

Multiple-antenna two-hop relaying for bi-directional transmission in wireless communication systems

Vom Fachbereich 18
Elektrotechnik und Informationstechnik
der Technischen Universität Darmstadt
zur Erlangung der Würde eines
Doktor-Ingenieurs (Dr.-Ing.)
genehmigte Dissertation

von
Dipl.-Ing. Timo Unger
geboren am 07.07.1979 in Groß-Gerau

Referent:	Prof. Dr.-Ing. Anja Klein
Korreferent:	Prof. Dr.-Ing. Armin Wittneben
Tag der Einreichung:	18. November 2008
Tag der mündlichen Prüfung:	04. Juni 2009

D 17
Darmstädter Dissertation
Darmstadt 2009

Danksagung

Diese Arbeit konnte nur entstehen, weil ich von einer Vielzahl von Menschen unterstützt worden bin, denen ich mit den folgenden Zeilen danken möchte.

Zuerst bedanke ich mich bei den Kollegen und Angestellten am Fachgebiet Kommunikationstechnik der TU Darmstadt. Die angenehme Arbeitsatmosphäre und die vielen lustigen Stunden vor und nach Feierabend mit Euch werden mir in sehr guter Erinnerung bleiben. Unsere intensiven Gesprächsrunden haben mir geholfen so manche fachliche Hürde zu überspringen.

Mein ganz besonderer Dank geht an meine Betreuerin Professor Anja Klein. Sie hat mich stets angetrieben, unterstützt und gefördert. Mit ihren Fragen, Ideen und Vorschlägen in unzähligen wertvollen Diskussionen hat sie wesentlich zu dieser Arbeit beigetragen. Desweiteren danke ich Professor Armin Wittneben, dass er das Korreferat für meine Dissertation übernommen hat und mit seinen Anmerkungen bei meinem Besuch in Zürich wichtige Impulse gegeben hat.

Ein weiterer Dank geht an alle Verantwortlichen der TU Darmstadt, die mir meine Promotion durch das gewährte Stipendium überhaupt erst ermöglicht haben. In diesem Zusammenhang möchte ich auch alle Studenten erwähnen, deren Betreuung bei Diplom- und Studienarbeiten mir sehr viel Freude bereitet hat.

Bei meinem Freundeskreis bedanke ich mich für die nötige Ablenkung außerhalb der Uni. In den freien Stunden mit Euch konnte ich sehr gut abschalten.

Besonders viel habe ich meinen Eltern zu verdanken, die mich jederzeit bei meinen Plänen unterstützt haben und immer ein verlässlicher Rückhalt waren.

Zuletzt danke ich meiner Partnerin Carolin für ihre Liebe, Geduld und Aufmunterung gerade in den wichtigen Momenten. Ich konnte mich stets auf ihre Unterstützung verlassen und widme ihr daher diese Arbeit.

Darmstadt, Juni 2009

Timo Unger

Kurzfassung

In derzeitigen drahtlosen Kommunikationssystemen wird gewöhnlich die sogenannte Punkt-zu-Punkt Übertragungstechnik verwendet. In Fällen, in denen diese Technik eine direkte Übertragung zwischen zwei Knoten S1 und S2 nicht ermöglicht, da beispielsweise eine Abschattung des Empfängers durch Hindernisse oder eine zu geringe Sendeleistung vorliegen, stellen Zwei-Hop Relaisverfahren eine vielversprechende Alternative dar. Bei den Zwei-Hop Relaisverfahren wird die Übertragung zwischen S1 und S2 durch eine zwischengeschaltete Relaisstation (RS) unterstützt. In dieser Arbeit werden nicht-regenerative Zwei-Hop Relaisverfahren betrachtet, wobei nicht-regenerativ bedeutet, dass das Empfangssignal an der RS weder dekodiert noch neu kodiert wird, sondern nur lineare Signalverarbeitung (SV) an der RS angewendet wird. Erst seit kurzem werden Zwei-Hop Relaisverfahren auch in Verbindung mit Mehrantennenverfahren untersucht, wodurch erhebliche Gewinne bezüglich der erreichbaren Datenraten erwartet werden. In dieser Arbeit werden an S1, S2 und der RS mehrere Antennen benutzt, um räumliche Multiplexverfahren mit adaptiver Strahlformung (SF) verwenden zu können.

Die vorliegende Arbeit untersucht zwei verschiedene Zwei-Hop Relaisverfahren für die bidirektionale Übertragung zwischen S1 und S2, welche Ein-Weg und Zwei-Wege Relaisverfahren genannt werden. Beim Ein-Weg Relaisverfahren werden wegen des Halbduplexbetriebes ein Zeitschlitz für die Übertragung von S1 zur RS und ein weiterer Zeitschlitz für die Übertragung von der RS zu S2 benötigt. Aufgrund der bidirektionalen Übertragung werden zwei weitere Zeitschlitze für die Übertragung von S2 über die RS zu S1 benötigt. Vergleicht man mit der bidirektionalen Punkt-zu-Punkt Übertragung zwischen S1 und S2, bei der nur ein Zeitschlitz für die Übertragung von S1 zu S2 und ein weiterer Zeitschlitz für die Übertragung von S2 zu S1 benötigt werden, wird beim Ein-Weg Relaisverfahren insgesamt die doppelte Menge an Zeitschlitzen benötigt. Das kürzlich vorgestellte Zwei-Wege Relaisverfahren ist bei bidirektionaler Übertragung sehr vielversprechend, da es nur zwei Zeitschlitze benötigt. Bei diesem Relaisverfahren senden S1 und S2 ihr jeweiliges Signal gleichzeitig im ersten Zeitschlitz zur RS, die dann die Summe der Signale von S1 und S2 im zweiten Zeitschlitz zurücksendet. Somit enthält das Empfangssignal an jedem Knoten auch das Signal, das vom jeweiligen Empfangsknoten selbst gesendet wurde. Falls ausreichend Kanalzustandsinformation (KZI) am Empfangsknoten verfügbar ist, kann dieser das gewünschte Signal bestimmen, indem er das eigene Signal subtrahiert. Dieses Verfahren wird Subtraktion der Duplexstörung (SDS) genannt.

In dieser Arbeit wird ein einheitliches Systemmodell für das Ein-Weg und Zwei-

Wege Relaisverfahren entwickelt. Für beide Relaisverfahren ist es von besonderem Interesse, auf welche Art adaptiver SF die Summenrate des Systems maximiert werden kann. Die erzielbare Summenrate hängt wesentlich von den Systemfähigkeiten ab, die durch die Verfügbarkeit von KZI und die SV Fähigkeiten an S1, S2 und der RS definiert werden. Da die Systemfähigkeiten die anwendbaren SF Algorithmen beeinflussen, werden neue Summenraten-Maximierungsprobleme identifiziert. Zur Einordnung dieser Probleme werden folgende vier Fälle von Systemfähigkeiten unterschieden:

- Ein System mit unbeschränkten Fähigkeiten, in dem S1 und S2 adaptive SF und SDS anwenden und die RS adaptive SF anwendet.
- Ein System mit eingeschränkten Fähigkeiten an der RS, in dem nur S1 und S2 adaptive SF und SDS anwenden.
- Ein System mit eingeschränkten Fähigkeiten an S1 und S2, in dem nur die RS adaptive SF anwendet.
- Ein System mit lokaler KZI, in dem S1 und S2 SDS anwenden und nur die RS adaptive SF anwendet.

Diese verschiedenen Fälle werden für das Ein-Weg und Zwei-Wege Relaisverfahren betrachtet und die entsprechenden maximalen Summenraten werden bestimmt. Für das Ein-Weg Relaisverfahren wird ein bereits bekannter analytischer SF Algorithmus zur Summenratenmaximierung in dem System mit unbeschränkten Fähigkeiten analysiert. Für alle anderen neu auftretenden Fälle werden numerische Lösungen der Probleme präsentiert. Für das System mit eingeschränkten Fähigkeiten an der RS werden neue suboptimale analytische SF Algorithmen mit einem nahezu optimalen Ergebnis vorgeschlagen. Es wird gezeigt, dass der maximale räumliche Multiplexgewinn für das Ein-Weg Relaisverfahren dem Minimum der Anzahl der Antennen an der RS und der Anzahl der Antennen an S1 und S2 entspricht, und für das Zwei-Wege Relaisverfahren dem Minimum der Anzahl der Antennen an der RS und der doppelten Anzahl der Antennen an S1 und S2. Desweiteren wird gezeigt, dass im Zwei-Wege Relaisverfahren die Summenrate beinahe doppelt so hoch ist wie im Ein-Weg Relaisverfahren.

Neben den adaptiven SF Algorithmen, die die Summenrate maximieren, sind andere adaptive SF Algorithmen, die den mittleren quadratischen Fehler (MQF) minimieren, den MQF unter der Zero-Forcing Bedingung minimieren und das Signal-zu-Rausch-Verhältnis maximieren, dafür bekannt, dass sie gute Ergebnisse für die Punkt-zu-Punkt Übertragung liefern. Da adaptive SF, die nur an S1 und S2 angewendet wird, bereits vielfach für die Punkt-zu-Punkt Übertragung untersucht wurde, wird in dieser Arbeit

besonderes Augenmerk auf das neue Feld der Systeme, in denen adaptive SF nur an der RS angewendet wird, gerichtet. Für diese Systeme werden sowohl im Ein-Weg als auch im Zwei-Wege Relaisverfahren die zuvor erwähnten Optimierungsprobleme neu formuliert, gelöst und analysiert. Vielversprechende Ergebnisse werden vor allem mit dem adaptiven SF Algorithmus, der den MQF minimiert, erzielt.

Um KZI in den verschiedenen Fällen von Systemfähigkeiten zu erlangen, werden neue Pilotübertragungsverfahren und die zugehörigen Kanalschätzalgorithmen entwickelt. Desweiteren werden die Auswirkungen nicht-perfekter KZI betrachtet. Zuletzt wird anhand von zwei beispielhaften Szenarien mit zusätzlichen Knoten ein erster Einblick in Problemstellungen gewährt, die sich durch Vielfachzugriffe im Zwei-Wege Relaisverfahren ergeben.

Abstract

In today's wireless communication systems, usually the point-to-point transmission technique is used for the transmission between two nodes S1 and S2. If a point-to-point transmission between S1 and S2 is not possible, e.g., due to shadowing or limited transmit powers, two-hop relaying is a promising technique, in which the transmission between S1 and S2 is assisted by an intermediate relay station (RS). In this thesis, non-regenerative two-hop relaying is considered which means that the received signals at the RS are neither decoded nor re-encoded, but only linear signal processing (SP) is employed at the RS. Just recently, two-hop relaying has been investigated in conjunction with multiple-antenna techniques which promises significant performance gains in terms of achievable data rates. In this work, multiple antennas are used at S1, S2 and the RS in order to perform spatial multiplexing by adaptive beamforming (BF).

This thesis investigates two different two-hop relaying schemes for bi-directional transmission between S1 and S2, namely one-way and two-way relaying. In one-way relaying due to the half-duplex constraint, one time slot is required for the first hop transmission from S1 to the RS, and another time slot is required for the second hop transmission from the RS to S2. For bi-directional transmission, another two time slots are required for the transmission from S2 via the RS to S1 resulting in a requirement of four time slots in total. Thus, compared to a bi-directional point-to-point transmission between S1 and S2, which requires only one time slot for the transmission from S1 to S2 and another time slot for the transmission from S2 to S1, the number of required time slots is doubled in one-way relaying. In case of bi-directional transmission, the recently proposed two-way relaying scheme is a very promising scheme in terms of resource efficiency since it requires only two time slots. In two-way relaying, S1 and S2 transmit their signals simultaneously in the first time slot to the RS which retransmits a superposition of the signals of S1 and S2 in the second time slot. Thus, the received signal at each node contains the signal which has been transmitted by the respective receive node itself. If sufficient channel state information (CSI) is available at the receive node, it can determine the desired signal by subtracting the own transmitted signal. This subtraction is termed cancellation of duplex interference (CDI).

In this work, a unified system model for one-way and two-way relaying is developed. For both relaying schemes, it is of particular interest how the sum rate of the system can be maximized by adaptive BF. The achievable sum rates depend considerably on the system capabilities, which are defined by the CSI availability and the SP capabilities at S1, S2 and the RS. Since the system capabilities influence the applicable adaptive BF algorithms, novel sum rate maximization problems are identified and classified by a framework consisting of four different cases of system capabilities:

- A system with full capabilities, in which S1 and S2 perform adaptive BF and CDI, and the RS performs adaptive BF.
- A system with limited capabilities at the RS, in which only S1 and S2 perform adaptive BF and CDI.
- A system with limited capabilities at S1 and S2, in which only the RS performs adaptive BF.
- A system with local CSI at S1 and S2, in which S1 and S2 perform CDI, and only the RS performs adaptive BF.

The different cases are considered for one-way and two-way relaying, and the respective maximum sum rates are determined. In one-way relaying, an analytical BF algorithm for maximizing the sum rate in the system with full capabilities is reviewed. For the other new cases of system capabilities in one-way and two-way relaying, numerical solutions to the sum rate maximization problems are given. For the systems with limited capabilities at the RS in one-way and two-way relaying, new sub-optimum analytical BF algorithms with close-to-optimum performances are proposed. It is shown that the maximum spatial multiplexing gain corresponds to the minimum of the number of antennas at the RS and the number of antennas at S1 and S2 in one-way relaying, and to the minimum of the number of antennas at the RS and twice the number of antennas at S1 and S2 in two-way relaying. Furthermore, it is demonstrated that the sum rate in two-way relaying is almost twice as high as the sum rate in one-way relaying.

Beside the adaptive BF algorithms maximizing the sum rate, other adaptive BF algorithms minimizing the mean square error (MSE), minimizing the MSE under the zero forcing constraint, and maximizing the signal-to-noise ratio are known to provide reasonable performance in point-to-point transmission. Since adaptive BF only performed at nodes S1 and S2 has already been investigated in several works regarding point-to-point transmission, in this thesis special attention is paid to the recent field of systems in which adaptive BF is only performed at the RS. For such systems in one-way as well as in two-way relaying, the aforementioned optimization problems, are newly formulated, solved, and analyzed. Promising performance results are especially obtained by the adaptive BF algorithm minimizing the MSE.

In order to obtain CSI in the different cases of system capabilities, novel pilot transmission schemes and the respective channel estimation algorithms are developed. Furthermore, the impact of imperfect CSI on the performance of two-way relaying is considered. Finally, two scenarios with multiple nodes are introduced exemplarily in order to give a first insight into the problems arising from multiple access in two-way relaying.

Contents

1	Introduction	1
1.1	Multiple-antenna two-hop relaying for bi-directional transmission . . .	1
1.1.1	Scenario	1
1.1.2	Considered two-hop relaying techniques	5
1.1.3	System capabilities	7
1.2	State-of-the-art	11
1.3	Open problems	15
1.4	Thesis contributions and overview	17
2	System model	19
2.1	Introduction	19
2.2	System assumptions	19
2.3	General system model	22
2.4	Sum rate definition	26
2.5	Application of the general system model to particular relaying schemes	29
2.5.1	One-way relaying	29
2.5.2	Two-way relaying	30
3	One-way relaying	33
3.1	Introduction	33
3.2	Maximization of the sum rate	34
3.2.1	General problem formulation	34
3.2.2	System with full capabilities	35
3.2.3	System with limited capabilities at the RS	38
3.2.4	System with limited capabilities at S1 and S2	41
3.3	Linear beamforming in a system with limited capabilities at S1 and S2	44
3.3.1	Introduction	44
3.3.2	Minimization of the MSE	45
3.3.3	Minimization of the MSE under the ZF constraint	47
3.3.4	Maximization of the SNR	50
3.4	Performance analysis	52
3.4.1	Simulation assumptions	52
3.4.2	Sum rate analysis	52
3.4.3	Bit error rate analysis	58
3.5	Conclusions	62
4	Two-way relaying	65

4.1	Introduction	65
4.2	Maximization of the sum rate	66
4.2.1	General problem formulation	66
4.2.2	System with full capabilities	69
4.2.3	System with limited capabilities at the RS	74
4.2.4	System with limited capabilities at S1 and S2	77
4.2.5	System with local CSI at S1 and S2	79
4.3	Linear beamforming in a system with limited capabilities at S1 and S2	80
4.3.1	Introduction	80
4.3.2	Minimization of the MSE	81
4.3.3	Minimization of the MSE under the ZF constraint	83
4.3.4	Maximization of the SNR	84
4.4	Linear beamforming in a system with local CSI at S1 and S2	86
4.4.1	Introduction	86
4.4.2	Minimization of the MSE	87
4.4.3	Minimization of the MSE under the ZF constraint	89
4.4.4	Maximization of the SNR	92
4.5	Performance analysis	94
4.5.1	Simulation assumptions	94
4.5.2	Sum rate analysis	95
4.5.3	Bit error rate analysis	105
4.6	Conclusions	110
5	Topics of relevance for the practical implementation of two-way re- laying	113
5.1	Introduction	113
5.2	Pilot assisted channel estimation	114
5.2.1	Introduction	114
5.2.2	Local CSI at S1, S2, and global CSI at the RS	115
5.2.3	Global CSI at S1 and S2	116
5.2.4	Pilot transmission schemes for different cases of system capabilities	119
5.2.5	Sum rate degradation	123
5.2.6	Performance analysis	124
5.3	Imperfect CSI	126
5.3.1	Introduction	126
5.3.2	Modeling imperfect CSI	127
5.3.3	Performance analysis	128
5.4	Multiple source-destination pairs	131
5.4.1	Introduction	131

5.4.2	Multiple single-antenna source-destination pairs	131
5.4.3	Asymmetric rate requirements of multiple source-destination pairs	133
6	Conclusions	137
	Appendix	139
A.1	Derivation of (3.38) and (3.39) for the MMSE-BF algorithm in one-way relaying	139
A.2	Derivation of (3.48) and (3.49) for the ZF-BF algorithm in one-way relaying	140
A.3	Derivation of (3.57) and (3.58) for the MF-BF algorithm in one-way relaying	141
A.4	The vectorization, the Kronecker product, and the matrix inversion . .	142
A.5	Derivation of (4.65) and (4.67) for the MMSE-BF algorithm in two-way relaying	143
A.6	Derivation of (4.75) and (4.77) for the ZF-BF algorithm in two-way relaying	145
A.7	Derivation of (4.83) and (4.85) for the MF-BF algorithm in two-way relaying	146
	List of Acronyms	149
	List of Symbols	151
	Bibliography	155

Chapter 1

Introduction

1.1 Multiple-antenna two-hop relaying for bi-directional transmission

1.1.1 Scenario

One major challenge for future wireless communication systems is the ubiquitous demand of high transmission rates [STMLM02, IST07b]. In present wireless communication systems, typically point-to-point transmission is used which means that a source node directly transmits its data to the corresponding destination node. However, due to the requirement of high transmission rates at any location of the system the point-to-point transmission technique meets its limits.

In order to establish a reliable transmission, which means that the destination node can determine the data of the source node with a tolerable error rate, the destination node requires a sufficient receive power of the desired signal. In case of a sufficient receive power, the desired signal may be detected within the mixture of signals and inherent receiver noise [Pro01] at the destination node. However, a sufficient receive power cannot always be provided by the point-to-point transmission technique. In order to obtain a sufficient receive power at the destination node, two effects of the radio channel between transmitter and receiver have to be taken into account. Firstly, the receive power decreases with the increasing distance squared between the source and destination node in free space. Due to reflection, diffraction and shadowing by obstacles, the receive power decreases even more rapidly [STIST05]. Secondly, the receive power decreases with increasing center frequency which is a critical issue since future wireless communication systems are expected to be operated at higher center frequencies than the frequencies in today's systems. For example, center frequencies of about 5GHz are proposed for the fourth generation (4G) [STIST07a] of wireless communication systems while the third generation (3G) [GP3GP06] is operated at about 2GHz. Since the receive power at the destination node increases with increasing transmit power of the source node, one could suggest to increase the transmit power as a counter measure to the two aforementioned effects. However, as the transmit power in wireless transmissions cannot be increased arbitrarily, e.g., due to electromagnetic compatibility (EMC) reasons or due to health reasons or due to cost reasons [Loy01,

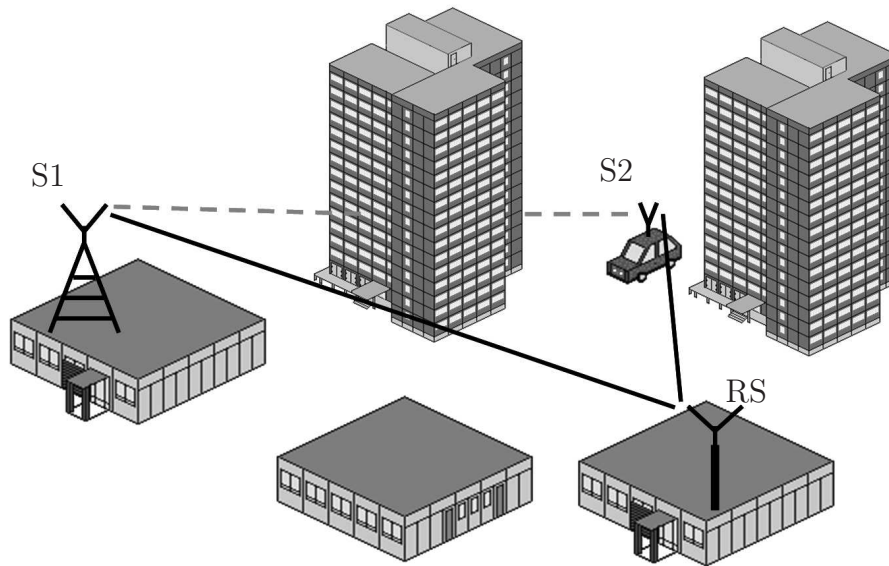


Figure 1.1. Two-hop relaying in an urban cellular scenario with insufficient receive power at node S2 for a point-to-point transmission from node S1 to node S2.

Lin03, Tim05, ZK01], increasing the transmit power is no feasible counter measure. Thus, the receive power at the destination node is a critical issue and techniques in order to obtain a sufficient receive power are required if high transmission rates are desired [PWS⁺04]. Figure 1.1 depicts a typical urban scenario in a cellular system which exemplifies the problem of insufficient receive power for the point-to-point transmission of two nodes S1 and S2. Let us consider the transmission from node S1 which is a base station to node S2 which is a mobile user node. In this example, S1 corresponds to the source node and S2 corresponds to the destination node. Nodes S1 and S2 form a source-destination pair. Due to the shadowing by the high building, the receive power at the destination node, is such low that a point-to-point transmission from the source node to the destination node is not possible. Note that S1 and S2 may exchange their roles while still being faced with the problem of insufficient receive power due to shadowing in the scenario of Figure 1.1. Throughout the thesis, it is assumed that a point-to-point transmission between source and destination node is impossible.

Nevertheless, a reliable transmission from the source node to the destination node can still be established if another node which is termed relay station (RS) assists the transmission. In the depicted scenario of Figure 1.1, the source node can establish a reliable transmission to the RS, and the RS can establish a reliable transmission to the destination node. Thus, the RS receives the data of the source node and retransmits the data to the destination node. Since the overall transmission requires two hops, one from the source node to the RS and another from the RS to the destination node, the technique is termed two-hop relaying [LLW⁺03]. For multi-hop relaying

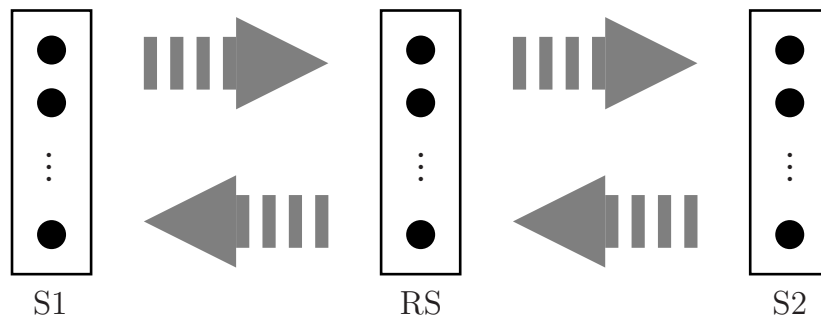


Figure 1.2. Considered bi-directional two-hop relaying scenario with source and destination nodes S1 and S2, and the RS, all equipped with multiple antennas.

[DLV⁺06,BFY04], there are multiple RSs between source and destination node, i.e., the data is retransmitted several times until it is received at the destination node. However, this thesis only considers two-hop relaying, since every additional hop increases the delay between the transmission of the source node and the reception at the destination node, and since two hops are reasonable in many application cases. Furthermore, the generalization from two-hop relaying to multi-hop relaying is straightforward in most of the cases. In cellular scenarios, either dedicated nodes with fixed locations [PWS⁺04, SPI03,HU06] as depicted in Figure 1.1 and/or mobile user nodes [Yan02] may serve as a RS. Relaying can also be applied in sensor networks as proposed in [DLV⁺06,LVZD07], for example. Figure 1.1 gives only one descriptive example for a possible application of two-hop relaying in cellular networks, but the two-hop relaying techniques presented in this thesis can also be applied in many other wireless communication systems.

In the following, the system which is considered throughout the thesis is introduced. The system consists of three nodes, namely S1, S2, and the RS. In the system, bi-directional transmission [OB08] is performed which means that S1 transmits data to S2, and S2 transmits data to S1. Hence, S1 and S2 are source nodes as well as destination nodes. Throughout the thesis, the terms source node S1 (S2) and destination node S1 (S2) are used if it is important which role is taken by S1 (S2) in the current context. If it is not important, simply the term S1 (S2) is used. Typical services requiring bi-directional transmissions with high transmission rates are video conferencing and gaming, for example. Figure 1.2 gives a schematic representation of the system under consideration. The two gray arrows from the left to the right and the two gray arrows from the right to the left indicate the four required transmissions for one overall bi-directional transmission between S1 and S2. In order to enable the four transmissions, channel resources in time and frequency need to be allocated to them. Since the resources in time and frequency are interchangeable in most of the cases, only one frequency resource and multiple time resources which are named time

slots are considered throughout the thesis.

Besides channel resources in time and frequency, channel resources may also be defined in the spatial domain by using multiple-input-multiple-output (MIMO) techniques [Tel99, KBB⁺05]. From point-to-point transmissions, it is known that MIMO techniques promise significant performance gains in terms of achievable transmission rate. Just recently, MIMO techniques are also applied in two-hop relaying expecting similar performance gains [HKE⁺07, DGA03]. In order to exploit the spatial domain, the different nodes need to be equipped with multiple antennas indicated by the big dots in Figure 1.2. These multiple antennas enhance the performance of the transmission by exploiting spatial diversity [PNG03] and/or applying spatial multiplexing [Tel99, LT02]. In case of spatial diversity schemes, the transmission rate may be improved by smartly transmitting and/or receiving one data stream at several antennas which provides several independent replicas of the same data stream at the receiver. In order to apply spatial diversity schemes, the transmitter does not need to know the current transfer function of the time variant and frequency selective radio channel between transmitter and receiver. This knowledge is defined as transmit channel state information (CSI) and can be obtained by pilot assisted channel estimation (PACE) for example [TSD04]. However, if the transmitter has transmit CSI, significantly higher performance gains in terms of transmission rate can be achieved by applying spatial multiplexing schemes. In case of spatial multiplexing schemes, multiple data streams are transmitted simultaneously on the same channel resources in time and frequency by separating the data streams in the spatial domain. This means that the required amount of channel resources in time and frequency needs not to be increased in order to increase the transmission rate. Since high transmission rates are desired for the systems of this thesis, only spatial multiplexing schemes are regarded in the following. Separating multiple data streams in the spatial domain can be achieved by adaptive beamforming (BF). In order to apply adaptive BF at the transmitter side which is also referred to as spatial precoding [MBQ04, JUN05, PNG03], the transmitter requires transmit CSI. In order to apply adaptive BF at the receiver side which is also referred to as joint decoding [Mue01, HM72], the receiver needs to know the current transfer function of the radio channel between transmitter and receiver. This knowledge is defined as receive CSI and can be obtained by PACE, too. Throughout the thesis, channel reciprocity is assumed since the time between transmission and reception of a node is chosen to be shorter than the channel coherence time [Pro01]. This means that the transmit CSI equals the receive CSI. Unless otherwise stated, the term CSI is used for both kinds of CSI in the following. The investigations of this thesis are limited to a single source-destination pair since the challenges for adaptive BF in two-hop relaying already appear for this simple system and the developed BF algorithms can be used

as a basis for an extension to multiple source-destination pairs.

1.1.2 Considered two-hop relaying techniques

In this section, the considered two-hop relaying techniques are presented. There exist many two-hop relaying techniques which can be classified by two criteria, namely the signal processing (SP) approach at the RS and the relaying scheme which is defined by the channel resource allocation [ZK01]. In the following, firstly the SP approaches are considered, and secondly the relaying schemes.

There exist two main approaches for the SP at the RS, which define how the received data streams at the RS are processed before the retransmission. For the regenerative approach which is also referred to as decode-and-forward (DF) or digital relaying [Yan02, OB06], the received data streams from the source node are decoded and re-encoded at the RS before the retransmission to the destination node. For the non-regenerative approach which is sometimes referred to as analog relaying [BUK⁺09, Yan02], the received data streams at the RS are neither decoded nor re-encoded, but only linear SP is employed. A well-known non-regenerative approach is amplify-and-forward (AF) relaying [PSP06, PS07] where the received data streams are just amplified by a weighting factor at the RS before the retransmission to the destination node. Other non-regenerative approaches employ advanced linear SP at the RS, e.g. linear adaptive BF where linear combinations of the received data streams can be retransmitted from the RS [HW06, TH07, UK08a].

In regenerative relaying, the receiver noise at the RS is eliminated due to decoding. In this case, decoding errors may appear. In non-regenerative relaying, the receiver noise at the RS is propagated to the destination node. Intuitively, one might expect that regenerative relaying always outperforms non-regenerative relaying due to the elimination of the receiver noise at the RS. However, there exist several works which show that this is not necessarily the case [Yan02, FATY07]. For example, the RS selection in regenerative relaying is a more challenging task than the RS selection in non-regenerative relaying since the selection of an improper RS causes decoding errors at the RS which propagate to the destination node [LTW04].

In regenerative relaying, the decoding and re-encoding of the data streams at the RS cause additional delay to the overall transmission from the source node to the destination node, while the linear SP in non-regenerative relaying is less critical in terms of delay. Time diversity in fading radio channels can be exploited by introducing

temporal interleaving [JT94] in conjunction with channel coding. Especially if the temporal interleaving depth is high, the delay caused by decoding and re-encoding at the RS increases.

In regenerative relaying, the RS needs to know and support the modulation and coding schemes [BHIM05] agreed between source and destination node, while non-regenerative relaying is transparent regarding the modulation and coding schemes. Let us consider a system which consists of source and destination nodes of different capabilities, e.g., some mobile nodes are able to support high transmission rates using advanced modulation and coding schemes while other mobile nodes do not support these advanced modulation and coding schemes. In regenerative relaying, the RS needs to support all modulation and coding schemes used in the system, otherwise it cannot decode and re-encode the received data streams. In non-regenerative relaying, the RS can support all modulation and coding schemes inherently without knowing them since the RS only retransmits linearly processed versions of the received data streams without considering the actual modulation and coding scheme. Due to the mentioned advantages of non-regenerative relaying, this thesis focuses on non-regenerative relaying exclusively.

In the following, the second criterion for the classification of the relaying techniques is considered, namely the relaying scheme. There exist several relaying schemes which differently allocate the channel resources to the different transmissions in the system. There exists a hardware limitation which imposes a constraint on all relaying schemes. Due to the high dynamic range between the signal powers of received and transmitted signals, typical transceivers at S1, S2, and the RS cannot receive and transmit simultaneously. This constraint is often referred to as half-duplex constraint [RW07] and is typically solved by transmitting and receiving on two orthogonal time slots. In this thesis, two relaying schemes satisfying the half-duplex constraint are investigated, namely one-way relaying and two-way relaying. The time slot allocation of the one-way relaying scheme is depicted in the upper part of Figure 1.3. The name on the left of the arrow gives the respective transmit node and the name on the right of the arrow gives the respective receive node of the transmission of the regarded time slot. Since spatial multiplexing is applied in the system, each transmission of a single time slot may consist of multiple data streams. The first and second time slot are allocated to the two-hop transmission from S1 to S2 and the third and fourth time slot are allocated to the two-hop transmission from S2 to S1. More precisely, the first time slot is allocated to the transmission of the data streams from S1 to the RS. In the second time slot, the RS retransmits a linear combination of its received data streams of the first time slot to S2. The third time slot is allocated to the transmission of the data streams from S2 to the RS. In the fourth time slot, the RS retransmits a linear combination of its received

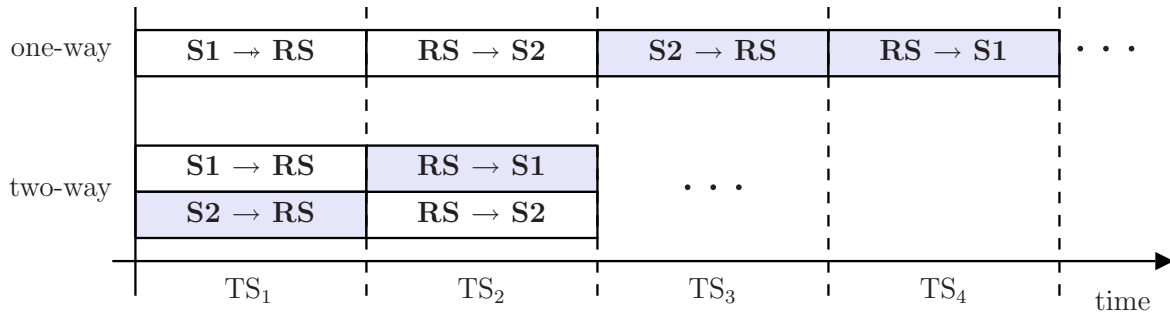


Figure 1.3. Time slot allocation for the one-way and the two-way relaying schemes with time slots TS_t , $t = 1, \dots, 4$.

data streams of the third time slot to $S1$. Compared to a bi-directional point-to-point transmission between $S1$ and $S2$ without intermediate RS , which requires only one time slot for the transmission from $S1$ to $S2$ and another time slot for the transmission from $S2$ to $S1$, the number of required time slots is doubled in one-way relaying.

In case of bi-directional transmission between $S1$ and $S2$, two-way relaying which has been first proposed by Rankov and Wittneben [RW05] is a very promising scheme in terms of resource efficiency since it requires only two time slots. The time slot allocation of the two-way relaying scheme is depicted in the lower part of Figure 1.3. In the first time slot, the source nodes $S1$ and $S2$ transmit simultaneously to the RS which retransmits a superposition of the data streams of $S1$ and $S2$ in the second time slot. The destination nodes $S1$ and $S2$ can determine the desired data streams by subtracting their own transmitted but interfering data streams from the received superposition of the data streams of $S1$ and $S2$ [RW07]. This kind of self interference which only appears in two-way relaying and not in one-way relaying is termed duplex interference and the applied subtraction is termed cancellation of duplex interference (CDI) in the following.

1.1.3 System capabilities

In this section, a new framework for classifying systems with different capabilities in one-way and two-way relaying is introduced. There are two main criteria which define the system capabilities, namely if CSI can be made available at $S1$, $S2$ and/or the RS , and the SP capabilities at $S1$, $S2$ and the RS . Before introducing the different system capabilities, CSI availability and SP capabilities are explained in detail.

In the considered system of Figure 1.2, either no CSI or local CSI or global CSI may be available at the nodes. If no CSI is available at a node, the node has no knowledge

about the channels. If local CSI is available at a node, the node knows the channel which is used for the transmission and reception of the node. Regarding Figure 1.2, knowing the channel between S1 (S2) and the RS at S1 (S2) corresponds to local CSI at S1 (S2), and knowing the channels between the RS and S1 and between the RS and S2 at the RS corresponds to local CSI at the RS. If global CSI is available at a node, the node knows all channels in the system. Regarding Figure 1.2, global CSI at S1 (S2) corresponds to knowledge about the channel between S1 (S2) and the RS, and the channel between S2 (S1) and the RS. Finally, from the definition of local CSI and global CSI it becomes obvious that both correspond to each other at the RS. However, only the term global CSI at the RS is used in the following. Obtaining local CSI is relatively simple for all nodes since the nodes can directly 'see' the respective channels. Obtaining global CSI at S1 and S2 is more challenging since both nodes also require CSI about a channel which they do not 'see' directly.

In order to perform adaptive BF at S1 and S2 which is adapted to both hops of a two-hop transmission, global CSI is required at S1 and S2. In order to perform adaptive BF for both directions of the bi-directional transmission at the RS, global CSI is required at the RS. In order to apply CDI in two-way relaying, only local CSI is required at S1 and S2.

Furthermore, the applied SP at the nodes does not only depend on the available CSI, but also on the SP capabilities of the nodes where the SP capabilities reflect the computational effort that can be spent at the nodes. In the following, the SP capabilities of the nodes are defined which may be either full or limited. It is assumed that source and destination nodes with full SP capabilities can perform adaptive BF, i.e., the source nodes can perform spatial precoding and the destination nodes can perform joint decoding. A RS with full SP capabilities can also perform adaptive BF. In the following, the applied SP at a source node, a destination node or a RS with full SP capabilities is always termed adaptive BF. It is assumed that source and destination nodes with limited SP capabilities cannot perform adaptive BF. In this case, it is assumed the source node only distributes the available transmit power equally between all transmit antennas and each antenna transmits one data stream. Analogous to the SP at the source node, the destination node with limited SP capabilities only performs an equal weighting of each received data stream. It is assumed that a RS with limited SP capabilities cannot perform adaptive BF. Thus, the RS only distributes the available transmit power equally between all transmit antennas and an amplified replica of the received data streams is retransmitted from each antenna. In the following, the applied SP at a source node, a destination node or a RS with limited SP capabilities is always termed equal weighting. It is assumed that limited SP capabilities are already sufficient in order to apply CDI at the destination nodes since CDI only requires a

system capabilities					
available CSI	at S1/S2	global	global	none	local
	at RS	global	none	global	global
SP capabilities	at S1/S2	full	full	limited	limited
	at RS	full	limited	full	full
applied SP	at S1/S2	BF & CDI	BF & CDI	equal weighting	equal weighting & CDI
	at RS	BF	equal weighting	BF	BF

relaying scheme	one-way relaying	maximization of sum rate	maximization of sum rate	<ul style="list-style-type: none"> • maximization of sum rate • minimization of MSE • minimization of MSE under ZF constraint • maximization of SNR 	
	two-way relaying	maximization of sum rate	maximization of sum rate	<ul style="list-style-type: none"> • maximization of sum rate • minimization of MSE • minimization of MSE under ZF constraint • maximization of SNR 	<ul style="list-style-type: none"> • maximization of sum rate • minimization of MSE • minimization of MSE under ZF constraint • maximization of SNR
		System with full capabilities	System with limited capabilities at the RS	System with limited capabilities at S1 and S2	System with local CSI at S1 and S2

Figure 1.4. Overview of considered optimization problems depending on the system capabilities and the relaying schemes.

simple subtraction of the own data streams which are multiplied with the local CSI. Due to the symmetry in bi-directional transmissions, S1 and S2 are always assumed to have the same capabilities.

With the above given explanation of CSI availability and SP capabilities, the new framework can be summarized by Figure 1.4. The matrix organization of the figure can be read as follows. The vertical axis with the dark gray shade gives the considered relaying scheme which is either one-way or two-way relaying. The horizontal axis with the light gray shade consists of three lines which are linked to the system capabilities. The first and second line of the horizontal axis in the figure give the available CSI and the SP capabilities at the nodes, respectively. The third line gives the SP applied at

S1 and S2, and the RS, which results from the assumptions in the first and second line. Depending on the available CSI and the SP capabilities of the nodes, four different cases of system capabilities are defined at the bottom of Figure 1.4 which correspond to the four columns outlined by the thick black frames:

- **System with full capabilities:** Global CSI is available at S1, S2, and the RS. S1, S2, and the RS have full SP capabilities. Thus, all nodes perform adaptive BF.
- **System with limited capabilities at the RS:** Global CSI is available at S1 and S2, and S1 and S2 have full SP capabilities. Thus, S1 and S2 perform adaptive BF. No CSI is available at the RS, and the RS has only limited SP capabilities. Thus, the RS only performs equal weighting.
- **System with limited capabilities at S1 and S2:** No CSI is available at S1 and S2, and S1 and S2 have limited SP capabilities. Thus, S1 and S2 only perform equal weighting. Global CSI is available at the RS, and the RS has full SP capabilities. Thus, the RS performs adaptive BF.
- **System with local CSI at S1 and S2:** Only local CSI is available at S1 and S2, and S1 and S2 have limited SP capabilities. Thus, S1 and S2 only perform equal weighting and CDI. Global CSI is available at the RS, and the RS has full SP capabilities. Thus, the RS performs adaptive BF.

In Figure 1.4, the matrix with the two rows corresponding to the two different relaying schemes and the four columns corresponding to the four different system capabilities consists of seven boxes with a thick black frame where each box contains typical optimization problems in the system of Figure 1.2. One typical optimization problem is given by the maximization of the sum rate where the sum rate gives the sum of the transmission rates of the two directions of transmission in bi-directional transmissions. Other typical optimization problem known from point-to-point transmissions are the minimization of the mean square error (MSE), the minimization of the MSE under the zero forcing (ZF) constraint, and the maximization of the signal-to-noise ratio (SNR). The formulation of the optimization problems depends on the system capabilities and the relaying schemes. All optimization problems indicated in Figure 1.4 are considered in detail in the following sections. Since duplex interference does not appear in one-way relaying, a system with local CSI and limited SP capabilities at S1 and S2 is not reasonable in one-way relaying. Thus, no optimization problems are formulated for a system with local CSI at S1 and S2, cf. first row and fourth column of the framework in Figure 1.4.

1.2 State-of-the-art

This section gives a review on the state-of-the-art regarding the one-way and two-way relaying schemes.

In [vdM71], the relay channel has been investigated for the first time assuming uni-directional transmission which means that only one direction of the transmission is considered. It is assumed that the transmission between the single-antenna source node and the single-antenna destination is assisted by the single-antenna RS. In general, the relay channel consists of three links: the direct link from the source node to the destination node which is indicated by the dashed line in Figure 1.1, the link from the source node to the RS, and the link from the RS to the destination node. Assuming these links, cooperation is a promising technique in order to improve the performance of the transmission between source and destination node [LW03, LTW04]. In the relay channel, cooperation implies that the source node and the RS jointly optimize their transmissions to the destination node and the destination node exploits that the desired signals are received over two independent links. Thus, cooperation exploits two main characteristics of relaying: it exploits the broadcast nature of the wireless channel and the diversity coming from the relay channel [ZHF03, HZF04b, ZHF04]. The capacity of the described relay channel is still unknown and only bounds are given [CEG79, CT06]. Thus, the term maximum transmission rate and not capacity is used in the following. The maximum transmission rate and the maximum sum rate may be determined under the assumption of a specific relaying technique classified by the SP approach and the relaying scheme.

In the following, firstly two-hop relaying schemes for single-antenna nodes are reviewed, and secondly a review on literature about multiple-antenna two-hop relaying is given.

The one-way relaying scheme as introduced by the time slot allocation of Figure 1.3 is the most simple relaying scheme since only the link from the source node to the RS, and the link from the RS to the destination node are considered. There exist several cooperative relaying schemes which are based on the one-way relaying scheme and which exploit different cooperation gains. Cooperation between multiple RSs assisting the transmission between one source-destination pair may provide spatial diversity [DDA02, DGA03], e.g., by applying distributed space-time coding [MH04, YSL06, UK07c, UK06]. A scheme which saves time-slots for one source-destination pair assisted by two RSs is proposed in [RW07]. This scheme is termed two-path relaying. In the first time slot, one RS receives from the source node and

the other RS transmits to the destination node. In the second time slot, the RSs change their roles. Since the source node may transmit in every time slot, the number of required time slots is the same as in point-to-point transmissions. However, since the two RSs use the same time slots, there may exist co-channel interference. Further work on the two-path relaying scheme considering the direct link between the source node and the destination node in order to exploit additional cooperation gains is presented in [FWTP07]. Cooperation between multiple users in one-way relaying provides user cooperative diversity [SEA03a,SEA03b]. Cooperative relaying schemes which save time slots in one-way relaying by making a smart reuse of the time slots for multiple source-destination pairs are proposed in [SAY06,MVA04,HYFP04]. In [SAY06], multiple RSs are divided into two groups that alternately receive and transmit signals, i.e., while one group is receiving signals from the source nodes, the other group is transmitting signals to the destination nodes. Since the source nodes transmit all the time in this scheme, the number of required time slots is the same as in point-to-point transmissions. However, the performance of the scheme can be significantly degraded by co-channel interference between the two groups of RSs. In [MVA04], one source node communicates with K different destination nodes via K different RSs. Firstly, the source node transmits consecutively to the K RSs using K time slots. Secondly, all RSs transmit simultaneously to their assigned destination nodes in the relay time slot $K + 1$. Obviously, this scheme does not require double number of time slots compared to a point-to-point transmission, but only $(K + 1)/K$ -times more. However, the performance may be significantly degraded by co-channel interference from the RSs at the destination nodes. The problem of co-channel interference is also addressed in [HYFP04], where the co-channel interference is kept low by a smart selection of simultaneously transmitting RSs in the relay time slot.

All aforementioned schemes aim at saving time slots in two-hop relaying by modifying the one-way relaying scheme. Two-way relaying [RW05] constitutes a completely new scheme which is especially developed for bi-directional transmissions. From Figure 1.3, it can be seen that two-way relaying requires the same number of time slots as a bi-directional point-to-point transmission. The two-way relaying scheme can be combined with a regenerative and a non-regenerative SP approach at the RS, respectively. Furthermore, two-way relaying is closely connected to network coding [ACW00]. Originally, in network coding data packets of different sources in a multi-node computer network are jointly encoded at intermediate network nodes, thus saving network resources. Applying network coding for wireless communications is referred to as physical layer network coding [DEH⁺05]. Beside two-way relaying, there exist other schemes which also apply physical layer network coding. In all schemes, there exist two phases, namely the multiple access phase for the transmission from S1 and S2 to the RS and the

broadcast phase for the transmission from the RS to S1 and S2. In the single-antenna regenerative relaying schemes of [PY07, LJS06, HH06], three orthogonal time slots are used. The first two time slots are allocated to the multiple access phase which means that S1 transmits in the first time slot to the RS and S2 transmits in the second time slot to the RS. At the RS, the decoded data streams of S1 and S2 are combined by an bit-wise exclusive OR (XOR) operation. The third time slot is used for the broadcast phase of the combined data streams. The destination nodes may determine the desired data stream by a bit-wise XOR operation of the received data stream and the own known data stream. In [PY07], the regenerative relaying scheme with three time slots is compared to non-regenerative two-way relaying. The comparison in [PY07] shows that non-regenerative two-way relaying provides a better performance for low noise levels at the RS than the regenerative relaying scheme with three time slots due to the smaller number of required time slots in non-regenerative two-way relaying.

In regenerative two-way relaying which also uses two time slots as introduced in Figure 1.3, the simultaneously transmitted data streams of S1 and S2 in the first time slot have to be separated by the decoding at the RS. As in the regenerative relaying scheme proposed in [PY07], the decoded data streams of S1 and S2 are re-combined by an bit-wise XOR operation before the retransmission in the second time slot. The destination nodes may determine the desired data stream by a bit-wise XOR operation of the received data stream and the own known data stream. In [RW06, OB07], the achievable rate regions of regenerative two-way relaying for single-antenna nodes are investigated. The optimal relative sizes of the first and second time slot in order to maximize the achievable sum rate of regenerative two-way relaying is given in [OB07, OB08]. A more practical issue is addressed in [KEHW06], where it is shown how regenerative two-way relaying can be integrated into the existing IEEE 802.11n (WLAN) standard promising an improved resource efficiency and a reduced delay for two-hop transmissions in IEEE 802.11n.

All of the aforementioned works on one-way and two-way relaying are restricted to single-antenna nodes. In the following, firstly the literature regarding optimization problems for systems with multiple antennas in one-way relaying, and secondly the literature regarding optimization problems for systems with multiple antennas in two-way relaying are reviewed using the framework of Figure 1.4.

Maximizing the transmission rate for non-regenerative one-way relaying with multiple antenna nodes in a system with full capabilities, cf. the box in the first row and first column in Figure 1.4, is considered in several works. The adaptive BF algorithms in order to maximize the transmission rate are given in [MVA05, MVA07, HW06, TH07]. In [MVA05, MVA07], the optimum BF at the RS is derived for a fixed BF at the source

node. The authors in [HW06] give the optimum BF at the source node if the BF at the RS is fixed. Furthermore, they present the joint optimization of the BF at the source node and the BF at the RS which finally gives the maximum transmission rate. While the joint optimization requires global CSI at all nodes, the schemes with fixed BF either at the source node or at the RS require global CSI at the RS and only local CSI at S1 and S2. In [Her05], the impact of average CSI instead of instantaneous CSI at the RS on the achievable transmission rate is investigated.

In [HZF04a], it is shown how the transmission rate can be determined for non-regenerative one-way relaying in a system with limited capabilities at the RS, cf. the first row and the second column of Figure 1.4. BF is only performed at the source and destination nodes and the received data streams at the RS are retransmitted with an equal weighting factor at all antennas of the RS. The authors in [HZF04a] only give the calculation of the transmission rate, but the BF algorithm which maximizes the transmission rate is not considered. Linear transmit and receive BF algorithms in point-to-point transmissions which minimize the MSE, minimize the MSE under the ZF constraint and maximize the SNR for either source nodes or destination nodes with limited capabilities are considered in [MBQ04, Joh04, JUN05]. Applying these BF algorithms in a system with limited capabilities at the RS is straightforward.

A system setup similar to a system with limited capabilities at S1 and S2, cf. the first row and the third column in Figure 1.4, is addressed in [BW05, OP06, EBW07]. In these works, BF is exclusively performed by multiple single-antenna RSs by jointly adapting the phases and amplitudes of the weighting factors at each single-antenna RS assuming availability of global CSI at the RSs. Since the antennas at the RSs are not co-located, they cannot exchange the currently received data streams. Thus, only an adaptation of the BF to the CSI but not to the currently received data streams is possible.

Just recently, two-way relaying with multiple-antenna nodes has attracted attention. Thus, there exist only few works on this topic and a detailed classification of these works according to the framework of Figure 1.4 is only possible in parts.

While this thesis considers multiple antennas at all nodes, [LZ08] assumes single antennas at S1 and S2 and multiple antennas only at the RS in non-regenerative two-way relaying. For single-antenna source and destination nodes, the maximization of the sum rate by exclusive BF at the RS and applying CDI at the destination nodes is considered in [LZ08]. The problem corresponds to a system with full capabilities, cf. second row and first column of Figure 1.4, as well as to a system with local CSI at S1 and S2, cf. second row and fourth column in Figure 1.4, since single-antenna source and

destination nodes can only apply equal weighting in the system with full capabilities, too. The proposed sub-optimum BF algorithm by [LZ08] based on a matched filter approach [Pro01] for the sum rate maximization works well in systems with similar link qualities for the transmissions from S1 to the RS and from S2 to the RS, respectively. However, for different link qualities the performance of this algorithm degrades.

Maximizing the sum rate for a system with full capabilities in regenerative multiple-antenna two-way relaying is addressed in [HKE⁺07]. The sum rates for two different precoding schemes exploiting global CSI at the RS are analyzed. In the first precoding scheme, the sum of individually precoded data streams for each direction of transmission is retransmitted by the RS. In the second precoding scheme, the bit-wise XOR of the data streams of each direction of transmission is retransmitted. The rate regions of regenerative two-way relaying using multiple-antenna nodes are derived in [WOB08]. In [VH07], it is shown how the sum rate in regenerative MIMO two-way relaying scales with the number of antennas at the RS and with the number of RSs. For large networks with multiple RSs between the source node and the destination node, the achievable sum rate scales linearly with the number of antennas at the RS and logarithmically with the number of RSs. Recently, the multiple access problem in regenerative multiple-antenna two-way relaying has been addressed in [EW08]. The sum rate maximization problem in a cellular scenario with a single base station, a single RS, and multiple mobile nodes is solved by an iterative algorithm based on semi-definite programming.

1.3 Open problems

In this section, the open problems coming from the comparison of the review of existing literature in Section 1.2 with the framework for systems of different capabilities introduced in Figure 1.4 are summarized:

1. A system model is required which allows to describe one-way and two-way relaying in a common framework. With the system model, it has to be possible to describe several linear optimization problems where the different system capabilities of Figure 1.4 are considered by introducing additional constraints.
2. The maximum sum rates in one-way relaying for all cases of system capabilities need to be determined, cf. first row and first three columns in Figure 1.4. While the BF algorithm which maximizes the sum rate in a system with full capabilities is well-known [HW06], the BF algorithms which maximize the sum rate for the

systems with limited capabilities at the RS and limited capabilities at S1 and S2 have to be derived.

3. In one-way relaying, linear BF algorithms are required for the system with limited capabilities at S1 and S2, cf. first row and third column in Figure 1.4. Typical optimization problems in point-to-point transmissions whose solutions are known to provide reasonable performance need to be adapted to the constraints and requirements of a system with limited capabilities at S1 and S2 in one-way relaying. A formulation of the optimization problems and the BF algorithms solving the problems are required.
4. BF algorithms which maximize the sum rate in non-regenerative two-way relaying are required for all defined cases of system capabilities. Thus, all sum rate maximization problems of the second row in Figure 1.4 need to be formulated and solved. Especially, the sub-optimum BF algorithm at the RS for the sum rate maximization in case of single-antenna source and destination nodes introduced in [LZ08] has to be improved in order to support systems with different link qualities of the transmissions from S1 to the RS and from S2 to the RS, respectively.
5. In two-way relaying, linear BF algorithms are required for the systems with limited capabilities at S1 and S2, cf. second row and third column in Figure 1.4. Typical optimization problems in point-to-point transmissions whose solutions are known to provide reasonable performance need to be adapted to the constraints and requirements of a system with limited capabilities at S1 and S2 in two-way relaying. A formulation of the optimization problems and the BF algorithms solving the problems are required.
6. In two-way relaying, linear BF algorithms are required for the systems with local CSI at S1 and S2, cf. second row and fourth column in Figure 1.4. Typical optimization problems in point-to-point transmissions whose solutions are known to provide reasonable performance need to be adapted to the constraints and requirements of a system with local CSI at S1 and S2 in two-way relaying. A formulation of the optimization problems and the BF algorithms solving the problems are required.
7. In order to give a fair comparison between the systems of different capabilities, the required effort for providing CSI to the nodes has to be considered. For that purpose, schemes in order to provide the CSI need to be developed and the resulting effort has to be considered in the determination of the sum rates.

8. The impact of imperfect CSI, e.g., due to noisy channel estimates or outdated estimates, on the considered BF algorithms is an open question which needs to be addressed.
9. Since the multiple access problem has only been addressed for regenerative two-way relaying so far, multiple access for non-regenerative two-way relaying is an open problem which needs to be considered.

1.4 Thesis contributions and overview

This section gives an overview of the thesis by summarizing the main contributions which solve the open problems introduced in Section 1.3.

1. A system model which allows to describe one-way and two-way relaying in a common framework is given in Chapter 2. All optimization problems presented in Figure 1.4 may be described by using this system model. Furthermore, the sum rate is defined in Chapter 2. For the sum rate maximization problems in one-way and two-way relaying, a general formulation of the optimization problems is given in Chapters 3 and 4, respectively. Different system capabilities may be considered by introducing additional constraints to the general formulation.
2. A sub-optimum analytical BF algorithm for maximizing the sum rate in one-way relaying for a system with limited capabilities at the RS is proposed in Chapter 3. For the system with limited capabilities at S1 and S2, a numerical solution to the sum rate maximization problem is given and it is shown how the number of required optimization variables for the numerical solution may be reduced. The sum rate performances of the different system capabilities are compared to each other by means of computer simulations in the same chapter.
3. In Chapter 3, also the typical optimization problems from point-to-point transmissions which describe the minimization of the MSE, the minimization of the MSE under the ZF constraint, and the maximization of the SNR are adapted to the requirements of the system with limited capabilities at S1 and S2 in one-way relaying. The BF algorithms solving these optimization problems are also derived. The sum rate and the bit error rate (BER) performances of the different algorithms are compared to each other by means of computer simulations.
4. For all cases of system capabilities in two-way relaying, the maximum sum rates are determined by numerical methods in Chapter 4. It is shown how the number

of required optimization variables in the numerical solution may be reduced for the system with full capabilities, the system with limited capabilities at S1 and S2 and the system with local CSI at S1 and S2. For the system with limited capabilities at the RS, a sub-optimum analytical BF algorithm is proposed. Furthermore, a sub-optimum analytical BF algorithm at the RS in case of single-antenna source and destination nodes is proposed which outperforms the BF algorithm of [LZ08] if there are different link qualities of the transmissions from S1 to the RS and from S2 to the RS, respectively. The sum rate performances of the different BF algorithms are compared to each other by means of computer simulations in the same chapter.

5. In Chapter 4, also the typical optimization problems from point-to-point transmissions which minimize the MSE, minimize the MSE under the ZF constraint, and maximize SNR are adapted to the requirements of the system with limited capabilities at S1 and S2 in two-way relaying. The BF algorithms solving these optimization problems are also derived. The sum rate and the BER performances of the different algorithms are compared to each other by means of computer simulations.
6. In Chapter 4, also the typical optimization problems from point-to-point transmissions which minimize the MSE, minimize the MSE under the ZF constraint, and maximize SNR are adapted to the requirements of the system with local CSI at S1 and S2 in two-way relaying. The BF algorithms solving these optimization problems are also derived. The sum rate and the BER performances of the different algorithms are compared to each other by means of computer simulations.
7. In Chapter 5, pilot transmission schemes and channel estimation algorithms for PACE are proposed which are used to provide the required CSI for the different cases of system capabilities in two-way relaying. In order to give a fair comparison of the different cases of system capabilities, a measure for considering the effort of PACE in the sum rate is presented.
8. The impact of imperfect CSI on the sum rate performance of the considered BF algorithms is investigated by means of computer simulations in Chapter 5, too.
9. In Chapter 5, also two scenarios with multiple source-destination pairs are introduced exemplarily in order to give a first insight into the problems arising from multiple access in non-regenerative two-way relaying.

Chapter 2

System model

2.1 Introduction

This chapter presents the derivation of a common system model for one-way and two-way relaying. In [HZF04a], a system model for multiple-antenna one-way relaying is given while [RW05] provides a system model for single-antenna two-way relaying. This chapter provides a system model which jointly describes both relaying schemes for multiple-antenna nodes. Furthermore, the system model is applicable to any of the four system capabilities in the introduced framework of Figure 1.4.

In this chapter, the sum rate is introduced as a performance measure for the two relaying schemes in the systems of different capabilities. The determination of the sum rate for the cases allowing adaptive BF at the source and destination nodes, cf. the first two columns in Figure 1.4, is different compared to the determination of the sum rate for the cases only allowing an equal weighting of data streams at the source and destination nodes, cf. the last two columns of Figure 1.4. This chapter presents how the sum rates are determined for adaptive BF and for equal weighting at S1 and S2.

The chapter is organized as follows. Section 2.2 discusses the system assumptions for the system introduced in Figure 1.2. The general system model is given in Section 2.3. The determination of the sum rate is explained in Section 2.4, and the application of the general system model in one-way relaying and two-way relaying is given in Section 2.5.

2.2 System assumptions

Throughout the thesis unless otherwise stated, the system which is introduced in Section 1.1.1 and depicted in Figure 1.2 is considered. There are two multiple-antenna nodes S1 and S2 which establish a bi-directional transmission via a multiple-antenna RS since a point-to-point transmission from S1 to S2 is not possible. In this section, the assumptions for this system are given.

S1 and S2 are equipped with $M^{(1)}$ and $M^{(2)}$ antennas, respectively. From point-to-point transmissions it is known that a source node which is equipped with \tilde{M} antennas

can multiplex \tilde{M} data streams simultaneously if the different radio channels between the antennas are uncorrelated [PNG03]. In order to separate the data streams multiplexed by the source node, the destination node requires at least \tilde{M} antennas, too. Since both nodes, S1 and S2, are source node as well as destination node, the maximum number of multiplexed data streams by a source node is given by the minimum of $M^{(1)}$ and $M^{(2)}$ in general. This characteristic from point-to-point transmissions is also valid for two-hop relaying as long as the number of antennas L at the RS is sufficiently high. How much antennas are needed at the RS in order to multiplex the minimum of $M^{(1)}$ and $M^{(2)}$ data streams depends on the relaying scheme and is considered in Chapters 3 and 4.

In the following, the assumptions regarding the number of antennas, the transmit powers of the nodes, the considered radio channels, the synchronization of the nodes and the considered BF algorithms are presented which are valid throughout the thesis unless otherwise stated.

- For simplicity but without loss of generality, it is assumed that S1 and S2 are equipped with the same number of antennas, i.e., $M^{(1)} = M^{(2)} = M$. Thus, it is ensured that none of the source nodes transmits more data streams than the respective destination node can separate spatially. For $M^{(1)} > M^{(2)}$, a precoding which distributes $M^{(2)}$ data streams over $M^{(1)}$ antennas would be required at S1 and vice versa [PNG03].
- It is assumed that each node has a transmit power constraint. The power values $E^{(1)}$, $E^{(2)}$, and $E^{(0)}$ denote the maximum transmit powers of S1, S2, and the RS, respectively.
- A flat fading channel is assumed. The reason for this assumption is explained in the following. In an orthogonal frequency division multiplexing (OFDM) system [vNP00] which is proposed for 4G wireless communication systems for example, the available bandwidth is divided into a number of orthogonal sub-carriers. If the bandwidth of the sub-carriers is smaller than the channel coherence bandwidth [Pro01], flat fading may be assumed which means that each sub-carrier is such narrow that its transfer function is well approximated by one complex channel fading coefficient in the frequency domain.
- It is assumed that the overall channel resources are divided into small units which are orthogonal in time and frequency and denoted as time-frequency units. A single time-frequency unit corresponds to one time slot as introduced in Figure 1.3 and one sub-carrier. In OFDM for example, the sub-carriers are orthogonal inherently [PNG03]. In a time-dispersive channel, temporal intersymbol interference

is circumvented by introducing a guard interval as a cyclic prefix whose duration is longer than the maximum channel delay [vNP00].

- It is assumed that a source node always transmits M data symbols per time-frequency unit if the time-frequency unit is allocated to the respective source node, i.e., from each transmit antenna of the source node one data symbol is transmitted per sub-carrier and during one time slot. Since the time-frequency units are orthogonal to each other, transmitting NM data symbols within N time-frequency units is straightforward and omitted in this thesis.
- It is assumed that the transfer functions of all considered radio channels are constant during one bi-directional transmission interval, where one bi-directional transmission interval consists of the transmission of M data symbols from S1 to S2 and M data symbols from S2 to S1. This means that the channel coherence time is greater than the time required to transmit M data symbols from S1 to S2 plus the time required to transmit M data symbols from S2 to S1. Considering the time slot allocation of Figure 1.3, the radio channels are constant during at least four time slots in one-way relaying and at least two time slots in two-way relaying.
- Channel reciprocity is assumed which means that the channel fading coefficient for the transmission from an antenna m at node S1 (S2) to an antenna l at the RS equals the channel fading coefficient for the transmission from the same antenna l at the RS to the same antenna m at node S1 (S2) [CLW⁺06]. With the previous assumption of constant radio channels during one bi-directional transmission interval, channel reciprocity is inherently obtained.
- It is assumed that if CSI is available at a node, this CSI corresponds to the instantaneous channel transfer function. Unless otherwise stated, the CSI is error-free which is often referred to as perfect CSI.
- It is assumed that the transmitted OFDM symbols of the nodes are synchronized in time. In an OFDM system, the impact of imperfect time synchronization of the OFDM symbols can be minimized by an appropriate length of the guard interval. The duration of the guard interval has to be greater than the maximum channel delay, and additionally the duration of the guard interval needs to cover the maximum time offset between the transmitter and the receiver. For practical applications, there exist several techniques which enable the required time synchronization [MVBL03].
- It is assumed that the transmitted and received signals at the nodes are frequency synchronous. The frequency shifts between the transmitted signal and the re-

ceived signal, e.g., due to imperfect oscillators [vNP00], can be compensated by frequency synchronization techniques [MVBL03]. Furthermore, the impact of the Doppler spread [vNP00] can be neglected in scenarios with nodes of low mobility and needs to be compensated in scenarios with nodes of higher mobility [EBP00].

- It is assumed that the transmitted and received signals at the co-located antennas of each node are phase synchronous. In practical applications, phase synchronization over co-located transmit and receive antennas, respectively, is inherently achieved due to one central clock at each node [BW08].
- Only linear BF algorithms are assumed in the following. In general, the linear BF algorithms can be outperformed by non-linear BF algorithms, like the Tomlinson-Harashima precoding [Tom71, HM72], at the cost of significantly increased computational complexity [Joh04].

2.3 General system model

In this section, a general system model is developed for the scenario depicted in Figure 1.2 with bi-directional transmission between S1 and S2 via the RS under the assumptions of Section 2.2. The general system model is valid for one-way relaying as well as for two-way relaying.

Figure 2.1 presents the general system model. The upper two blocks on the left-hand side which are framed by the dashed lines denote the receiver and transmitter part of node S1, respectively, while the lower two blocks on the left-hand side denote the receiver and transmitter part of S2, respectively. The single block on the right-hand side which is framed by the dashed lines corresponds to the RS which also consists of a transmitter and a receiver part. The transmitters and receivers are linked via the respective radio channels between them.

Throughout the thesis, the equivalent low-pass frequency domain is considered [Pro01, Kes07]. Signals and radio channels are represented by their complex valued samples in the frequency domain. Each sample is valid for one specific time-frequency unit. Lower case bold face letters and upper case bold face letters denote complex valued vectors and matrices, respectively. Let $[\cdot]^T$, $[\cdot]^*$, $[\cdot]^H$, $E\{\cdot\}$, \mathbf{I}_M , and $\mathbf{0}_{L \times M}$ denote the transpose, the conjugate, the Hermitian, the expectation, an identity matrix of size M , and an all-zero matrix with L rows and M columns.

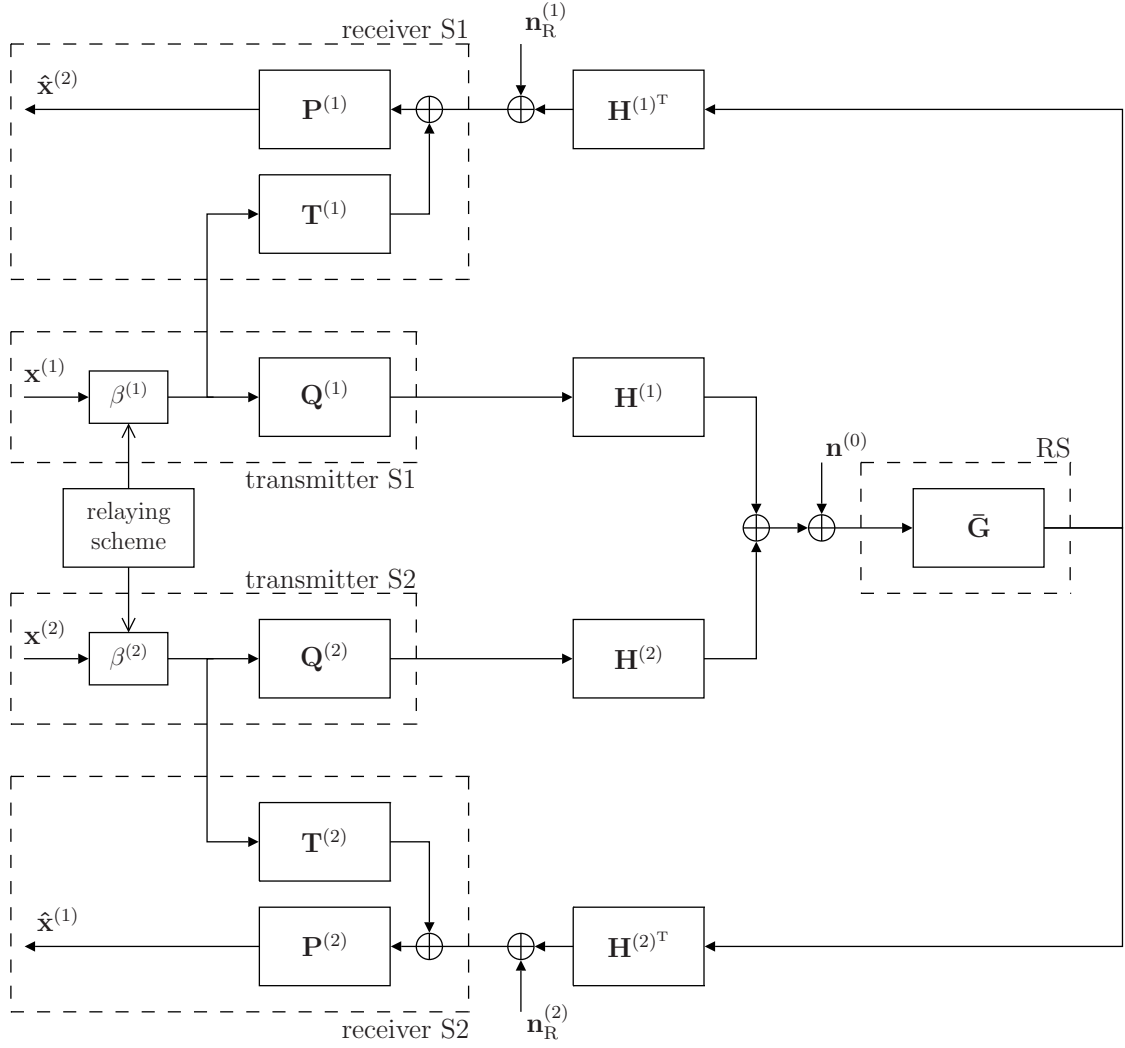


Figure 2.1. General system model valid for one-way and two-way relaying.

Data vector

$$\mathbf{x}^{(i)} = [x_1^{(i)}, \dots, x_M^{(i)}]^T \quad (2.1)$$

consists of the data symbols $x_m^{(i)}$, $m = 1, \dots, M$, and is transmitted from source node S_i to destination node S_k for

$$k = \begin{cases} 1 & \text{if } i = 2, \\ 2 & \text{if } i = 1. \end{cases} \quad (2.2)$$

In the following, index (i) always corresponds to the source node and index (k) which depends on index (i) via Eq. (2.2) corresponds to the respective destination node. Thus, matrices and vectors corresponding to the transmission from source node S_i to the RS are denoted by index (i) , and matrices and vectors corresponding to the transmission from the RS to destination node S_k are denoted by index (k) . The data symbols $x_m^{(i)}$, $m = 1, \dots, M$, are zero-mean, independent, circularly symmetric, complex Gaussian random variables with variance one. Hence, the covariance matrix $\mathbf{R}_{\mathbf{x}^{(i)}}$ of $\mathbf{x}^{(i)}$ results

	$\beta^{(1)}$	$\beta^{(2)}$
one-way relaying: S1 to S2	1	0
one-way relaying: S2 to S1	0	1
two-way relaying	1	1

Table 2.1. The different directions of transmission in one-way and two-way relaying described by the choice of $\beta^{(1)}$ and $\beta^{(2)}$.

in

$$\mathbf{R}_{\mathbf{x}^{(i)}} = \text{E} \left\{ \mathbf{x}^{(i)} \mathbf{x}^{(i)\text{H}} \right\} = \mathbf{I}_M. \quad (2.3)$$

In Figure 2.1, factors $\beta^{(i)} \in \{0, 1\}$, $i = 1, 2$, represent switches which either let pass a signal for $\beta^{(i)} = 1$ or block a signal for $\beta^{(i)} = 0$. By the joint choice of factors $\beta^{(1)}$ and $\beta^{(2)}$ depending on the relaying scheme, one can determine which direction of transmission is considered in the system model of Figure 2.1. The factors $\beta^{(i)}$ are also a representation of the time slot allocation of Figure 1.3. Table 2.1 summarizes how $\beta^{(1)}$ and $\beta^{(2)}$ have to be chosen in order to describe the transmissions in one-way and two-way relaying, respectively. For the transmission from S1 to S2 in one-way relaying, only data vector $\mathbf{x}^{(1)}$ is transmitted by source node S1, i.e., $\beta^{(1)} = 1$ and $\beta^{(2)} = 0$. For the transmission from S2 to S1 in one-way relaying, only data vector $\mathbf{x}^{(2)}$ is transmitted by source node S2, i.e., $\beta^{(1)} = 0$ and $\beta^{(2)} = 1$. In two-way relaying, data vectors $\mathbf{x}^{(1)}$ and $\mathbf{x}^{(2)}$ are transmitted simultaneously, i.e., $\beta^{(1)} = \beta^{(2)} = 1$.

Before the transmission over the radio channel, the data vector $\mathbf{x}^{(i)}$ is spatially precoded which is indicated by the transmit BF matrix $\mathbf{Q}^{(i)} \in \mathbb{C}^{M \times M}$. The transmit BF matrix $\mathbf{Q}^{(i)}$ may be optimized depending on the optimization problems introduced in the framework of Figure 1.4. The radio channel for the transmission from node S_i to the RS is described by the channel matrix

$$\mathbf{H}^{(i)} = \left[\mathbf{h}_1^{(i)}, \mathbf{h}_2^{(i)}, \dots, \mathbf{h}_M^{(i)} \right] \in \mathbb{C}^{L \times M}, \quad (2.4)$$

with channel vectors

$$\mathbf{h}_m^{(i)} = \left[h_{1,m}^{(i)}, h_{2,m}^{(i)}, \dots, h_{L,m}^{(i)} \right]^T, \quad m = 1, 2, \dots, M, \quad (2.5)$$

where $h_{l,m}^{(i)}$ for $l = 1, \dots, L$ and $m = 1, \dots, M$ are complex fading coefficients describing the fading channel between transmit antenna m and receive antenna l . The noise at the receive antennas of the RS is assumed as additive white Gaussian noise (AWGN) and described by vector $\mathbf{n}^{(0)} \in \mathbb{C}^{L \times 1}$ where the elements of $\mathbf{n}^{(0)}$ are zero-mean, independent, circularly symmetric, complex Gaussian random variables with variance $\sigma_{\mathbf{n}^{(0)}}^2$ yielding the noise covariance matrix

$$\mathbf{R}_{\mathbf{n}^{(0)}} = \text{E} \left\{ \mathbf{n}^{(0)} \mathbf{n}^{(0)\text{H}} \right\} = \sigma_{\mathbf{n}^{(0)}}^2 \mathbf{I}_L. \quad (2.6)$$

The received data streams at the RS are sums of all data streams transmitted simultaneously by the source nodes over the respective radio channels plus the AWGN at the RS. Before the retransmission, the received data streams are filtered by a linear BF matrix $\bar{\mathbf{G}} \in \mathbb{C}^{L \times L}$. The BF matrix $\bar{\mathbf{G}}$ at the RS depends on the relaying scheme, i.e., it also depends on the choice of the factors $\beta^{(i)}$, $i = 1, 2$. Furthermore, matrix $\bar{\mathbf{G}}$ may be optimized depending on the optimization problems introduced in the framework of Figure 1.4. Due to the assumption of constant radio channels during one bi-directional transmission interval and due to the assumption of channel reciprocity, the channel matrix for the transmission from the RS to node Sk is given by $\mathbf{H}^{(k)\text{T}}$. At the receive antennas of Sk , AWGN with variance $\sigma_{\mathbf{n}_R}^2$ is assumed which is described by the noise vector $\mathbf{n}_R^{(k)} \in \mathbb{C}^{M \times 1}$ with noise covariance matrix

$$\mathbf{R}_{\mathbf{n}_R^{(k)}} = \text{E} \left\{ \mathbf{n}_R^{(k)} \mathbf{n}_R^{(k)\text{H}} \right\} = \sigma_{\mathbf{n}_R^{(k)}}^2 \mathbf{I}_M. \quad (2.7)$$

Let $\text{diag}_b[\mathbf{Z}_1, \mathbf{Z}_2, \dots, \mathbf{Z}_N]$ denote a block diagonal matrix given by

$$\text{diag}_b[\mathbf{Z}_1, \mathbf{Z}_2, \dots, \mathbf{Z}_N] = \begin{bmatrix} \mathbf{Z}_1 & \mathbf{0} & \mathbf{0} & \cdots & \mathbf{0} \\ \mathbf{0} & \mathbf{Z}_2 & \mathbf{0} & \cdots & \mathbf{0} \\ \mathbf{0} & \mathbf{0} & \ddots & \mathbf{0} & \vdots \\ \vdots & \vdots & \mathbf{0} & \mathbf{Z}_{N-1} & \mathbf{0} \\ \mathbf{0} & \mathbf{0} & \cdots & \mathbf{0} & \mathbf{Z}_N \end{bmatrix},$$

where the all-zero matrices $\mathbf{0}$ have to be adapted to the sizes of the arbitrarily sized complex matrices \mathbf{Z}_n , $n = 1, \dots, N$. Furthermore, let $\text{diag}[\cdot]$ denote a diagonal matrix consisting of the main diagonal matrix elements if the argument is a matrix, and consisting of the vector elements if the argument is a vector. The noise at the RS and the noise at the destination node Sk , which are mutually independent, are concatenated to the overall noise vector

$$\mathbf{n}^{(k)} = \left[\mathbf{n}^{(0)\text{T}}, \mathbf{n}_R^{(k)\text{T}} \right]^{\text{T}} \in \mathbb{C}^{(M+L) \times 1}, \quad (2.8)$$

with the overall noise covariance matrix

$$\mathbf{R}_{\mathbf{n}^{(k)}} = \text{diag}_b \left[\sigma_{\mathbf{n}^{(0)}}^2 \mathbf{I}_L, \sigma_{\mathbf{n}_R^{(k)}}^2 \mathbf{I}_M \right]. \quad (2.9)$$

In order to describe the output of the receiver Sk , the following matrices are required. Matrix $\mathbf{T}^{(k)} \in \mathbb{C}^{M \times M}$ is introduced in order to describe the application of CDI at the destination node Sk . The receive BF matrix $\mathbf{P}^{(k)} \in \mathbb{C}^{M \times M}$ is applied after the application of CDI. The CDI matrix $\mathbf{T}^{(k)}$ and the receive BF matrix $\mathbf{P}^{(k)}$ at the receiver in Figure 2.1 depend on the relaying scheme and may be optimized depending on the

optimization problems introduced in Figure 1.4. Furthermore, matrices

$$\mathbf{A}^{(k)} = \text{diag} \left[\mathbf{H}^{(k)\text{T}} \bar{\mathbf{G}} \mathbf{H}^{(i)} \mathbf{Q}^{(i)} \right] \in \mathbb{C}^{M \times M}, \quad (2.10a)$$

$$\mathbf{F}^{(k)} = \mathbf{H}^{(k)\text{T}} \bar{\mathbf{G}} \mathbf{H}^{(i)} \mathbf{Q}^{(i)} - \mathbf{A}^{(k)} \in \mathbb{C}^{M \times M}, \quad (2.10b)$$

$$\mathbf{D}^{(k)} = \mathbf{H}^{(k)\text{T}} \bar{\mathbf{G}} \mathbf{H}^{(k)} \mathbf{Q}^{(k)} + \mathbf{T}^{(k)} \in \mathbb{C}^{M \times M}, \quad (2.10c)$$

$$\mathbf{B}^{(k)} = \left[\mathbf{H}^{(k)\text{T}} \bar{\mathbf{G}}, \mathbf{I}_M \right] \in \mathbb{C}^{M \times (M+L)}, \quad (2.10d)$$

are linked with the desired data vector $\mathbf{x}^{(i)}$, with the intersymbol interference between the data symbols of the data symbol vector $\mathbf{x}^{(i)}$, with the duplex interference vector containing the interference caused by the data vector $\mathbf{x}^{(k)}$, and with the overall noise vector $\mathbf{n}^{(k)}$, respectively. Using these definitions, the estimate $\hat{\mathbf{x}}^{(i)}$ of data vector $\mathbf{x}^{(i)}$ at the output of receiver Sk is given by

$$\hat{\mathbf{x}}^{(i)} = \mathbf{P}^{(k)} \left((\mathbf{A}^{(k)} + \mathbf{F}^{(k)}) \mathbf{x}^{(i)} + \mathbf{D}^{(k)} \mathbf{x}^{(k)} + \mathbf{B}^{(k)} \mathbf{n}^{(k)} \right). \quad (2.11)$$

2.4 Sum rate definition

In the following, the sum rate of the system in Figure 1.2 is defined. The sum rate is a measure how much information can be exchanged between S1 and S2 per time-frequency unit in the bi-directional scenario of Figure 1.2. It depends on the time slot allocation of the relaying scheme depicted in Figure 1.3 and on the system capabilities defined in the framework of Figure 1.4.

Regarding the time slot allocation, one-way relaying and two-way relaying require a different overall number S of time slots for one bi-directional transmission interval. This fact is considered by the sum rate normalization factor r which is defined as

$$r = \frac{1}{S}. \quad (2.12)$$

In [HZF04a], the transmission rate of a non-regenerative MIMO two-hop relaying system is considered. In order to determine the transmission rate with the approach from [HZF04a], one needs to identify the useful signals at the destination node and the disturbances at the destination node consisting of AWGN and interferences. With the general system model for one-way and two-way relaying in Eq. (2.11), it possible to determine the useful signals and the disturbances.

Regarding the system capabilities, two cases have to be distinguished in order to determine the sum rate. Firstly, for the system with full capabilities and the system

with limited capabilities at the RS which correspond to the first and second column in Figure 1.4, respectively, adaptive BF can be applied at S1 and S2 since both nodes have full SP capabilities. Secondly, for the system with limited capabilities at S1 and S2 and the system with local CSI at S1 and S2 which correspond to the third and fourth column in Figure 1.4, respectively, only equal weighting of the data streams can be applied at S1 and S2 since both nodes have only limited SP capabilities and limited CSI. In the following, the sum rate is firstly determined for adaptive BF at S1 and S2, and secondly for equal weighting of the data streams at S1 and S2.

In case of adaptive BF at S1 and S2, beside the useful signal indicated by matrix $\mathbf{P}^{(k)}\mathbf{A}^{(k)}$ in Eq. (2.11) the intersymbol interference represented by matrix $\mathbf{P}^{(k)}\mathbf{F}^{(k)}$ can also be exploited by applying joint decoding at destination node Sk [Mue01]. Thus, the overall matrix linked with useful signal vector $\mathbf{x}^{(i)}$ is given by

$$\mathbf{P}^{(k)}\tilde{\mathbf{A}}^{(k)} = \mathbf{P}^{(k)}(\mathbf{A}^{(k)} + \mathbf{F}^{(k)}). \quad (2.13)$$

The disturbances at the destination node Sk consist of the duplex interference represented by matrix $\mathbf{P}^{(k)}\mathbf{D}^{(k)}$ and the AWGN represented by matrix $\mathbf{P}^{(k)}\mathbf{B}^{(k)}$. Thus, using adaptive BF at S1 and S2 in the system described by Eq. (2.11), yields the following transmission rate for the uni-directional transmission from node Si to node Sk :

$$C_{\text{BF}}^{(k)} = \log_2 \left(\det \left[\mathbf{I}_M + \left(\tilde{\mathbf{A}}^{(k)}\mathbf{R}_{\mathbf{x}^{(i)}}\tilde{\mathbf{A}}^{(k)\text{H}} \right) \left(\mathbf{D}^{(k)}\mathbf{R}_{\mathbf{x}^{(k)}}\mathbf{D}^{(k)\text{H}} + \mathbf{B}^{(k)}\mathbf{R}_{\mathbf{n}^{(k)}}\mathbf{B}^{(k)\text{H}} \right)^{-1} \right] \right), \quad (2.14)$$

[HZF04a], where $\log_2(\cdot)$ and $\det[\cdot]$ denote the logarithm to the base 2 and the determinant, respectively. Note that the receive BF matrix $\mathbf{P}^{(k)}$ is not included in Eq. (2.14) since the useful signal part corresponding to the term $\tilde{\mathbf{A}}^{(k)}\mathbf{R}_{\mathbf{x}^{(i)}}\tilde{\mathbf{A}}^{(k)\text{H}}$ and the overall disturbances corresponding to the term $\mathbf{D}^{(k)}\mathbf{R}_{\mathbf{x}^{(k)}}\mathbf{D}^{(k)\text{H}} + \mathbf{B}^{(k)}\mathbf{R}_{\mathbf{n}^{(k)}}\mathbf{B}^{(k)\text{H}}$ are both filtered by the same BF matrix $\mathbf{P}^{(k)}$. Thus, matrix $\mathbf{P}^{(k)}$ does not change the determinant in Eq. (2.14). With the transmission rate $C_{\text{BF}}^{(k)}$ of Eq. (2.14), the sum rate in case of adaptive BF at S1 and S2 for one-way as well as for two-way relaying results in

$$C_{\text{BF}}^{(\text{sum})} = r \left(C_{\text{BF}}^{(1)} + C_{\text{BF}}^{(2)} \right). \quad (2.15)$$

In Eq. (2.15), the sum rate normalization factor r of Eq. (2.12) is included as a pre-factor.

If equal weighting of the data streams is applied at S1 and S2, the precoding matrix $\mathbf{Q}^{(i)}$ at source node Si is represented by one scalar weighting factor $q^{(i)}$ assuming that the transmit power $E^{(i)}$ of Si is equally distributed between all transmit antennas since no CSI is available at Si and since Si has only limited capabilities, i.e., $\mathbf{Q}^{(i)} = q^{(i)}\mathbf{I}_M$ with $q^{(i)} = \sqrt{E^{(i)}/M}$. Furthermore, the receive BF matrix at destination node Sk is

represented by one scalar weighting factor $p^{(k)}$, i.e., $\mathbf{P}^{(k)} = p^{(k)}\mathbf{I}_M$. As the useful signal and the disturbances are both multiplied with the scalar receive filter $p^{(k)}$, the filter is omitted in the following derivation of the sum rate in case of equal weighting.

Although the receive nodes do not have global CSI in case of equal weighting, the channel decoders of the destination nodes have to be provided with the overall channel $q^{(i)}\mathbf{H}^{(k)\text{T}}\bar{\mathbf{G}}\mathbf{H}^{(i)}$. This problem can only be circumvented if the channel decoders may assume a pre-defined overall channel, e.g., $q^{(i)}\mathbf{H}^{(k)\text{T}}\bar{\mathbf{G}}\mathbf{H}^{(i)} = \mathbf{I}$. In this case, the BF matrix $\bar{\mathbf{G}}$ at the RS has to ensure that this pre-defined overall channel is achieved. This assumption is valid for all proposed analytical BF algorithms of this thesis.

If equal weighting of the data streams is applied at S1 and S2, it is defined that the m -th transmit antenna of the source node S_i and the m -th receive antenna of the destination node S_k form a transmit-receive antenna pair. This means that the data stream transmitted by the m -th transmit antenna of the source node S_i is dedicated to the m -th receive antenna of the destination node S_k . Pairing the m -th transmit antenna with the m -th receive antenna is reasonable, since no global CSI is available at the source and destination nodes. Of course, if CSI was available at S1 and S2 the pairing of the transmit and receive antennas could be optimized. The transmission rate of the data stream of each transmit-receive antenna pair can be treated independently from the other transmission rates. In order to determine the transmission rate of each single data stream, the signal-to-noise-plus-interference ratio (SINR) of each data stream at the corresponding receive antenna of destination node S_k is required.

The SINR gives the ratio between the useful power and the sum power of all disturbances consisting of interference and noise. The required powers are derived in the following. For each antenna at the destination node, only one data stream is desired. The power of the desired data stream at the m -th antenna of node S_k is given by

$$A_m^{(k)} = q^{(i)^2} \mathbf{h}_m^{(k)\text{T}} \bar{\mathbf{G}} \mathbf{h}_m^{(i)} \mathbf{h}_m^{(i)\text{H}} \bar{\mathbf{G}}^{\text{H}} \mathbf{h}_m^{(k)*}, \quad (2.16)$$

which corresponds to the average power of the m -th row of the vector $\mathbf{A}^{(k)}\mathbf{x}^{(i)}$ in Eq. (2.11). In contrast to the case of adaptive BF at S1 and S2, intersymbol interference power coming from the sum of the $M - 1$ interfering data streams dedicated to the $M - 1$ other antennas of S_k has to be considered as a part of the disturbances in case of equal weighting of the data streams at S1 and S2. The intersymbol interference power is given by

$$F_m^{(k)} = q^{(i)^2} \mathbf{h}_m^{(k)\text{T}} \bar{\mathbf{G}} \left(\sum_{\substack{l=1, \\ l \neq m}}^M \mathbf{h}_l^{(i)} \mathbf{h}_l^{(i)\text{H}} \right) \bar{\mathbf{G}}^{\text{H}} \mathbf{h}_m^{(k)*}, \quad (2.17)$$

which corresponds to the average power of the m -th row of the vector $\mathbf{F}^{(k)}\mathbf{x}^{(i)}$ in Eq. (2.11). Furthermore, the duplex interference power coming from the M transmitted data streams of S_k dedicated to S_i has to be considered. Let $\mathbf{t}_m^{(k)\text{T}}$ denote the m -th row of CDI matrix $\mathbf{T}^{(k)}$. Then, the duplex interference power is given by

$$D_m^{(k)} = \left(q^{(k)} \mathbf{h}_m^{(k)\text{T}} \bar{\mathbf{G}} \mathbf{H}^{(k)} - \mathbf{t}_m^{(k)\text{T}} \right) \left(q^{(k)} \mathbf{h}_m^{(k)\text{T}} \bar{\mathbf{G}} \mathbf{H}^{(k)} - \mathbf{t}_m^{(k)\text{T}} \right)^{\text{H}}. \quad (2.18)$$

The duplex interference power $D_m^{(k)}$ corresponds to the average power of the m -th row of vector $\mathbf{D}^{(k)}\mathbf{x}^{(k)}$ in Eq. (2.11). Finally, the overall noise power has to be considered which is given by

$$B_m^{(k)} = \left(\sigma_{\mathbf{n}^{(0)}}^2 \mathbf{h}_m^{(k)\text{T}} \bar{\mathbf{G}} \bar{\mathbf{G}}^{\text{H}} \mathbf{h}_m^{(k)*} + \sigma_{\mathbf{n}_{\text{R}}^{(k)}}^2 \right), \quad (2.19)$$

which corresponds to the average power of the m -th row in vector $\mathbf{B}^{(k)}\mathbf{n}^{(k)}$ of Eq. (2.11). With these powers, the SINR at the m -th receive antenna of destination node S_k results in

$$\text{SINR}_m^{(k)} = \frac{A_m^{(k)}}{F_m^{(k)} + D_m^{(k)} + B_m^{(k)}}. \quad (2.20)$$

The transmission rate for the transmission from source node S_i to destination node S_k is the sum of the independent transmission rates of each transmit-receive antenna pair given by

$$C_{\text{EW}}^{(k)} = \sum_{m=1}^M \log_2 \left(1 + \text{SINR}_m^{(k)} \right). \quad (2.21)$$

With the transmission rate of Eq. (2.21), the sum rate in case of equal weighting of the data streams at S_1 and S_2 in one-way and two-way relaying results in

$$C_{\text{EW}}^{(\text{sum})} = r \left(C_{\text{EW}}^{(1)} + C_{\text{EW}}^{(2)} \right), \quad (2.22)$$

with the sum rate normalization factor r as introduced in Eq. (2.12).

2.5 Application of the general system model to particular relaying schemes

2.5.1 One-way relaying

In this section, the general system model of Section 2.3 is applied to the one-way relaying scheme. The BF matrix $\bar{\mathbf{G}}$ can be individually adapted for both transmissions from S_i to S_k , for $i = 1, 2$. Hence, BF matrix $\bar{\mathbf{G}}$ at the RS depends on the choice of the

factors $\beta^{(i)}$. The following denotation is made in order to distinguish both directions of the transmission:

$$\bar{\mathbf{G}} = \begin{cases} \mathbf{G}^{(2,1)} & \text{for } \beta^{(1)} = 1, \beta^{(2)} = 0, \\ \mathbf{G}^{(1,2)} & \text{for } \beta^{(1)} = 0, \beta^{(2)} = 1. \end{cases} \quad (2.23)$$

In Eq. (2.23), BF matrix $\mathbf{G}^{(2,1)}$ corresponds to the transmission from S1 to S2 and BF matrix $\mathbf{G}^{(1,2)}$ corresponds to the transmission from S2 to S1.

In one-way relaying, S1 and S2 do not transmit simultaneously which means that there exists no duplex interference from $\mathbf{x}^{(k)}$ at Sk due the orthogonal transmission in time domain. Hence, no gains can be achieved by knowing $\mathbf{x}^{(k)}$ at Sk and CDI matrix $\mathbf{T}^{(k)}$ is set to zero yielding

$$\mathbf{T}^{(k)} = \mathbf{D}^{(k)} = \mathbf{0}_{M \times M}. \quad (2.24)$$

From the time slot allocation for the one-way relaying scheme as depicted in the upper part of Figure 1.3, it can be seen that each source node transmits one data symbol vector during $S = 4$ orthogonal time slots. Hence, the sum rate normalization factor of Eq. (2.12) results in

$$r_{\text{ow}} = \frac{1}{4}. \quad (2.25)$$

2.5.2 Two-way relaying

In this section, the general system model of Section 2.3 is applied to the two-way relaying scheme. BF matrix $\bar{\mathbf{G}}$ can only be adapted to the sum of both transmitted signals. Hence, BF matrix $\bar{\mathbf{G}}$ is valid for both directions of the transmission, namely from S1 to S2 and from S2 to S1, and is denoted by

$$\bar{\mathbf{G}} = \mathbf{G} \quad \text{for } \beta^{(1)} = \beta^{(2)} = 1, \quad (2.26)$$

in the following.

In contrast to one-way relaying, S1 and S2 transmit simultaneously in two-way relaying. For that reason, duplex interference from $\mathbf{x}^{(k)}$ may appear at Sk . Depending on the considered system capabilities of the framework in Figure 1.4, this duplex interference can either be cancelled by CDI at the destination nodes or not. The application of CDI requires an appropriate choice of CDI matrix $\mathbf{T}^{(k)}$. CDI is applied in the cases of the first, second, and fourth column of Figure 1.4, which yields the following set of equations

$$\mathbf{T}^{(k)} = -\mathbf{H}^{(k)\text{T}} \mathbf{G} \mathbf{H}^{(k)} \mathbf{Q}^{(k)}, \quad (2.27)$$

$$\mathbf{D}^{(k)} = \mathbf{0}_{M \times M}. \quad (2.28)$$

If CDI cannot be applied at the destination nodes, which corresponds to the case in the third column of Figure 1.4, the following set of equations is applied:

$$\mathbf{T}^{(k)} = \mathbf{0}_{M \times M}, \quad (2.29)$$

$$\mathbf{D}^{(k)} = \mathbf{H}^{(k)\text{T}} \mathbf{G} \mathbf{H}^{(k)} \mathbf{Q}^{(k)}. \quad (2.30)$$

From the time slot allocation for the two-way relaying scheme as depicted in the lower part of Figure 1.3, it can be seen that each source node transmits one data symbol vector during $S = 2$ orthogonal time slots. Hence, the sum rate normalization factor of Eq. (2.12) results in

$$r_{\text{TW}} = \frac{1}{2}. \quad (2.31)$$

Chapter 3

One-way relaying

3.1 Introduction

In this chapter, all optimization problems in one-way relaying introduced in the first row of the matrix organization in Figure 1.4 are considered. Firstly, the optimization problems are formulated, and secondly, the respective BF algorithms which solve the problems are derived.

For one-way relaying, three systems of different capabilities are considered, namely the system with full capabilities, the system with limited capabilities at the RS, and the system with limited capabilities at S1 and S2. For all three systems which correspond to the first three columns in Figure 1.4, the maximization of the sum rate is considered in Section 3.2. Among those three, the system with full capabilities achieves the highest sum rate since all nodes have full SP capabilities and global CSI is provided to all nodes. Thus, all nodes may perform adaptive BF. In the system with limited capabilities at the RS, the RS cannot perform adaptive BF and in the system with limited capabilities at S1 and S2, the source and destination nodes cannot perform adaptive BF. The limited capabilities in both systems correspond to additional constraints in the sum rate maximization problems. These constraints are defined in Section 3.2 and included into the optimization problems.

Depending on the considered system capabilities, the optimum BF algorithms can be described analytically or only numerical solutions are available. For the system with full capabilities, an analytical BF algorithm in order to maximize the sum rate is presented. However, for the system with limited capabilities at the RS and the system with limited capabilities at S1 and S2, only numerical solutions to the sum rate maximization problem can be given. Since numerical methods require high computational effort, analytical solutions are desired which may even provide a sub-optimum performance if the computational effort is reduced significantly. Thus, for the system with limited capabilities at the RS a sub-optimum analytical BF algorithm in order to maximize the sum rate is derived. For the system with limited capabilities at S1 and S2, further optimization problems whose solutions are known to provide reasonable performance in point-to-point transmissions are newly formulated for one-way relaying in Section 3.3, and the corresponding BF algorithms are derived. These optimization

problems can also be formulated for the system with limited capabilities at the RS. Since the problems can be solved by straightforward adaptations of transmit and receive BF algorithms known from point-to-point transmissions [MBQ04, Joh04, JUN05], they are omitted for the system with limited capabilities at the RS in this thesis.

The performances of the proposed BF algorithms are investigated in Section 3.4 and the main conclusions of this chapter are drawn in Section 3.5.

3.2 Maximization of the sum rate

3.2.1 General problem formulation

In this Section 3.2, the maximization of the sum rate for the three different cases of system capabilities in one-way relaying is considered, which corresponds to the sum rate maximization problems in the first three columns of the first row in the matrix organization of Figure 1.4.

The sum rates defined in Section 2.4 can be maximized by adapting the BF matrices $\mathbf{Q}^{(i)}$ and $\mathbf{G}^{(k,i)}$ at the source node S_i and at the RS, respectively, introduced in Figure 2.1. From the sum rate definitions in Section 2.4, it is known that the sum rate is always independent of the receive BF matrix $\mathbf{P}^{(k)}$. Thus, $\mathbf{P}^{(k)}$ can be omitted in the sum rate maximization problems. Due to the orthogonality between the transmissions from S_1 to S_2 and from S_2 to S_1 in one-way relaying, transmission rate $C^{(2)}$ is independent of transmission rate $C^{(1)}$. In this case, the sum rate is maximized if each transmission rate is maximized individually, and the BF matrices $\mathbf{G}^{(2,1)}$ and $\mathbf{Q}^{(1)}$ can be designed independently of $\mathbf{G}^{(1,2)}$ and $\mathbf{Q}^{(2)}$.

Based on the aforementioned assumptions, a general sum rate maximization problem with transmit power constraints is formulated which can be adapted to each case of system capabilities by introducing additional constraints to the problem and by using the respective sum rate of Section 2.4, i.e., either Eq. (2.15) for adaptive BF at S_1 and S_2 or Eq. (2.22) for equal weighting at S_1 and S_2 . Let $\arg \max_{\{a\}} b$ return the value of a which maximizes b and let $\text{tr}\{\cdot\}$ denote the trace of a matrix. The general sum rate maximization problem consists of two independent transmission rate maximization problems where each of the problems with $i = 1, 2$ and k according to Eq. (2.2)

may be formulated in the following way:

$$\left\{ \mathbf{G}_{\text{opt}}^{(k,i)}, \mathbf{Q}_{\text{opt}}^{(i)} \right\} = \arg \max_{\left\{ \mathbf{G}^{(k,i)}, \mathbf{Q}^{(i)} \right\}} C^{(k)}, \quad (3.1a)$$

$$\text{subject to: } \text{tr} \left\{ \mathbf{Q}^{(i)} \mathbf{R}_{\mathbf{x}^{(i)}} \mathbf{Q}^{(i)\text{H}} \right\} = E^{(i)}, \quad (3.1b)$$

$$\text{tr} \left\{ \mathbf{G}^{(k,i)} \left(\mathbf{H}^{(i)} \mathbf{Q}^{(i)} \mathbf{R}_{\mathbf{x}^{(i)}} \mathbf{Q}^{(i)\text{H}} \mathbf{H}^{(i)\text{H}} + \mathbf{R}_{\mathbf{n}^{(0)}} \right) \mathbf{G}^{(k,i)\text{H}} \right\} = E^{(0)}. \quad (3.1c)$$

Eq. (3.1b) corresponds to the transmit power constraint at the source node S_i and Eq. (3.1c) corresponds to the transmit power constraint at the RS.

3.2.2 System with full capabilities

In this section, the BF algorithm for the maximization of the transmission rate in problem (3.1) is given for a system with full capabilities. The problem corresponds to the optimization problem in the first row and the first column of Figure 1.4. Note that the maximization of the transmission rate in a system with full capabilities is completely described by the problem formulation (3.1) without any additional constraint. The BF matrices $\mathbf{Q}^{(i)}$ and $\mathbf{G}^{(k,i)}$ of Figure 2.1 which provide the maximum transmission rate in one-way relaying with full capabilities at S_1 , S_2 , and the RS have already been derived in [HW06]. In [HW06], three different algorithms are proposed. The first BF algorithm determines the optimum BF matrix at the RS for a fixed BF matrix at the source node. The second BF algorithm determines the optimum BF matrix at the source node for a fixed BF matrix at the RS. This second BF algorithm works according to the same principles as the first BF algorithm. The third BF algorithm jointly optimizes the BF matrix at the source node and the BF matrix at the RS by alternating between the solutions of the first and the second BF algorithm. While the third BF algorithm providing the optimum solution requires global CSI at all nodes, the first and second scheme require global CSI at the RS and only local CSI at S_1 and S_2 . In [HW06], it is shown that the first and second BF algorithm come very close to the optimum solution of the third BF algorithm requiring significantly less computational effort than the third BF algorithm. Since the basic idea behind all three BF algorithms is the same, only the first BF algorithm is presented in this section. It is used to give some insight into the differences between maximizing the sum rate in one-way relaying and maximizing the sum rate in two-way relaying which is regarded in Chapter 4.

Since there are no capability constraints, all nodes are provided with CSI and may perform adaptive BF in order to maximize the transmission rates at S_1 and S_2 given

by Eq. (2.14). In order to determine the optimum BF matrix at the RS for a fixed BF matrix at the source node S_i , the spatial sub-channels, which correspond to the eigenmodes of the channels between source node and destination node, need to be orthogonalized [Ham06]. In the following, it is assumed that the rank of the channel is given by M which means that there exist M spatial sub-channels if all channel coefficients are uncorrelated and $L \geq M$. In order to orthogonalize the M sub-channels, the singular value decomposition (SVD) of the first hop channel $\mathbf{H}^{(i)}$ is required. In the following, the columns of matrix $\mathbf{U}^{(i)} \in \mathbb{C}^{L \times L}$ denote the left eigenvectors of $\mathbf{H}^{(i)}$, the columns of matrix $\mathbf{V}^{(i)} \in \mathbb{C}^{M \times M}$ denote the right eigenvectors of $\mathbf{H}^{(i)}$, and the diagonal matrix

$$\mathbf{\Lambda}^{(i)1/2} = \text{diag} \left[\sqrt{\lambda_1^{(i)}}, \dots, \sqrt{\lambda_M^{(i)}} \right], \quad (3.2)$$

contains the square roots of the eigenvalues $\lambda_m^{(i)}$, $m = 1, \dots, M$, of $\mathbf{H}^{(i)}$. Thus, the SVD of the channel $\mathbf{H}^{(i)}$ is given by

$$\mathbf{H}^{(i)} = \mathbf{U}^{(i)} \begin{bmatrix} \mathbf{\Lambda}^{(i)1/2} \\ \mathbf{0}_{(L-M) \times M} \end{bmatrix} \mathbf{V}^{(i)\text{H}}. \quad (3.3)$$

Due to the assumed channel reciprocity, the SVD of the second hop channel $\mathbf{H}^{(k)\text{T}}$ is given by

$$\mathbf{H}^{(k)\text{T}} = \mathbf{V}^{(k)*} \begin{bmatrix} \mathbf{\Lambda}^{(i)1/2} \\ \mathbf{0}_{M \times (L-M)} \end{bmatrix} \mathbf{U}^{(k)\text{T}}. \quad (3.4)$$

The BF matrix $\mathbf{G}^{(k,i)}$ at the RS which needs to be optimized is separated into three parts [Ham06] given by the receive BF matrix $\mathbf{G}_\text{R}^{(i)}$, the transmit BF matrix $\mathbf{G}_\text{T}^{(k)}$, and the RS power allocation matrix $\mathbf{W}^{(k,i)} = \text{diag} \left[w_1^{(k,i)}, \dots, w_L^{(k,i)} \right]$, with the positive real-valued power allocation factors $w_m^{(k,i)} \in \mathbb{R}^+$, $m = 1, \dots, M$. This separation yields

$$\mathbf{G}^{(k,i)} = \mathbf{G}_\text{T}^{(k)} \mathbf{W}^{(k,i)} \mathbf{G}_\text{R}^{(i)}. \quad (3.5)$$

In [Ham06], it is proposed to use the following BF matrices in order to orthogonalize the spatial sub-channels:

$$\mathbf{Q}^{(i)} = \sqrt{\frac{E^{(i)}}{M}} \mathbf{V}^{(i)}, \quad (3.6a)$$

$$\mathbf{G}_\text{R}^{(i)} = \mathbf{U}^{(i)\text{H}}, \quad (3.6b)$$

$$\mathbf{G}_\text{T}^{(k)} = \mathbf{U}^{(k)*}, \quad (3.6c)$$

$$\mathbf{P}^{(k)} = \mathbf{V}^{(k)\text{T}}. \quad (3.6d)$$

Intuitively, the BF matrices $\mathbf{Q}^{(i)}$ and $\mathbf{G}_\text{R}^{(i)}$ orthogonalize the first hop channel $\mathbf{H}^{(i)}$ by a transmit-side and a receive-side adaptation to the eigenmodes of $\mathbf{H}^{(i)}$. Furthermore, BF matrices $\mathbf{G}_\text{T}^{(k)}$ and $\mathbf{P}^{(k)}$ perform a transmit-side and a receive-side adaptation to

the eigenmodes of the second hop channel $\mathbf{H}^{(k)\text{T}}$. Note that any other BF matrix $\mathbf{P}^{(k)}$, which contains neither an all-zero column vector nor an all-zero row vector, could have been chosen at the destination node Sk in order to maximize the transmission rate which is independent of $\mathbf{P}^{(k)}$. However, only the choice of Eq. (3.6d) orthogonalizes the spatial sub-channels and allows to use a channel decoder which decodes each data stream separately. Otherwise, joint decoding is required at the destination nodes [Mue01]. BF matrix $\mathbf{Q}^{(i)}$ already fulfills the transmit power constraint (3.1b) at the source node Si and is not changed in the following optimization process. Inserting the BF matrices of (3.6) into Eq. (2.14), the transmission rate results in

$$C_{\text{BF}}^{(k)} = \sum_{m=1}^M \log_2 \left(1 + \frac{E^{(i)}}{M} \frac{|w_m^{(k,i)}|^2 \lambda_m^{(i)} \lambda_m^{(k)}}{|w_m^{(k,i)}|^2 \lambda_m^{(k)} \sigma_{\mathbf{n}^{(0)}}^2 + \sigma_{\mathbf{n}_R^{(k)}}^2} \right), \quad (3.7)$$

where $|\cdot|$ denotes the absolute value. Note that the sorting of the eigenvalues in the SVDs of Eqs. (3.3) and (3.4) has to be such that the resulting pairs of eigenmodes of the first and second hop channel provide the highest transmission rate [MVA07]. In order to maximize Eq. (3.7) under the remaining transmit power constraint (3.1c) at the RS, the power allocation factors $|w_m^{(k,i)}|^2$ have to be determined, i.e., instead of optimizing the BF matrix $\mathbf{G}^{(k,i)}$ only the power allocation matrix $\mathbf{W}^{(k,i)}$ needs to be optimized due to the separation of Eq. (3.5). This kind of problem is similar to the famous waterfilling problem in point-to-point transmission [PF05]. The second summand in the logarithm of Eq. (3.7) corresponds to a SNR value. The useful signal power at Sk given in the numerator contains the eigenvalues $\lambda_m^{(i)}$ and $\lambda_m^{(k)}$ of the first and second hop channel, respectively, which are weighted by the power allocation factor $|w_m^{(k,i)}|^2$. The denominator contains the overall noise at the destination node Sk . In contrast to the point-to-point transmission, the noise does not only consist of the receiver noise but also of the noise at the RS which is also weighted by the eigenvalue $\lambda_m^{(k)}$ of the second hop channel and the power allocation factor $|w_m^{(k,i)}|^2$. Thus, the mathematical structure of the rate maximization problem with objective function (3.7) is different and more complicated compared to the waterfilling problem in point-to-point transmission. However, the solution can be determined as follows. Let $\rho^{(k)}$ be defined by

$$\rho^{(k)} = \frac{\sigma_{\mathbf{n}_R^{(k)}}^2}{\sigma_{\mathbf{n}^{(0)}}^2}. \quad (3.8)$$

Furthermore, $(y)^+$ denotes

$$(y)^+ = \begin{cases} y & \text{for } y \geq 0, \\ 0 & \text{for } y < 0. \end{cases} \quad (3.9)$$

Since Eq. (3.7) is concave in $|w_m^{(k,i)}|^2$, the maximum transmission rate $C_{\text{BF}}^{(k)}$ under the RS transmit power constraint (3.1c) can be found by Lagrangian optimization, yielding

$$|w_m^{(k,i)}|^2 = \frac{\left[\sqrt{\left(\rho^{(k)} \frac{E^{(i)} \lambda_m^{(i)}}{2M \lambda_m^{(k)}} \right)^2 + \mu^{(k)} \rho^{(k)} \frac{E^{(i)} \lambda_m^{(i)}}{M \lambda_m^{(k)}} - \rho^{(k)} \frac{E^{(i)} \lambda_m^{(i)}}{2M \lambda_m^{(k)}} - \frac{\sigma_{\mathbf{R}}^2}{\lambda_m^{(k)}}} \right]^+}{\frac{E^{(i)} \lambda_m^{(i)}}{M} + \sigma_{\mathbf{n}(0)}^2}, \quad (3.10)$$

[Ham06]. Similar to the waterfilling problem, the Lagrangian multiplier $\mu^{(k)}$ has to be chosen such that the RS transmit power constraint (3.1c) is satisfied.

3.2.3 System with limited capabilities at the RS

In this section, a BF algorithm for the maximization of the transmission rate in problem (3.1) is proposed for a system with limited capabilities at the RS. The optimization problem can be found in the first row and the second column of Figure 1.4. In a system with limited capabilities at the RS, only S1 and S2 perform BF. Since precoding and joint decoding are possible in this system, the transmission rate is determined by Eq. (2.14). The RS with limited SP capabilities cannot retransmit linear combinations of the received data streams of each receive antenna. Thus, each antenna of the RS retransmits its received data stream which is simply amplified by a positive real-valued weighting factor $g^{(k,i)}$ equal for all antennas. Note that weighting factor $g^{(k,i)}$ could also be complex-valued. But since any phase rotation due to a complex weighting factor at the RS can be compensated at the destination node, weighting factor $g^{(k,i)}$ is restricted to positive real values. Thus, the BF matrix $\mathbf{G}^{(k,i)}$ at the RS simplifies to

$$\mathbf{G}^{(k,i)} = g^{(k,i)} \mathbf{I}_L, \quad g^{(k,i)} \in \mathbb{R}^+. \quad (3.11)$$

With this constraint on the system with limited capabilities at the RS, problem (3.1) may be rewritten as follows:

$$\left\{ g_{\text{opt}}^{(k,i)}, \mathbf{Q}_{\text{opt}}^{(i)} \right\} = \arg \max_{\{g^{(k,i)}, \mathbf{Q}^{(i)}\}} C_{\text{BF}}^{(k)}, \quad (3.12a)$$

$$\text{subject to:} \quad \text{tr} \left\{ \mathbf{Q}^{(i)} \mathbf{R}_{\mathbf{x}^{(i)}} \mathbf{Q}^{(i)\text{H}} \right\} = E^{(i)}, \quad (3.12b)$$

$$\text{tr} \left\{ g^{(k,i)^2} \left(\mathbf{H}^{(i)} \mathbf{Q}^{(i)} \mathbf{R}_{\mathbf{x}^{(i)}} \mathbf{Q}^{(i)\text{H}} \mathbf{H}^{(i)\text{H}} + \mathbf{R}_{\mathbf{n}(0)} \right) \right\} = E^{(0)}. \quad (3.12c)$$

Since the BF matrix $\mathbf{G}^{(k,i)}$ of Eq. (3.11) cannot be adapted to the eigenmodes of the first hop and second hop channels, an orthogonalization of the sub-channels as introduced in Section 3.2.2 is not possible. The weighting factor $g^{(k,i)}$ directly depends

on the BF matrix $\mathbf{Q}^{(i)}$ via the RS transmit power constraint (3.12c) which requires a joint optimization of $\mathbf{Q}^{(i)}$ and $g^{(k,i)}$. In order to solve problem (3.12), numerical methods are required since the problem in its current formulation is neither convex nor concave [BV04]. As the problem may have several minima or maxima, it is difficult to determine if the numerical optimization finds the global or a local optimum. Since numerical methods require high computational effort, analytical solutions are desired which may even provide a sub-optimum performance if the computational effort is reduced significantly.

In the following, a new sub-optimum analytical BF algorithm for the maximization of the sum rate in a system with limited capabilities at the RS is proposed. Since the received signal at the RS is simply amplified by a real-valued weighting factor $g^{(k,i)}$, the overall channel between the source node and the destination node is just a multiplication of the first hop channel $\mathbf{H}^{(i)}$ with the second hop channel $\mathbf{H}^{(k)\text{T}}$ scaled by $g^{(k,i)}$. Except for the retransmission of the noise and the adaptive weighting factor $g^{(k,i)}$ at the RS, the transmission in a system with limited capabilities at the RS corresponds to a point-to-point transmission from the source node to the destination node using the overall channel

$$\mathbf{H}^{(k,i)} = \mathbf{H}^{(k)\text{T}} \mathbf{H}^{(i)}. \quad (3.13)$$

Thus, the well-known BF algorithm which maximizes the transmission rate in point-to-point transmissions [PNG03] is partly adapted to the transmission in a system with limited capabilities at the RS in the following. Let $\mathbf{U}^{(k,i)} \in \mathbb{C}^{M \times M}$ denote the left eigenvectors and $\mathbf{V}^{(k,i)} \in \mathbb{C}^{M \times M}$ denote the right eigenvectors of the overall channel $\mathbf{H}^{(k,i)}$, and let

$$\mathbf{\Lambda}^{(k,i)1/2} = \text{diag} \left[\sqrt{\lambda_1^{(k,i)}}, \sqrt{\lambda_2^{(k,i)}}, \dots, \sqrt{\lambda_M^{(k,i)}} \right], \quad (3.14)$$

contain the square roots of the eigenvalues $\lambda_m^{(k,i)}$, for $m = 1, 2, \dots, M$. Then, the SVD of the overall channel $\mathbf{H}^{(k,i)}$ is given by

$$\mathbf{H}^{(k,i)} = \mathbf{U}^{(k,i)} \mathbf{\Lambda}^{(k,i)1/2} \mathbf{V}^{(k,i)\text{H}}. \quad (3.15)$$

Now, the transmission from S_i to S_k is adapted to the eigenmodes of the overall channel $\mathbf{H}^{(k,i)}$. As known from the point-to-point transmission, a power allocation matrix $\mathbf{S}^{(i)}$ at source node S_i is required in order to distribute the overall transmit power $E^{(i)}$ at S_i with respect to the weights of the eigenmodes of the overall channel $\mathbf{H}^{(k,i)}$. Thus, power allocation matrix $\mathbf{S}^{(i)}$ is defined as

$$\mathbf{S}^{(i)} = \text{diag} \left[s_1^{(i)}, s_2^{(i)}, \dots, s_M^{(i)} \right], \quad (3.16)$$

with the positive real-valued power allocation factors $s_m^{(i)} \in \mathbb{R}^+$, $m = 1, \dots, M$. Furthermore, the BF matrices at S_i and S_k are chosen according to

$$\mathbf{Q}^{(i)} = \mathbf{V}^{(k,i)} \mathbf{S}^{(i)}, \quad (3.17)$$

$$\mathbf{P}^{(k)} = \mathbf{U}^{(k,i)\text{H}}. \quad (3.18)$$

By the choices of Eqs. (3.17) and (3.18), and after calculating the noise covariance matrix $\mathbf{R}_{\tilde{\mathbf{n}}_R^{(k)}}$ at the destination node S_k by

$$\mathbf{R}_{\tilde{\mathbf{n}}_R^{(k)}} = g^{(k,i)^2} \sigma_{\mathbf{n}^{(0)}}^2 \mathbf{U}^{(k,i)\text{H}} \mathbf{H}^{(k)\text{T}} \mathbf{H}^{(k)*} \mathbf{U}^{(k,i)} + \sigma_{\mathbf{n}_R^{(k)}}^2 \mathbf{I}_M, \quad (3.19)$$

the transmission rate of Eq. (2.14) results in

$$C_{\text{BF}}^{(k)} = \log_2 \left(\det \left[\mathbf{I}_M + g^{(k,i)^2} \boldsymbol{\Lambda}^{(k,i)} \mathbf{S}^{(i)^2} \mathbf{R}_{\tilde{\mathbf{n}}_R^{(k)}}^{-1} \right] \right). \quad (3.20)$$

Although the M data streams of source node S_i are orthogonalized by the choices of Eqs. (3.17) and (3.18), the noise at the destination node is no longer spatially white since the noise of the RS is transmitted over the second hop channel $\mathbf{H}^{(k)\text{T}}$. This can be seen from the first summand in the noise covariance matrix $\mathbf{R}_{\tilde{\mathbf{n}}_R^{(k)}}$ in Eq. (3.19). However, in order to provide an approximate analytical solution to the sum rate maximization problem in a system with limited capabilities at the RS, the noise is assumed to be spatially white Gaussian with the average noise power

$$\sigma_{\tilde{\mathbf{n}}_R^{(k)}}^2 = \frac{\text{tr} \left\{ \mathbf{R}_{\tilde{\mathbf{n}}_R^{(k)}} \right\}}{M}, \quad (3.21)$$

per receive antenna. After substituting $\mathbf{R}_{\tilde{\mathbf{n}}_R^{(k)}}$ of Eq. (3.19) by $\sigma_{\tilde{\mathbf{n}}_R^{(k)}}^2 \mathbf{I}_M$ in Eq. (3.20), the following simplified version of optimization problem (3.12) for a system with limited capabilities at the RS is obtained:

$$\{\mathbf{g}_{\text{opt}}^{(k,i)}, s_{m,\text{opt}}^{(i)}\} = \arg \max_{\{\mathbf{g}^{(k,i)}, s_m^{(i)}\}} \sum_{m=1}^M \log_2 \left(1 + \frac{g^{(k,i)^2}}{\sigma_{\tilde{\mathbf{n}}_R^{(k)}}^2} \lambda_m^{(k,i)} s_m^{(i)^2} \right), \quad (3.22a)$$

$$\text{subject to: } \sum_{m=1}^M s_m^{(i)^2} = E^{(i)}, \quad (3.22b)$$

$$g^{(k,i)^2} \text{tr} \left\{ \mathbf{H}^{(i)} \mathbf{V}^{(k,i)} \mathbf{S}^{(i)} \mathbf{S}^{(i)\text{H}} \mathbf{V}^{(k,i)\text{H}} \mathbf{H}^{(i)\text{H}} + \mathbf{R}_{\mathbf{n}^{(0)}} \right\} = E^{(0)}. \quad (3.22c)$$

In problem (3.22), the weighting factor $g^{(k,i)}$ at the RS and the power allocation factors $s_m^{(i)}$ at the source node S_i still have to be optimized jointly. It is proposed to separate the problem into two sub-problems and to solve the two sub-problems alternately which may yield a sub-optimum solution to problem (3.22). Firstly, the sub-problem of

determining $g^{(k,i)}$ for fixed power allocation factors $s_m^{(i)}$ and the corresponding power allocation matrix $\mathbf{S}^{(i)}$ of Eq. (3.16) is solved. By using the constraint (3.22c), $g^{(k,i)}$ is calculated as

$$g^{(k,i)} = \sqrt{\frac{E^{(0)}}{\text{tr} \{ \mathbf{H}^{(i)} \mathbf{V}^{(k,i)} \mathbf{S}^{(i)} \mathbf{S}^{(i)\text{H}} \mathbf{V}^{(k,i)\text{H}} \mathbf{H}^{(i)\text{H}} + \mathbf{R}_{\mathbf{n}^{(0)}} \}}}. \quad (3.23)$$

The initial power allocation factors $s_m^{(i)}$ at S_i are very important because an eigenmode will never be used if zero power is allocated to it initially. For that reason, it is proposed to start with an equal power allocation to the eigenmodes which means that no eigenmode is preferred in the beginning, i.e., $s_m^{(i)2} = \frac{E^{(i)}}{M}$. Secondly, the sub-problem given by (3.22a) and (3.22b) is solved for the fixed weighting factor $g^{(k,i)}$ at the RS which means that the RS power constraint (3.22c) is omitted for the optimization of $s_m^{(i)}$. Since the resulting problem is a typical waterfilling problem, the solution to the power allocation factors $s_m^{(i)2}$ is given by

$$s_m^{(i)2} = \left(\mu^{(i)} - \frac{\sigma_{\mathbf{n}_R}^2}{g^{(k,i)2} \lambda^{(k,i)}} \right)^+, \quad (3.24)$$

[PF05]. The coefficients $s_m^{(i)2}$ and the waterfilling level $\mu^{(i)}$ are found by the well-known iterative waterpouring algorithm [PF05] where $\mu^{(i)}$ is chosen to satisfy the transmit power constraint (3.22b) at S_i . After the power allocation factors $s_m^{(i)}$ and the corresponding power allocation matrix $\mathbf{S}^{(i)}$ have been determined, the weighting factor $g^{(k,i)}$ can be determined by using Eq. (3.23) again. This alternation between the two sub-problems is repeated until the solutions for $s_m^{(i)}$ and $g^{(k,i)}$ do not change more than tolerated by a predefined accuracy. Typically, two to four alternations are required in order to obtain a relative change of $g^{(k,i)}$ which is less than 10^{-4} . Since the optimization result depends on the initial power allocation at S_i , it cannot be guaranteed that the alternation between the calculation of weighting factor $g^{(k,i)}$ and the calculation of the power allocation factors at S_i yields an optimum of the relaxed problem (3.22). Nevertheless, the simulation results show that the performance of the algorithm comes close to the numerical solution to the original optimization problem (3.12).

3.2.4 System with limited capabilities at S1 and S2

In this section, the linear BF for the maximization of the transmission rate in problem (3.1) is considered for a system with limited capabilities at S1 and S2. The optimization problem is mentioned in the first row and the third column of Figure 1.4. In a system with limited capabilities at S1 and S2, no CSI is available at S1 and S2.

The source node Si assigns the same weighting factor $q^{(i)}$ to all transmit antennas and from each transmit antenna one data stream is transmitted. Thus, the BF matrix $\mathbf{Q}^{(i)}$ simplifies to

$$\mathbf{Q}^{(i)} = q^{(i)} \mathbf{I}_M. \quad (3.25)$$

The destination node Sk cannot perform a joint decoding of the incoming data streams since no CSI is available at S1 and S2. The destination node Sk assigns the same weighting factor $p^{(k)}$ to all receive antennas and each antenna receives one dedicated data stream. Thus, the receive BF matrix $\mathbf{P}^{(k)}$ at Sk is simplified to

$$\mathbf{P}^{(k)} = p^{(k)} \mathbf{I}_M. \quad (3.26)$$

Since the scalar value $p^{(k)}$ does not influence the problem of maximizing the transmission rate, it can be chosen arbitrarily except for $p^{(k)} = 0$. The transmission rate for a system with limited capabilities at S1 and S2 is determined with respect to Eq. (2.21). With these constraints on the system with limited capabilities at S1 and S2, problem (3.1) may be rewritten as follows:

$$\left\{ \mathbf{G}_{\text{opt}}^{(k,i)}, q_{\text{opt}}^{(i)} \right\} = \arg \max_{\left\{ \mathbf{G}^{(k,i)}, q^{(i)} \right\}} C_{EW}^{(k)}, \quad (3.27a)$$

$$\text{subject to: } \text{tr} \left\{ q^{(i)2} \mathbf{R}_{\mathbf{x}^{(i)}} \right\} = E^{(i)}, \quad (3.27b)$$

$$\text{tr} \left\{ \mathbf{G}^{(k,i)} \left(q^{(i)2} \mathbf{H}^{(i)} \mathbf{R}_{\mathbf{x}^{(i)}} \mathbf{H}^{(i)\text{H}} + \mathbf{R}_{\mathbf{n}^{(0)}} \right) \mathbf{G}^{(k,i)\text{H}} \right\} = E^{(0)}. \quad (3.27c)$$

In order to satisfy the transmit power constraint (3.27b) at Si , the scalar weighting factor is chosen as follows:

$$q_{\text{opt}}^{(i)} = \sqrt{\frac{E^{(i)}}{M}}, \quad (3.28)$$

which means that the overall transmit power $E^{(i)}$ is equally distributed between all transmit antennas of Si . Hence, the optimum weighting factor $q_{\text{opt}}^{(i)}$ in problem (3.27) is already determined and the transmit power constraint (3.27b) at the source node is satisfied by the choice of $q_{\text{opt}}^{(i)}$ in Eq. (3.28). This means that constraint (3.27b) needs not to be considered in the following.

As in the previous case of Section 3.2.3, the sub-channels of the first and second hop channels cannot be orthogonalized if BF can only be performed either at the receiver-side or the transmitter-side of a link. To the best of the author's knowledge, the optimum BF matrix $\mathbf{G}^{(k,i)}$ which solves problem (3.27) can only be found by numerical methods.

However, the optimization problem (3.27) can be transformed into an equivalent and simpler optimization problem, if the RS is equipped with more antennas than the

source and destination nodes, i.e., for the case $L > M$. In this case, the channel has only M eigenmodes in maximum while $\mathbf{G}^{(k,i)} \in \mathbb{C}^{L \times L}$ could be adapted to L eigenmodes. Hence, there are linear dependencies between the variables in $\mathbf{G}^{(k,i)}$. These linear dependencies may be removed by the following BF approach. Let $\tilde{\mathbf{U}}^{(i)} \in \mathbb{C}^{L \times M}$ contain the first M left eigenvectors corresponding to the range of channel matrix $\mathbf{H}^{(i)}$ and let matrix $\bar{\mathbf{U}}^{(i)} \in \mathbb{C}^{L \times (L-M)}$ contain the last $L - M$ left eigenvectors corresponding to the null space of $\mathbf{H}^{(i)}$. Thus, the SVD of the first hop channel $\mathbf{H}^{(i)}$ of Eq. (3.3) can be modified to

$$\mathbf{H}^{(i)} = \begin{bmatrix} \tilde{\mathbf{U}}^{(i)} & \bar{\mathbf{U}}^{(i)} \end{bmatrix} \begin{bmatrix} \mathbf{\Lambda}^{(i)1/2} \\ \mathbf{0}_{(L-M) \times M} \end{bmatrix} \mathbf{V}^{(i)H}. \quad (3.29)$$

Similarly, the SVD of the second hop channel $\mathbf{H}^{(k)T}$ of Eq. (3.4) can be modified to

$$\mathbf{H}^{(k)T} = \mathbf{V}^{(k)*} \begin{bmatrix} \mathbf{\Lambda}^{(i)1/2} & \mathbf{0}_{M \times (L-M)} \end{bmatrix} \begin{bmatrix} \tilde{\mathbf{U}}^{(k)T} \\ \bar{\mathbf{U}}^{(k)T} \end{bmatrix}. \quad (3.30)$$

Since Matrix $\tilde{\mathbf{U}}^{(i)}$ forms an orthogonal basis for the range of $\mathbf{H}^{(i)}$, matrix $\tilde{\mathbf{U}}^{(i)H}$ may be used as an adaptation to the non-zero eigenmodes of the first hop channel $\mathbf{H}^{(i)}$ at the RS. For the same reason, matrix $\tilde{\mathbf{U}}^{(k)*}$ may be used as an adaptation to the non-zero eigenmodes of the second hop channel $\mathbf{H}^{(k)T}$ at the RS. In the equivalent optimization problem, the BF matrix $\mathbf{G}^{(k,i)}$ is separated into three parts, namely the receive BF matrix $\tilde{\mathbf{U}}^{(i)H}$, the transmit BF matrix $\tilde{\mathbf{U}}^{(k)*}$ and an unknown matrix $\tilde{\mathbf{G}}^{(k,i)} \in \mathbb{C}^{M \times M}$. Thus, matrix $\mathbf{G}^{(k,i)}$ is given by

$$\mathbf{G}^{(k,i)} = \tilde{\mathbf{U}}^{(k)*} \tilde{\mathbf{G}}^{(k,i)} \tilde{\mathbf{U}}^{(i)H}. \quad (3.31)$$

Due to the unitary BF in Eq. (3.31) by the matrices $\tilde{\mathbf{U}}^{(i)H}$ and $\tilde{\mathbf{U}}^{(k)*}$, the non-zero eigenmodes of the first hop channel $\mathbf{H}^{(i)}$ and the second hop channel $\mathbf{H}^{(k)T}$ are preserved. By the BF approach of Eq. (3.31) the original sum rate maximization problem (3.27) with BF matrix $\mathbf{G}^{(k,i)}$ is transformed into an equivalent optimization problem where the unknown BF matrix $\mathbf{G}^{(k,i)}$ is replaced by the unknown BF matrix $\tilde{\mathbf{G}}^{(k,i)}$. Since BF matrix $\tilde{\mathbf{G}}^{(k,i)}$ only contains M^2 complex optimization variables, the equivalent optimization problem is simpler compared to the original one where BF matrix $\mathbf{G}^{(k,i)}$ contains L^2 complex optimization variables. Nevertheless, BF matrix $\tilde{\mathbf{G}}^{(k,i)}$ has to be determined by numerical methods, e.g., by sequential quadratic programming (SQP) algorithms which can be found in the MATLAB[®] optimization toolbox.

3.3 Linear beamforming in a system with limited capabilities at S1 and S2

3.3.1 Introduction

In this section 3.3, three additional optimization problems in the system with limited capabilities at S1 and S2 are considered. The three optimization problems consider the minimization of the MSE, the minimization of the MSE under the ZF constraint, and the maximization of the SNR, cf. first row and third column of the framework in Figure 1.4. In Section 3.2.4, no analytical solution to the maximization of the sum rate in the system with limited capabilities at S1 and S2 could be found. However, the three additional optimization problems are well-known from point-to-point transmissions and the corresponding BF algorithms are known to provide reasonable performance in point-to-point transmissions. For that reason, the optimization problems are newly formulated for the one-way relaying scheme with exclusive BF at the RS, and the respective BF algorithms are derived.

Since source node S_i is assumed to be a source node with limited SP capabilities and without CSI, the source node S_i assigns the same weighting factor $q^{(i)}$ to all transmit antennas, and from each transmit antenna one data stream is transmitted. From the transmit power constraint (3.1b) at S_i , the optimum $q_{\text{opt}}^{(i)}$ is directly given by Eq. (3.28). Thus, the transmit power constraint at the source node S_i can be omitted in the following optimization problems and $q^{(i)} = q_{\text{opt}}^{(i)}$ can be assumed as a fixed parameter in the optimization problems.

Since S_k is assumed to be a destination node with limited capabilities, the receive BF matrix $\mathbf{P}^{(k)}$ is given by Eq. (3.26), which means that the weighting factor $p^{(k)}$ is equal for all receive antennas. Besides the optimization of the BF matrix $\mathbf{G}^{(k,i)}$ at the RS, the proposed BF algorithms which minimize the MSE, minimize the MSE under the ZF constraint, and maximize the SNR consider the optimization of the weighting factor $p^{(k)}$ explicitly. Since the destination nodes are not provided with CSI according to the classifications of Figure 1.4, $p^{(k)}$ cannot be determined by the destination nodes by using CSI. Thus, another approach is required which is explained in the following.

For practical implementations, the weighting factor $p^{(k)}$ at the destination nodes can be chosen arbitrarily if all symbols of the modulation alphabet have the same amplitude which is the case for all phase shift keying (PSK) modulation schemes for example [Pro01]. For modulation schemes with symbols of different amplitudes, the

weighting factor $p^{(k)}$ is required in order to resize the received symbols to the original constellation of the transmitted symbols. Without CSI, $p^{(k)}$ can be determined by an observation of the received power of multiple received symbols under the assumption that all symbols are equiprobable. In this case, the weighting factor $p^{(k)}$ corresponds to the ratio between the expected average received power and the actually average received power at destination node Sk . Thus, weighting factor $p^{(k)}$ is chosen as $p^{(k)} = \mathbb{E} \left\{ \mathbf{y}^{(k)\text{H}} \mathbf{x}^{(i)} \right\} / \mathbb{E} \left\{ \mathbf{y}^{(k)\text{H}} \mathbf{y}^{(k)} \right\}$ where $\mathbf{y}^{(k)}$ is the received vector at the receive antennas of Sk before the weighting factor $p^{(k)}$ is applied.

3.3.2 Minimization of the MSE

In this section, the problem of minimizing the MSE is formulated and the respective MMSE-BF algorithm which solves the problem is derived. In literature, there exist MSE minimizations for point-to-point transmissions which are unconstrained concerning the transmit power, e.g., in [VJ98]. These optimizations may lead to unfeasible solutions since the available transmit power can be exceeded. For point-to-point transmission, the transmit power constraint can also be included into the optimization problem. In [Joh04], for example, the resulting solution is referred to as Wiener filter solution [Wie40]. The MMSE-BF of this section is derived considering the same principles as in [Joh04].

The BF matrix $\mathbf{G}^{(k,i)}$ at the RS and the weighting factor $p^{(k)}$ at destination node Sk have to be designed such that the MSE between the transmitted vector $\mathbf{x}^{(i)}$ of Eq. (2.1) and the estimated vector $\hat{\mathbf{x}}^{(i)}$ of Eq. (2.11) is minimized under the RS transmit power constraint. Let $\|\cdot\|_2^2$ and $\Re\{\cdot\}$ denote the Euclidean norm of a vector and the real value of the complex-valued argument, respectively. Thus, the minimization of the MSE is formulated as follows:

$$\left\{ p_{\text{MMSE}}^{(k)}, \mathbf{G}_{\text{MMSE}}^{(k,i)} \right\} = \arg \min_{\{p^{(k)}, \mathbf{G}^{(k,i)}\}} \mathbb{E} \left\{ \left\| \mathbf{x}^{(i)} - \hat{\mathbf{x}}^{(i)} \right\|_2^2 \right\}, \quad (3.32a)$$

$$\text{subject to: } \text{tr} \left\{ \mathbf{G}^{(k,i)} \left(q^{(i)2} \mathbf{H}^{(i)} \mathbf{R}_{\mathbf{x}^{(i)}} \mathbf{H}^{(i)\text{H}} + \mathbf{R}_{\mathbf{n}^{(0)}} \right) \mathbf{G}^{(k,i)\text{H}} \right\} = E^{(0)}, \quad (3.32b)$$

where Eq. (3.32b) constitutes the RS transmit power constraint.

In the following, the MMSE-BF algorithm which provides the solution to optimization problem (3.32) is derived. By applying the definitions of Eqs. (2.10a) to (2.10d)

and inserting $\hat{\mathbf{x}}^{(i)}$ of Eq. (2.11) into the MSE objective function in Eq. (3.32a), the MSE at the receiver output of Sk results in

$$\begin{aligned} \mathbb{E} \left\{ \|\hat{\mathbf{x}}^{(i)} - \mathbf{x}^{(i)}\|_2^2 \right\} &= \text{tr} \{ \mathbf{R}_{\mathbf{x}^{(i)}} \} - 2\Re \left\{ p^{(k)} q^{(i)} \text{tr} \left\{ \mathbf{H}^{(k)\text{T}} \mathbf{G}^{(k,i)} \mathbf{H}^{(i)} \mathbf{R}_{\mathbf{x}^{(i)}} \right\} \right\} \\ &\quad + p^{(k)2} q^{(i)2} \text{tr} \left\{ \mathbf{H}^{(k)\text{T}} \mathbf{G}^{(k,i)} \mathbf{H}^{(i)} \mathbf{R}_{\mathbf{x}^{(i)}} \mathbf{H}^{(i)\text{H}} \mathbf{G}^{(k,i)\text{H}} \mathbf{H}^{(k)*} \right\} \\ &\quad + p^{(k)2} \text{tr} \left\{ \mathbf{H}^{(k)\text{T}} \mathbf{G}^{(k,i)} \mathbf{R}_{\mathbf{n}^{(0)}} \mathbf{G}^{(k,i)\text{H}} \mathbf{H}^{(k)*} + \mathbf{R}_{\mathbf{n}_R^{(k)}} \right\}. \end{aligned} \quad (3.33)$$

In [Joh04], it is shown that the MSE objective function in point-to-point transmissions is neither convex nor concave, since the objective function is quadratic in the optimization variable. Since the MSE of Eq. (3.33) is also quadratic in $\mathbf{G}^{(k,i)}$, the MSE minimization problem for the one-way relaying scheme is neither convex nor concave, too. Nevertheless, as introduced in [Joh04] for point-to-point transmission, Lagrangian optimization [BV04] is applied knowing that the resulting solution is not necessarily unique. Let $\mathbf{\Upsilon}^{(i)}$ denote the covariance matrix of the received signal at the RS which is given by

$$\mathbf{\Upsilon}^{(i)} = \mathbb{E} \left\{ (q^{(i)} \mathbf{H}^{(i)} \mathbf{x}^{(i)} + \mathbf{n}^{(0)}) (q^{(i)} \mathbf{H}^{(i)} \mathbf{x}^{(i)} + \mathbf{n}^{(0)})^{\text{H}} \right\} = q^{(i)2} \mathbf{H}^{(i)} \mathbf{R}_{\mathbf{x}^{(i)}} \mathbf{H}^{(i)\text{H}} + \mathbf{R}_{\mathbf{n}^{(0)}}. \quad (3.34)$$

With Eq. (3.34), the Lagrangian function for problem (3.32) yields

$$\begin{aligned} L(p^{(k)}, \mathbf{G}^{(k,i)}, \eta^{(k)}) &= \text{tr} \{ \mathbf{R}_{\mathbf{x}^{(i)}} \} - 2\Re \left\{ p^{(k)} q^{(i)} \text{tr} \left\{ \mathbf{H}^{(k)\text{T}} \mathbf{G}^{(k,i)} \mathbf{H}^{(i)} \mathbf{R}_{\mathbf{x}^{(i)}} \right\} \right\} \\ &\quad + p^{(k)2} q^{(i)2} \text{tr} \left\{ \mathbf{H}^{(k)\text{T}} \mathbf{G}^{(k,i)} \mathbf{H}^{(i)} \mathbf{R}_{\mathbf{x}^{(i)}} \mathbf{H}^{(i)\text{H}} \mathbf{G}^{(k,i)\text{H}} \mathbf{H}^{(k)*} \right\} \\ &\quad + p^{(k)2} \text{tr} \left\{ \mathbf{H}^{(k)\text{T}} \mathbf{G}^{(k,i)} \mathbf{R}_{\mathbf{n}^{(0)}} \mathbf{G}^{(k,i)\text{H}} \mathbf{H}^{(k)*} + \mathbf{R}_{\mathbf{n}_R^{(k)}} \right\} \\ &\quad + \eta^{(k)} \left(\text{tr} \left\{ \mathbf{G}^{(k,i)} \mathbf{\Upsilon}^{(i)} \mathbf{G}^{(k,i)\text{H}} \right\} - E^{(0)} \right), \end{aligned} \quad (3.35)$$

with the Lagrangian multiplier $\eta^{(k)}$. The Karush-Kuhn-Tucker (KKT) conditions [BV04] are only necessary conditions for the global optimum and are given by

$$\begin{aligned} \frac{\partial L}{\partial p^{(k)}} &= -q^{(i)} \text{tr} \left\{ \mathbf{H}^{(k)\text{T}} \mathbf{G}^{(k,i)} \mathbf{H}^{(i)} \mathbf{R}_{\mathbf{x}^{(i)}} \right\} \\ &\quad + p^{(k)*} |q^{(i)}|^2 \text{tr} \left\{ \mathbf{H}^{(k)\text{T}} \mathbf{G}^{(k,i)} \mathbf{H}^{(i)} \mathbf{R}_{\mathbf{x}^{(i)}} \mathbf{H}^{(i)\text{H}} \mathbf{G}^{(k,i)\text{H}} \mathbf{H}^{(k)*} \right\} \\ &\quad + p^{(k)*} \text{tr} \left\{ \mathbf{H}^{(k)\text{T}} \mathbf{G}^{(k,i)} \mathbf{R}_{\mathbf{n}^{(0)}} \mathbf{G}^{(k,i)\text{H}} \mathbf{H}^{(k)*} + \mathbf{R}_{\mathbf{n}_R^{(k)}} \right\} \stackrel{!}{=} 0, \end{aligned} \quad (3.36a)$$

$$\frac{\partial L}{\partial \mathbf{G}^{(k,i)}} = |p^{(k)}|^2 \mathbf{H}^{(k)} \mathbf{H}^{(k)\text{H}} \mathbf{G}^{(k,i)*} \mathbf{\Upsilon}^{(i)\text{T}} - p^{(k)} q^{(i)} \mathbf{H}^{(k)} \mathbf{R}_{\mathbf{x}^{(i)}}^{\text{T}} \mathbf{H}^{(i)\text{T}} + \eta^{(k)} \mathbf{G}^{(k,i)*} \mathbf{\Upsilon}^{(i)\text{T}} \stackrel{!}{=} 0, \quad (3.36b)$$

$$\eta^{(k)} \left(\text{tr} \left\{ \mathbf{G}^{(k,i)} \mathbf{\Upsilon}^{(i)} \mathbf{G}^{(k,i)\text{H}} \right\} - E^{(0)} \right) \stackrel{!}{=} 0. \quad (3.36c)$$

Let matrix $\mathbf{\Upsilon}^{(k)}$ be defined as

$$\mathbf{\Upsilon}^{(k)} = \mathbf{H}^{(k)*} \mathbf{H}^{(k)\text{T}} + \frac{\text{tr} \left\{ \mathbf{R}_{\mathbf{n}_R^{(k)}} \right\}}{E^{(0)}} \mathbf{I}_L. \quad (3.37)$$

With $\Upsilon^{(k)}$ of Eq. (3.37), the solution to problem (3.32) results in

$$\mathbf{G}_{\text{MMSE}}^{(k,i)} = \frac{q^{(i)}}{p_{\text{MMSE}}^{(k)}} \Upsilon^{(k)-1} \mathbf{H}^{(k)*} \mathbf{R}_{\mathbf{x}^{(i)}} \mathbf{H}^{(i)\text{H}} \Upsilon^{(i)-1}, \quad (3.38)$$

and

$$p_{\text{MMSE}}^{(k)} = \sqrt{\frac{q^{(i)2} \text{tr} \{ \mathbf{H}^{(i)} \mathbf{R}_{\mathbf{x}^{(i)}} \mathbf{H}^{(k)\text{T}} \Upsilon^{(k)-2} \mathbf{H}^{(k)*} \mathbf{R}_{\mathbf{x}^{(i)}} \mathbf{H}^{(i)\text{H}} \Upsilon^{(i)-1} \}}{E^{(0)}}} \in \mathbb{R}^+. \quad (3.39)$$

The derivation of the BF matrix $\mathbf{G}_{\text{MMSE}}^{(k,i)}$ at the RS and the weighting factor $p_{\text{MMSE}}^{(k)}$ at Sk from the KKT conditions (3.36) can be found in Appendix A.1. Note that the proposed MMSE-BF algorithm requires knowledge about the noise covariance matrix $\mathbf{R}_{\mathbf{n}^{(0)}}$ of the RS which can be estimated by the RS itself, but also about the noise covariance matrix $\mathbf{R}_{\mathbf{n}_R^{(k)}}$ of the destination node Sk . Assuming AWGN, this means that the noise variance $\sigma_{\mathbf{n}_R^{(k)}}^2$, which is estimated at Sk , needs to be signaled via a feedback channel from destination nodes Sk to the RS. However, the effort for such a feedback is very low.

In order to give an insight into the derived MMSE-BF algorithm, BF matrix $\mathbf{G}^{(k,i)}$ is separated into a receive BF matrix $\mathbf{G}_R^{(i)}$ and a transmit BF matrix $\mathbf{G}_T^{(k)}$ yielding

$$\mathbf{G}^{(k,i)} = \mathbf{G}_T^{(k)} \mathbf{G}_R^{(i)}. \quad (3.40)$$

Identifying the receive BF matrix

$$\mathbf{G}_{R,\text{MMSE}}^{(i)} = q^{(i)} \mathbf{R}_{\mathbf{x}^{(i)}} \mathbf{H}^{(i)\text{H}} \Upsilon^{(i)-1}, \quad (3.41)$$

and the transmit BF matrix

$$\mathbf{G}_{T,\text{MMSE}}^{(k)} = \frac{1}{p_{\text{MMSE}}^{(k)}} \Upsilon^{(k)-1} \mathbf{H}^{(k)*}, \quad (3.42)$$

in Eq. (3.38), it turns out that the receive BF matrix $\mathbf{G}_{R,\text{MMSE}}^{(i)}$ is only linked with the first hop transmission from Si to the RS, and that the transmit BF matrix $\mathbf{G}_{T,\text{MMSE}}^{(k)}$ is only linked with the second hop transmission from the RS to Sk .

3.3.3 Minimization of the MSE under the ZF constraint

In this section, the minimization of the MSE under the ZF constraint is considered for a system with limited capabilities at S1 and S2 in one-way relaying, and the corresponding ZF-BF algorithm is derived. The minimization of the MSE under the ZF

constraint is a modification of the minimization of the MSE presented in Section 3.3.2. Due to the ZF constraint, the whole intersymbol interference between simultaneously transmitted data streams is removed additionally [PNG03]. In other words, the ZF constraint means that in case of zero AWGN, the transmitted and received data streams are equal. In the following, the ZF constraint is introduced as an additional constraint to the MSE optimization problem (3.32). Thus, the minimization of the MSE under the ZF constraint is formulated as follows:

$$\left\{ p_{\text{ZF}}^{(k)}, \mathbf{G}_{\text{ZF}}^{(k,i)} \right\} = \arg \min_{\{p^{(k)}, \mathbf{G}^{(k,i)}\}} \mathbb{E} \left\{ \|\mathbf{x}^{(i)} - \hat{\mathbf{x}}^{(i)}\|_2^2 \right\}, \quad (3.43a)$$

$$\text{subject to: } \hat{\mathbf{x}}^{(i)} = \mathbf{x}^{(i)} \quad \text{for } \mathbf{n}^{(0)} = \mathbf{0}_{L \times 1} \text{ and } \mathbf{n}_{\text{R}}^{(k)} = \mathbf{0}_{M \times 1}, \quad (3.43b)$$

$$\text{tr} \left\{ \mathbf{G}^{(k,i)} \left(q^{(i)2} \mathbf{H}^{(i)} \mathbf{R}_{\mathbf{x}^{(i)}} \mathbf{H}^{(i)\text{H}} + \mathbf{R}_{\mathbf{n}^{(0)}} \right) \mathbf{G}^{(k,i)\text{H}} \right\} = E^{(0)}, \quad (3.43c)$$

where Eq. (3.43b) is the mentioned ZF constraint.

In the following, the ZF-BF algorithm which provides the solution to the optimization problem (3.43) is given. With Eqs. (2.10) and (2.11), the ZF constraint (3.43b) can also be described by

$$p^{(k)} q^{(i)} \mathbf{H}^{(k)\text{T}} \mathbf{G}^{(k,i)} \mathbf{H}^{(i)} = \mathbf{I}_M. \quad (3.44)$$

By applying the definitions of Eqs. (2.10a) to (2.10d) and inserting $\hat{\mathbf{x}}^{(i)}$ of Eq. (2.11) into the MSE objective function (3.43a) and using Eq. (3.44), it turns out that the MSE corresponds to the overall noise power at the receiver output of Sk . Thus, the MSE under the ZF constraint is given by

$$\mathbb{E} \left\{ \|\hat{\mathbf{x}}^{(i)} - \mathbf{x}^{(i)}\|_2^2 \right\} = p^{(k)2} \text{tr} \left\{ \mathbf{H}^{(k)\text{T}} \mathbf{G}^{(k,i)} \mathbf{R}_{\mathbf{n}^{(0)}} \mathbf{G}^{(k,i)\text{H}} \mathbf{H}^{(k)*} + \mathbf{R}_{\mathbf{n}_{\text{R}}^{(k)}} \right\}. \quad (3.45)$$

As for the minimization of the MSE in Section 3.3.2, the objective function (3.45) is neither convex nor concave since the function is quadratic in $\mathbf{G}^{(k,i)}$. Furthermore, the ZF constraint is a complex-valued constraint. With the definition of Lagrangian functions for complex-valued constraints [Joh04], the Lagrangian function yields

$$\begin{aligned} L(p^{(k)}, \mathbf{G}^{(k,i)}, \mathbf{\Gamma}^{(k)}, \eta^{(k)}) = & p^{(k)2} \text{tr} \left\{ \mathbf{H}^{(k)\text{T}} \mathbf{G}^{(k,i)} \mathbf{R}_{\mathbf{n}^{(0)}} \mathbf{G}^{(k,i)\text{H}} \mathbf{H}^{(k)*} + \mathbf{R}_{\mathbf{n}_{\text{R}}^{(k)}} \right\} \\ & - 2\Re \left\{ \text{tr} \left\{ \mathbf{\Gamma}^{(k)} \left(q^{(i)} p^{(k)} \mathbf{H}^{(k)\text{T}} \mathbf{G}^{(k,i)} \mathbf{H}^{(i)} - \mathbf{I}_M \right) \right\} \right\} \\ & + \eta^{(k)} \left(\text{tr} \left\{ \mathbf{G}^{(k,i)} \mathbf{\Upsilon}^{(i)} \mathbf{G}^{(k,i)\text{H}} \right\} - E^{(0)} \right), \end{aligned} \quad (3.46)$$

with the Lagrangian multipliers $\mathbf{\Gamma}^{(k)}$ and $\eta^{(k)}$. The KKT conditions are only necessary

conditions for the global optimum and are given by

$$\frac{\partial L}{\partial p^{(k)}} = p^{(k)*} \operatorname{tr} \left\{ \mathbf{H}^{(k)\top} \mathbf{G}^{(k,i)} \mathbf{R}_{\mathbf{n}^{(0)}} \mathbf{G}^{(k,i)\text{H}} \mathbf{H}^{(k)*} + \mathbf{R}_{\mathbf{n}_{\text{R}}^{(k)}} \right\} - \operatorname{tr} \left\{ \mathbf{\Gamma}^{(k)} \mathbf{H}^{(k)\top} \mathbf{G}^{(k,i)} \mathbf{H}^{(i)} \right\} \stackrel{!}{=} 0, \quad (3.47\text{a})$$

$$\frac{\partial L}{\partial \mathbf{G}^{(k,i)}} = p^{(k)2} \mathbf{H}^{(k)} \mathbf{H}^{(k)\text{H}} \mathbf{G}^{(k,i)*} \mathbf{R}_{\mathbf{n}^{(0)}}^{\top} - p^{(k)} q^{(i)} \mathbf{H}^{(k)} \mathbf{\Gamma}^{(k)\top} \mathbf{H}^{(i)\top} + \eta^{(k)} \mathbf{G}^{(k,i)*} \mathbf{\Upsilon}^{(i)\top} \stackrel{!}{=} \mathbf{0}, \quad (3.47\text{b})$$

$$\frac{\partial L}{\partial \mathbf{\Gamma}^{(k)}} = p^{(k)} q^{(i)} \mathbf{H}^{(i)\top} \mathbf{G}^{(k,i)\top} \mathbf{H}^{(k)} - \mathbf{I}_M \stackrel{!}{=} \mathbf{0}, \quad (3.47\text{c})$$

$$\eta^{(k)} \left(\operatorname{tr} \left\{ \mathbf{G}^{(k,i)} \mathbf{\Upsilon}^{(i)} \mathbf{G}^{(k,i)\text{H}} \right\} - E^{(0)} \right) \stackrel{!}{=} 0. \quad (3.47\text{d})$$

The solution to problem (3.43) is obtained under the simplifying assumption that the noise $\mathbf{n}^{(0)}$ at the RS does not contribute to the MSE of Eq. (3.45), cf. Appendix A.2. In this case, problem (3.43) is solved by

$$\mathbf{G}_{\text{ZF}}^{(k,i)} = \frac{1}{p_{\text{ZF}}^{(k)} q^{(i)}} \mathbf{H}^{(k)*} \left(\mathbf{H}^{(k)\top} \mathbf{H}^{(k)*} \right)^{-1} \left(\mathbf{H}^{(i)\text{H}} \mathbf{R}_{\mathbf{n}^{(0)}}^{-1} \mathbf{H}^{(i)} \right)^{-1} \mathbf{H}^{(i)\text{H}} \mathbf{R}_{\mathbf{n}^{(0)}}^{-1}, \quad (3.48)$$

and

$$p_{\text{ZF}}^{(k)} = \frac{1}{q^{(i)}} \sqrt{\frac{\operatorname{tr} \left\{ \left(\mathbf{H}^{(i)\text{H}} \mathbf{\Upsilon}^{(i)-1} \mathbf{H}^{(i)} \right)^{-1} \left(\mathbf{H}^{(k)\top} \mathbf{H}^{(k)*} \right)^{-1} \right\}}{E^{(0)}}} \in \mathbb{R}^+. \quad (3.49)$$

The derivation of the BF matrix $\mathbf{G}_{\text{ZF}}^{(k,i)}$ at the RS and the weighting factor $p_{\text{ZF}}^{(k)}$ at Sk from the KKT conditions (3.47) can be found in Appendix A.2. In contrast to the MMSE-BF algorithm of Section 3.3.2, the ZF-BF algorithm only requires knowledge about the noise covariance matrix $\mathbf{R}_{\mathbf{n}^{(0)}}$ of the RS, but not about the noise covariance matrix $\mathbf{R}_{\mathbf{n}_{\text{R}}^{(k)}}$ of the destination node Sk , i.e., no feedback from Sk to the RS is required.

As for the MMSE-BF algorithm of Section 3.3.2, in order to give an insight into the derived ZF-BF algorithm, BF matrix $\mathbf{G}^{(k,i)}$ is separated into a receive BF matrix $\mathbf{G}_{\text{R}}^{(i)}$ and a transmit BF matrix $\mathbf{G}_{\text{T}}^{(k)}$ introduced in Eq. (3.40). Identifying the receive BF matrix

$$\mathbf{G}_{\text{R,ZF}}^{(i)} = \frac{1}{q^{(i)}} \left(\mathbf{H}^{(i)\text{H}} \mathbf{R}_{\mathbf{n}^{(0)}}^{-1} \mathbf{H}^{(i)} \right)^{-1} \mathbf{H}^{(i)\text{H}} \mathbf{R}_{\mathbf{n}^{(0)}}^{-1}, \quad (3.50)$$

and the transmit BF matrix

$$\mathbf{G}_{\text{T,ZF}}^{(k)} = \frac{1}{p_{\text{ZF}}^{(k)}} \mathbf{H}^{(k)*} \left(\mathbf{H}^{(k)\top} \mathbf{H}^{(k)*} \right)^{-1}, \quad (3.51)$$

in Eq. (3.48), it turns out that the receive BF matrix $\mathbf{G}_{\text{R,ZF}}^{(i)}$ is only linked with the first hop transmission from Si to the RS, and that the transmit BF matrix $\mathbf{G}_{\text{T,ZF}}^{(k)}$ is only linked with the second hop transmission from the RS to Sk .

3.3.4 Maximization of the SNR

In this section, the problem of maximizing the SNR at the receiver output of Sk is formulated for a system with limited capabilities at S1 and S2 in one-way relaying. The corresponding BF algorithm is derived, too. In literature, the BF algorithm which maximizes the SNR is also known as the matched filter (MF) solution. Thus, the BF algorithm which maximizes the SNR is termed MF-BF algorithm in the following. The receive MF [Pro01] and the transmit MF [Cav00] are well-known BF approaches in point-to-point multiple-antenna systems. From [Joh04], it is known that receive and transmit filters are based on similar optimization approaches. In this section, the MF definitions of [Joh04] are adapted to the one-way relaying problem with BF matrix $\mathbf{G}^{(k,i)}$ at the RS. In one-way relaying, the SNR gives the ratio between the average power of the useful signal part in the estimated data vector $\hat{\mathbf{x}}^{(i)}$ and the average power of the noise parts at the receiver output. After separating $\hat{\mathbf{x}}^{(i)}$ of Eq. (2.11) into the useful signal parts and the noise parts using the definitions in Eqs. (2.10a) to (2.10d), the maximization of the SNR under the RS transmit power constraint may be formulated as follows:

$$\left\{ p_{\text{MF}}^{(k)}, \mathbf{G}_{\text{MF}}^{(k,i)} \right\} = \arg \max_{\left\{ p^{(k)}, \mathbf{G}^{(k,i)} \right\}} \frac{\left| \mathbb{E} \left\{ \mathbf{x}^{(i)\text{H}} \hat{\mathbf{x}}^{(i)} \right\} \right|^2}{\mathbb{E} \left\{ \|\mathbf{x}^{(i)}\|_2^2 \right\} \mathbb{E} \left\{ \left\| p^{(k)} \left(\mathbf{H}^{(k)\text{T}} \mathbf{G}^{(k,i)} \mathbf{n}^{(0)} + \mathbf{n}_{\text{R}}^{(k)} \right) \right\|_2^2 \right\}}, \quad (3.52a)$$

$$\text{subject to: } \text{tr} \left\{ \mathbf{G}^{(k,i)} \left(q^{(i)2} \mathbf{H}^{(i)} \mathbf{R}_{\mathbf{x}^{(i)}} \mathbf{H}^{(i)\text{H}} + \mathbf{R}_{\mathbf{n}^{(0)}} \right) \mathbf{G}^{(k,i)\text{H}} \right\} = E^{(0)}. \quad (3.52b)$$

In the following, the MF-BF algorithm is derived which provides the solution to the optimization problem (3.52). Firstly, with Eqs. (2.10) and (2.11) the three expectation values in Eq. (3.52a) are determined as follows:

$$\left| \mathbb{E} \left\{ \mathbf{x}^{(i)\text{H}} \hat{\mathbf{x}}^{(i)} \right\} \right|^2 = p^{(k)2} q^{(i)2} \left| \text{tr} \left\{ \mathbf{H}^{(k)\text{T}} \mathbf{G}^{(k,i)} \mathbf{H}^{(i)} \mathbf{R}_{\mathbf{x}^{(i)}} \right\} \right|^2, \quad (3.53a)$$

$$\mathbb{E} \left\{ \|\mathbf{x}^{(i)}\|_2^2 \right\} = \text{tr} \left\{ \mathbf{R}_{\mathbf{x}^{(i)}} \right\}, \quad (3.53b)$$

$$\mathbb{E} \left\{ \left\| p^{(k)} \left(\mathbf{H}^{(k)\text{T}} \mathbf{G}^{(k,i)} \mathbf{n}^{(0)} + \mathbf{n}_{\text{R}}^{(k)} \right) \right\|_2^2 \right\} = p^{(k)2} \text{tr} \left\{ \mathbf{H}^{(k)\text{T}} \mathbf{G}^{(k,i)} \mathbf{R}_{\mathbf{n}^{(0)}} \mathbf{G}^{(k,i)\text{H}} \mathbf{H}^{(k)*} + \mathbf{R}_{\mathbf{n}_{\text{R}}^{(k)}} \right\}. \quad (3.53c)$$

Secondly, with the results of Eqs. (3.53a) to (3.53c) the Lagrangian function can be written as

$$\begin{aligned} L \left(p^{(k)}, \mathbf{G}^{(k,i)}, \eta^{(k)} \right) = & - \frac{q^{(i)2} \left| \text{tr} \left\{ \mathbf{H}^{(k)\text{T}} \mathbf{G}^{(k,i)} \mathbf{H}^{(i)} \mathbf{R}_{\mathbf{x}^{(i)}} \right\} \right|^2}{\text{tr} \left\{ \mathbf{R}_{\mathbf{x}^{(i)}} \right\} \text{tr} \left\{ \mathbf{H}^{(k)\text{T}} \mathbf{G}^{(k,i)} \mathbf{R}_{\mathbf{n}^{(0)}} \mathbf{G}^{(k,i)\text{H}} \mathbf{H}^{(k)*} + \mathbf{R}_{\mathbf{n}_{\text{R}}^{(k)}} \right\}} \\ & + \eta^{(k)} \left(\text{tr} \left\{ \mathbf{G}^{(k,i)} \mathbf{\Upsilon}^{(i)} \mathbf{G}^{(k,i)\text{H}} \right\} - E^{(0)} \right), \end{aligned} \quad (3.54)$$

with the Lagrangian multiplier $\eta^{(k)}$. Obviously, the Lagrangian function is independent of the weighting factor $p^{(k)}$, which means that $p^{(k)}$ is arbitrary and the solution to the optimization problem (3.52) is not unique. Using the following definition

$$\alpha^{(k)} = \frac{\text{tr} \left\{ \mathbf{H}^{(k)\text{T}} \mathbf{G}^{(k,i)} \mathbf{H}^{(i)} \mathbf{R}_{\mathbf{x}^{(i)}} \right\}}{\text{tr} \left\{ \mathbf{R}_{\mathbf{x}^{(i)}} \right\} \text{tr} \left\{ \mathbf{H}^{(k)\text{T}} \mathbf{G}^{(k,i)} \mathbf{R}_{\mathbf{n}^{(0)}} \mathbf{G}^{(k,i)\text{H}} \mathbf{H}^{(k)*} + \mathbf{R}_{\mathbf{n}_R^{(k)}} \right\}}, \quad (3.55)$$

the KKT conditions are given by

$$\frac{\partial L}{\partial \mathbf{G}^{(k,i)}} = -q^{(i)^2} \alpha^{(k)*} \mathbf{H}^{(k)} \mathbf{R}_{\mathbf{x}^{(i)}}^{\text{T}} \mathbf{H}^{(i)\text{T}} + q^{(i)^2} |\alpha^{(k)}|^2 \text{tr} \left\{ \mathbf{R}_{\mathbf{x}^{(i)}} \right\} \mathbf{H}^{(k)} \mathbf{H}^{(k)\text{H}} \mathbf{G}^{(k,i)*} \mathbf{R}_{\mathbf{n}^{(0)}}^{\text{T}} + \eta^{(k)} \mathbf{G}^{(k,i)*} \mathbf{\Upsilon}^{(i)\text{T}} \stackrel{!}{=} \mathbf{0}, \quad (3.56a)$$

$$\eta^{(k)} \left(\text{tr} \left\{ \mathbf{G}^{(k,i)} \mathbf{\Upsilon}^{(i)} \mathbf{G}^{(k,i)\text{H}} \right\} - E^{(0)} \right) \stackrel{!}{=} 0. \quad (3.56b)$$

The MF-BF algorithm which solves problem (3.52) is obtained under the assumption that the noise $\mathbf{n}^{(0)}$ at the RS does not contribute to the overall noise at the receiver output given in the denominator of the objective function (3.52a), cf. Appendix A.3. In this case, problem (3.52) is solved by

$$\mathbf{G}_{\text{MF}}^{(k,i)} = \frac{1}{p_{\text{MF}}^{(k)}} \mathbf{H}^{(k)*} \mathbf{R}_{\mathbf{x}^{(i)}} \mathbf{H}^{(i)\text{H}} \mathbf{\Upsilon}^{(i)-1}, \quad (3.57)$$

and

$$p_{\text{MF}}^{(k)} = \sqrt{\frac{\text{tr} \left\{ \mathbf{H}^{(k)*} \mathbf{R}_{\mathbf{x}^{(i)}} \mathbf{H}^{(i)\text{H}} \mathbf{\Upsilon}^{(i)-1} \mathbf{H}^{(i)} \mathbf{R}_{\mathbf{x}^{(i)}} \mathbf{H}^{(k)\text{T}} \right\}}{E^{(0)}}} \in \mathbb{R}^+. \quad (3.58)$$

The derivation of BF matrices $\mathbf{G}_{\text{MF}}^{(k,i)}$ at the RS and the weighting factor $p_{\text{MF}}^{(k)}$ at Sk from the KKT conditions (3.56) can be found in Appendix A.3. In contrast to the MMSE-BF algorithm of Section 3.3.2, the MF-BF algorithm only requires knowledge about the noise covariance matrix $\mathbf{R}_{\mathbf{n}^{(0)}}$ of the RS, but not about the noise covariance matrix $\mathbf{R}_{\mathbf{n}_R^{(k)}}$ of the destination node, i.e., no feedback from Sk to the RS is required.

As for the MMSE-BF algorithm and the ZF-BF algorithm, in order to give an insight into the derived MF-BF algorithm, BF matrix $\mathbf{G}^{(k,i)}$ is separated into a receive BF matrix $\mathbf{G}_{\text{R}}^{(i)}$ and a transmit BF matrix $\mathbf{G}_{\text{T}}^{(k)}$ introduced in Eq. (3.40). Identifying the receive BF matrix

$$\mathbf{G}_{\text{R, MF}}^{(i)} = q^{(i)} \mathbf{R}_{\mathbf{x}^{(i)}} \mathbf{H}^{(i)\text{H}} \mathbf{\Upsilon}^{(i)-1}, \quad (3.59)$$

and the transmit BF matrix

$$\mathbf{G}_{\text{T, MF}}^{(k)} = \frac{1}{p_{\text{MF}}^{(k)}} \mathbf{H}^{(k)*}, \quad (3.60)$$

in Eq. (3.57), it turns out that the receive BF matrix $\mathbf{G}_{\text{R, MF}}^{(i)}$ is only linked with the first hop transmission from Si to the RS, and that the transmit BF matrix $\mathbf{G}_{\text{T, MF}}^{(k)}$ is only linked with the second hop transmission from the RS to Sk .

3.4 Performance analysis

3.4.1 Simulation assumptions

In this Section 3.4, the BF algorithms of Sections 3.2 and 3.3 are analyzed by means of simulations. The presented results are obtained by Monte Carlo simulations assuming Rayleigh block fading channels [KS95]. The channel coefficients of channels $\mathbf{H}^{(1)}$ and $\mathbf{H}^{(2)}$ are zero-mean, independent, circularly symmetric, complex Gaussian random variables with variance $\sigma^{(1)^2}$ and $\sigma^{(2)^2}$, respectively. Nodes S1, S2, and the RS use the same transmit powers, i.e., $E^{(0)} = E^{(1)} = E^{(2)} = E = 1$, and the same noise variances are assumed at all nodes, i.e., $\sigma_{\mathbf{n}^{(0)}}^2 = \sigma_{\mathbf{n}^{(1)}}^2 = \sigma_{\mathbf{n}^{(2)}}^2 = \sigma_{\mathbf{n}}^2 = 1$. Due to the assumption of channel reciprocity introduced in Section 2.2, the average SNR for the transmission from S_i to the RS is equal to the average SNR for the transmission from the RS to S_i . Thus, the average SNR⁽ⁱ⁾ of the link between S_i and the RS is defined by:

$$\text{SNR}^{(i)} = \sigma^{(i)^2}, \quad \text{for } i = 1, 2. \quad (3.61)$$

The three different cases of system capabilities in one-way relaying are distinguished by the following notation:

- CASE1: system with full capabilities,
- CASE2: system with limited capabilities at the RS,
- CASE3: system with limited capabilities at S1 and S2.

Concerning the maximization of the sum rate, the following abbreviations indicate how the respective results are obtained: All results which are obtained by numerical methods of the MATLAB[®] optimization toolbox are denoted by N-BF, and all results obtained by analytical BF algorithms proposed in Section 3.2 are denoted by A-BF.

3.4.2 Sum rate analysis

In this section, the average sum rates of the different BF algorithms in one-way relaying introduced in Sections 3.2 and 3.3 are analyzed. The average sum rate is obtained by averaging over the instantaneous sum rates of multiple channel realizations defined in Eqs. (2.15) and (2.22). Since the transmission from S1 to S2 is independent of the

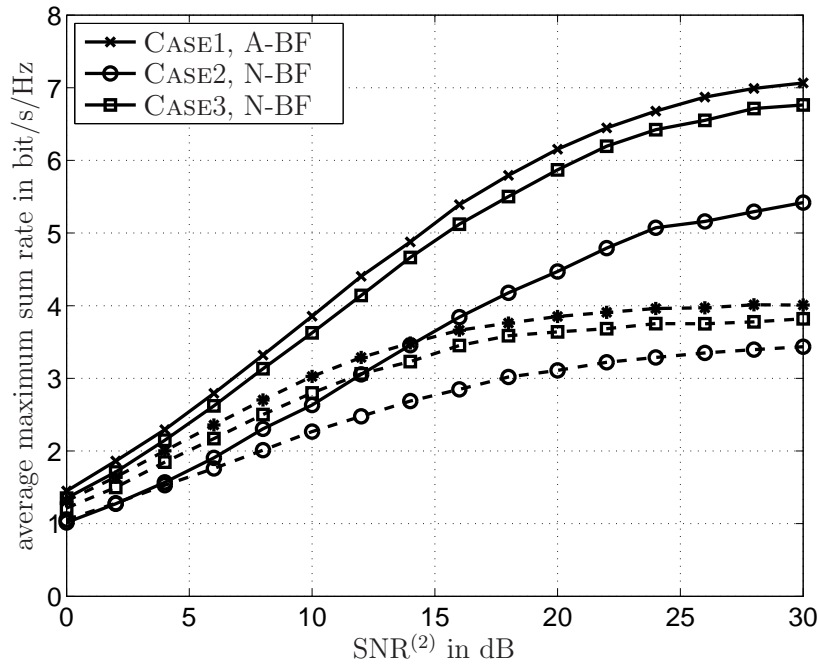


Figure 3.1. Average maximum sum rate vs. $\text{SNR}^{(2)}$ for CASE1, CASE2, and CASE3, $M = 2$ and $L = 4$, dashed lines: $\text{SNR}^{(1)} = 10\text{dB}$, solid lines: $\text{SNR}^{(1)} = 20\text{dB}$.

transmission from S2 to S1, one could only consider the individual transmission rate for one of the two transmissions in order to compare different BF algorithms in one-way relaying. However, for the sake of comparison to the performance results of two-way relaying, where only the sum rate provides a reasonable performance measure for the whole system, the BF algorithms in one-way relaying are also compared to each other by means of the sum rate.

In the following, the average maximum sum rates of CASE1, CASE2, and CASE3 are considered so that the different cases of system capabilities in one-way relaying introduced in the new framework of Figure 1.4 can be investigated jointly. Figure 3.1 gives the average maximum sum rate in bit/s/Hz vs. $\text{SNR}^{(2)}$ in dB for CASE1, CASE2, and CASE3, for two fixed values of $\text{SNR}^{(1)}$, namely $\text{SNR}^{(1)} = 10\text{dB}$ and $\text{SNR}^{(1)} = 20\text{dB}$. Nodes S1 and S2 are equipped with $M = 2$ antennas and the RS is equipped with $L = 4$ antennas. The maximum sum rate of CASE1 is obtained by the A-BF algorithm proposed by [HW06], and the sum rates of CASE2 and CASE3 are obtained by numerical methods. Note that the applied SQP algorithms [BV04] of the MATLAB[®] optimization toolbox provide an optimum which is not necessarily the global one.

In any of the cases, the maximum sum rate is limited. For each direction of the transmission, the data streams are transmitted over both channels $\mathbf{H}^{(1)}$ and $\mathbf{H}^{(2)}$. Hence, even if the SNR value of one channel goes to infinity, the SNR value of the

worse channel limits the achievable sum rate in both directions of the transmission, i.e., the maximum sum rate converges to an upper bound for increasing $\text{SNR}^{(2)}$ if $\text{SNR}^{(1)}$ is fixed to a certain value.

In the following, the different cases of system capabilities are compared to each other. For both values of $\text{SNR}^{(1)}$, the relations between the average maximum sum rates of the different cases are the same. The best performance is obtained in CASE1, since adaptive BF can be applied at S1, S2, and the RS. In CASE3, the RS can also perform adaptive BF. However, since equal weighting is applied at S1 and S2, which means that the data streams are encoded and decoded stream-wise for each antenna at the source and destination node, respectively, the performance is degraded compared to CASE1. Compared to CASE1, the relative loss in sum rate is about 5% for $\text{SNR}^{(1)} = 20\text{dB}$ as well as for $\text{SNR}^{(1)} = 10\text{dB}$ and all values of $\text{SNR}^{(2)}$ in CASE3. In CASE2, adaptive BF can be applied at the source and destination nodes but the RS only retransmits the received data streams with a constant weighting factor equal at all antennas of the RS. In this case, the high number L of antennas at the RS cannot be exploited and the performance is considerably degraded by about 20% in average sum rate compared to CASE1 for $\text{SNR}^{(1)} = 20\text{dB}$.

In the following, the influence of the number L of antennas at the RS on the sum rate performance is investigated which provides an insight to the different performance gains, namely multiplexing gain, array gain, and diversity gain, which can be obtained due to multiple antennas at the RS in one-way relaying. In Figure 3.2, the average maximum sum rate vs. the number L of antennas at the RS is depicted for CASE1 with the A-BF algorithm proposed by [HW06], CASE2 with the N-BF solution, CASE2 with the proposed sub-optimum A-BF algorithm of Section 3.2.3, and CASE3 with the N-BF solution. The SNR values are fixed to $\text{SNR}^{(1)} = \text{SNR}^{(2)} = 10\text{dB}$, and the number of antennas at S1 and S2 is fixed to $M = 2$.

In any case of system capabilities for $L = 1$ antenna at the RS, only one data stream can be transmitted by the $M = 2$ antennas of the source node since the rank of the channel is limited by the minimum of L and M . In the particular case of $L = 1$, this means that only one spatial sub-channel is available for the transmission from the source to the destination node. For $L = 1$ in CASE1 and CASE2 where adaptive BF can be applied at S1 and S2, the sum rate is higher than the sum rate in CASE3 due to the fact that diversity and array gains are provided by the $M = 2$ antennas at the source node and at the destination node. The spatial diversity is provided since the source node transmits from two antennas, and the array gain is provided since the destination node receives with two antennas increasing the overall received power [PNG03]. For CASE3, the sum rate is lower than in CASE1 and CASE2, since S1 and S2 cannot

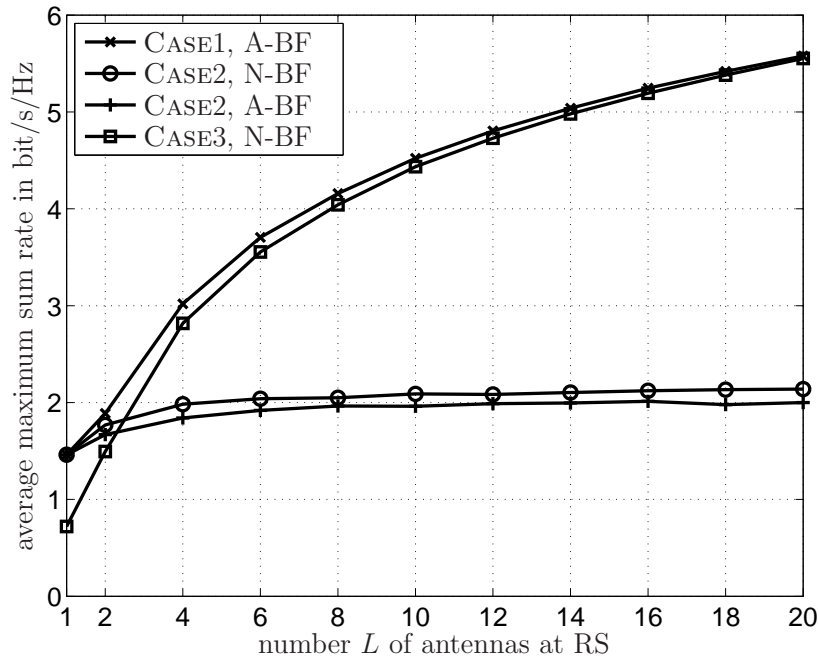


Figure 3.2. Average maximum sum rate vs. number L of antennas at the RS for CASE1, CASE2, and CASE3, $\text{SNR}^{(1)} = \text{SNR}^{(2)} = 10\text{dB}$, $M = 2$.

perform adaptive BF due to their limited SP capabilities and the RS cannot perform adaptive BF since only $L = 1$ antenna is available at the RS. This means that neither diversity and array gain nor spatial multiplexing gain can be expected in a system with limited capabilities at S1 and S2 for $L = 1$.

Increasing the number L of antennas at the RS from $L = 1$ to $L = 2$, provides spatial multiplexing gain for all cases of system capabilities. This can be seen especially for CASE3 where one additional antenna at the RS increases the sum rate by almost 1bit/s/Hz, i.e., one additional data stream may be transmitted for one additional antenna so that two data streams can be transmitted by the source node for $L = 2$. The increase in the sum rate for CASE1 and CASE2 is lower than 1bit/s/Hz, since for $L = 1$ spatial diversity and array gain can already be obtained by BF at the source and destination node. However, for $L = 2$ no spatial diversity and no array gain are exploited in CASE1 and CASE2 but only spatial multiplexing gain. From the fact that the sum rate does not increase by 2bit/s/Hz if the number L of antennas at the RS is increased by two from $L = 2$ to $L = 4$ it can be seen that the full spatial multiplexing gain is already obtained if $L = M$. The maximum spatial multiplexing gain is limited by the minimum number of antennas per node which is given by $M = 2$ at S1 and S2 in Figure 3.2. Nevertheless, for $L > M$ in CASE1 and CASE3, the sum rate increases with increasing number L of antennas at the RS. This increase is coming from the array

gain at the receive antennas of the RS and the spatial diversity for the retransmission from the RS. Furthermore, the sum rate in CASE3 converges to the sum rate in CASE1 for high numbers L of antennas at the RS. For high values of L , the equal weighting with stream-wise encoding and decoding at S1 and S2 in CASE3 performs as well as the adaptive BF at S1 and S2 for $M = 2$ data streams. This means that the spatial separation of the data streams by the BF at the RS in both cases improves with the number L of antennas at the RS since sharper beams may be transmitted by the RS. Simultaneously, the influence of the additional coding gain which can be obtained in CASE1 is decreasing so that the sum rate performances of CASE1 and CASE3 converge.

For $L = M = 2$, CASE2 achieves the full spatial multiplexing gain corresponding to the two transmit and receive antennas at the source and destination node. The performance is slightly better than in CASE3. This shows that spatial precoding at the source node and joint decoding at the destination node provide a coding gain which cannot be obtained by the spatial separation of the data streams by exclusive adaptive BF at the RS. However, with increasing number L of antennas at the RS this drawback of CASE3 can be compensated, and for $L > 3$, CASE3 already outperforms CASE2. For $L > M$, the sum rate of CASE2 is significantly smaller than the sum rates of CASE1 and CASE3, and for $L > 4$ it is even constant. This effect can be explained as follows. For equal weighting at the transmit antennas of the source node, the potential of multiple antennas at the RS is not exploited. In CASE2, increasing the number L of antennas at the RS does not provide array and diversity gains since no adaptation to the current channel fading is applied. In order to achieve some array gain, e.g., maximum-ratio combining [Pro01] would be required for the receive signal at the RS. In order to achieve some diversity gain, e.g., space-time coding [PNG03] applied to the transmit signal of the RS would be required. Since none of these combining and/or diversity techniques are applied at the RS, no gains can be expected. In CASE2, the performance of the proposed analytical BF algorithm of Section 3.2.3 comes very close to the performance of the numerical solution. The performance degradation of the A-BF algorithm comes from the two simplifying assumptions for the A-BF algorithm, namely the assumption of spatially white noise at the destination node and the assumption that the two sub-problems of determining the weighting factor $g^{(k,i)}$ at the RS and determining the power allocation at the source node are independent of each other.

In the following, the sum rate performances of the MMSE-BF, ZF-BF, and MF-BF algorithms in CASE3 derived in Section 3.3 are considered. On the one hand, the sum rates of these BF algorithms which are known from point-to-point transmission shall be compared among each other, and on the other hand the sum rates shall be compared to the maximum achievable sum rate in CASE3 known from the previous two figures. In Figure 3.3, the average sum rate vs. $\text{SNR}^{(2)}$ is depicted for $\text{SNR}^{(1)} = 20\text{dB}$ and

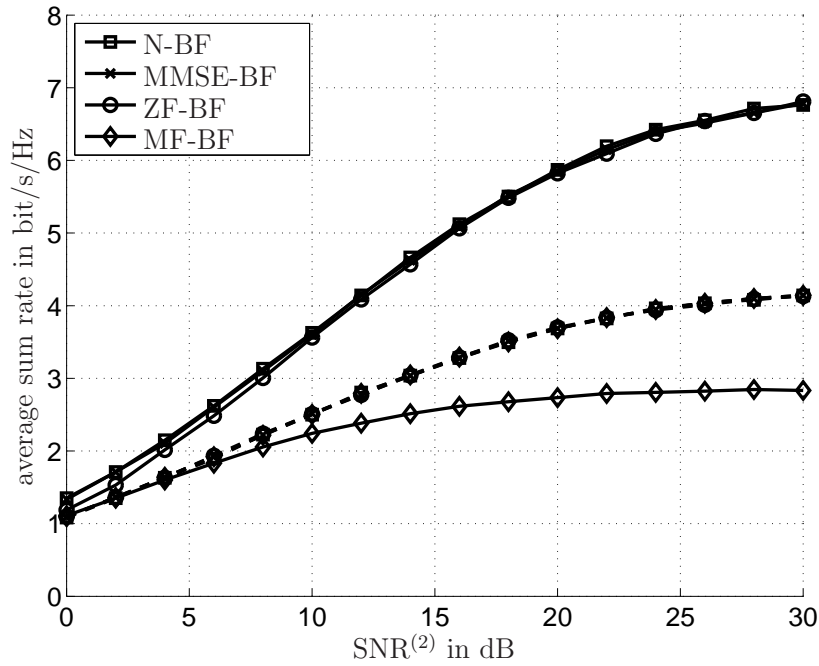


Figure 3.3. Average sum rate vs. $\text{SNR}^{(2)}$ for different BF algorithms in CASE3, $\text{SNR}^{(1)} = 20\text{dB}$, $L = 4$, dashed lines: $M = 1$, solid lines: $M = 2$.

$L = 4$. S1 and S2 are equipped with either $M = 1$ (dashed lines) or $M = 2$ (solid lines) antennas.

For $M = 1$, all BF algorithms provide the same performance. This comes from the fact that intersymbol interference cannot appear if only one data stream is transmitted in each time slot. In this case, the MMSE-BF and the ZF-BF algorithm provide the same BF solution as the MF-BF algorithm which is optimum for $M = 1$. Hence, the three analytical BF algorithms perform as well as the N-BF algorithm. If the number M of antennas at S1 and S2 is increased to $M = 2$, the MMSE-BF algorithm achieves almost the same performance as the numerical solution. In this case, $L = 4$ antennas at the RS may be used in order to separate $M = 2$ data streams. Since there are significantly more antennas at the RS than data streams to transmit, the data streams can be separated very efficiently in space. For the case $M = L$, which is omitted here, it can be shown more clearly that the sum rate performance of the MMSE-BF algorithm is worse than the sum rate performance of the N-BF solution since there are only as much antennas at the RS as data streams to transmit. For $M = 2$, the ZF-BF algorithm has a slightly degraded sum rate performance compared to the MMSE-BF algorithm. Due to the ZF constraint, some power is spent in order to completely suppress the intersymbol interference which reduces the power efficiency compared to the MMSE-BF algorithm which does not completely suppress the intersymbol interference. Obviously

for $M = 2$, the MF-BF algorithm performs considerably worse compared to the MMSE-BF algorithm and the ZF-BF algorithm. This comes from the fact that only the SNR is maximized. Since the intersymbol interference is not considered in case of the MF-BF algorithm, the intersymbol interference increases which leads to a significant performance degradation.

3.4.3 Bit error rate analysis

In this section, the average uncoded bit error rate (BER) of the linear BF algorithms of Section 3.3 for CASE3 is analyzed. The individual uncoded BER corresponds to the ratio of the number of incorrectly detected bits at a destination node divided by the number of overall transmitted bits by the respective source node. Beside the individual uncoded BER at S1 and S2, respectively, the joint uncoded BER of S1 and S2 is of particular interest. It gives the ratio of the sum of incorrectly detected bits at both destination nodes divided by the sum of transmitted bits by both source nodes. All BER results are presented for quadrature phase shift keying (QPSK) modulated data bit streams.

In the following, the average joint uncoded BERs of the MMSE-BF, ZF-BF, and MF-BF algorithm are considered in order to evaluate the performances of the algorithms in case of different numbers of antennas at S1, S2, and the RS. Figure 3.4 gives the average joint uncoded BER vs. $\text{SNR}^{(2)}$ for $M = 1$ antenna at S1 and S2, and $L = 4$ antennas at the RS for two different values of $\text{SNR}^{(1)}$, namely $\text{SNR}^{(1)} = 10\text{dB}$ and $\text{SNR}^{(1)} = 20\text{dB}$. The joint BER is depicted for the three proposed BF algorithms of Section 3.3, namely the MMSE-BF, ZF-BF, and MF-BF algorithm.

In case of $M = 1$ antenna at S1 and S2, only one data stream is transmitted by the source node. For that reason, intersymbol interference does not exist. Without intersymbol interference, the SNR is maximized by all three BF algorithms and, accordingly, the same BER performance is obtained by all algorithms. For $\text{SNR}^{(1)} = 10\text{dB}$, an error floor can be observed in the BER performance. As the sum rate, the joint BER is also limited by the worst value of $\text{SNR}^{(1)}$ and $\text{SNR}^{(2)}$. For $\text{SNR}^{(1)} = 20\text{dB}$, there also exists an error floor, but since $\text{SNR}^{(1)}$ of the channel between S1 and the RS is already relatively high, the error floor is below 10^{-6} and cannot be seen in Figure 3.4.

In the following, the number of antennas at S1 and S2 is increased in order to investigate the impact of intersymbol interference on the performance of the BF algorithms. In Figure 3.5, the average joint uncoded BER vs. $\text{SNR}^{(2)}$ for $M = 2$ antennas at S1 and S2 is given. All other parameters are chosen as introduced for Figure 3.4.

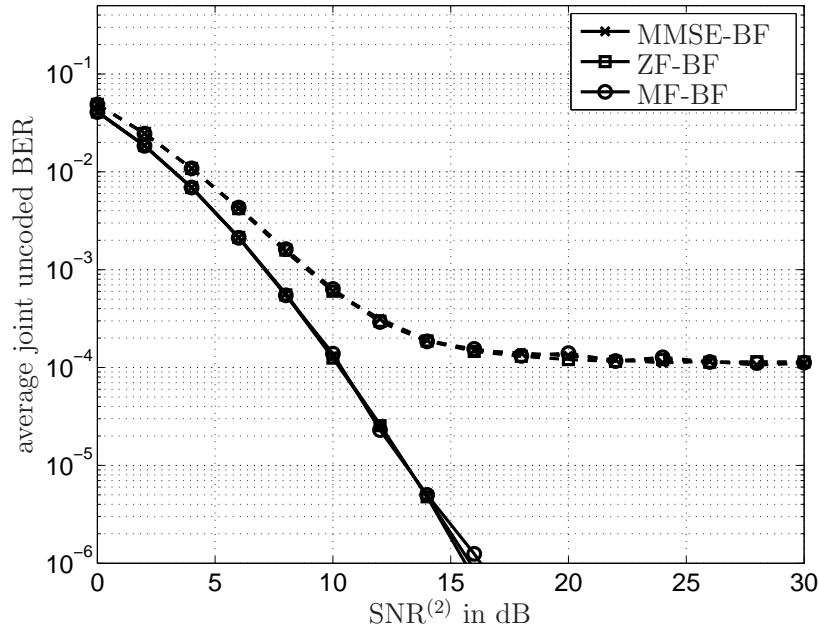


Figure 3.4. Average joint uncoded BER vs. $\text{SNR}^{(2)}$ for different BF algorithms, $M = 1$ and $L = 4$, dashed lines: $\text{SNR}^{(1)} = 10\text{dB}$, solid lines: $\text{SNR}^{(1)} = 20\text{dB}$.

For the parameters of Figure 3.5, the source node transmits two independent data streams and intersymbol interference may appear. Since intersymbol interference is treated differently in the considered BF algorithms, they provide different performance results. As for $M = 1$, the error floor in the BER comes from the limitation by the worst value of $\text{SNR}^{(1)}$ and $\text{SNR}^{(2)}$. Since $M = 2$ data streams have to be separated spatially by the BF algorithms at the RS, the performance of all algorithms is worse than in case of $M = 1$ where the antennas at the RS need not to be used for spatial multiplexing, but can be used exclusively in order to maximize the effective SNR at the destination node. For $M = 2$, the best performance is achieved by the MMSE-BF algorithm. The ZF-BF algorithm comes quite close to this performance. The difference between both BF algorithms comes from the fact that for the ZF-BF algorithm some power is spent in order to completely suppress the intersymbol interference which is unnecessary for the MMSE-BF algorithm. The MF-BF algorithm provides the worst performance due to the disregard of the intersymbol interference.

In the following, the impact of the number of antennas at S1, S2 and the RS on the BER performance is investigated in order to identify diversity and array gains in the BER results. Figure 3.6 exclusively considers the BER performance of the MMSE-BF algorithm for $\text{SNR}^{(1)} = 20\text{dB}$ for four different antenna configurations. The ZF-BF algorithm and the MF-BF algorithm are omitted here since the relative behavior of the performances of the different antenna configurations is the same as for the MMSE-BF

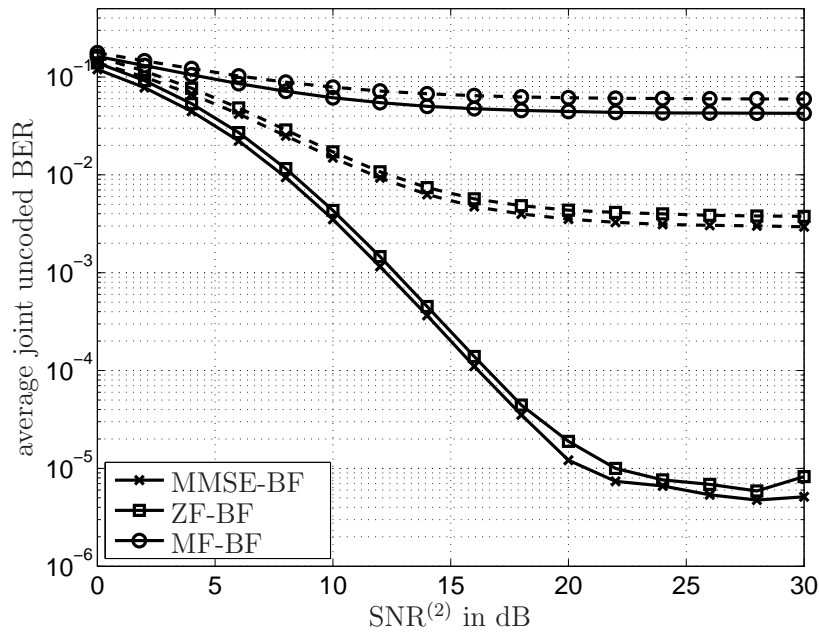


Figure 3.5. Average joint uncoded BER vs. $\text{SNR}^{(2)}$ for different BF algorithms, $M = 2$ and $L = 4$, dashed lines: $\text{SNR}^{(1)} = 10\text{dB}$, solid lines: $\text{SNR}^{(1)} = 20\text{dB}$.

algorithm. The case $M = 1$ antenna at S1 and S2 and $L = 2$ antennas at the RS, provides the worst BER performance. Increasing the number L of antennas at the RS from $L = 2$ to $L = 4$ improves the performance significantly since the BF algorithm provides sharper antenna beams, i.e., the antenna beams can be steered more precisely into the direction of the source and destination nodes. The increase of the slope of the curve corresponds to a diversity gain coming from multiple independent propagation paths and the shift to the left corresponds to an array gain coming from the increased received power at the RS.

If the number M of antennas at S1 and S2 is increased from $M = 1$ to $M = 2$ while L is fixed to $L = 4$, the BER is degraded again since two data streams are transmitted by the source node. This means that the $L = 4$ antennas at the RS are now required in order to multiplex two different data streams in space. Hence, for each single data stream the antenna beam is widened again leading to a performance degradation. Intuitively, it can be assumed for $M = 2$ and $L = 4$ that two antennas at the RS are required in order to multiplex two data streams by BF at the RS and the remaining two antennas can be used to sharpen the antenna beams of the two data streams. Increasing the number L of antennas at the RS also provides a diversity gain which can be seen from the increased slope of the BER curve for $M = 2$ and $L = 4$ compared to the BER curve for $M = 1$ and $L = 2$. Finally, the case $M = 2$ and $L = 8$ provides the best BER performance since the array gain is increased compared to the

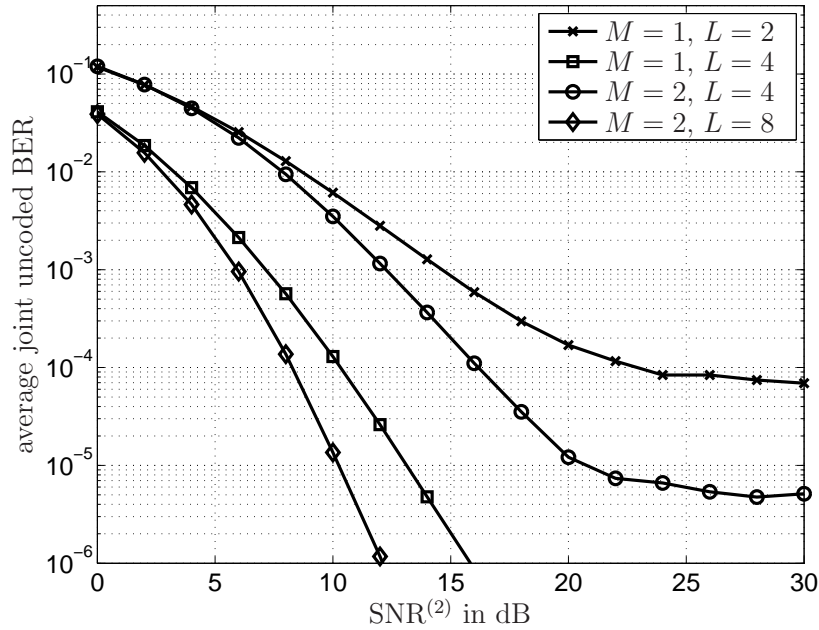


Figure 3.6. Average joint uncoded BER vs. $\text{SNR}^{(2)}$ for MMSE-BF for different antenna configurations, $\text{SNR}^{(1)} = 20\text{dB}$.

case $M = 2$ and $L = 4$ and the diversity gain is increased compared to the case $M = 1$ and $L = 4$.

The introduced joint uncoded BER is strongly influenced by the destination node with the worst channel conditions. Hence, the joint uncoded BER as well as the sum rate reflect the overall system performance of the applied BF algorithms. However, since S1 and S2 are two independent destination nodes, their average individual uncoded BER performances are of interest, too. Thus, the individual BER performances at S1 and S2 are considered in the following. The solid lines in Figure 3.7 give the average individual uncoded BER vs. $\text{SNR}^{(2)}$ at destination node S1 and the dashed lines give the average uncoded BER vs. $\text{SNR}^{(2)}$ at destination node S2 for $\text{SNR}^{(1)} = 10\text{dB}$. Nodes S1 and S2 are equipped with $M = 2$ antennas and the RS is equipped with $L = 4$ and $L = 8$ antennas, respectively.

The results are obtained for the MMSE-BF algorithm, but concerning the relative behavior between the BER at S1 and the BER at S2, the ZF-BF and MF-BF algorithms provide similar results. Furthermore, the BER performances at S1 and S2 show the same relative behavior for $L = 4$ and $L = 8$ so that both cases can be analyzed together. The ratio between the BER at S1 and the BER at S2 depends on the ratio between $\text{SNR}^{(1)}$ and $\text{SNR}^{(2)}$. For $\text{SNR}^{(1)} = \text{SNR}^{(2)} = 10\text{dB}$, both BER values are the same. For $\text{SNR}^{(2)} > \text{SNR}^{(1)}$, the BER at S1 is lower than the BER at S2 and vice versa. While

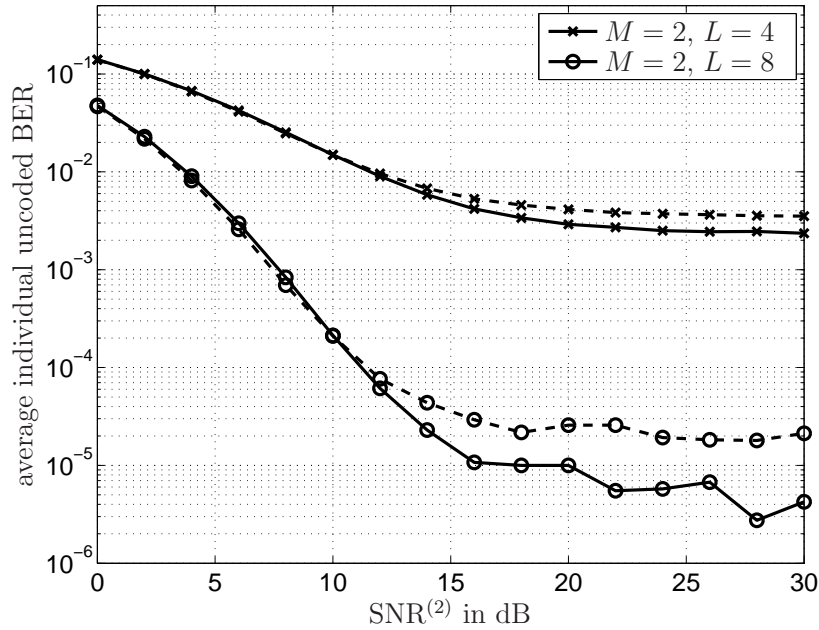


Figure 3.7. Average individual uncoded BER vs. SNR⁽²⁾ for MMSE-BF, SNR⁽¹⁾ = 10dB, dashed lines: BER at S2, solid lines: BER at S1.

SNR⁽²⁾ is the SNR for the first hop of the transmission from S2 to S1, SNR⁽¹⁾ is the SNR for the second hop of the transmission from S2 to S1. This means that the SNR for the first hop has a higher impact on the BER than the SNR for the second hop because bad first hop channel conditions cannot be compensated by good second hop channel conditions. Indeed, a bad SNR for the first hop causes that the high noise value at the RS is amplified and retransmitted on the second hop.

3.5 Conclusions

This chapter has been about linear BF in non-regenerative one-way relaying with multiple-antenna nodes. The sum rate maximization problem has been considered for three different cases of system capabilities which have been newly defined in the framework of Figure 1.4. For a system with full capabilities, a review of the BF algorithm which maximizes the sum rate has been given [Ham06]. For the system with limited capabilities at the RS, a novel sub-optimum analytical BF algorithm has been proposed in order to maximize the sum rate. Furthermore, the BF algorithms which minimize the MSE, minimize the MSE under the ZF constraint, and maximize the SNR by BF at the RS have been newly derived for the system with limited capabilities at

S1 and S2. The analyses of the different proposed BF algorithms provide the following main conclusions:

- The highest sum rate in multi-antenna one-way relaying is only achieved if BF is performed at all nodes of the system. In this case, all nodes have to provide full SP capabilities and need to be provided with global CSI. The optimum BF algorithm can be determined by analytical methods.
- The full spatial multiplexing gain in one-way relaying for independently Rayleigh fading channel coefficients corresponds to the minimum of the number L of antennas at the RS and the number M of antennas at S1 and S2.
- In case of limited capabilities at the RS and in case of limited capabilities at S1 and S2, the maximum sum rate needs to be determined by numerical methods. However, for a system with limited capabilities at S1 and S2, the MMSE-BF algorithm almost achieves the maximum sum rate for equal weighting at the source and destination nodes, respectively.
- For high numbers L of antennas at the RS, the system with limited capabilities at S1 and S2 outperforms the system with limited capabilities at the RS, since BF at the RS provides significant diversity and array gains in addition to the multiplexing gains available in both systems.
- The MMSE-BF algorithm outperforms the ZF-BF algorithm and the MF-BF algorithm in the system with limited capabilities at S1 and S2.

Chapter 4

Two-way relaying

4.1 Introduction

In this chapter, all optimization problems in two-way relaying introduced in the second row of the matrix organization in Figure 1.4 are considered. Firstly, the optimization problems are formulated, and secondly, the respective BF algorithms which solve the problems are derived.

For two-way relaying, four different cases of system capabilities are considered, namely the system with full capabilities, the system with limited capabilities at the RS, the system with limited capabilities at S1 and S2, and the system with local CSI at S1 and S2. The system with local CSI at S1 and S2 which corresponds to the fourth column in Figure 1.4 constitutes an additional case compared to one-way relaying where only the first three cases are considered. The reasons for this additional case are explained in the following. In two-way relaying, a significant performance gain can be obtained if CDI is performed at the destination nodes. In order to perform CDI, local CSI is required at the destination nodes while global CSI is not required. Hence, a system with local CSI at S1 and S2 but without global CSI at S1 and S2 is defined as an additional case of system capabilities compared to one-way relaying where CDI is not required. This system has more capabilities than the system with limited capabilities at S1 and S2 since local CSI is available at the destination nodes so that CDI can be performed, but it has less capabilities than the system with full capabilities since global CSI is not available at S1 and S2 so that no adaptive BF can be applied at S1 and S2.

For all four cases which correspond to the four columns in Figure 1.4, the maximization of the sum rate is considered in Section 4.2. Among those four, the system with full capabilities achieves the highest sum rate since all nodes may apply adaptive BF and CDI can be performed. In the system with limited capabilities at the RS, the RS cannot perform BF while BF and CDI can be applied at S1 and S2. In the system with limited capabilities at S1 and S2, the RS can perform BF, but S1 and S2 cannot perform BF and CDI cannot be applied, too. In the system with local CSI at S1 and S2, the RS can perform BF. Although S1 and S2 cannot perform BF, CDI can be applied at the destination nodes. The limited capabilities in the systems of

the last three columns of Figure 1.4 correspond to additional constraints in the sum rate maximization problems. These constraints are defined in Section 4.2 and included into the optimization problems. There are significant differences in the mathematical structure of the sum rate maximization problems in two-way relaying compared to one-way relaying of Chapter 3. These differences are explained and it is shown that there exist only numerical solutions which maximize the sum rate in two-way relaying for every case of system capabilities. Therefore, either BF algorithms which minimize the effort for the numerical solution, or BF algorithms which provide sub-optimum analytical solutions requiring less effort are proposed depending on the respective system capabilities.

For the system with limited capabilities at S1 and S2 and the system with local CSI at S1 and S2, additional optimization problems whose analytical solutions are known to provide reasonable performance in point-to-point transmissions are newly formulated for two-way relaying in Sections 4.3 and 4.4, respectively. The corresponding BF algorithms solving the problems are derived, too.

The performances of the proposed BF algorithms are investigated in Section 4.5, and the main conclusions of this chapter are drawn in Section 4.6.

4.2 Maximization of the sum rate

4.2.1 General problem formulation

In this Section 4.2, the sum rate maximization problems are considered for the four different cases of system capabilities in two-way relaying, which are denoted in the four columns of the second row in the matrix organization of Figure 1.4. Our work [UK08b] addresses the maximization of the sum rate for a system with full capabilities and a system with limited capabilities at S1 and S2.

In contrast to the one-way relaying scheme, the transmission from S1 to S2 is not orthogonal to the transmission from S2 to S1 since both transmissions are performed within the same time slots. For that reason, the transmission rates $C^{(1)}$ and $C^{(2)}$ are not independent of each other. Maximizing only $C^{(1)}$ would result in a low $C^{(2)}$ and vice versa. From the system perspective, maximizing the sum of both individual transmission rates is a more reasonable optimization goal than maximizing only one

individual transmission rate. The sum rates defined in Section 2.4 can only be maximized by simultaneously adapting the BF matrices $\mathbf{Q}^{(1)}$, $\mathbf{Q}^{(2)}$ and \mathbf{G} at the nodes S1, S2 and at the RS, respectively, introduced in the system model of Figure 2.1. In order to maximize the sum rate in two-way relaying, it may also be beneficial not to exploit the maximum transmit powers of nodes S1 and S2. For a large difference between the individual transmission rates $C^{(1)}$ and $C^{(2)}$ due to different SNRs of the channels $\mathbf{H}^{(1)}$ and $\mathbf{H}^{(2)}$, reducing the transmit power of the node with the higher transmission rate leads only to a small degradation of its own transmission rate while the other node can increase its transmission rate significantly due to the reduced interference of the first node. This fact has to be reflected by the transmit power constraints of nodes S1 and S2. As for one-way relaying, the sum rate in two-way relaying is also maximized if the maximum transmit power of the RS is exploited. From the sum rate definitions in Section 2.4 it is known that the sum rate is always independent of the receive BF matrices $\mathbf{P}^{(1)}$ and $\mathbf{P}^{(2)}$. Thus, $\mathbf{P}^{(1)}$ and $\mathbf{P}^{(2)}$ can be omitted in the sum rate maximization problems.

In the following, a general sum rate maximization problem with transmit power constraints is formulated which can be adapted to each case of system capabilities by introducing additional constraints to the problem and by using the respective sum rate of Section 2.4, i.e., either $C_{\text{BF}}^{(\text{sum})}$ of Eq. (2.15) for adaptive BF at S1 and S2 or $C_{\text{EW}}^{(\text{sum})}$ of Eq. (2.22) for equal weighting at S1 and S2. The general sum rate maximization problem in two-way relaying for the simultaneous transmission from S1 to S2 and from S2 to S1 can be written as follows:

$$\left\{ \mathbf{G}_{\text{opt}}, \mathbf{Q}_{\text{opt}}^{(1)}, \mathbf{Q}_{\text{opt}}^{(2)} \right\} = \arg \max_{\{\mathbf{G}, \mathbf{Q}^{(1)}, \mathbf{Q}^{(2)}\}} C^{(\text{sum})}, \quad (4.1a)$$

$$\text{subject to: } \text{tr} \left\{ \mathbf{Q}^{(i)} \mathbf{R}_{\mathbf{x}^{(i)}} \mathbf{Q}^{(i)\text{H}} \right\} \leq E^{(i)}, \quad i = 1, 2, \quad (4.1b)$$

$$\text{tr} \left\{ \mathbf{G} \left(\sum_{i=1}^2 \mathbf{H}^{(i)} \mathbf{Q}^{(i)} \mathbf{R}_{\mathbf{x}^{(i)}} \mathbf{Q}^{(i)\text{H}} \mathbf{H}^{(i)\text{H}} + \mathbf{R}_{\mathbf{n}^{(0)}} \right) \mathbf{G}^{\text{H}} \right\} = E^{(0)}, \quad (4.1c)$$

where the sum rate is maximized under the two transmit power constraints (4.1b) at the source nodes S_i , $i = 1, 2$, which are inequalities, and the transmit power constraint (4.1c) at the RS which is an equality. In contrast to one-way relaying, the transmit power constraint (4.1c) at the RS includes both transmit BF matrices $\mathbf{Q}^{(1)}$ and $\mathbf{Q}^{(2)}$, since the data streams of S1 and S2 are received simultaneously.

In order to understand some characteristics of two-way relaying in more detail, an equivalent system model of the system introduced in Chapter 2 is proposed in the following. This equivalent system model is only valid for two-way relaying and allows to

describe the simultaneous transmission from S1 and S2 to the RS and the simultaneous retransmission from the RS to S1 and S2. All vectors and matrices corresponding either to S1 or to S2 in the original system model of Figure 2.1 are considered jointly in the equivalent system model. The joint data vector is defined by

$$\mathbf{x} = \left[\mathbf{x}^{(1)\text{T}}, \mathbf{x}^{(2)\text{T}} \right]^{\text{T}}, \quad (4.2)$$

with the joint data covariance matrix

$$\mathbf{R}_{\mathbf{x}} = \text{diag}_{\text{b}} [\mathbf{R}_{\mathbf{x}^{(1)}}, \mathbf{R}_{\mathbf{x}^{(2)}}]. \quad (4.3)$$

The joint transmit BF matrix of the source nodes S1 and S2 is defined by the block diagonal matrix

$$\mathbf{Q} = \text{diag}_{\text{b}} [\mathbf{Q}^{(1)}, \mathbf{Q}^{(2)}]. \quad (4.4)$$

The joint first hop channel matrix \mathbf{H}_{R} for the simultaneous transmission from S1 and S2 to the RS is a concatenation of $\mathbf{H}^{(1)}$ and $\mathbf{H}^{(2)}$ which is given by

$$\mathbf{H}_{\text{R}} = [\mathbf{H}^{(1)}, \mathbf{H}^{(2)}] \in \mathbb{C}^{L \times 2M}. \quad (4.5)$$

Let matrices \mathbf{V}_{R} and \mathbf{U}_{R} contain the right and left eigenvectors of \mathbf{H}_{R} , respectively. Furthermore, let matrix $\Lambda_{\text{R}}^{1/2}$ contain the singular values of \mathbf{H}_{R} . Thus, the SVD of the joint first hop channel \mathbf{H}_{R} yields

$$\mathbf{H}_{\text{R}} = \mathbf{U}_{\text{R}} \Lambda_{\text{R}}^{1/2} \mathbf{V}_{\text{R}}^{\text{H}}. \quad (4.6)$$

The joint second hop channel matrix \mathbf{H}_{T} for the retransmission from the RS to S1 and S2 is a concatenation of $\mathbf{H}^{(2)\text{T}}$ and $\mathbf{H}^{(1)\text{T}}$ which is given by

$$\mathbf{H}_{\text{T}} = \begin{bmatrix} \mathbf{H}^{(2)\text{T}} \\ \mathbf{H}^{(1)\text{T}} \end{bmatrix} \in \mathbb{C}^{2M \times M}. \quad (4.7)$$

Due to the channel reciprocity, \mathbf{H}_{T} is a simple permutation of \mathbf{H}_{R} . Using permutation matrix

$$\mathbf{\Pi} = \begin{bmatrix} \mathbf{0}_{M \times M} & \mathbf{I}_M \\ \mathbf{I}_M & \mathbf{0}_{M \times M} \end{bmatrix}, \quad (4.8)$$

\mathbf{H}_{T} may also be described by

$$\mathbf{H}_{\text{T}} = \mathbf{\Pi} \mathbf{H}_{\text{R}}^{\text{T}}. \quad (4.9)$$

Since the joint second hop channel matrix \mathbf{H}_{T} is a simple permutation of \mathbf{H}_{R} according to Eq. (4.9), the SVD of \mathbf{H}_{T} is just the transpose of the SVD of \mathbf{H}_{R} in Eq. (4.6) and both channels possess the same eigenmodes. Note that the eigenmodes of the joint channel are completely different compared to the eigenmodes of the two individual channels $\mathbf{H}^{(1)}$ and $\mathbf{H}^{(2)}$. In the equivalent system model, the joint receive BF matrix \mathbf{P} at the destination nodes is defined by a block diagonal matrix

$$\mathbf{P} = \text{diag}_{\text{b}} [\mathbf{P}^{(2)}, \mathbf{P}^{(1)}], \quad (4.10)$$

and the joint CDI matrix \mathbf{T} is also given by a block matrix

$$\mathbf{T} = \begin{bmatrix} \mathbf{0}_{M \times M} & \mathbf{T}^{(2)} \\ \mathbf{T}^{(1)} & \mathbf{0}_{M \times M} \end{bmatrix}. \quad (4.11)$$

The joint noise vector

$$\mathbf{n}_R = \left[\mathbf{n}_R^{(2)\text{T}}, \mathbf{n}_R^{(1)\text{T}} \right]^T, \quad (4.12)$$

denotes the overall noise vector of S2 and S1 with joint noise covariance matrix

$$\mathbf{R}_{\mathbf{n}_R} = \text{diag}_{\mathcal{G}_b} \left[\mathbf{R}_{\mathbf{n}_R^{(1)}}, \mathbf{R}_{\mathbf{n}_R^{(2)}} \right]. \quad (4.13)$$

With the definitions of Eqs. (4.2) to (4.13), the joint estimated data vector

$$\hat{\mathbf{x}} = \left[\hat{\mathbf{x}}^{(1)\text{T}}, \hat{\mathbf{x}}^{(2)\text{T}} \right]^T, \quad (4.14)$$

may be described by

$$\hat{\mathbf{x}} = \mathbf{P} \left((\mathbf{H}_T \mathbf{G} \mathbf{H}_R \mathbf{Q} + \mathbf{T}) \mathbf{x} + \mathbf{H}_T \mathbf{G} \mathbf{n}^{(0)} + \mathbf{n}_R \right). \quad (4.15)$$

While Eq. (2.11) gives an individual description of each direction of the transmission, Eq. (4.15) gives a joint description of both directions of the transmission. Depending on the considered problem either the individual description or the joint description is preferable.

4.2.2 System with full capabilities

In this section, the sum rate maximization problem (4.1) in two-way relaying for a system with full capabilities is considered, cf. the second row and first column of Figure 1.4. In this system, adaptive BF may be performed at all nodes since global CSI is available at all nodes and all nodes have full SP capabilities. Hence, the sum rate is determined by Eq. (2.15). Furthermore, the duplex interference can be completely cancelled by CDI at the destination nodes by choosing CDI matrix $\mathbf{T}^{(k)}$ according to Eq. (2.27), which is introduced as an additional constraint to the general problem formulation (4.1). With these constraints on the system with full capabilities, problem (4.1) may be rewritten as follows:

$$\left\{ \mathbf{G}_{\text{opt}}, \mathbf{Q}_{\text{opt}}^{(1)}, \mathbf{Q}_{\text{opt}}^{(2)} \right\} = \arg \max_{\{\mathbf{G}, \mathbf{Q}^{(1)}, \mathbf{Q}^{(2)}\}} C_{\text{BF}}^{(\text{sum})}, \quad (4.16a)$$

$$\text{subject to: } \mathbf{T}^{(k)} = -\mathbf{P}^{(k)} \mathbf{H}^{(k)\text{T}} \mathbf{G} \mathbf{H}^{(k)} \mathbf{Q}^{(k)}, \quad k = 1, 2, \quad (4.16b)$$

$$\text{tr} \left\{ \mathbf{Q}^{(i)} \mathbf{R}_{\mathbf{x}^{(i)}} \mathbf{Q}^{(i)\text{H}} \right\} \leq E^{(i)}, \quad i = 1, 2, \quad (4.16c)$$

$$\text{tr} \left\{ \mathbf{G} \left(\sum_{i=1}^2 \mathbf{H}^{(i)} \mathbf{Q}^{(i)} \mathbf{R}_{\mathbf{x}^{(i)}} \mathbf{Q}^{(i)\text{H}} \mathbf{H}^{(i)\text{H}} + \mathbf{R}_{\mathbf{n}^{(0)}} \right) \mathbf{G}^{\text{H}} \right\} = E^{(0)}. \quad (4.16d)$$

In order to give an upper bound for the achievable sum rate in two-way relaying, the individual description of each direction of the transmission given by the system model of Eq. (2.11) is used. Let us concentrate on a single receive node S_k for that purpose. On the one hand, S_k may cancel the duplex interference of its own data streams by CDI so that it is not disturbed by the simultaneous retransmission into both directions by the RS. However, from the perspective of destination node S_k the RS wastes some part of its overall available transmit power in order to retransmit already known data streams yielding $\mathbf{D}^{(k)}\mathbf{x}^{(k)}$ in Eq. (2.11). Hence, the individual transmission rate for the transmission from S_i to S_k in two-way relaying is smaller than the individual transmission rate for the transmission from S_i to S_k in one-way relaying where all the available transmit power at the RS can be used to transmit the unknown data streams yielding $(\mathbf{A}^{(k)} + \mathbf{F}^{(k)})\mathbf{x}^{(i)}$ in Eq. (2.11). For that reason, an upper bound for the achievable sum rate in two-way relaying is given by the sum of the two individual transmission rates coming from the orthogonal transmission in one-way relaying where each direction of transmission is optimized independently.

The maximum sum rate in two-way relaying is achieved if the maximum spatial multiplexing gain is exploited. In order to give the maximum spatial multiplexing gain in two-way relaying, the joint description of both directions of the transmission by Eq. (4.15) is used. Since the sum rate is linked with both directions of the transmission, the joint description of Eq. (4.15) allows to consider the maximum spatial multiplexing gain in two-way relaying. The maximum spatial multiplexing gain corresponds to the number of independent sub-channels of the simultaneously used radio channels. For that reason, the maximum spatial multiplexing gain is given by the rank of the joint channels \mathbf{H}_R and \mathbf{H}_T which is the same for both channels due to the identity of Eq. (4.9). Assuming that all channel coefficients are uncorrelated, the rank of the joint channels \mathbf{H}_R and \mathbf{H}_T corresponds to the minimum of L and $2M$, i.e., the maximum spatial multiplexing gain in two-way relaying is given by the minimum of L and $2M$.

In order to provide an insight into the BF algorithm which maximizes the sum rate in two-way relaying, the corresponding BF algorithm for one-way relaying introduced in Section 3.2.2 is reviewed. As shown in Section 3.2.2, the sum rate in one-way relaying is maximized by BF matrices adapted to the eigenmodes of the first hop channel $\mathbf{H}^{(i)}$ and by BF matrices adapted to the eigenmodes of the second hop channel $\mathbf{H}^{(k)T}$. Applying these adaptations to the eigenmodes, the two channels can be separated into their spatial sub-channels. In two-way relaying, S_1 and S_2 transmit simultaneously to the RS over two independent first hop channels $\mathbf{H}^{(1)}$ and $\mathbf{H}^{(2)}$. These transmissions correspond to a multiple access phase in two-way relaying. Due to this multiple access phase, the BF at the RS cannot be adapted simultaneously to the independent eigenmodes of the two first hop channels. Furthermore, in two-way relaying the RS transmits

simultaneously to S1 and S2 over two independent second hop channels $\mathbf{H}^{(1)\text{T}}$ and $\mathbf{H}^{(2)\text{T}}$. These transmissions correspond to a broadcast phase in two-way relaying. As in the multiple access phase, the BF at the RS cannot be adapted simultaneously to the eigenmodes of the two second hop channels in the broadcast phase. Nevertheless, in two-way relaying, an adaptation to the eigenmodes of the joint first hop channel and the joint second hop channel with the SVD of Eq. (4.6) could be performed at the RS. However, since the source nodes S1 and S2 do not cooperate with each other, the joint transmit BF matrix \mathbf{Q} of Eq. (4.4) cannot be adapted to the joint channels. The problem of optimizing block diagonal matrix \mathbf{Q} with sub-matrices $\mathbf{Q}^{(1)}$ and $\mathbf{Q}^{(2)}$ corresponds to a multiple access problem which has even no closed-form solution in point-to-point transmission [KBB⁺05]. In conjunction with the optimization of the BF matrix \mathbf{G} at the RS, the multiple access problem even becomes more complicated. To the best of the author's knowledge, the optimum BF matrices $\mathbf{Q}^{(1)}$, $\mathbf{Q}^{(2)}$, and \mathbf{G} solving the sum rate maximization problem (4.16) can only be determined by numerical methods.

Although there exist only numerical solutions to the sum rate maximization problem (4.16) in the system with full capabilities, the optimization problem can be transformed into an equivalent and simpler optimization problem, if the RS is equipped with more antennas than the sum of the antennas at S1 and S2, i.e., if $L > 2M$. The proposed transformation is based on a similar approach introduced in one-way relaying for the system with limited capabilities at S1 and S2 in Section 3.2.4. For the transformation, the joint description of both directions of the transmission according to Eq. (4.15) is required. For $L > 2M$, let matrices $\tilde{\mathbf{U}}_{\text{R}} \in \mathbb{C}^{L \times 2M}$ and $\bar{\mathbf{U}}_{\text{R}} \in \mathbb{C}^{L \times (L-2M)}$ contain the first $2M$ left eigenvectors corresponding to the range of \mathbf{H}_{R} and the last $L - 2M$ left eigenvectors corresponding to the null space of \mathbf{H}_{R} , respectively. Thus, the SVD of the joint first hop channel \mathbf{H}_{R} may be rewritten as

$$\mathbf{H}_{\text{R}} = \left[\tilde{\mathbf{U}}_{\text{R}}, \bar{\mathbf{U}}_{\text{R}} \right] \begin{bmatrix} \Lambda_{\text{R}}^{1/2} \\ \mathbf{0}_{(L-2M) \times M} \end{bmatrix} \mathbf{V}_{\text{R}}^{\text{H}}. \quad (4.17)$$

For $L > 2M$, the joint channels \mathbf{H}_{R} and \mathbf{H}_{T} have only a maximum of $2M$ eigenmodes while $\mathbf{G} \in \mathbb{C}^{L \times L}$ could be adapted to L eigenmodes. Hence, there are linear dependencies between the variables in \mathbf{G} . These linear dependencies may be removed by the following BF approach. The BF matrix \mathbf{G} is separated into three parts, namely the receive BF matrix $\mathbf{G}_{\text{R}} \in \mathbb{C}^{2M \times L}$, the transmit BF matrix $\mathbf{G}_{\text{T}} \in \mathbb{C}^{L \times 2M}$ and an unknown matrix $\tilde{\mathbf{G}} \in \mathbb{C}^{2M \times 2M}$, yielding

$$\mathbf{G} = \mathbf{G}_{\text{T}} \tilde{\mathbf{G}} \mathbf{G}_{\text{R}}. \quad (4.18)$$

The receive BF matrix \mathbf{G}_{R} is used as a projection to the range of the joint first hop channel \mathbf{H}_{R} which has only $2M$ dimensions. Furthermore, the transmit BF matrix \mathbf{G}_{T}

is used as a projection to the range of the joint second hop channel \mathbf{H}_T which has only $2M$ dimensions, too. Since matrix $\tilde{\mathbf{U}}_R$ of Eq. (4.17) forms an orthogonal basis for the range of \mathbf{H}_R , it may be used as an adaptation to the non-zero eigenmodes of the joint first hop channel \mathbf{H}_R , which leads to the following choice of \mathbf{G}_R :

$$\mathbf{G}_R = \tilde{\mathbf{U}}_R^H. \quad (4.19)$$

Since matrix $\tilde{\mathbf{U}}_R^T$ forms an orthogonal basis for the range of \mathbf{H}_T , it may be used as an adaptation to the non-zero eigenmodes of the joint second hop channel \mathbf{H}_T , which leads to the following choice of \mathbf{G}_T :

$$\mathbf{G}_T = \tilde{\mathbf{U}}_R^*. \quad (4.20)$$

Due to the unitary BF by the matrices $\tilde{\mathbf{U}}_R^H$ and $\tilde{\mathbf{U}}_R^*$, the non-zero eigenmodes of the joint first hop channel \mathbf{H}_R and the joint second hop channel \mathbf{H}_T are preserved. By the BF approach of Eqs. (4.18) to (4.20) the original sum rate maximization problem (4.16) with BF matrix \mathbf{G} is transformed into an equivalent optimization problem where the unknown BF matrix \mathbf{G} is replaced by the unknown BF matrix $\tilde{\mathbf{G}}$. Since BF matrix $\tilde{\mathbf{G}}$ only contains $(2M)^2$ complex optimization variables, the equivalent optimization problem is simpler compared to the original one where BF matrix \mathbf{G} contains L^2 complex optimization variables. Nevertheless, BF matrix $\tilde{\mathbf{G}}$ has to be determined by numerical methods.

In the following, a sub-optimum analytical BF algorithm for the particular case of single-antenna S1 and S2, i.e., $M = 1$, is proposed which comes close to the performance of the numerical solution of the sum rate maximization problem. For $M = 1$, the transmit BF matrices at S1 and S2 are reduced to scalar weighting factors. The weighting factors are chosen to fulfill the transmit power constraints at source nodes S_i with equality yielding $\mathbf{Q}^{(i)} = q^{(i)} = \sqrt{E^{(i)}}$, for $i = 1, 2$. Note that assuming equality in the transmit power constraints at source nodes S_i is already a sub-optimum approach which reduces the complexity of the problem. For $M = 1$, channel matrices $\mathbf{H}^{(i)}$ and $\mathbf{H}^{(k)T}$ are reduced to channel vectors $\mathbf{H}^{(i)} = \mathbf{h}^{(i)}$ and $\mathbf{H}^{(k)T} = \mathbf{h}^{(k)T}$, respectively. The duplex interference indicated by $\mathbf{D}^{(k)}$ in Eq. (2.11) is always cancelled by CDI at the destination nodes. Furthermore, there exists no intersymbol interference indicated by $\mathbf{F}^{(k)}$ in Eq. (2.11), since only one data stream is transmitted per source node. Without interference, the SINR value of Eq. (2.20) reduces to a SNR value and the transmission rate $C_{\text{BF}}^{(k)}$ of Eq. (2.14) equals the transmission rate $C_{\text{EW}}^{(k)}$ of Eq. (2.21). For the sub-optimum BF algorithm, it is proposed to adapt the BF at the RS to the joint first hop and joint second hop channel. For that purpose, the BF matrix \mathbf{G} at the RS is again decomposed into three parts according to Eq. (4.18). Firstly, matrices \mathbf{G}_R and \mathbf{G}_T are determined in order to maximize the SNR of the first hop transmissions and

the second hop transmissions, respectively. Secondly, matrix $\tilde{\mathbf{G}}$ is used to combine the SNR maximization of the first and second hop.

Matrices \mathbf{G}_R and \mathbf{G}_T are determined as follows: The receive SNR of data symbol $x_1^{(i)}$ at the RS is maximized for the receive MF $\mathbf{h}^{(i)H}$ matched to channel $\mathbf{h}^{(i)}$ [Pro01]. Hence, the overall receive MF matrix \mathbf{G}_R applied to the two received data streams of the RS is a concatenation of the MFs to channels $\mathbf{h}^{(1)}$ and $\mathbf{h}^{(2)}$ given by

$$\mathbf{G}_R = \begin{bmatrix} \mathbf{h}^{(1)H} \\ \mathbf{h}^{(2)H} \end{bmatrix}. \quad (4.21)$$

The receive SNR at node Sk for data symbol $x_1^{(i)}$ is maximized for the transmit MF $\mathbf{h}^{(k)*}$ matched to channel $\mathbf{h}^{(k)T}$ [Cav00]. Hence, the overall transmit MF matrix \mathbf{G}_T applied to the two transmitted data streams of the RS is a concatenation of the MFs to channels $\mathbf{h}^{(2)T}$ and $\mathbf{h}^{(1)T}$ given by

$$\mathbf{G}_T = [\mathbf{h}^{(2)*}, \mathbf{h}^{(1)*}]. \quad (4.22)$$

After maximizing the SNR of the first hop and the second hop transmission by the MFs of Eqs. (4.21) and (4.22), the optimum linear combination of the two received data streams at the RS has to be determined in order to maximize the sum rate. The optimum linear combination is described by matrix $\tilde{\mathbf{G}} \in \mathbb{C}^{2 \times 2}$ consisting of four complex optimization variables and can only be determined by numerical methods. Since there are only two data streams at the RS, the following approximation can be performed: Instead of finding the optimum linear combination, simply different powers could be allocated to the two data streams. This leads to the following simplification of matrix $\tilde{\mathbf{G}}$:

$$\tilde{\mathbf{G}} = \text{diag}[w_1, w_2], \quad (4.23)$$

with real-valued power allocation factors $w_1 \in \mathbb{R}^+$ and $w_2 \in \mathbb{R}^+$. With this simplification, the number of optimization variables in the numeric optimization is further reduced to two real-valued power allocation factors. In the following, an analytical approach for determining the power allocation factors is proposed. With the receive and transmit MFs of Eqs. (4.21) and (4.22), respectively, the transmission rates $C_{\text{BF}}^{(k)}$ of Eq. (2.21) result in

$$C_{\text{BF}}^{(k)} = \frac{1}{2} \log_2 \left(1 + \frac{E^{(i)} |\mathbf{h}^{(i)}|^4 |\mathbf{h}^{(k)}|^4 w_i^2}{\sigma_{\mathbf{n}^{(0)}}^2 \mathbf{h}^{(k)T} \mathbf{G} \mathbf{G}^H \mathbf{h}^{(k)*} + \sigma_{\mathbf{n}_R}^{(k)}} \right), \quad i = 1, 2. \quad (4.24)$$

For \mathbf{G} of Eq. (4.18) and $\tilde{\mathbf{G}}$ of Eq. (4.23), the filtered noise of the RS which is the first summand in the denominator of Eq. (4.24) depends on w_i and w_k . With respect to the absolute value $|\mathbf{h}^{(k)}|$, this first summand is a polynomial of the order four.

Considering only the summand of the highest order, i.e., $|\mathbf{h}^{(k)}|^4$, which is the dominant one, Eq. (4.24) may be approximated by

$$C_{\text{BF}}^{(k)} \approx \frac{1}{2} \log_2 \left(1 + \frac{E^{(i)} |\mathbf{h}^{(i)}|^4 |\mathbf{h}^{(k)}|^4 w_i^2}{\sigma_{\mathbf{n}^{(0)}}^2 |\mathbf{h}^{(k)}|^4 w_i^2 + \sigma_{\mathbf{n}^{(k)}}^2} \right). \quad (4.25)$$

Now, the transmission rate $C_{\text{BF}}^{(k)}$ only depends on power allocation factor w_i . For maximizing the sum rate of Eq. (4.25) under the RS power constraint (4.1c), power allocation factor w_i can be determined by Lagrangian optimization. Since Eq. (4.25) has the same structure as Eq. (3.7), the derivation of the power allocation factor w_i is similar to the derivation of the power allocation factors in Eq. (3.10). Thus, the derivation is omitted here. With

$$\nu^{(i)} = E^{(i)} \frac{|\mathbf{h}^{(i)}|^2}{|\mathbf{h}^{(k)}|^4}, \quad (4.26)$$

and

$$\rho^{(k)} = \frac{\sigma_{\mathbf{n}^{(k)}}^2}{\sigma_{\mathbf{n}^{(0)}}^2}, \quad (4.27)$$

the power allocation factors w_i , $i = 1, 2$, result in

$$w_i^2 = \frac{\left[\sqrt{\left(\frac{\rho^{(k)} \nu^{(i)}}{2} \right)^2 + \tilde{\mu} \rho^{(k)} \nu^{(i)}} - \frac{\rho^{(k)} \nu^{(i)}}{2} - \frac{\sigma_{\mathbf{n}^{(k)}}^2}{|\mathbf{h}^{(k)}|^4} \right]^+}{E^{(i)} |\mathbf{h}^{(i)}|^4 + \sigma_{\mathbf{n}^{(0)}}^2 |\mathbf{h}^{(i)}|^2}. \quad (4.28)$$

The Lagrangian multiplier $\tilde{\mu}$ has to be chosen such that the RS power constraint (4.1c) is satisfied. With w_i of Eq. (4.28), $\tilde{\mathbf{G}}$ of Eq. (4.23), \mathbf{G}_T of Eq. (4.22), and \mathbf{G}_R of Eq. (4.21), the sub-optimum BF matrix \mathbf{G} of Eq. (4.18) can be determined for $M = 1$.

A similar sub-optimum BF algorithm which combines receive and transmit MFs for $M = 1$ in two-way relaying is proposed in [LZ08], namely maximal-ratio reception maximal-ratio transmission (MRR-MRT). In MRR-MRT two-way relaying, also receive and transmit MFs as given by Eqs. (4.21) and (4.22) are used at the RS, but the combination of the two independent MF solutions by an adaptation of matrix $\tilde{\mathbf{G}}$ is omitted. This means that $\tilde{\mathbf{G}} = w \mathbf{I}_2$ is chosen inherently in [LZ08], where $w \in \mathbb{R}^+$ is chosen to satisfy the RS transmit power constraint (4.1c). In the performance evaluation of Section 4.5, it is shown that MRR-MRT two-way relaying only performs well if the SNRs of the channels $\mathbf{h}^{(1)}$ and $\mathbf{h}^{(2)}$ are in a similar range.

4.2.3 System with limited capabilities at the RS

In this section, a BF algorithm for the maximization of the sum rate in problem (4.1) is proposed for a system with limited capabilities at the RS. The optimization problem

is introduced in the second row and the second column of Figure 1.4. In a system with limited capabilities at the RS, S1 and S2 can perform adaptive BF. Furthermore, the duplex interference can be completely cancelled by CDI at the destination nodes by choosing CDI matrix $\mathbf{T}^{(k)}$ according to Eq. (2.27). Due to the joint precoding and the joint decoding, the sum rate is determined by Eq. (2.15). Since no CSI is available at the RS and since the RS has only limited SP capabilities, the RS cannot retransmit linear combinations of the received data streams of each receive antenna, but at each antenna of the RS its received data stream is only amplified by a positive real-valued weighting factor g , which is equal for all antennas and chosen to satisfy the RS transmit power constraint (4.1c). In this case, the BF matrix at the RS simplifies to

$$\mathbf{G} = g\mathbf{I}, \quad g \in \mathbb{R}^+. \quad (4.29)$$

With these constraints on the system with limited capabilities at the RS, problem (4.1) may be rewritten as follows:

$$\left\{ g_{\text{opt}}, \mathbf{Q}_{\text{opt}}^{(1)}, \mathbf{Q}_{\text{opt}}^{(2)} \right\} = \arg \max_{\{g, \mathbf{Q}^{(1)}, \mathbf{Q}^{(2)}\}} C_{\text{BF}}^{(\text{sum})}, \quad (4.30a)$$

$$\text{subject to: } \mathbf{T}^{(k)} = -g\mathbf{P}^{(k)}\mathbf{H}^{(k)\text{T}}\mathbf{H}^{(k)}\mathbf{Q}^{(k)}, \quad k = 1, 2, \quad (4.30b)$$

$$\text{tr} \left\{ \mathbf{Q}^{(i)}\mathbf{R}_{\mathbf{x}^{(i)}}\mathbf{Q}^{(i)\text{H}} \right\} \leq E^{(i)}, \quad i = 1, 2, \quad (4.30c)$$

$$\text{tr} \left\{ g^2 \left(\sum_{i=1}^2 \mathbf{H}^{(i)}\mathbf{Q}^{(i)}\mathbf{R}_{\mathbf{x}^{(i)}}\mathbf{Q}^{(i)\text{H}}\mathbf{H}^{(i)\text{H}} + \mathbf{R}_{\mathbf{n}^{(0)}} \right) \right\} = E^{(0)}. \quad (4.30d)$$

Since the RS cannot apply BF, an adaptation to the eigenmodes of the joint first hop channel \mathbf{H}_{R} of Eq. (4.5) and the joint second hop channel \mathbf{H}_{T} of Eq. (4.7) as introduced in Section 4.2.2 is not possible in order to solve problem (4.30). Furthermore, the weighting factor g directly depends on the two BF matrices $\mathbf{Q}^{(1)}$ and $\mathbf{Q}^{(2)}$ via the RS transmit power constraint (4.1c) which requires a joint optimization of $\mathbf{Q}^{(1)}$, $\mathbf{Q}^{(2)}$ and g . This optimization requires numerical methods, and since problem (4.30) in its current formulation is neither convex nor concave [BV04], several minima or maxima may exist. As numerical methods require high computational effort, analytical solutions are desired which require less computational effort.

In the following, a new sub-optimum analytical BF algorithm for the maximization of the sum rate in case of limited capabilities at the RS is proposed which is based on the algorithm introduced for one-way relaying in Section 3.2.3. In the one-way relaying case, the sum rate can be maximized by maximizing each transmission rate $C_{\text{BF}}^{(k)}$ of Eq. (2.14) individually due to the orthogonality of the transmissions. In two-way relaying, the transmissions from S1 to S2 and from S2 to S1 are no longer orthogonal. However, due to the fact that the RS only performs a weighting of the received

data streams by the scalar g and due to the fact that CDI is applied at the destination nodes, the two transmission rates are only coupled via the RS transmit power constraint (4.1c). For both transmissions from S1 to S2 as well as from S2 to S1, the overall channel between source node S_i and destination node S_k is just a multiplication of the respective first hop channel $\mathbf{H}^{(i)}$ with the respective second hop channel $\mathbf{H}^{(k)\text{T}}$ scaled by weighting factor g . Except for the retransmission of the noise and the coupling by the adaptive weighting factor g at the RS, the two transmissions in a system with limited capabilities at the RS correspond to a point-to-point transmission from the source node to the destination node using the overall channels $\mathbf{H}^{(k,i)}$ of Eq. (3.13) for $i = 1, 2$. Thus, the well-known BF algorithm which maximizes the transmission rate in point-to-point transmissions [PNG03] is adapted to two-way relaying in a system with limited capabilities at the RS in the following. For simplification, it is assumed that source nodes S1 and S2 both transmit with their maximum available transmit power. The BF matrices $\mathbf{Q}^{(i)}$ and $\mathbf{P}^{(k)}$ are chosen as proposed for the respective one-way relaying problem yielding Eqs. (3.17) and (3.18), respectively. Following the steps in one-way relaying from Section 3.2.3, the sum rate maximization problem (4.30) for a system with limited SP capabilities at the RS in two-way relaying results in

$$\{g_{\text{opt}}, s_{m,\text{opt}}^{(1)}, s_{m,\text{opt}}^{(2)}\} = \arg \max_{\{g, s_m^{(1)}, s_m^{(2)}\}} \frac{1}{2} \sum_{i=1}^2 \sum_{m=1}^M \log_2 \left(1 + \frac{g_{\text{opt}}^2}{\sigma_{\tilde{\mathbf{n}}_{\text{R}}}^2} \lambda_m^{(k,i)} s_m^{(i)2} \right), \quad (4.31a)$$

$$\text{subject to: } \sum_{m=1}^M s_m^{(i)2} = E^{(i)}, \quad i = 1, 2, \quad (4.31b)$$

$$g^2 \text{tr} \left\{ \sum_{i=1}^2 \mathbf{H}^{(i)} \mathbf{V}^{(k,i)} \mathbf{S}^{(i)} \mathbf{S}^{(i)\text{H}} \mathbf{V}^{(k,i)\text{H}} \mathbf{H}^{(i)\text{H}} + \mathbf{R}_{\mathbf{n}^{(0)}} \right\} = E^{(0)}, \quad (4.31c)$$

where all variables are defined in the same way as introduced in Section 3.2.3. In problem (4.31), the weighting factor g at the RS and the power allocation factors $s_m^{(i)}$ at both source nodes S_i , $i = 1, 2$, have to be optimized jointly.

It is proposed to approximate problem (4.31) by separating it into two independent sub-problems which are solved alternately. Firstly, the sub-problem of satisfying the RS transmit power constraint (4.31c) by weighting factor g is solved for fixed power allocation factors $s_m^{(i)}$ at source nodes S_i , $i = 1, 2$. By using the constraint (4.31c), g is calculated as

$$g = \sqrt{\frac{E^{(0)}}{\text{tr} \left\{ \sum_{i=1}^2 \mathbf{H}^{(i)} \mathbf{V}^{(k,i)} \mathbf{S}^{(i)} \mathbf{S}^{(i)\text{H}} \mathbf{V}^{(k,i)\text{H}} \mathbf{H}^{(i)\text{H}} + \mathbf{R}_{\mathbf{n}^{(0)}} \right\}}}. \quad (4.32)$$

As in one-way relaying, the initial power allocation factors at S1 and S2 are very important because if a sub-channel is allocated zero power initially, it will never be used. For that reason, it is proposed to start with an equal power allocation to the sub-channels at S_i which means that no sub-channel is preferred in the beginning, i.e., $s_m^{(i)2} = \frac{E^{(i)}}{M}$. Secondly, the sub-problem with objective function (4.31a) and constraint (4.31b) is solved for the fixed weighting factor g at the RS. Since $C_{\text{BF}}^{(1)}$ only depends on $s_m^{(2)}$ and $C_{\text{BF}}^{(2)}$ only depends on $s_m^{(1)}$, both transmission rates in the sum of Eq. (4.31a) can be maximized independently, yielding two typical waterfilling problems, which can be solved in parallel. The solutions to the power allocation factors $s_m^{(i)2}$, $i = 1, 2$, are given by

$$s_m^{(i)2} = \left(\mu^{(i)} - \frac{\sigma_{\tilde{\mathbf{n}}_{\text{R}}^{(k)}}^2}{g^2 \lambda^{(k,i)}} \right)^+, \quad i = 1, 2, \quad (4.33)$$

[PF05]. The coefficients $s_m^{(i)2}$ and the waterfilling levels $\mu^{(i)}$ are found by the well-known iterative waterpouring algorithm [PF05] where $\mu^{(1)}$ and $\mu^{(2)}$ are chosen to satisfy the transmit power constraints (4.31b) at source nodes S1 and S2, respectively. After the power allocation factors $s_m^{(i)}$, for $i = 1, 2$, and the corresponding power allocation matrices $\mathbf{S}^{(i)}$, for $i = 1, 2$, have been determined, the weighting factor g can be determined from Eq. (4.32) again. This alternation between the two sub-problems is repeated until the solutions to $s_m^{(i)}$ and g do not change more than tolerated by a predefined accuracy. Typically, two to four alternations are required in order to obtain a relative change of g which is less than 10^{-4} . Since the optimization result depends on the initial power allocation at S1 and S2, it cannot be guaranteed that the alternation between the calculation of weighting factor g and the calculation of the power allocation factors $s_m^{(1)}$ and $s_m^{(2)}$ at S1 and S2 yields an optimum of the relaxed problem (4.31).

4.2.4 System with limited capabilities at S1 and S2

In this section, the sum rate maximization problem of Eq. (4.1) for a system with limited capabilities at S1 and S2 in two-way relaying is considered. The problem is depicted in the second row and third column of Figure 1.4. In such a system without CSI at the source nodes S_i , $i = 1, 2$, each source node uses the maximum available transmit power $E^{(i)}$ and assigns the same weighting factor $q^{(i)}$, $i = 1, 2$, to all its transmit antennas and from each transmit antenna one data stream is transmitted. Thus, the transmit power constraints of Eq. 4.1b are satisfied with equality and the BF matrices $\mathbf{Q}^{(i)}$, $i = 1, 2$, simplify to

$$\mathbf{Q}^{(i)} = q^{(i)} \mathbf{I}_M, \quad i = 1, 2. \quad (4.34)$$

The destination nodes cannot perform a joint decoding of the received data streams since no CSI is available at S1 and S2. Due to the equal weighting by a single scalar $p^{(k)}$, $k = 1, 2$, at all receive antennas of S_k , the receive BF matrices $\mathbf{P}^{(k)}$ simplify to

$$\mathbf{P}^{(k)} = p^{(k)} \mathbf{I}_M, \quad k = 1, 2. \quad (4.35)$$

As in one-way relaying, the scalar weighting factor $p^{(k)}$ does not influence the transmission rate for the transmission from S_i to S_k . Due to the equal weighting, the sum rate in the system with limited capabilities at S1 and S2 is given by Eq. (2.22). Since no CSI is available at S1 and S2, the duplex interference caused by node S_k cannot be cancelled at S_k by CDI, i.e., $\mathbf{T}^{(k)} = \mathbf{0}_{M \times M}$. With these constraints on the system with limited capabilities at S1 and S2, problem (4.1) may be rewritten as follows:

$$\left\{ \mathbf{G}_{\text{opt}}, q_{\text{opt}}^{(1)}, q_{\text{opt}}^{(2)} \right\} = \arg \max_{\{\mathbf{G}, q^{(1)}, q^{(2)}\}} C_{\text{EW}}^{(\text{sum})}, \quad (4.36a)$$

$$\text{subject to: } \mathbf{T}^{(k)} = \mathbf{0}_{M \times M}, \quad k = 1, 2, \quad (4.36b)$$

$$\text{tr} \left\{ q^{(i)2} \mathbf{R}_{\mathbf{x}^{(i)}} \right\} = E^{(i)}, \quad i = 1, 2, \quad (4.36c)$$

$$\text{tr} \left\{ \mathbf{G} \left(\sum_{i=1}^2 q^{(i)2} \mathbf{H}^{(i)} \mathbf{R}_{\mathbf{x}^{(i)}} \mathbf{H}^{(i)\text{H}} + \mathbf{R}_{\mathbf{n}^{(0)}} \right) \mathbf{G}^{\text{H}} \right\} = E^{(0)}, \quad (4.36d)$$

In order to satisfy the transmit power constraints (4.36c) at nodes S_i , the scalar weighting factors are chosen as follows:

$$q_{\text{opt}}^{(i)} = \sqrt{\frac{E^{(i)}}{M}}, \quad i = 1, 2, \quad (4.37)$$

which means that the overall transmit power $E^{(i)}$ is equally distributed between all transmit antennas of source node S_i . Hence, the optimum weighting factors $q_{\text{opt}}^{(i)}$ in problem (4.36) are already determined and the transmit power constraints (4.36c) at the source nodes are satisfied by the choices of $q_{\text{opt}}^{(i)}$ in Eq. (4.37). This means that constraints (4.36c) need not to be considered in the following.

With constraint (4.36b), the duplex interference caused by data streams of S_k can be treated exactly as the intersymbol interference caused by data streams of S_i . Thus, all $2M$ received data streams at the RS from S1 and S2 have to be spatially separated by BF at the RS which has global CSI and full SP capabilities. In order to separate $2M$ data streams by BF, the RS has to be equipped with $L \geq 2M$ antennas. Regarding the sum rate maximization problem (4.36), the BF approach at the RS with BF matrix \mathbf{G} of Eqs. (4.18) to (4.20) can also be applied in a system with limited capabilities at S1 and S2. This means that by an adaptation to the non-zero eigenmodes of the joint first

and second hop channels the number of optimization variables can be reduced from L^2 in BF matrix \mathbf{G} to $(2M)^2$ in BF matrix $\tilde{\mathbf{G}}$ for $L > 2M$. As in the system with full capabilities, numerical methods are required in order to determine the optimum BF matrix $\tilde{\mathbf{G}}$. However, the numerical effort is significantly lower for the system with limited capabilities at S1 and S2, since BF matrices $\mathbf{Q}^{(1)}$ and $\mathbf{Q}^{(2)}$ are already given by Eq. (4.34) which means that $\tilde{\mathbf{G}}$ can be determined independently and no joint optimization of $\mathbf{Q}^{(1)}$, $\mathbf{Q}^{(2)}$, and $\tilde{\mathbf{G}}$ is required.

4.2.5 System with local CSI at S1 and S2

This section considers the sum rate maximization problem of Eq. (4.1) for a system with local CSI at S1 and S2 in two-way relaying. In this system, S1 and S2 cannot perform BF, since global CSI would be required for that purpose. Without global CSI each source node S_i uses the maximum available transmit power $E^{(i)}$, so that the source nodes transmit one data stream per transmit antenna assigning equal weighting factors to all transmit antennas. As for the system with limited capabilities at S1 and S2 in Section 4.2.4, the transmit BF matrices $\mathbf{Q}^{(i)}$, $i = 1, 2$, are given by Eq. (4.34) and the receive BF matrices $\mathbf{P}^{(k)}$, $k = 1, 2$, are given by Eq. (4.35). Since equal weighting is performed at S1 and S2, the sum rate for the system with local CSI at S1 and S2 is determined by Eq. (2.22). In contrast to the system with limited capabilities at S1 and S2, the destination nodes may cancel the duplex interference by CDI in the system with local CSI at S1 and S2. In order to apply CDI which requires the calculation of matrices $\mathbf{T}^{(k)}$, $k = 1, 2$, with respect to Eq. (2.27), local CSI is sufficient at the destination nodes. With these constraints on the system with local CSI at S1 and S2, problem (4.1) may be rewritten as follows:

$$\left\{ \mathbf{G}_{\text{opt}}, q_{\text{opt}}^{(1)}, q_{\text{opt}}^{(2)} \right\} = \arg \max_{\{\mathbf{G}, q^{(1)}, q^{(2)}\}} C_{\text{EW}}^{(\text{sum})}, \quad (4.38a)$$

$$\text{subject to: } \mathbf{T}^{(k)} = -pq^{(k)}\mathbf{H}^{(k)\text{T}}\mathbf{G}\mathbf{H}^{(k)}, \quad k = 1, 2, \quad (4.38b)$$

$$\text{tr} \left\{ q^{(i)2} \mathbf{R}_{\mathbf{x}^{(i)}} \right\} = E^{(i)}, \quad i = 1, 2, \quad (4.38c)$$

$$\text{tr} \left\{ \mathbf{G} \left(\sum_{i=1}^2 q^{(i)2} \mathbf{H}^{(i)} \mathbf{R}_{\mathbf{x}^{(i)}} \mathbf{H}^{(i)\text{H}} + \mathbf{R}_{\mathbf{n}^{(0)}} \right) \mathbf{G}^{\text{H}} \right\} = E^{(0)}. \quad (4.38d)$$

In order to satisfy the transmit power constraints (4.38c) at nodes S_i , the optimum scalar weighting factors $\mathbf{q}_{\text{opt}}^{(i)}$ are given by Eq. (4.37). Hence, the optimum weighting factors $q_{\text{opt}}^{(i)}$ in problem (4.38) are already determined and the transmit power constraints (4.38c) at the source nodes are satisfied by the choices of $q_{\text{opt}}^{(i)}$ in Eq. (4.37). This means that constraints (4.38c) need not to be considered in the following.

The optimum BF matrix \mathbf{G} at the RS for maximizing the sum rate can only be determined by numerical methods again. But as in Sections 4.2.2 and 4.2.4, the number of optimization variables can be reduced from L^2 in BF matrix \mathbf{G} to $(2M)^2$ in BF matrix $\tilde{\mathbf{G}}$ for $L > 2M$ by using the adaptation to the non-zero eigenmodes of the joint first-hop and second-hop channels described by the BF matrix \mathbf{G} of Eqs. (4.18) to (4.20).

4.3 Linear beamforming in a system with limited capabilities at S1 and S2

4.3.1 Introduction

In this Section 4.3, three additional optimization problems in the system with limited capabilities at S1 and S2 are considered. The optimization problems consider the minimization of the MSE, the minimization of the MSE under the ZF constraint, and the maximization of the SNR, cf. second row and third column of the framework in Figure 1.4. In Section 4.2.4, no analytical solution to the maximization of the sum rate in the system with limited capabilities at S1 and S2 could be found. However, the three additional optimization problems are well-known from point-to-point transmission and the corresponding BF algorithms are known to provide reasonable performance in point-to-point transmission. For that reason, the optimization problems are newly formulated for the two-way relaying scheme with exclusive BF at the RS in a system with limited capabilities at S1 and S2, and the respective BF algorithms are derived. The BF algorithm which minimizes the MSE and the BF algorithm which minimizes the MSE under the ZF constraint are introduced in our works [UK07d, UK07b, UK07a, UK08a].

Since it is assumed that no CSI is available at source nodes S_i , $i = 1, 2$, each source node S_i uses the maximum available transmit power $E^{(i)}$ and assigns the same weighting factor $q^{(i)}$ to all transmit antennas. Furthermore, one data stream is transmitted from each transmit antenna. From the transmit power constraints (4.36c) at nodes S_i , $i = 1, 2$, the optima $q_{\text{opt}}^{(i)}$ are directly given by Eq. (4.37). Thus, the transmit power constraints at the source nodes S_i , $i = 1, 2$, can be omitted in the following optimization problems and $q^{(i)} = q_{\text{opt}}^{(i)}$, $i = 1, 2$, can be assumed as fixed parameters in the optimization problems.

Since S1 and S2 are assumed to have limited SP capabilities, the receive BF matrices $\mathbf{P}^{(k)}$, $k = 1, 2$, are given by Eq. (4.35), which means that the weighting factors

$p^{(k)}$ are equal for all receive antennas of the respective destination node. Furthermore, $p^{(1)} = p^{(2)} = p$ is assumed in the following. Besides the optimization of the BF matrix \mathbf{G} at the RS, the proposed BF algorithms which minimize the MSE, minimize the MSE under the ZF constraint, and maximize the SNR explicitly consider the optimization of the weighting factor p . Since no CSI is available at the destination nodes, p cannot be calculated by the destination nodes by using CSI. However, as introduced in Section 3.3.1 the weighting factor p corresponds to the ratio between the expected average received power and the actually average received power at the destination nodes. Thus, p can be easily determined at the destination nodes after measuring the received power.

Since no CSI is available at S1 and S2, CDI cannot be applied at the destination nodes. In this case, the CDI matrices $\mathbf{T}^{(k)}$, $k = 1, 2$, are set to zero, i.e., $\mathbf{T}^{(k)}$ is chosen according to Eq. (2.29). In the following optimization problems for a system with limited capabilities at S1 and S2, Eq. (2.29) is always included as a constraint.

4.3.2 Minimization of the MSE

In this section, the problem of minimizing the MSE is considered for a system with limited capabilities at S1 and S2 in two-way relaying, and the corresponding MMSE-BF algorithm solving the problem is given.

For one-way relaying in a system with limited capabilities at S1 and S2, the MSE is minimized independently for the transmission from S1 to S2 and for the transmission from S2 to S1 as introduced in Section 3.3.2. In two-way relaying, both transmissions are processed simultaneously. Thus, BF matrix \mathbf{G} of Eq. (2.26) at the RS and the scalar weighting factor p at the destination nodes have to be designed such that the MSE between the joint data vector \mathbf{x} of Eq. (4.2) and the joint estimated vector $\hat{\mathbf{x}}$ of Eq. (4.15) is minimized. Furthermore, it has to be considered that S1 and S2 transmit simultaneously to the RS which increases the overall received power at the RS and changes the RS transmit power constraint. Thus, the minimization of the MSE is formulated as follows:

$$\{p_{\text{MMSE}}, \mathbf{G}_{\text{MMSE}}\} = \arg \min_{\{p, \mathbf{G}\}} \text{E} \left\{ \|\mathbf{x} - \hat{\mathbf{x}}\|_2^2 \right\}, \quad (4.39a)$$

$$\text{subject to: } \mathbf{T}^{(k)} = \mathbf{0}_{M \times M}, \quad k = 1, 2, \quad (4.39b)$$

$$\text{tr} \left\{ \mathbf{G} \left(\sum_{i=1}^2 q^{(i)2} \mathbf{H}^{(i)} \mathbf{R}_{\mathbf{x}^{(i)}} \mathbf{H}^{(i)\text{H}} + \mathbf{R}_{\mathbf{n}^{(0)}} \right) \mathbf{G}^{\text{H}} \right\} = E^{(0)}. \quad (4.39c)$$

In the following, the MMSE-BF algorithm which solves problem (4.39) is given. For that purpose, the equivalent system model for the joint description of both directions of the transmission in Section 4.2.2 is reviewed for the system with limited capabilities at S1 and S2. With $\mathbf{P} = p\mathbf{I}_M$ and $\mathbf{T} = \mathbf{0}_{2M \times 2M}$ in the system with limited capabilities at S1 and S2, the joint estimated data vector $\hat{\mathbf{x}}$ of Eq. (4.15) simplifies to

$$\hat{\mathbf{x}} = p \left(\mathbf{H}_T \mathbf{G} \mathbf{H}_R \mathbf{Q} \mathbf{x} + \mathbf{H}_T \mathbf{G} \mathbf{n}^{(0)} + \mathbf{n}_R \right). \quad (4.40)$$

Now, the joint estimated data vector $\hat{\mathbf{x}}$ of Eq. (4.40) is compared to the estimated data vector $\hat{\mathbf{x}}^{(i)}$ of Eq. (2.11) for one-way relaying in the system with limited capabilities at S1 and S2. Knowing that $\mathbf{Q}^{(i)} = q^{(i)}\mathbf{I}_M$, $\mathbf{P}^{(k)} = p^{(k)}\mathbf{I}_M$, and $\mathbf{T}^{(k)} = \mathbf{D}^{(k)} = \mathbf{0}_{M \times M}$ as introduced in Eq. (2.24), $\hat{\mathbf{x}}^{(i)}$ of Eq. (2.11) simplifies to

$$\hat{\mathbf{x}}^{(i)} = p^{(k)} \left(\mathbf{H}^{(k)T} \mathbf{G}^{(k,i)} \mathbf{H}^{(i)} q^{(i)} \mathbf{x}^{(i)} + \mathbf{H}^{(k)T} \mathbf{G}^{(k,i)} \mathbf{n}^{(0)} + \mathbf{n}_R^{(k)} \right). \quad (4.41)$$

Comparing Eq. (4.40) and Eq. (4.41) shows that both system equations have exactly the same mathematical structure. For example, the joint data vector \mathbf{x} and the joint estimated data vector $\hat{\mathbf{x}}$ in two-way relaying correspond to the data vector $\mathbf{x}^{(i)}$ and the estimated data vector $\hat{\mathbf{x}}^{(i)}$ in one-way relaying, respectively. Table 4.1 summarizes all correspondences between the variables of Eq. (4.40) and Eq. (4.41).

one-way relaying		two-way relaying
$\mathbf{x}^{(i)}$	\iff	\mathbf{x}
$\hat{\mathbf{x}}^{(i)}$	\iff	$\hat{\mathbf{x}}$
$\mathbf{n}^{(0)}$	\iff	$\mathbf{n}^{(0)}$
$\mathbf{n}_R^{(k)}$	\iff	\mathbf{n}_R
$\mathbf{H}^{(i)} q^{(i)}$	\iff	$\mathbf{H}_R \mathbf{Q}$
$\mathbf{H}^{(k)T}$	\iff	\mathbf{H}_T
$\mathbf{G}^{(k,i)}$	\iff	\mathbf{G}
$p^{(k)}$	\iff	p
$\mathbf{R}_{\mathbf{x}^{(i)}}$	\iff	$\mathbf{R}_{\mathbf{x}}$
$\mathbf{R}_{\mathbf{n}^{(0)}}$	\iff	$\mathbf{R}_{\mathbf{n}^{(0)}}$
$\mathbf{R}_{\mathbf{n}_R^{(k)}}$	\iff	$\mathbf{R}_{\mathbf{n}_R}$
$\Upsilon_R^{(i)}$	\iff	Υ_R
$\Upsilon^{(k)}$	\iff	Υ_T

Table 4.1. Correspondences between one-way relaying and two-way relaying for a system with limited capabilities at S1 and S2

Furthermore, it gives the resulting correspondences of the respective covariance matrices, where the covariance matrix Υ_R of the received signal at the RS is given by

$$\Upsilon_R = \mathbf{H}_R \mathbf{Q} \mathbf{R}_{\mathbf{x}} \mathbf{Q}^H \mathbf{H}_R^H + \mathbf{R}_{\mathbf{n}^{(0)}}, \quad (4.42)$$

and matrix Υ_T is defined as

$$\Upsilon_T = \mathbf{H}_T^H \mathbf{H}_T + \frac{\text{tr}\{\mathbf{R}_{\mathbf{n}_R}\}}{E^{(0)}} \mathbf{I}_L. \quad (4.43)$$

Due to the same mathematical structure of Eqs. (4.40) and (4.41), the derivation of the BF matrix \mathbf{G} and the scalar weighting factor p for the minimization of the MSE in two-way relaying follows the same steps as the derivation of the BF matrix $\mathbf{G}^{(k,i)}$ and the scalar weighting factor $p^{(k)}$ for the minimization of the MSE in one-way relaying presented in Section 3.3.2. With the correspondences of Table 4.1, all variables of the MMSE-BF algorithm in one-way relaying which is given by Eqs. (3.38) and (3.39) can be replaced by their correspondences in two-way relaying, which leads to the following MMSE-BF algorithm in two-way relaying:

$$\mathbf{G}_{\text{MMSE}} = \frac{1}{p_{\text{MMSE}}} \Upsilon_T^{-1} \mathbf{H}_T^H \mathbf{R}_x \mathbf{Q}^H \mathbf{H}_R^H \Upsilon_R^{-1}, \quad (4.44)$$

with

$$p_{\text{MMSE}} = \sqrt{\frac{\text{tr}\{\mathbf{H}_R \mathbf{Q} \mathbf{R}_x \mathbf{H}_T \Upsilon_T^{-2} \mathbf{H}_T^H \mathbf{R}_x \mathbf{Q}^H \mathbf{H}_R^H \Upsilon_R^{-1}\}}{E^{(0)}}} \in \mathbb{R}^+. \quad (4.45)$$

As explained for the MMSE-BF algorithm in one-way relaying in Section 3.3.2, a feedback of the noise variance $\sigma_{\mathbf{n}_R}^2$ from nodes S_k to the RS is required for the MMSE-BF algorithm in two-way relaying. Furthermore, two parts can be identified in the BF matrix \mathbf{G}_{MMSE} of Eq. (4.44), namely the receive BF matrix

$$\mathbf{G}_{R,\text{MMSE}} = \mathbf{R}_x \mathbf{Q}^H \mathbf{H}_R^H \Upsilon_R^{-1}, \quad (4.46)$$

and the transmit BF matrix

$$\mathbf{G}_{T,\text{MMSE}} = \frac{1}{p_{\text{MMSE}}} \Upsilon_T^{-1} \mathbf{H}_T^H. \quad (4.47)$$

4.3.3 Minimization of the MSE under the ZF constraint

This section considers the minimization of the MSE under the ZF constraint for a system with limited capabilities at S1 and S2 in two-way relaying, and the corresponding ZF-BF algorithm is given. The optimization problem is a modification of the minimization of the MSE in Section 4.3.2 where all interferences, namely intersymbol and duplex interferences, between simultaneously transmitted data streams are removed additionally. For that purpose, the MSE optimization problem (4.39) is extended by the

additional ZF constraint. Thus, the minimization of the MSE under the ZF constraint is formulated as follows:

$$\{p_{\text{ZF}}, \mathbf{G}_{\text{ZF}}\} = \arg \min_{\{p, \mathbf{G}\}} E \{ \|\mathbf{x} - \hat{\mathbf{x}}\|_2^2 \}, \quad (4.48a)$$

$$\text{subject to: } \mathbf{T}^{(k)} = \mathbf{0}_{M \times M} \quad k = 1, 2, \quad (4.48b)$$

$$\hat{\mathbf{x}} = \mathbf{x} \quad \text{for } \mathbf{n}^{(0)} = \mathbf{0}_{L \times 1} \text{ and } \mathbf{n}_{\text{R}} = \mathbf{0}_{2M \times 1}, \quad (4.48c)$$

$$\text{tr} \left\{ \mathbf{G} \left(\sum_{i=1}^2 q^{(i)^2} \mathbf{H}^{(i)} \mathbf{R}_{\mathbf{x}^{(i)}} \mathbf{H}^{(i)\text{H}} + \mathbf{R}_{\mathbf{n}^{(0)}} \right) \mathbf{G}^{\text{H}} \right\} = E^{(0)}. \quad (4.48d)$$

In the following, the solution to optimization problem (4.48) is given. As introduced for the MMSE-BF algorithm in Section 4.3.2, the derivation of the BF matrix \mathbf{G} and the scalar weighting factor p for the minimization of the MSE under the ZF constraint in two-way relaying follows the same steps as the derivation of the BF matrix $\mathbf{G}^{(k,i)}$ and the scalar weighting factor $p^{(k)}$ for the minimization of the MSE under the ZF constraint in one-way relaying presented in Section 3.3.3. With the correspondences of Table 4.1, all variables of the ZF-BF algorithm in one-way relaying which is given by Eqs. (3.48) and (3.49) can be replaced by their correspondences in two-way relaying, which leads to the following ZF-BF algorithm in two-way relaying:

$$\mathbf{G}_{\text{ZF}} = \frac{1}{p_{\text{ZF}}} \mathbf{H}_{\text{T}}^{\text{H}} (\mathbf{H}_{\text{T}} \mathbf{H}_{\text{T}}^{\text{H}})^{-1} (\mathbf{Q}^{\text{H}} \mathbf{H}_{\text{R}}^{\text{H}} \mathbf{R}_{\mathbf{n}^{(0)}}^{-1} \mathbf{H}_{\text{R}} \mathbf{Q})^{-1} \mathbf{Q}^{\text{H}} \mathbf{H}_{\text{R}}^{\text{H}} \mathbf{R}_{\mathbf{n}^{(0)}}^{-1}, \quad (4.49)$$

with

$$p_{\text{ZF}} = \sqrt{\frac{\text{tr} \left\{ (\mathbf{Q}^{\text{H}} \mathbf{H}_{\text{R}}^{\text{H}} \mathbf{R}_{\text{R}}^{-1} \mathbf{H}_{\text{R}} \mathbf{Q})^{-1} (\mathbf{H}_{\text{T}} \mathbf{H}_{\text{T}}^{\text{H}})^{-1} \right\}}{E^{(0)}}} \in \mathbb{R}^+. \quad (4.50)$$

As explained for the ZF-BF algorithm in one-way relaying in Section 3.3.3, no feedback of the noise variances $\sigma_{\mathbf{n}_{\text{R}}^{(k)}}^2$ from nodes S_k to the RS is required for the ZF-BF algorithm in two-way relaying. Furthermore, two parts can be identified in the BF matrix \mathbf{G}_{ZF} of Eq. (4.49), namely the receive BF matrix

$$\mathbf{G}_{\text{R,ZF}} = (\mathbf{Q}^{\text{H}} \mathbf{H}_{\text{R}}^{\text{H}} \mathbf{R}_{\mathbf{n}^{(0)}}^{-1} \mathbf{H}_{\text{R}} \mathbf{Q})^{-1} \mathbf{Q}^{\text{H}} \mathbf{H}_{\text{R}}^{\text{H}} \mathbf{R}_{\mathbf{n}^{(0)}}^{-1}, \quad (4.51)$$

and the transmit BF matrix

$$\mathbf{G}_{\text{T,ZF}} = \frac{1}{p_{\text{ZF}}} \mathbf{H}_{\text{T}}^{\text{H}} (\mathbf{H}_{\text{T}} \mathbf{H}_{\text{T}}^{\text{H}})^{-1}. \quad (4.52)$$

4.3.4 Maximization of the SNR

In this section, the maximization of the SNR is considered for a system with limited capabilities at S1 and S2 in two-way relaying. In two-way relaying, the SNR gives the

ratio between the average power of the useful signal part in the joint estimated data vector $\hat{\mathbf{x}}$ and the average power of the overall noise of both receiver outputs of the destination nodes. Hence, the maximization of the SNR is formulated as follows:

$$\{p_{\text{MF}}, \mathbf{G}_{\text{MF}}\} = \arg \max_{\{p, \mathbf{G}\}} \frac{|\mathbb{E}\{\mathbf{x}^{\text{H}}\hat{\mathbf{x}}\}|^2}{\mathbb{E}\{\|\mathbf{x}\|_2^2\} \mathbb{E}\{\|p\mathbf{H}_{\text{T}}\mathbf{G}\mathbf{n}^{(0)} + \mathbf{P}\mathbf{n}_{\text{R}}\|_2^2\}}, \quad (4.53\text{a})$$

$$\text{subject to: } \mathbf{T}^{(k)} = \mathbf{0}_{M \times M} \quad k = 1, 2, \quad (4.53\text{b})$$

$$\text{tr} \left\{ \mathbf{G} \left(\sum_{i=1}^2 q^{(i)^2} \mathbf{H}^{(i)} \mathbf{R}_{\mathbf{x}^{(i)}} \mathbf{H}^{(i)\text{H}} + \mathbf{R}_{\mathbf{n}^{(0)}} \right) \mathbf{G}^{\text{H}} \right\} = E^{(0)}. \quad (4.53\text{c})$$

In the following, the MF-BF algorithm solving the optimization problem (4.53) is given. As introduced for the MMSE-BF algorithm in Section 4.3.2, the derivation of the BF matrix \mathbf{G} and the scalar weighting factor p for the maximization of the SNR in two-way relaying follows the same steps as the derivation of the BF matrix $\mathbf{G}^{(k,i)}$ and the scalar weighting factor $p^{(k)}$ for the maximization of the SNR in one-way relaying presented in Section 3.3.4. With the correspondences of Table 4.1, all variables of the MF-BF algorithm in one-way relaying which is given by Eqs. (3.57) and (3.58) can be replaced by their correspondences in two-way relaying, which leads to the following MF-BF algorithm in two-way relaying:

$$\mathbf{G}_{\text{MF}} = \frac{1}{p_{\text{MF}}} \mathbf{H}_{\text{T}}^{\text{H}} \mathbf{R}_{\mathbf{x}} \mathbf{Q}^{\text{H}} \mathbf{H}_{\text{R}}^{\text{H}} \boldsymbol{\Upsilon}_{\text{R}}^{-1}, \quad (4.54)$$

and

$$p_{\text{MF}} = \sqrt{\frac{\text{tr} \{ \mathbf{H}_{\text{T}}^{\text{H}} \mathbf{R}_{\mathbf{x}} \mathbf{Q}^{\text{H}} \mathbf{H}_{\text{R}}^{\text{H}} \boldsymbol{\Upsilon}_{\text{R}}^{-1} \mathbf{H}_{\text{R}} \mathbf{Q} \mathbf{R}_{\mathbf{x}} \mathbf{H}_{\text{T}} \}}{E^{(0)}}}} \in \mathbb{R}^+. \quad (4.55)$$

As explained for the MF-BF algorithm in one-way relaying in Section 3.3.4, no feedback of the noise variances $\sigma_{\mathbf{n}_{\text{R}}}^2$ from nodes S_k to the RS is required for the MF-BF algorithm in two-way relaying. Furthermore, two parts can be identified in the BF matrix \mathbf{G}_{MF} of Eq. (4.54), namely the receive BF matrix

$$\mathbf{G}_{\text{R, MF}} = \mathbf{R}_{\mathbf{x}} \mathbf{Q}^{\text{H}} \mathbf{H}_{\text{R}}^{\text{H}} \boldsymbol{\Upsilon}_{\text{R}}^{-1}, \quad (4.56)$$

and the transmit BF matrix

$$\mathbf{G}_{\text{T, MF}} = \frac{1}{p_{\text{MF}}} \mathbf{H}_{\text{T}}^{\text{H}}. \quad (4.57)$$

4.4 Linear beamforming in a system with local CSI at S1 and S2

4.4.1 Introduction

In this Section 4.4, three additional optimization problems in the system with local CSI at S1 and S2 are considered. The optimization problems consider the minimization of the MSE, the minimization of the MSE under the ZF constraint, and the maximization of the SNR, cf. second row and fourth column of the framework in Figure 1.4. In Section 4.2.5, no analytical solution to the maximization of the sum rate in the system with local CSI at S1 and S2 could be found. However, the three additional optimization problems are well-known from point-to-point transmission and the corresponding BF algorithms are known to provide reasonable performance in point-to-point transmission. For that reason, the optimization problems are newly formulated for the two-way relaying scheme with exclusive BF at the RS in a system with local CSI at S1 and S2, and the respective BF algorithms are derived.

Since it is assumed that only local CSI is available at source nodes S_i , $i = 1, 2$, each source node S_i uses the maximum available transmit power $E^{(i)}$ and assigns the same weighting factor $q^{(i)}$ to all transmit antennas. Furthermore, one data stream is transmitted from each transmit antenna. From the transmit power constraints (4.38c) at S_i , $i = 1, 2$, the optima $q_{\text{opt}}^{(i)}$ are directly given by Eq. (4.37). Thus, the transmit power constraints at the source nodes S_i , $i = 1, 2$, can be omitted in the following optimization problems and $q^{(i)} = q_{\text{opt}}^{(i)}$, $i = 1, 2$, can be assumed as fixed parameters in the optimization problems.

Since it is assumed that only local CSI is available at S1 and S2, the receive BF matrices $\mathbf{P}^{(k)}$, $k = 1, 2$, are given by Eq. (4.35). As already proposed for the system with limited capabilities at S1 and S2 in Section 4.3, the weighting factors $p^{(1)}$ and $p^{(2)}$ are assumed to be equal, i.e., $p^{(1)} = p^{(2)} = p$. Besides the optimization of the BF matrix \mathbf{G} of Eq. (2.26), the proposed BF algorithms which minimize the MSE, minimize the MSE under the ZF constraint, and maximize the SNR explicitly consider the optimization of the weighting factor p . As introduced in Section 3.3.1, the weighting factor p corresponds to the ratio between the expected average received power and the actually average received power at the destination nodes. Thus, p can be easily determined at the destination nodes after measuring the received power.

In contrast to the system with limited capabilities at S1 and S2, the duplex interference can be cancelled at the destination nodes S_k , $k = 1, 2$, by applying CDI in the

system with local CSI at S1 and S2, since local CSI is sufficient in order to determine matrices $\mathbf{T}^{(k)}$, $k = 1, 2$, according to Eq. (2.27). The application of CDI in the system with local CSI can be included into the following optimization problems by introducing Eq. (2.27) for $k = 1, 2$, as additional constraints.

4.4.2 Minimization of the MSE

In this section, the minimization of the MSE is considered for a system with local CSI at S1 and S2 in two-way relaying, and the respective MMSE-BF algorithm solving the problem is derived. The application of CDI is included into the optimization problem (4.39) by changing the additional constraints for CDI matrices $\mathbf{T}^{(k)}$, $k = 1, 2$, of Eq. (2.29) to Eq. (2.27). Furthermore, the MSE is written such that the contribution of the transmission from S1 to S2 can be distinguished from the contribution of the transmission from S2 to S1 which means that the overall MSE is given by the sum of the two individual MSEs of the two transmissions yielding

$$\mathbb{E} \{ \|\mathbf{x} - \hat{\mathbf{x}}\|_2^2 \} = \mathbb{E} \left\{ \sum_{i=1}^2 \|\mathbf{x}^{(i)} - \hat{\mathbf{x}}^{(i)}\|_2^2 \right\}. \quad (4.58)$$

Thus, the minimization of the MSE in a system with local CSI at S1 and S2 can be written as follows:

$$\{p_{\text{MMSE}}, \mathbf{G}_{\text{MMSE}}\} = \arg \min_{\{p, \mathbf{G}\}} \mathbb{E} \left\{ \sum_{i=1}^2 \|\mathbf{x}^{(i)} - \hat{\mathbf{x}}^{(i)}\|_2^2 \right\}, \quad (4.59a)$$

$$\text{subject to: } \mathbf{T}^{(k)} = -pq^{(k)} \mathbf{H}^{(k)\text{T}} \mathbf{G} \mathbf{H}^{(k)}, \quad k = 1, 2, \quad (4.59b)$$

$$\text{tr} \left\{ \mathbf{G} \left(\sum_{i=1}^2 q^{(i)2} \mathbf{H}^{(i)} \mathbf{R}_{\mathbf{x}^{(i)}} \mathbf{H}^{(i)\text{H}} + \mathbf{R}_{\mathbf{n}^{(0)}} \right) \mathbf{G}^{\text{H}} \right\} = E^{(0)}. \quad (4.59c)$$

In the following, the MMSE-BF algorithm solving problem (4.59) is derived. Compared to the BF algorithm proposed in Section 4.3.2 without CDI at the destination nodes, the constraint (4.59b) significantly changes the MMSE-BF algorithm for the minimization of the MSE in a system with local CSI at S1 and S2. The constraint (4.59b) which describes the application of CDI at the destination nodes yields $\mathbf{D}^{(k)} = \mathbf{0}_{M \times M}$, for $k = 1, 2$, in Eq. (2.11). Using $\mathbf{D}^{(k)} = \mathbf{0}_{M \times M}$, and inserting

Eqs. (2.10) and (2.11) into the MSE of the objective function (4.59a), yields

$$\begin{aligned} E \{ \|\hat{\mathbf{x}} - \mathbf{x}\|_2^2 \} &= \sum_{i=1}^2 \text{tr} \{ \mathbf{R}_{\mathbf{x}^{(i)}} \} - 2\Re \left\{ p \sum_{i=1}^2 q^{(i)} \text{tr} \left\{ \mathbf{H}^{(k)\text{T}} \mathbf{G} \mathbf{H}^{(i)} \mathbf{R}_{\mathbf{x}^{(i)}} \right\} \right\} \\ &\quad + p^2 \sum_{i=1}^2 q^{(i)2} \text{tr} \left\{ \mathbf{H}^{(k)\text{T}} \mathbf{G} \mathbf{H}^{(i)} \mathbf{R}_{\mathbf{x}^{(i)}} \mathbf{H}^{(i)\text{H}} \mathbf{G}^{\text{H}} \mathbf{H}^{(k)*} \right\} \\ &\quad + p^2 \sum_{k=1}^2 \text{tr} \left\{ \mathbf{H}^{(k)\text{T}} \mathbf{G} \mathbf{R}_{\mathbf{n}^{(0)}} \mathbf{G}^{\text{H}} \mathbf{H}^{(k)*} + \mathbf{R}_{\mathbf{n}_{\text{R}}^{(k)}} \right\}. \end{aligned} \quad (4.60)$$

Since the MSE of Eq. (4.60) is quadratic in \mathbf{G} , the MSE minimization problem for two-way relaying is neither convex nor concave. Nevertheless, as introduced in [Joh04] for point-to-point transmission, Lagrangian optimization is applied knowing that the resulting solution is not necessarily unique. The overall covariance matrix $\mathbf{\Upsilon}$ of the received signal at the RS is given by

$$\mathbf{\Upsilon} = \sum_{i=1}^2 |q^{(i)}|^2 \mathbf{H}^{(i)} \mathbf{R}_{\mathbf{x}^{(i)}} \mathbf{H}^{(i)\text{H}} + \mathbf{R}_{\mathbf{n}^{(0)}}. \quad (4.61)$$

Using covariance matrix $\mathbf{\Upsilon}$ of Eq. (4.61) in Eq. (4.60) and rewriting the RS transmit power constraint (4.59c) by considering $\mathbf{\Upsilon}$, the Lagrangian function results in

$$\begin{aligned} L(p, \mathbf{G}, \eta) &= \sum_{i=1}^2 \text{tr} \{ \mathbf{R}_{\mathbf{x}^{(i)}} \} - 2\Re \left\{ p \sum_{i=1}^2 q^{(i)} \text{tr} \left\{ \mathbf{H}^{(k)\text{T}} \mathbf{G} \mathbf{H}^{(i)} \mathbf{R}_{\mathbf{x}^{(i)}} \right\} \right\} \\ &\quad + p^2 \sum_{i=1}^2 \text{tr} \left\{ \mathbf{H}^{(k)\text{T}} \mathbf{G} \mathbf{\Upsilon}^{(i)} \mathbf{G}^{\text{H}} \mathbf{H}^{(k)*} + \mathbf{R}_{\mathbf{n}_{\text{R}}^{(k)}} \right\} + \eta (\text{tr} \{ \mathbf{G} \mathbf{\Upsilon} \mathbf{G}^{\text{H}} \} - E^{(0)}), \end{aligned} \quad (4.62)$$

with the Lagrangian multiplier η and $\mathbf{\Upsilon}^{(i)}$ of Eq. (3.34). From the Lagrangian function, the KKT conditions which are only necessary conditions for the global optimum result in

$$\frac{\partial L}{\partial p} = - \sum_{i=1}^2 q^{(i)} \text{tr} \left\{ \mathbf{H}^{(k)\text{T}} \mathbf{G} \mathbf{H}^{(i)} \mathbf{R}_{\mathbf{x}^{(i)}} \right\} + p^* \sum_{i=1}^2 \text{tr} \left\{ \mathbf{H}^{(k)\text{T}} \mathbf{G} \mathbf{\Upsilon}^{(i)} \mathbf{G}^{\text{H}} \mathbf{H}^{(k)*} + \mathbf{R}_{\mathbf{n}_{\text{R}}^{(k)}} \right\} \stackrel{!}{=} 0, \quad (4.63a)$$

$$\frac{\partial L}{\partial \mathbf{G}} = - p \sum_{i=1}^2 q^{(i)} \mathbf{H}^{(k)} \mathbf{R}_{\mathbf{x}^{(i)}}^{\text{T}} \mathbf{H}^{(i)\text{T}} + |p|^2 \sum_{i=1}^2 \mathbf{H}^{(k)} \mathbf{H}^{(k)\text{H}} \mathbf{G}^* \mathbf{\Upsilon}^{(i)\text{T}} + \eta \mathbf{G}^* \mathbf{\Upsilon}^{\text{T}} \stackrel{!}{=} \mathbf{0}, \quad (4.63b)$$

$$\eta (\text{tr} \{ \mathbf{G} \mathbf{\Upsilon} \mathbf{G}^{\text{H}} \} - E^{(0)}) \stackrel{!}{=} 0. \quad (4.63c)$$

With the definitions of the vectorization $\text{vec}[\cdot]$, its reversion $\text{vec}_{L,L}^{-1}[\cdot]$, and the Kronecker product $\mathbf{Z} \otimes \mathbf{X}$ of two matrices \mathbf{Z} and \mathbf{X} , that can be found in Appendix A.4,

matrix \mathbf{K} is defined as

$$\mathbf{K} = \sum_{i=1}^2 \left(\boldsymbol{\Upsilon}^{(i)\text{T}} \otimes \left(\mathbf{H}^{(k)*} \mathbf{H}^{(k)\text{T}} \right) \right) + \left(\boldsymbol{\Upsilon} \otimes \frac{1}{E^{(0)}} \text{tr} \left\{ \sum_{k=1}^2 \mathbf{R}_{\mathbf{n}_R^{(k)}} \right\} \mathbf{I}_L \right). \quad (4.64)$$

Using Eq. (4.64), the BF matrix at the RS for the MMSE-BF algorithm which solves problem (4.59) is given by

$$\mathbf{G}_{\text{MMSE}} = \frac{1}{p_{\text{MMSE}}} \text{vec}_{L,L}^{-1} \left[\mathbf{K}^{-1} \text{vec} \left[\sum_{i=1}^2 q^{(i)} \mathbf{H}^{(k)*} \mathbf{R}_{\mathbf{x}^{(i)}} \mathbf{H}^{(i)\text{H}} \right] \right]. \quad (4.65)$$

With auxiliary matrix

$$\tilde{\mathbf{G}}_{\text{MMSE}} = \text{vec}_{L,L}^{-1} \left[\mathbf{K}^{-1} \text{vec} \left[\sum_{i=1}^2 q^{(i)} \mathbf{H}^{(k)*} \mathbf{R}_{\mathbf{x}^{(i)}} \mathbf{H}^{(i)\text{H}} \right] \right], \quad (4.66)$$

the scalar weighting factor p_{MMSE} results in

$$p_{\text{MMSE}} = \sqrt{\frac{\text{tr} \left\{ \tilde{\mathbf{G}}_{\text{MMSE}} \boldsymbol{\Upsilon} \tilde{\mathbf{G}}_{\text{MMSE}}^{\text{H}} \right\}}{E^{(0)}}} \in \mathbb{R}^+. \quad (4.67)$$

The derivation of the BF matrix \mathbf{G}_{MMSE} and the scalar weighting factor p_{MMSE} from the KKT conditions (4.63) can be found in Appendix A.5. Note that the proposed MMSE-BF algorithm requires knowledge about the noise covariance matrix $\mathbf{R}_{\mathbf{n}^{(0)}}$ of the RS which can be estimated by the RS itself, but also about the noise covariance matrices $\mathbf{R}_{\mathbf{n}_R^{(k)}}$, $k = 1, 2$, of the destination nodes. Assuming AWGN, this means that the noise variances $\sigma_{\mathbf{n}_R^{(k)}}^2$, $k = 1, 2$, which are estimated at S_k need to be signaled via a feedback channel from nodes S_k to the RS. However, the effort expected for such a feedback is very low.

4.4.3 Minimization of the MSE under the ZF constraint

In this section, the minimization of the MSE under the ZF constraint is considered for a system with local CSI at S1 and S2 in two-way relaying. The corresponding ZF-BF algorithm which solves the problem is derived in this section, too. In contrast to the minimization of the MSE of Eq. (4.59), two additional ZF constraints are introduced which ensure that data streams of the same source node are orthogonalized by the BF at the RS. An orthogonalization of the data streams of different source nodes by the BF at the RS as introduced for a system with limited capabilities at S1 and S2 in Section 4.3.3 is not required since the destination nodes can apply CDI. Under these

assumptions, the minimization of the MSE under the ZF constraint may be formulated as follows:

$$\{p_{\text{ZF}}, \mathbf{G}_{\text{ZF}}\} = \arg \min_{\{p, \mathbf{G}\}} \mathbb{E} \left\{ \sum_{i=1}^2 \|\mathbf{x}^{(i)} - \hat{\mathbf{x}}^{(i)}\|_2^2 \right\}, \quad (4.68a)$$

$$\text{subject to: } \mathbf{T}^{(k)} = -pq^{(k)} \mathbf{H}^{(k)\text{T}} \mathbf{G} \mathbf{H}^{(k)}, \quad k = 1, 2, \quad (4.68b)$$

$$\hat{\mathbf{x}}^{(i)} = \mathbf{x}^{(i)} \quad \text{for } \mathbf{n}^{(0)} = \mathbf{0}_{L \times 1} \text{ and } \mathbf{n}_{\text{R}}^{(k)} = \mathbf{0}_{M \times 1}, \quad i = 1, 2, \quad (4.68c)$$

$$\text{tr} \left\{ \mathbf{G} \left(\sum_{i=1}^2 q^{(i)2} \mathbf{H}^{(i)} \mathbf{R}_{\mathbf{x}^{(i)}} \mathbf{H}^{(i)\text{H}} + \mathbf{R}_{\mathbf{n}^{(0)}} \right) \mathbf{G}^{\text{H}} \right\} = E^{(0)}. \quad (4.68d)$$

The ZF-BF algorithm solving problem (4.68) is derived in the following. Using Eqs. (2.10) and (2.11), the two ZF constraints of Eq. (4.68c) can also be described by

$$pq^{(i)} \mathbf{H}^{(k)\text{T}} \mathbf{G} \mathbf{H}^{(i)} = \mathbf{I}_M, \quad i = 1, 2. \quad (4.69)$$

Note that Eq. (4.69) contains two ZF constraints which are coupled via \mathbf{G} . This coupling complicates the optimization problem compared to one-way relaying where only one overall ZF constraint is considered in Eq. (3.44). With the two ZF constraints of Eq. (4.69), Eq. (2.10) and Eq. (2.11), the MSE objective function of Eq. (4.68a) corresponds to the overall noise power at the receiver output of S_k , and reads as

$$\mathbb{E} \left\{ \left\| \sum_{i=1}^2 \hat{\mathbf{x}}^{(i)} - \mathbf{x}^{(i)} \right\|_2^2 \right\} = p^2 \sum_{k=1}^2 \text{tr} \left\{ \mathbf{H}^{(k)\text{T}} \mathbf{G} \mathbf{R}_{\mathbf{n}^{(0)}} \mathbf{G}^{\text{H}} \mathbf{H}^{(k)*} + \mathbf{R}_{\mathbf{n}_{\text{R}}^{(k)}} \right\}. \quad (4.70)$$

The Lagrangian function of problem (4.68) results in

$$\begin{aligned} L(p, \mathbf{G}, \eta, \mathbf{\Gamma}^{(1)}, \mathbf{\Gamma}^{(2)}) = & p^2 \sum_{k=1}^2 \text{tr} \left\{ \mathbf{H}^{(k)\text{T}} \mathbf{G} \mathbf{R}_{\mathbf{n}^{(0)}} \mathbf{G}^{\text{H}} \mathbf{H}^{(k)*} + \mathbf{R}_{\mathbf{n}_{\text{R}}^{(k)}} \right\} \\ & - 2\Re \left\{ \sum_{i=1}^2 \text{tr} \left\{ \mathbf{\Gamma}^{(k)} \left(pq^{(i)} \mathbf{H}^{(k)\text{T}} \mathbf{G} \mathbf{H}^{(i)} - \mathbf{I}_M \right) \right\} \right\} \\ & + \eta \left(\text{tr} \left\{ \mathbf{G} \mathbf{\Gamma} \mathbf{G}^{\text{H}} \right\} - E^{(0)} \right), \end{aligned} \quad (4.71)$$

with the Lagrangian multiplier η coming from the RS power constraint and the two Lagrangian multipliers $\mathbf{\Gamma}^{(k)}$, $k = 1, 2$, coming from the two complex-valued ZF constraints (4.69). The KKT conditions are only necessary conditions for the global opti-

mum and are given by

$$\frac{\partial L}{\partial p} = p^* \sum_{k=1}^2 \text{tr} \left\{ \mathbf{H}^{(k)\text{T}} \mathbf{G} \mathbf{R}_{\mathbf{n}^{(0)}} \mathbf{G}^{\text{H}} \mathbf{H}^{(k)*} + \mathbf{R}_{\mathbf{n}_{\text{R}}^{(k)}} \right\} - \sum_{i=1}^2 \text{tr} \left\{ \mathbf{\Gamma}^{(k)} \mathbf{H}^{(k)\text{T}} \mathbf{G} \mathbf{H}^{(i)} \right\} \stackrel{!}{=} 0, \quad (4.72a)$$

$$\frac{\partial L}{\partial \mathbf{G}} = p^2 \sum_{k=1}^2 \mathbf{H}^{(k)} \mathbf{H}^{(k)\text{H}} \mathbf{G}^* \mathbf{R}_{\mathbf{n}^{(0)}}^{\text{T}} - p \sum_{i=1}^2 q^{(i)} \mathbf{H}^{(k)} \mathbf{\Gamma}^{(k)\text{T}} \mathbf{H}^{(i)\text{T}} + \eta \mathbf{G}^* \mathbf{\Upsilon}^{\text{T}} \stackrel{!}{=} \mathbf{0}, \quad (4.72b)$$

$$\frac{\partial L}{\partial \mathbf{\Gamma}^{(k)}} = p q^{(i)} \mathbf{H}^{(i)\text{T}} \mathbf{G}^{\text{T}} \mathbf{H}^{(k)} - \mathbf{I}_M \stackrel{!}{=} \mathbf{0}, \quad i = 1, 2, \quad (4.72c)$$

$$\eta (\text{tr} \{ \mathbf{G} \mathbf{\Upsilon} \mathbf{G}^{\text{H}} \} - E^{(0)}) \stackrel{!}{=} 0, \quad (4.72d)$$

where Eq. (4.72c) gives two independent KKT conditions for $i = 1, 2$. An analytical solution to problem (4.68) can only be provided under the assumption that the noise at the RS does not contribute to the MSE in Eq. (4.70), cf. Appendix A.6. Thus, the following ZF-BF algorithm provides a sub-optimum solution to problem (4.68). Defining the matrices

$$\mathbf{X}_0^{(k)} = \mathbf{H}^{(k)\text{T}} \mathbf{H}^{(i)*} \left(\mathbf{H}^{(i)\text{T}} \mathbf{H}^{(i)*} \right)^{-1} \left(\mathbf{H}^{(k)\text{H}} \mathbf{\Upsilon}^{-1} \mathbf{H}^{(k)} \right)^{-1} \mathbf{H}^{(k)\text{H}} \mathbf{\Upsilon}^{-1} \mathbf{H}^{(i)}, \quad (4.73a)$$

$$\mathbf{X}_1^{(k)} = q^{(i)} \mathbf{H}^{(k)\text{T}} \mathbf{H}^{(k)*}, \quad (4.73b)$$

$$\mathbf{X}_2^{(k)} = \mathbf{H}^{(i)\text{H}} \mathbf{\Upsilon}^{-1} \mathbf{H}^{(i)}, \quad (4.73c)$$

$$\mathbf{X}_3^{(k)} = q^{(k)} \mathbf{H}^{(k)\text{T}} \mathbf{H}^{(i)*} \left(\mathbf{H}^{(i)\text{T}} \mathbf{H}^{(i)*} \right)^{-1} \mathbf{H}^{(i)\text{T}} \mathbf{H}^{(k)*}, \quad (4.73d)$$

$$\mathbf{X}_4^{(k)} = \mathbf{H}^{(i)\text{H}} \mathbf{\Upsilon}^{-1} \mathbf{H}^{(k)} \left(\mathbf{H}^{(k)\text{H}} \mathbf{\Upsilon}^{-1} \mathbf{H}^{(k)} \right)^{-1} \mathbf{H}^{(k)\text{H}} \mathbf{\Upsilon}^{-1} \mathbf{H}^{(i)}, \quad (4.73e)$$

and the modified Lagrangian multipliers

$$\tilde{\mathbf{\Gamma}}^{(k)\text{H}} = \text{vec}_{M,M}^{-1} \left[\left(\left(\mathbf{X}_2^{(k)\text{T}} \otimes \mathbf{X}_1^{(k)} \right) - \left(\mathbf{X}_4^{(k)\text{T}} \otimes \mathbf{X}_3^{(k)} \right) \right)^{-1} \text{vec} \left[\frac{1}{q^{(k)}} \mathbf{I}_M - \mathbf{X}_0^{(k)} \right] \right], \quad (4.74)$$

the BF matrix at the RS yields

$$\mathbf{G}_{\text{ZF}} = \frac{1}{p_{\text{ZF}}} \sum_{i=1}^2 q^{(i)} \mathbf{H}^{(k)*} \tilde{\mathbf{\Gamma}}^{(k)\text{H}} \mathbf{H}^{(i)\text{H}} \mathbf{\Upsilon}^{-1}. \quad (4.75)$$

With auxiliary matrix

$$\tilde{\mathbf{G}}_{\text{ZF}} = \sum_{i=1}^2 q^{(i)} \mathbf{H}^{(k)*} \tilde{\mathbf{\Gamma}}^{(k)\text{H}} \mathbf{H}^{(i)\text{H}} \mathbf{\Upsilon}^{-1}, \quad (4.76)$$

the scalar weighting factor p_{ZF} results in

$$p_{\text{ZF}} = \sqrt{\frac{\text{tr} \left\{ \tilde{\mathbf{G}}_{\text{ZF}} \mathbf{\Upsilon} \tilde{\mathbf{G}}_{\text{ZF}}^{\text{H}} \right\}}{E^{(0)}}} \in \mathbb{R}^+. \quad (4.77)$$

The derivation of the ZF-BF algorithm from the KKT conditions (4.72) can be found in Appendix A.6. In contrast to the MMSE-BF algorithm of Section 4.4.2, the ZF-BF algorithm only requires knowledge about the noise covariance matrix $\mathbf{R}_{\mathbf{n}^{(0)}}$ of the RS but not about the noise covariance matrices $\mathbf{R}_{\mathbf{n}_R^{(k)}}$, $k = 1, 2$, of the destination nodes, i.e., no feedback from S_k to the RS is required.

4.4.4 Maximization of the SNR

In this section, the maximization of the SNR is considered for a system with local CSI at S1 and S2 in two-way relaying and the corresponding MF-BF algorithm is derived. As in a system with limited capabilities at S1 and S2, the SNR gives the ratio between the average power of the useful signal part in the joint estimated data vector $\hat{\mathbf{x}}$ of Eq. (4.15) and the average power of the overall noise at the receiver output. The constraints for CDI matrices $\mathbf{T}^{(k)}$, $k = 1, 2$, in problem (4.53), are changed from Eq. (2.29) to Eq. (2.27) due to the application of CDI at the destination nodes. Thus, the problem is formulated as follows:

$$\{p_{\text{MF}}, \mathbf{G}_{\text{MF}}\} = \arg \max_{\{p, \mathbf{G}\}} \frac{|\mathbb{E}\{\mathbf{x}^H \hat{\mathbf{x}}\}|^2}{\mathbb{E}\{\|\mathbf{x}\|_2^2\} \mathbb{E}\left\{\left\|\sum_{k=1}^2 p \mathbf{H}^{(k)\text{T}} \mathbf{G} \mathbf{n}^{(0)} + p \mathbf{n}_R^{(k)}\right\|_2^2\right\}}, \quad (4.78a)$$

$$\text{subject to: } \mathbf{T}^{(k)} = -pq^{(k)} \mathbf{H}^{(k)\text{T}} \mathbf{G} \mathbf{H}^{(k)}, \quad k = 1, 2, \quad (4.78b)$$

$$\text{tr}\left\{\mathbf{G}\left(\sum_{i=1}^2 q^{(i)2} \mathbf{H}^{(i)} \mathbf{R}_{\mathbf{x}^{(i)}} \mathbf{H}^{(i)\text{H}} + \mathbf{R}_{\mathbf{n}^{(0)}}\right)\mathbf{G}^{\text{H}}\right\} = E^{(0)}. \quad (4.78c)$$

In the following, the MF-BF algorithm solving problem (4.78) is derived. For the maximization of the SNR in the system with local CSI at S1 and S2, the application of CDI indicated by constraint (4.78b) only changes the numerator in the objective function (4.78a) compared to the objective function (4.53a) in the system with limited capabilities at S1 and S2. In the system with limited capabilities at S1 and S2, the numerator contains the duplex interference power while this power is subtracted in the system with local CSI where $\mathbf{D}^{(k)} = \mathbf{0}_{M \times M}$ in Eq. (2.11). Regarding the overall noise power in the denominator, both systems are the same. Hence, with

Eqs. (2.10) and (2.11), the expectation values of Eq. (4.78a) are given by

$$|\mathbb{E} \{ \mathbf{x}^H \hat{\mathbf{x}} \}|^2 = \sum_{i=1}^2 \left| \mathbb{E} \{ \mathbf{x}^{(i)H} \hat{\mathbf{x}}^{(i)} \} \right|^2 = p^2 \sum_{i=1}^2 q^{(i)2} \left| \text{tr} \left\{ \mathbf{H}^{(k)T} \mathbf{G} \mathbf{H}^{(i)} \mathbf{R}_{\mathbf{x}^{(i)}} \right\} \right|^2, \quad (4.79a)$$

$$\mathbb{E} \{ \|\mathbf{x}\|_2^2 \} = \sum_{i=1}^2 \text{tr} \{ \mathbf{R}_{\mathbf{x}^{(i)}} \}, \quad (4.79b)$$

$$\mathbb{E} \left\{ \sum_{k=1}^2 \left\| p \mathbf{H}^{(k)T} \mathbf{G} \mathbf{n}^{(0)} + p \mathbf{n}_{\mathbf{R}}^{(k)} \right\|_2^2 \right\} = p^2 \sum_{k=1}^2 \text{tr} \left\{ \mathbf{H}^{(k)T} \mathbf{G} \mathbf{R}_{\mathbf{n}^{(0)}} \mathbf{G}^H \mathbf{H}^{(k)*} + \mathbf{R}_{\mathbf{n}_{\mathbf{R}}^{(k)}} \right\}. \quad (4.79c)$$

The Lagrangian function can be written as

$$L(p, \mathbf{G}, \eta) = - \frac{\sum_{i=1}^2 q^{(i)2} \left| \text{tr} \left\{ \mathbf{H}^{(k)T} \mathbf{G} \mathbf{H}^{(i)} \mathbf{R}_{\mathbf{x}^{(i)}} \right\} \right|^2}{\left(\sum_{i=1}^2 \text{tr} \{ \mathbf{R}_{\mathbf{x}^{(i)}} \} \right) \left(\sum_{k=1}^2 \text{tr} \left\{ \mathbf{H}^{(k)T} \mathbf{G} \mathbf{R}_{\mathbf{n}^{(0)}} \mathbf{G}^H \mathbf{H}^{(k)*} + \mathbf{R}_{\mathbf{n}_{\mathbf{R}}^{(k)}} \right\} \right)} + \eta \left(\text{tr} \{ \mathbf{G} \Upsilon \mathbf{G}^H \} - E^{(0)} \right), \quad (4.80)$$

with the Lagrangian multiplier η . Obviously, the Lagrangian function is independent of the scalar weighting factor p , which means that p can be chosen arbitrarily, except for $p = 0$, and the solution to the optimization problem (4.78) is not unique. Defining

$$\alpha^{(i)} = \frac{\text{tr} \left\{ \mathbf{H}^{(k)T} \mathbf{G} \mathbf{H}^{(i)} \mathbf{R}_{\mathbf{x}^{(i)}} \right\}}{\left(\sum_{l=1}^2 \text{tr} \{ \mathbf{R}_{\mathbf{x}^{(l)}} \} \right) \left(\sum_{l=1}^2 \text{tr} \left\{ \mathbf{H}^{(l)T} \mathbf{G} \mathbf{R}_{\mathbf{n}^{(0)}} \mathbf{G}^H \mathbf{H}^{(l)*} + \mathbf{R}_{\mathbf{n}_{\mathbf{R}}^{(l)}} \right\} \right)}, \quad i = 1, 2, \quad (4.81)$$

the KKT conditions result in

$$\frac{\partial L}{\partial \mathbf{G}} = - \sum_{i=1}^2 q^{(i)2} \alpha^{(i)*} \mathbf{H}^{(k)} \mathbf{R}_{\mathbf{x}^{(i)}}^T \mathbf{H}^{(i)T} + \left(\sum_{i=1}^2 \text{tr} \{ \mathbf{R}_{\mathbf{x}^{(i)}} \} \right) \left(\sum_{i=1}^2 q^{(i)2} |\alpha^{(i)}|^2 \right) \left(\sum_{k=1}^2 \mathbf{H}^{(k)} \mathbf{H}^{(k)H} \mathbf{G}^* \mathbf{R}_{\mathbf{n}^{(0)}}^T \right) + \eta \mathbf{G}^* \Upsilon^T \stackrel{!}{=} \mathbf{0}, \quad (4.82a)$$

$$\eta \left(\text{tr} \{ \mathbf{G} \Upsilon \mathbf{G}^H \} - E^{(0)} \right) \stackrel{!}{=} 0. \quad (4.82b)$$

An analytical solution to problem (4.78) can only be provided under the assumption that the noise at the RS which is retransmitted to the destination nodes does not contribute to the overall noise at the destination node, i.e., $\mathbf{R}_{\mathbf{n}^{(0)}} = \mathbf{0}_{L \times L}$ in Eq. (4.79c), cf. Appendix A.7. With this assumption, the BF matrix of the MF-BF algorithm is given by

$$\mathbf{G}_{\text{MF}} = \frac{1}{p_{\text{MF}}} \sum_{i=1}^2 \mathbf{H}^{(k)*} \mathbf{R}_{\mathbf{x}^{(i)}} \mathbf{H}^{(i)H} \Upsilon^{-1}. \quad (4.83)$$

With auxiliary matrix

$$\tilde{\mathbf{G}}_{\text{MF}} = \sum_{i=1}^2 \mathbf{H}^{(k)*} \mathbf{R}_{\mathbf{x}^{(i)}} \mathbf{H}^{(i)\text{H}} \boldsymbol{\Upsilon}^{-1}, \quad (4.84)$$

the scalar weighting factor p_{MF} results in

$$p_{\text{MF}} = \sqrt{\frac{\text{tr} \left\{ \tilde{\mathbf{G}}_{\text{MF}} \boldsymbol{\Upsilon} \tilde{\mathbf{G}}_{\text{MF}}^{\text{H}} \right\}}{E^{(0)}}} \in \mathbb{R}^+. \quad (4.85)$$

The derivation of the MF-BF algorithm from the KKT conditions (4.82) for a system with local CSI at S1 and S2 can be found in Appendix A.7. In contrast to the MMSE-BF algorithm of Section 4.4.2, the MF-BF algorithm only requires knowledge about the noise covariance matrix $\mathbf{R}_{\mathbf{n}^{(0)}}$ of the RS but not about the noise covariance matrices $\mathbf{R}_{\mathbf{n}^{(k)}}$, $k = 1, 2$, of the destination nodes, i.e., no feedback from S_k to the RS is required. Obviously, the BF matrix \mathbf{G}_{MF} of Eq. (4.83) consists of two summands. The first summand corresponds to the receive MF to channel $\mathbf{H}^{(1)}$ in conjunction with the transmit MF to channel $\mathbf{H}^{(2)\text{T}}$ for the transmission from S1 to S2. The second summand corresponds to the receive MF to channel $\mathbf{H}^{(2)}$ in conjunction with the transmit MF to channel $\mathbf{H}^{(1)\text{T}}$ for the transmission from S2 to S1.

4.5 Performance analysis

4.5.1 Simulation assumptions

In this Section 4.5, the BF algorithms of Sections 4.2, 4.3, and 4.4 are analyzed by means of simulations. The assumed channel model and the definition of $\text{SNR}^{(i)}$ is exactly the same as introduced for one-way relaying in Eq. 3.61. The transmit power of the RS is assumed as $E^{(0)} = 1$, and the noise variances of all nodes are assumed as $\sigma_{\mathbf{n}^{(0)}}^2 = \sigma_{\mathbf{n}^{(1)}}^2 = \sigma_{\mathbf{n}^{(2)}}^2 = \sigma_{\mathbf{n}}^2 = 1$. The transmit powers of S_i , $i = 1, 2$, are given by $E^{(i)} \leq 1$ considering the fact that the transmission powers of S_i may be below the maximum transmission powers in two-way relaying. The four different cases of system capabilities in two-way relaying are distinguished by the following notation:

- CASE1: system with full capabilities,
- CASE2: system with limited capabilities at the RS,
- CASE3: system with limited capabilities at S1 and S2,

- CASE4: system with local CSI at S1 and S2,

where CASE1, CASE2, and CASE3 directly correspond to the same cases of system capabilities in one-way relaying. As introduced in Section 3.4.1, all results which are obtained by numerical methods from the MATLAB[®] optimization toolbox are denoted by N-BF, and all results obtained by analytical BF algorithms proposed in Section 4.2 are denoted by A-BF.

4.5.2 Sum rate analysis

In this section, the average sum rates of the different BF algorithms in two-way relaying introduced in Sections 4.2, 4.3, and 4.4 are analyzed. The sum rate is a reasonable performance measure for two-way relaying since both transmissions, namely from S1 to S2 and from S2 to S1, are performed during the same time slots.

In the following, the average maximum sum rates of CASE1, CASE2, CASE3, and CASE4 are considered so that the performances of the different cases of system capabilities in two-way relaying introduced in the new framework of Figure 1.4 can be compared to each other. In Figure 4.1, the average maximum sum rate vs. SNR⁽²⁾ is depicted for CASE1, CASE2, CASE3, and CASE4 for $M = 2$ antennas at S1 and S2 and $L = 4$ antennas at the RS. For the sake of clarity, the sum rate performance is only presented for one value of SNR⁽¹⁾, namely SNR⁽¹⁾ = 20dB. As for one-way relaying, other values of SNR⁽¹⁾ do not provide new observations since the relative behavior of the curves does not change. The sum rates of all four cases are determined by numerical methods. Furthermore, Figure 4.1 contains the upper bound for the maximum sum rate in two-way relaying which comes from the sum of two independent one-way relaying transmissions as discussed in Section 4.2.2.

As expected, the highest sum rate is obtained in CASE1 where adaptive BF is performed at S1, S2 and the RS. For all values of SNR⁽²⁾ in CASE1, there exists a relative loss in sum rate of about 10% compared to the upper bound. As explained in Section 4.2.2, this loss comes from the fact that some fraction of the RS transmit power is used to transmit information to the destination nodes which they already know. In other words, two-way relaying cannot completely double the sum rate of one-way relaying but it compensates a significant fraction of the loss in sum rate due to the half-duplex constraint in two-hop relaying. These results show that in case of bi-directional transmission, two-way relaying considerably outperforms one-way relaying and should be preferred.

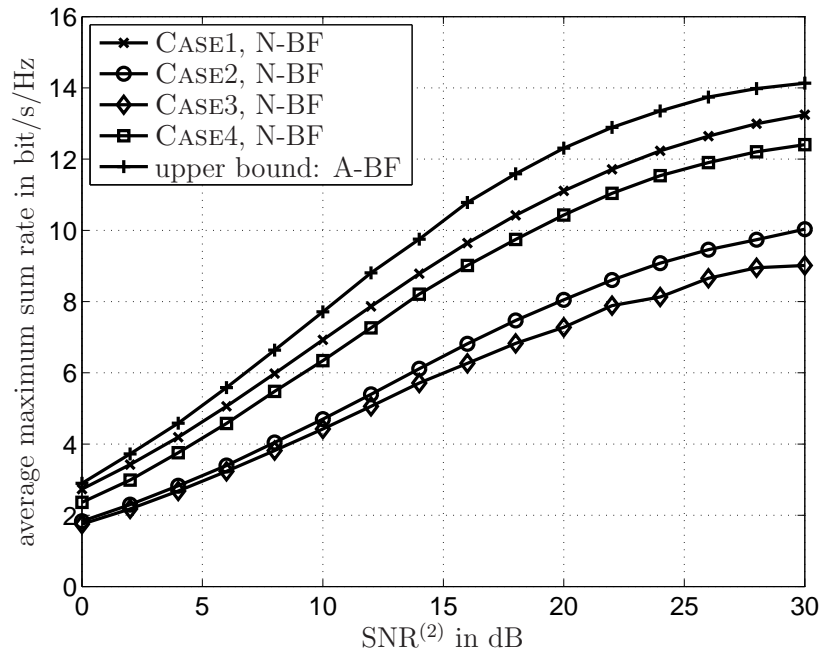


Figure 4.1. Average maximum sum rate vs. $\text{SNR}^{(2)}$ for CASE1, CASE2, CASE3, CASE4, and the upper bound, $\text{SNR}^{(1)} = 20\text{dB}$, $M = 2$ and $L = 4$.

Compared to CASE1, the relative loss in sum rate is about 6% for all values of $\text{SNR}^{(2)}$ in CASE4. This loss is caused by the equal weighting at S1 and S2 which implies that no coding gain due to joint decoding at the destination nodes can be obtained. In CASE2 as known from one-way relaying, the high number L of antennas at the RS cannot be exploited since the RS cannot perform adaptive BF but only equal weighting. This fact leads to the strong degradation compared to CASE1 and CASE4. The worst performance is obtained in CASE3 since the duplex interference is not eliminated at the destination nodes, and all antennas at the RS are required in order to multiplex the $2M$ data streams transmitted by the two source nodes. For those reasons, CASE3 performs worse than CASE2 in two-way relaying, while CASE3 performs better than CASE2 in one-way relaying where no duplex interference appears, and only M data streams transmitted by one source node have to be multiplex, cf. Figure 3.1.

In the following, the influence of the number L of antennas at the RS on the sum rate performance is investigated which provides an insight into the different performance gains, namely multiplexing gain, array gain, and diversity gain, which can be obtained due to multiple antennas at the RS in two-way relaying. Figure 4.2 gives the average maximum sum rate vs. the number L of antennas at the RS for all cases of system capabilities obtained by numerical methods and for the introduced upper bound which comes from the sum of two independent one-way relaying transmissions. Additionally, the sum rate performance for the A-BF algorithm proposed for CASE2 in Section 4.2.3

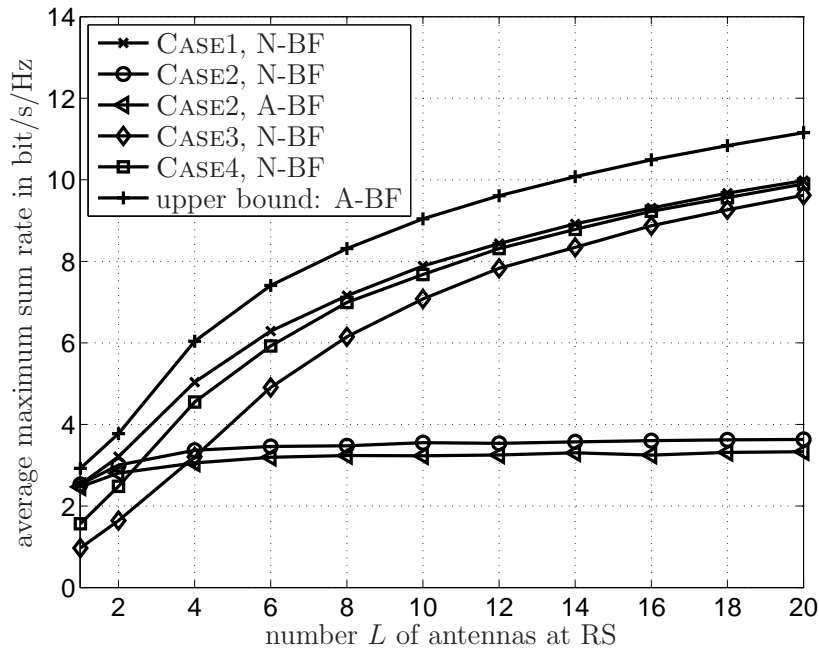


Figure 4.2. Average maximum sum rate vs. number L of antennas at the RS for CASE1, CASE2 (N-BF and A-BF), CASE3, CASE4, and the upper bound, $\text{SNR}^{(1)} = \text{SNR}^{(2)} = 10\text{dB}$, $M = 2$.

is depicted in the figure. The SNR values are fixed to $\text{SNR}^{(1)} = \text{SNR}^{(2)} = 10\text{dB}$, and the number M of antennas at S1 and S2 is fixed to $M = 2$.

The relative difference between the sum rate in CASE1 and the upper bound is between 10% for high numbers L of antennas at the RS and 15% for small numbers L of antennas at the RS. The relative difference comes from the transmit power loss at the RS due to the retransmission of already known information by the RS. Furthermore, for CASE1 it can be seen that the sum rate increases by 2bit/s/Hz if the number L of antennas at the RS is increased from $L = 2$ to $L = 4$ which corresponds to a spatial multiplexing gain of two. This means that the full spatial multiplexing gain in two-way relaying is not achieved until $L \geq 2M$. This observation constitutes a significant difference to one-way relaying where the full spatial multiplexing gain is already obtained for $L \geq M$. For $L > 2M$, the increase in sum rate in two-way relaying is coming from the array gain for the reception at the RS and the spatial diversity gain for the retransmission from the RS.

In CASE3 and CASE4, the full spatial multiplexing gain is obtained for $L \geq 2M$, too. Furthermore, both cases converge against the sum rate of CASE1 since the antenna beams are becoming sharper for higher numbers L of antennas at the RS. As in one-way relaying, the influence of the additional coding gain which can be obtained in

CASE1 is decreasing so that the sum rate performances of CASE1, CASE3, and CASE4 converge. However, the sum rate in CASE4 converges faster since the duplex interference is cancelled by CDI at the destination nodes in CASE4 while the $2M$ data streams of the two source nodes have to be separated exclusively by adaptive BF at the RS in CASE3.

For $L = M = 2$, the N-BF solution in CASE2 provides almost the same performance as the N-BF solution in CASE1, and the performance in CASE2 is slightly better than in CASE3. As in one-way relaying, this shows that spatial precoding at the source nodes and joint decoding at the destination nodes provide a coding gain which cannot be obtained by the spatial separation of the data streams by exclusive adaptive BF at the RS. However, for $L > M$ the performance in CASE2 is considerably worse than the performance in all other cases, even CASE3, since the array gain and the spatial diversity cannot be exploited for an equal weighting at all antennas of the RS. As in one-way relaying, no diversity gain can be achieved for the equal weighting at the RS in CASE2 which means that the sum rate remains constant even if the number L of antennas at the RS is increased. The highest sum rate is already obtained for $L = 4$ where the full spatial multiplexing gain can be exploited by the adaptive BF at the source and destination nodes. The performance of the proposed A-BF algorithm of Section 4.2.3 comes close to the performance of the N-BF solution, especially for $L = 1$ and $L = 2$. For $L \geq 4$, the relative difference between the sum rate of the proposed A-BF algorithm and the sum rate of the N-BF solution is about 8% which comes from the two simplifying assumptions of the A-BF algorithm, namely the assumption of spatially white noise at the destination nodes and the assumption that the two sub-problems of determining the weighting factor g at the RS and determining the power allocations at the source nodes are independent of each other. Nevertheless, due the considerably lower computational effort compared to the N-BF algorithm, the A-BF algorithm is of particular interest for practical applications, in which there are limited capabilities at the RS, i.e., in CASE2.

In the following, the transmission powers of the source nodes S1 and S2 are considered. In Section 4.2, it is explained that reducing the transmit power of the source node with the higher transmission rate may improve the overall sum rate in case of significantly different values of $\text{SNR}^{(1)}$ and $\text{SNR}^{(2)}$. Of course, S1 and S2 can adapt their transmission power only if global CSI is available at the source nodes which is valid for CASE1 and CASE2. If no global CSI is available at the source nodes, which is assumed in CASE3 and CASE4, the maximum transmission power has to be used. Since the evaluation of the sum rates of the different cases of system capabilities in the previous two figures does not include the required transmission powers in the different cases, Figure 4.3 gives the average required transmission powers $\bar{E}^{(i)}$, $i = 1, 2$, vs.

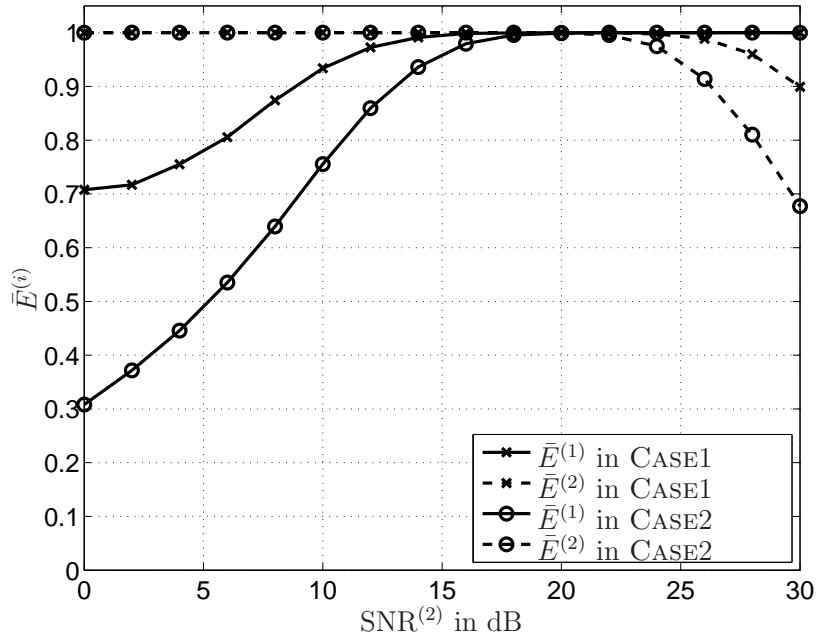


Figure 4.3. Average transmitted power $\bar{E}^{(i)}$ vs. $\text{SNR}^{(2)}$ for CASE1 and CASE2, $\text{SNR}^{(1)} = 20\text{dB}$, $M = 2$ and $L = 4$.

$\text{SNR}^{(2)}$ for CASE1 and CASE2. The RS is equipped with $L = 4$ antennas, and S1 and S2 are equipped with $M = 2$ antennas. $\text{SNR}^{(1)}$ is fixed to $\text{SNR}^{(1)} = 20\text{dB}$.

Without adaptation, the transmission powers of S_i , $i = 1, 2$, are always given by $\bar{E}^{(i)} = 1$ in CASE3 and CASE4. From Figure 4.3, it can be seen that a significant amount of the average transmit power may be saved in CASE1 and CASE2, if the values of $\text{SNR}^{(1)}$ and $\text{SNR}^{(2)}$ are significantly different. For $\text{SNR}^{(2)} < \text{SNR}^{(1)}$, the average transmit power of node S1 may be reduced and for $\text{SNR}^{(2)} > \text{SNR}^{(1)}$, the average transmit power of node S2 may be reduced. This means that the source node which transmits over the better channel to the RS, should reduce its own transmit power and transmission rate in order to reduce the interference at the RS and to allow the other node a higher transmission rate which yields a higher overall sum rate. If $\text{SNR}^{(2)} = \text{SNR}^{(1)}$, both source nodes should transmit with their maximum power in order to obtain the maximum sum rate.

In Figure 4.3, it can also be seen that the reduction of the transmit powers is significantly higher for CASE2 than for CASE1. This may be explained as follows. In CASE1, the different SNR values of the two channels cannot only be compensated by the source nodes but also the BF at the RS. In this case, the larger part of the RS transmit power is used for the retransmission over the channel with the lower SNR and the smaller part is used for the retransmission over the channel with the higher SNR.

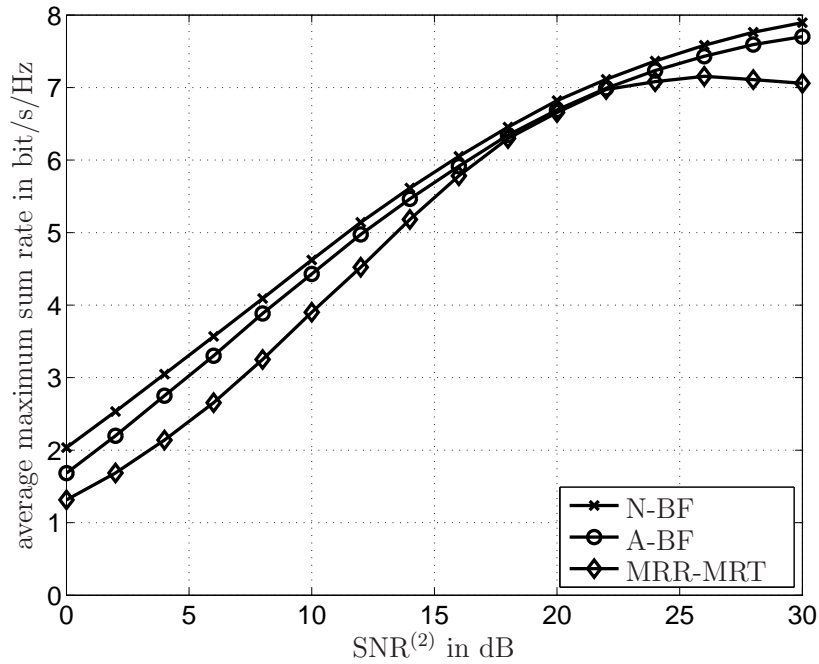


Figure 4.4. Average maximum sum rate vs. $\text{SNR}^{(2)}$ for N-BF, A-BF, and MRR-MRT in CASE1, $\text{SNR}^{(1)} = 20\text{dB}$, $M = 1$ and $L = 4$.

In CASE2, the different SNR values can only be compensated by the source nodes since the RS does not perform BF. Hence, the power reduction in CASE2 is higher than in CASE1.

In the following, the average maximum sum rate for the particular case of single-antenna source and destination nodes, i.e., $M = 1$, is considered in order to investigate the performance of the proposed sub-optimum A-BF algorithm of Section 4.2.2. In Figure 4.4, the average maximum sum rate vs. $\text{SNR}^{(2)}$ is depicted for $\text{SNR}^{(1)} = 20\text{dB}$ in CASE1. Nodes S1 and S2 are equipped with $M = 1$ antenna, and the RS is equipped with $L = 4$ antennas. Note that the sum rate maximization problems in CASE1 and CASE4 are the same optimization problems for $M = 1$ since only weighting by a single scalar factor is possible at the source and destination nodes.

As expected, the highest sum rate is obtained by the N-BF solution. However, the proposed A-BF algorithm of Section 4.2.2 which is based on a MF approach with adaptive power allocation to the different data streams at the RS performs almost as well as the N-BF solution. Furthermore, it is shown in Figure 4.4 that the MRR-MRT two-way relaying approach proposed in [LZ08] has a worse performance especially in case of significantly different SNRs for the two channels $\mathbf{h}^{(1)}$ and $\mathbf{h}^{(2)}$. For MRR-MRT two-way relaying, the average sum rate achieves the highest value for $\text{SNR}^{(2)} \approx 26\text{dB}$ and even decreases for $\text{SNR}^{(2)} > 26\text{dB}$. This comes from the fact that maximizing the

SNR for the transmission over the better channel $\mathbf{h}^{(2)\text{T}}$ by the transmit MF $\mathbf{h}^{(2)*}$ also decreases the SNR for the transmission over the worse channel $\mathbf{h}^{(1)\text{T}}$ due to the amplification of the noise of the RS. The noise at the RS is weighted by the MFs matched to both directions of the transmission where MF $\mathbf{h}^{(2)*}$ dominates the amplification of the RS noise since it has a higher absolute value than the MF $\mathbf{h}^{(1)*}$. For the retransmission over the channel $\mathbf{h}^{(2)\text{T}}$, the noise and the useful signal are both weighted by the dominant MF $\mathbf{h}^{(2)*}$ so that the amplification of the noise of the RS for the transmission to S2 is compensated by a high value of the received useful power at S2. However, for the retransmission over channel $\mathbf{h}^{(1)\text{T}}$, the noise is also mainly amplified by the MF $\mathbf{h}^{(2)*}$ which means that the noise is weighted by the MF of the strong channel while the useful signal is only weighted by the weak channel $\mathbf{h}^{(1)\text{T}}$. In the particular case, this means that $C^{(2)}$ is increased while $C^{(1)}$ is decreased. For $\text{SNR}^{(2)} > 26\text{dB}$, the increase in $C^{(2)}$ is smaller than the decrease in $C^{(1)}$ which means that the sum rate gets smaller for MRR-MRT two-way relaying. With respect to the results presented in Figure 4.4 for $M = 1$, it is proposed to perform adaptive power allocation to the data streams at the RS according to the A-BF algorithm of Section 4.2.2.

In the following, the individual rate performances of the transmission from S1 to S2 and the transmission from S2 to S1 are compared to each other for all cases of system capabilities. In Figure 4.5, the average maximum individual rate vs. $\text{SNR}^{(2)}$ is depicted for the transmission from S1 to S2 (solid lines) and for the transmission from S2 to S1 (dashed lines).

The relation between the individual rates of both directions of the transmission is the same in all cases of system capabilities so that all cases are analyzed jointly in the following. For $\text{SNR}^{(1)} = \text{SNR}^{(2)} = 20\text{dB}$, the individual rate is the same for both directions of the transmission. However, for $\text{SNR}^{(1)} > \text{SNR}^{(2)}$ the individual rate for the transmission from S1 to S2 is higher than the individual rate for the transmission from S2 to S1 and vice versa. This comes from the fact that the two first hop transmissions are processed simultaneously in two-way relaying. Hence, the data streams which are transmitted over the channel with the higher SNR are dominant in the sum of the received data streams at the RS. In order to maximize the sum rate, more transmit power of the RS is allocated to the data streams which are dominant at the RS. Thus, the data streams with the worse SNR value for their first hop transmission achieve a lower individual rate. In general, different SNR values for the two channels to the RS cause an imbalance of the performances of the two directions of the transmission.

In the following, the sum rate performances of the MMSE-BF, ZF-BF, and MF-BF algorithms in CASE3 derived in Section 4.3 are considered. In Figure 4.6, the average sum rate vs. $\text{SNR}^{(2)}$ is depicted for the different BF algorithms of Section 4.3.

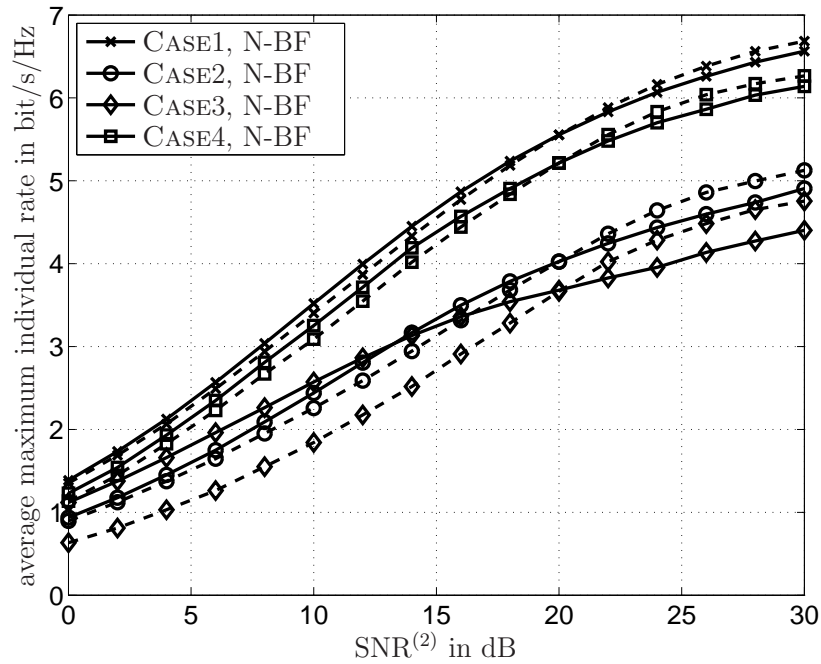


Figure 4.5. Average maximum individual rate vs. $\text{SNR}^{(2)}$ for CASE1, CASE2, CASE3, and CASE4, $\text{SNR}^{(1)} = 20\text{dB}$, $M = 2$ and $L = 4$, dashed lines: transmission from S2 to S1, solid lines: transmission from S1 to S2.

The average SNR between S1 and the RS is fixed to $\text{SNR}^{(1)} = 20\text{dB}$. S1 and S2 are equipped with either $M = 1$ (dashed lines) or $M = 2$ (solid lines) antennas, and the RS is equipped with $L = 4$ antennas.

For $M = 1$, the performance of the MMSE-BF algorithm is slightly worse than the performance of the N-BF solution. The ZF-BF algorithm performs worse than the MMSE-BF algorithm for low values of $\text{SNR}^{(2)}$ but converges to the performance of the MMSE-BF algorithm for high values of $\text{SNR}^{(2)}$. In contrast to one-way relaying where the ZF-BF algorithm and the MMSE-BF algorithm provide the same solutions for $M = 1$, the ZF-BF algorithm and the MMSE-BF algorithm provide different solutions for $M = 1$ in two-way relaying because there exists duplex interference between the data streams of S1 and S2 which has to be considered by the adaptive BF at the RS in CASE3. Indeed, from the interference perspective the BF algorithms for $M = 1$ in two-way relaying have to perform the same separation of data streams as the BF algorithms for $M = 2$ in one-way relaying considering that the intersymbol interference in one-way relaying corresponds to the duplex interference in two-way relaying. This relation between one-way relaying and two-way relaying in CASE3 becomes also clear for the MF-BF algorithm. While the MF-BF algorithm performs as well as the ZF-BF and MMSE-BF algorithms in one-way relaying for $M = 1$, the MF-BF algorithm performs much worse than the ZF-BF and MMSE-BF algorithms in two-way relaying

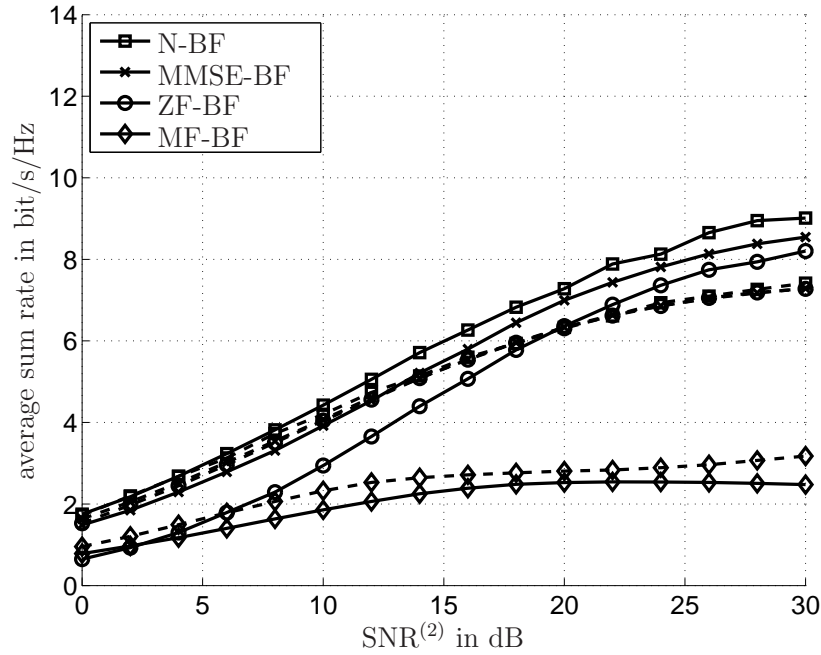


Figure 4.6. Average sum rate vs. $\text{SNR}^{(2)}$ for different BF algorithms in CASE3, $\text{SNR}^{(1)} = 20\text{dB}$, $L = 4$, dashed lines: $M = 1$, solid lines: $M = 2$.

due to the fact that the duplex interference is not considered in the MF-BF algorithm and cannot be cancelled by CDI at the destination nodes.

If the number M of antennas at S1 and S2 is increased from $M = 1$ to $M = 2$, the performances of the ZF-BF algorithm and the MMSE-BF algorithm become worse for low values of $\text{SNR}^{(2)}$ and become better for high values of $\text{SNR}^{(2)}$. In order to obtain performance gains by adaptive BF, good channel conditions in terms of SNR are required in order to steer the antenna beams into the correct directions. Since separating $M = 2$ data streams per source node by BF at the RS instead of separating $M = 1$ data stream per source node is more sensitive to low SNR values, the performance of the ZF-BF and MMSE-BF algorithms improves not until a certain SNR is exceeded, namely $\text{SNR}^{(2)} = 20\text{dB}$ for the ZF-BF algorithm and $\text{SNR}^{(2)} = 14\text{dB}$ for the MMSE-BF algorithm.

For $M = 2$, the relative difference in sum rate for the MMSE-BF algorithm compared to the N-BF algorithm is between 15% for small values of $\text{SNR}^{(2)}$ and 5% for large values of $\text{SNR}^{(2)}$. As mentioned before, the difference for small and large values of $\text{SNR}^{(2)}$ comes from the fact that good channel conditions in terms of SNR are required in order to steer the antenna beams into the correct directions. For $M = 2$, four data streams have to be separated by $L = 4$ antennas at the RS. In this case, the performance of the MMSE-BF algorithm is worse than the performance of the N-BF

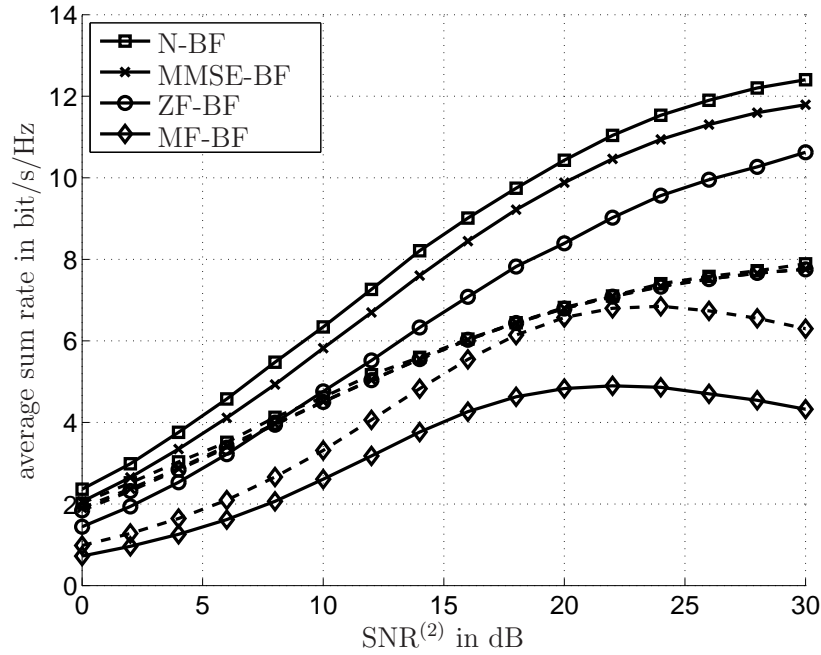


Figure 4.7. Average sum rate vs. $\text{SNR}^{(2)}$ for different BF algorithms in CASE4, $\text{SNR}^{(1)} = 20\text{dB}$, $L = 4$, dashed lines: $M = 1$, solid lines: $M = 2$.

solution. This result is also known from one-way relaying where no sharp antenna beams can be formed if the number of separated data streams equals the number L of antennas at the RS. Furthermore, the sum rate of the ZF-BF algorithm converges to the sum rate of the MMSE-BF algorithm. However, the speed of convergence is slower compared to one-way relaying for the same antenna configuration. This comes from the fact that the BF at the RS separates four data streams in case of two-way relaying instead of only two data streams in case of one-way relaying.

In Figure 4.7, the average sum rate vs. $\text{SNR}^{(2)}$ is depicted for CASE4. All other parameters are the same as introduced for Figure 4.6.

For the same reasons as in CASE3, the performances of the ZF-BF algorithm and the MMSE-BF become worse for low values of $\text{SNR}^{(2)}$ and become better for high values of $\text{SNR}^{(2)}$, if the number M of antennas at S1 and S2 is increased from $M = 1$ to $M = 2$.

In contrast to CASE3, the MMSE-BF algorithm and the ZF-BF algorithm provide almost the same performance for $M = 1$. This can be explained by the fact that no interference has to be considered for the BF at the RS since the duplex interference is cancelled by CDI at the destination nodes in CASE4. Both analytical BF algorithms come quite close to the N-BF solution and the slightly degraded performance of the

ZF-BF algorithm compared to the MMSE-BF algorithm comes from the proposed sub-optimum solution. The MF-BF algorithm performs worse than the ZF-BF algorithm and the MMSE-BF algorithm, and the sum rate of MF-BF algorithm does not increase monotonically with increasing $\text{SNR}^{(2)}$, but it even decreases with increasing $\text{SNR}^{(2)}$. The reasons are the same as introduced for the MRR-MRT two-way relaying approach presented in Figure 4.4. While the destination node with the better second hop channel is provided with a large SNR value by the MF of the RS, the destination node with the worse second hop channel suffers from the strong noise amplification due to the MF of the RS leading to a small receive SNR.

As in CASE3 for $M = 2$, the relative difference in sum rate for the MMSE-BF algorithm compared to the N-BF algorithm is between 15% for small values of $\text{SNR}^{(2)}$ and 5% for large values of $\text{SNR}^{(2)}$. Furthermore, the sum rate of the ZF-BF algorithm converges very slowly to the sum rate of the MMSE-BF algorithm. This slow speed of convergence comes from the fact that the optimization problem could only be solved analytically by relaxing the objective function with the assumption of zero noise at the RS which makes the proposed ZF-BF algorithm of Section 4.4.3 sub-optimum. The effect of this assumption only vanishes for very high values of the SNR. However, the performance of the ZF-BF algorithm is still significantly better than that of the MF-BF algorithm which suffers from the intersymbol interference appearing for more than $M = 1$ data stream per source node in CASE4.

4.5.3 Bit error rate analysis

In this section, the average uncoded BER of the linear BF algorithms of Sections 4.3 and 4.4 for CASE3 and CASE4, respectively, are analyzed. As in one-way relaying, all BER results are presented for QPSK modulated data bit streams.

In the following, the average joint uncoded BER of the MMSE-BF algorithm is considered at first in order to evaluate the performance of the algorithm in the different cases system capabilities, namely CASE3 and CASE4. Figure 4.8 presents the average joint uncoded BER vs. $\text{SNR}^{(2)}$ for the MMSE-BF algorithm for different numbers of antennas at S1, S2, and the RS. In the figure, the BER performances for CASE3 (dashed lines) and CASE4 (solid lines) are depicted. Since the relative behavior of the BER performance in the different antenna configurations is the same for all values of $\text{SNR}^{(1)}$, it is fixed to one value, namely $\text{SNR}^{(1)} = 20\text{dB}$.

Especially for small numbers L of antennas at the RS, the performance of CASE3 is significantly degraded compared to the performance of CASE4 due to the duplex

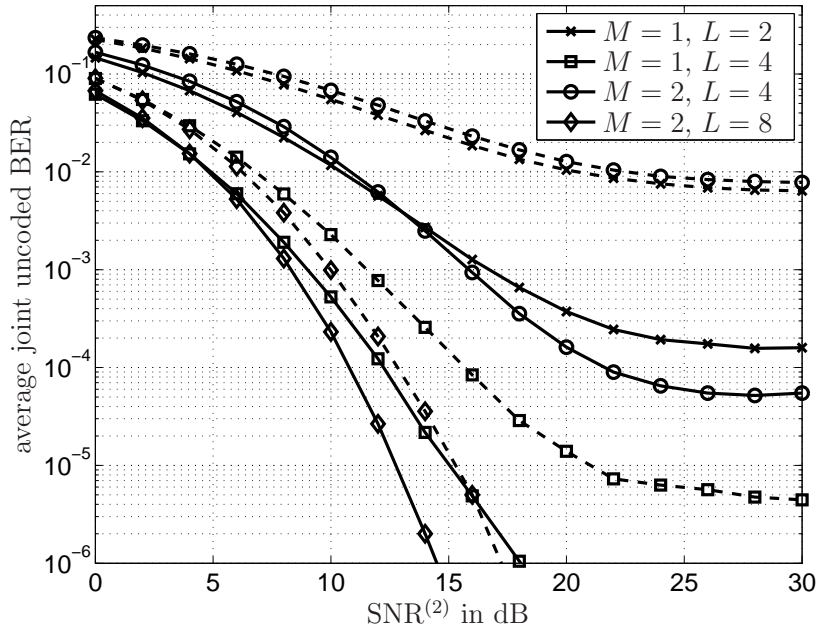


Figure 4.8. Average joint uncoded BER vs. $\text{SNR}^{(2)}$ for MMSE-BF for different antenna configurations, $\text{SNR}^{(1)} = 20\text{dB}$, dashed lines: CASE3, solid lines: CASE4.

interference which cannot be cancelled by CDI at the destination nodes in CASE3. With increasing number L of antennas at the RS, the BER of CASE3 is getting closer to the BER of CASE4, e.g., for the case $M = 2$ and $L = 8$, the SNR loss in CASE3 is only about 1.5dB compared to CASE4. However, the results of Figure 4.8 show that CDI should be performed at the destination nodes since CDI promises significant performance gains in CASE4 compared to CASE3 where no CDI is performed.

By comparing the antenna configuration of $M = 1$ and $L = 2$ with the antenna configuration of $M = 1$ and $L = 4$, it is seen that increasing the number L of antennas at the RS provides additional array and diversity gain. As for one-way relaying, the antenna beams can be steered more precisely in the direction of the source and destination nodes in case of more antennas at the RS. Regarding the antenna configuration of $M = 1$ and $L = 2$, and the antenna configuration of $M = 2$ and $L = 4$ where the ratio between M and L stays constant, a significant difference can be observed compared to one-way relaying. In one-way relaying, both antenna configurations provide the same array gain and the antenna configuration with the higher number L of antennas at the RS provides the higher diversity gain which can be seen from Figure 3.6. The diversity can be exploited in one-way relaying, since only M antennas of the $L = 2M$ antennas at the RS are required in order to multiplex M data streams transmitted by a source node. Thus, the remaining M antennas at the RS can be used in order to employ diversity schemes. For two-way relaying in CASE3 as well as in CASE4, there exists no

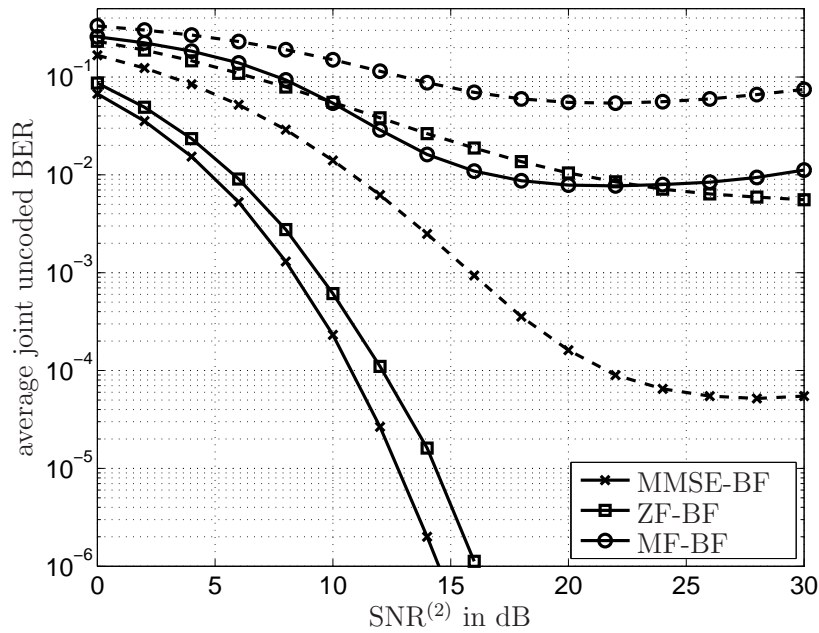


Figure 4.9. Average joint uncoded BER vs. $\text{SNR}^{(2)}$ for different BF algorithms in CASE4, $\text{SNR}^{(1)} = 20\text{dB}$, $M = 2$, dashed lines: $L = 4$, solid lines: $L = 8$.

array gain and no diversity gain. For both cases of system capabilities, the $L = 2M$ antennas at the RS are required in order to multiplex the $2M$ data streams of the two source nodes. Thus, no additional antennas are available for exploiting array and diversity gain. Since the ZF-BF and the MF-BF algorithms provide similar insights into the BER performance of two-way relaying in CASE3 and CASE4, their BER results regarding different antenna configurations are omitted here.

In the following, a comparison between the three BF algorithms is given for CASE4, since CASE4 performs significantly better than CASE3 which makes it more promising for real applications. In Figure 4.9, the average joint uncoded BER vs. $\text{SNR}^{(2)}$ is depicted for the three different BF algorithms in case of $\text{SNR}^{(1)} = 20\text{dB}$. Two antenna configurations are considered in the figure, namely $M = 2$ and $L = 8$ which is indicated by the solid lines, and $M = 2$ and $L = 4$ which is indicated by the dashed lines.

As already seen from the previous Figure 4.8, increasing the number L of antennas at the RS increases the diversity gain and the array gain if M is fixed. This observation holds for all BF algorithms. However, the MMSE-BF algorithm significantly outperforms the ZF-BF and the MF-BF algorithms. Typically, the difference in performance between MMSE-BF algorithms and ZF-BF algorithms is relatively small as seen in one-way relaying for example. The large difference in BER performance between the ZF-BF algorithm and the MMSE-BF algorithm in Figure 4.9 can be explained by the

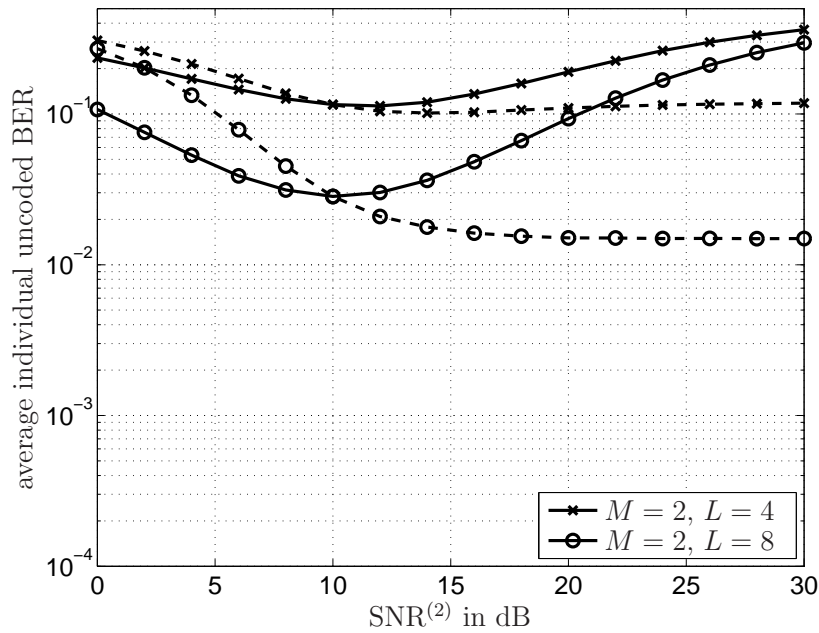


Figure 4.10. Average individual uncoded BER vs. $\text{SNR}^{(2)}$ for MF-BF in CASE4, $\text{SNR}^{(1)} = 10\text{dB}$, dashed lines: BER at S2, solid lines: BER at S1.

sub-optimum approach for solving the minimization of the MSE under the ZF constraint. For $M = 2$ and $L = 8$, the performance degradation of the ZF-BF algorithm due to the assumption of zero noise at the RS becomes smaller since the large number L of antennas at the RS can compensate the wrong assumption of zero noise at the RS by performing sharper antenna beams. Furthermore, the ZF-BF algorithm outperforms the MF-BF algorithm for all antenna configurations due to the fact that the MF-BF algorithm does not consider intersymbol interference. Regarding the BER of the MF-BF algorithm, a special characteristic of the MF-BF algorithm can be observed which is already known from the sum rate analysis and comes from the strong noise amplification for the worse second hop channel. Even with increasing $\text{SNR}^{(2)}$, the joint BER increases above a certain value of $\text{SNR}^{(2)}$, which is $\text{SNR}^{(2)} = 20\text{dB}$ in Figure 4.9.

In order to explain this special characteristic of the MF-BF algorithm in more detail, the average individual uncoded BER vs. $\text{SNR}^{(2)}$ at destination node S1 and the average individual uncoded BER vs. $\text{SNR}^{(2)}$ at destination node S2 are considered in Figure 4.10. The solid lines in the figure correspond to the average individual uncoded BER vs. $\text{SNR}^{(2)}$ at destination node S1 and the dashed lines correspond to the average individual uncoded BER vs. $\text{SNR}^{(2)}$ at destination node S2 for the MF-BF algorithm. Nodes S1 and S2 are equipped with $M = 2$ antennas and the RS is equipped with $L = 4$ and $L = 8$ antennas, respectively. $\text{SNR}^{(1)}$ is fixed to $\text{SNR}^{(1)} = 10\text{dB}$.

The BER performances at S1 and S2 show the same relative behavior for the case of $L = 4$ and the case of $L = 8$ which is explained and analyzed in the following. For equal values of $\text{SNR}^{(1)}$ and $\text{SNR}^{(2)}$, i.e. $\text{SNR}^{(1)} = \text{SNR}^{(2)} = 10\text{dB}$, the average BER values at S1 and S2 are the same. But for $\text{SNR}^{(2)} > \text{SNR}^{(1)}$, the BER at S2 is lower than the BER at S1 and vice versa. While $\text{SNR}^{(2)}$ is the SNR of the first hop of the transmission from S2 to S1, $\text{SNR}^{(1)}$ is the SNR of the second hop of the transmission from S2 to S1. In the BF matrix \mathbf{G}_{MF} of Eq. (4.83), the transmit and receive MF parts which are matched to the channel with the higher SNR are dominating. Since the RS noise is also filtered by the BF matrix \mathbf{G}_{MF} , the RS noise is transmitted with the same power to S1 and S2. For that reason, the destination node with the lower SNR receives more and more noise power without increasing the own receive power, if the SNR of the other channel increases more and more. Thus, the SNR at the receiver output decreases and the BER of destination node S1 even increases with increasing $\text{SNR}^{(2)}$ which explains the BER performance in Figure 4.10. Note that although the BER at S1 increases and the corresponding SNR at the receiver output of destination node S1 decreases with increasing $\text{SNR}^{(2)}$, the overall SNR defined in the objective function (4.78a) of the SNR maximization problem increases, i.e., the optimization goal is achieved nevertheless.

Compared to the MF-BF algorithm, the relative behavior of the average individual uncoded BERs at S1 and S2 is different for the MMSE-BF and ZF-BF algorithms. In order to show the differences, Figure 4.11 gives the average individual uncoded BERs of the MMSE-BF algorithm at S1 and S2. All parameters leading to the results in Figure 4.11 are exactly the same as introduced in Figure 4.10. Note that for the ZF-BF algorithm, the relative behavior of the BER performances at S1 and S2 is the same as for the MMSE-BF algorithm. Therefore, the results for the ZF-BF algorithm are omitted here.

In principle, the observations of the results in Figure 4.11 for the MMSE-BF algorithm are similar to the observations of the results for one-way relaying depicted in Figure 3.7. The ratio between the BER at S1 and at S2 depends on the ratio between $\text{SNR}^{(1)}$ and $\text{SNR}^{(2)}$. For equal values of $\text{SNR}^{(1)}$ and $\text{SNR}^{(2)}$, i.e. $\text{SNR}^{(1)} = \text{SNR}^{(2)} = 10\text{dB}$, the average BER values are the same. For $\text{SNR}^{(2)} > \text{SNR}^{(1)}$, the BER at S1 is lower than the BER at S2 and vice versa. However, compared to the BER performance in one-way relaying, the relative difference between the BER at S1 and at S2 is significantly higher which can be explained as follows. In two-way relaying, the two first hop transmissions are processed simultaneously. Hence, the data stream which is transmitted over the channel with the higher SNR is dominant in the sum of the two received data streams at the RS. Since the overall MSE is minimized in the optimization problem (4.59), the overall performance can be improved if more

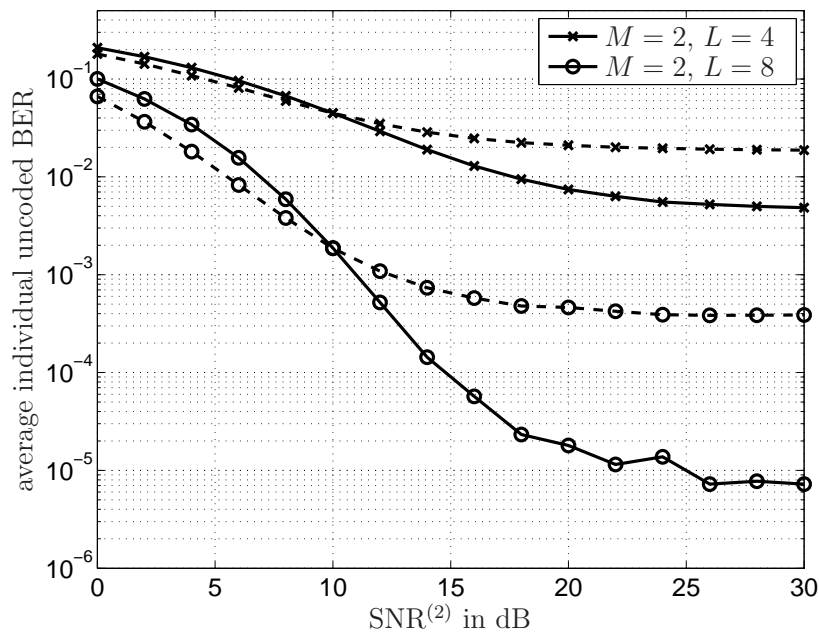


Figure 4.11. Average individual uncoded BER vs. $\text{SNR}^{(2)}$ for MMSE-BF in CASE4, dashed lines: BER at S2, solid lines: BER at S1, $\text{SNR}^{(1)} = 10\text{dB}$.

transmit power of the RS is allocated to the data stream which is dominant at the RS. Thus, the data stream with the worse SNR value for its first hop transmission achieves a relatively bad BER at its destination node. In general for all considered optimization problems in two-way relaying, different SNR values for the two channels to the RS cause an imbalance of the performances of the two directions of the transmission. Note that fairness of the two directions of the transmission is a topic which is beyond the scope of this thesis.

4.6 Conclusions

In this chapter, linear BF in non-regenerative two-way relaying with multiple-antenna nodes has been regarded. The sum rate maximization problem has been considered for four different cases of system capabilities which have been newly defined in the framework of Figure 1.4. For all cases, the maximum sum rates could only be determined numerically. Novel methods have been proposed in order to simplify the numerical optimizations by reducing the number of optimization variables for $L \geq 2M$. For the particular case of one antenna at the source and destination nodes a new sub-optimum analytical BF algorithm has been proposed. For the system with limited capabilities at S1 and S2, it has been shown that the BF algorithms which minimize the MSE,

minimize the MSE under the ZF constraint, and maximize the SNR by adaptive BF at the RS can be derived by introducing an equivalent system model and using the respective BF algorithms known from one-way relaying. For the system with local CSI at S1 and S2, BF algorithms which minimize the MSE, minimize the MSE under the ZF constraint, and maximize the SNR by BF at the RS have been proposed. All presented BF algorithms have been analyzed resulting in the following main conclusions:

- A significant amount of the loss in achievable sum rate due to the half-duplex constraint in two-hop transmissions can be compensated by two-way relaying. Compared to one-way relaying, the sum rate cannot be fully doubled since some transmit power of the RS is wasted in order to retransmit already known information to the destination nodes.
- The full spatial multiplexing gain in two-way relaying for independently Rayleigh fading channel coefficients corresponds to the minimum of the number L of antennas at the RS and twice the number M of antennas at S1 and S2.
- For the systems with full capabilities and with limited capabilities at the RS which have CSI at the source nodes, the sum rate is maximized by reducing the transmit power of the source node whose channel to the RS has a higher SNR.
- If the source nodes and destination nodes are equipped with $M = 1$ antenna, efficient analytical BF algorithms at the multiple-antenna RS are proposed in order to maximize the sum rate. For higher numbers M of antennas at the source and destination nodes, only numerical methods are known in order to maximize the sum rate.
- The comparison between the system with limited capabilities at S1 and S2 and the system with local CSI at S1 and S2 shows that significant gains in terms of sum rate and BER can be expected due to the cancellation of the duplex interference by CDI at the destination nodes. This motivates to provide at least local CSI to the destination nodes.
- The sum rate performance of the system with local CSI at S1 and S2 comes quite close to the sum rate performance of the system with full capabilities. Since the system with local CSI at S1 and S2 requires less effort, it is very promising for practical applications.
- In the system with local CSI at S1 and S2, the MMSE-BF algorithm provides a sum rate which comes quite close to the maximum sum rate in this case of system capabilities. Since the MMSE-BF algorithm is an analytical BF algorithm with

significantly less effort compared to numerical methods, it is very promising for practical applications.

- In the system with limited capabilities at S1 and S2 and in the system with local CSI at S1 and S2, the MMSE-BF algorithm always outperforms the ZF-BF algorithm and the MF-BF algorithm.
- For all considered optimization problems in two-way relaying, different channel conditions on the two channels to the RS cause an imbalance of the performances of the two directions of transmission.

Chapter 5

Topics of relevance for the practical implementation of two-way relaying

5.1 Introduction

In this chapter, several topics concerning the practical implementation of two-way relaying are discussed. For the investigations of Chapters 3 and 4, several simplifying assumptions have been made and only the limited scenario of Figure 1.2 has been considered. In the following, some of the simplifying assumptions introduced in Section 2.2 are revealed and advanced scenarios are considered. Most of the considered topics are also relevant to one-way relaying. However, since an adaptation of the following topics is straightforward in one-way relaying, it is omitted in the following.

In order to obtain CSI at the respective nodes, channel estimation has to be performed. Typically, channel estimation is based on pilot symbols and the resulting technique is termed PACE [TSD04]. The transmission of pilot symbols requires resources in time and frequency. Since these resources are not available for the data transmission, the sum rates presented in Chapters 3 and 4 are too optimistic for real systems. Furthermore, in the four cases of system capabilities in two-way relaying different kinds of CSI availability are assumed, so that different numbers of resources in time and frequency are required in order to perform PACE. Thus, it is expected that the sum rates of the four cases are degraded differently. In Section 5.2, pilot transmission schemes that define which node transmits a pilot on which resource in time and frequency are proposed for the different cases of system capabilities and the respective channel estimation algorithms are developed. Furthermore, the impact of the pilot transmission schemes on the sum rate performances is addressed.

The quality of the available CSI has also significant impact on the system performance. For the performance analysis in Chapters 3 and 4, perfect CSI is assumed which means that the estimated CSI equals the exact CSI. In real systems, this assumption cannot be met due to noisy estimates for example [KBB⁺05]. For that reason, Section 5.3 addresses the impact of imperfect CSI.

In the previous chapters, only a single source-destination pair has been considered. In Section 5.4, two-way relaying for multiple source-destination pairs is addressed. Two scenarios with multiple source-destination pairs are introduced exemplarily in order to give a first insight into the problems arising from multiple access in two-way relaying.

5.2 Pilot assisted channel estimation

5.2.1 Introduction

This Section 5.2 considers PACE [TSD04] for two-way relaying. For PACE, pilot symbols which are also known to the receive node are transmitted by the transmit node. With the knowledge about the transmitted pilot symbols, the receive node can obtain the CSI from the received pilot symbols which have been modified by the channel coefficients. As a general rule, a receive node which performs PACE needs to receive one pilot symbol per unknown channel coefficient. For a transmission using \tilde{M} transmit antennas and \tilde{L} receive antennas, this means that the receive node has to receive $\tilde{M}\tilde{L}$ orthogonal pilot symbols in order to perform PACE. In the following, only one frequency resource is considered and the number of required time slots for the pilot transmission scheme shall be minimized. Since \tilde{L} receive antennas provide \tilde{L} received pilot symbols per time slot, \tilde{M} orthogonal time slots are required in order to receive $\tilde{M}\tilde{L}$ orthogonal pilot symbols at the receive node. This requirement has to be satisfied by the following pilot transmission schemes.

In the following for the sake of simplicity but without loss of generality, the channel estimates shall fulfill the ZF constraint under the assumption of zero noise at all receive antennas. Note that also more advanced channel estimation algorithms may be applied [HH03, CGN07]. However, these algorithms are omitted since the proposed pilot transmission schemes can be used for each channel estimation algorithm, as long as the pilot transmission scheme provides a sufficient number of received pilot symbols. Furthermore, channel reciprocity and a sufficiently long channel coherence time are assumed which means that the CSI which is obtained for the receive channel of a node corresponds to the CSI which is valid for the transmission over the respective channel.

Since different CSI availabilities are defined for the different cases of system capabilities in Figure 1.4, a novel pilot transmission scheme is proposed for each case of system capabilities. In the different cases of system capabilities, a node requires either no CSI, local CSI or global CSI. If a node requires no CSI, no pilot symbols need to be transmitted to the node. If S1 and S2 require local CSI, a well-known pilot transmission scheme and the respective ZF channel estimation algorithm from point-to-point transmissions can be used which are reviewed in Section 5.2.2. Since global CSI at the RS directly corresponds to local CSI at the RS, the same pilot transmission scheme and the same ZF channel estimation algorithm can also be applied if the RS requires global CSI. If S1 and S2 require global CSI, another pilot transmission scheme and

the respective ZF channel estimation algorithm are required which are newly proposed in Section 5.2.3. The pilot transmission schemes for obtaining local CSI and global CSI have to be combined to the novel pilot transmission schemes which satisfy the CSI requirements of the four different cases of system capabilities. These pilot transmission schemes are presented in Section 5.2.4.

Section 5.2.5 gives a description of the degradation of the sum rate by the proposed pilot transmission schemes which allows a fair comparison of the sum rate performances of the different cases of system capabilities in Section 5.2.6.

5.2.2 Local CSI at S1, S2, and global CSI at the RS

In the following, a pilot transmission scheme as well as the respective ZF channel estimation algorithm in order to obtain local CSI at S1, S2, and global CSI at the RS are presented. The pilot transmission scheme and the ZF channel estimation algorithm are well-known from point-to-point transmissions. However, since they provide a basis for the newly developed pilot transmission scheme and the respective ZF channel estimation algorithm for obtaining global CSI at S1 and S2, they are reviewed here.

In the following, the pilot transmission scheme performed at node S_i and the channel estimation of channel $\mathbf{H}^{(i)}$ at the receiving RS are considered as an example. Note that adapting the pilot transmission scheme and the ZF channel estimation algorithm in order to obtain local CSI about channel $\mathbf{H}^{(k)\text{T}}$ at S_k is straightforward.

In order to receive the required ML pilot symbols at the L receive antennas of the RS, M time slots are required in the pilot transmission scheme of node S_i . The most obvious approach is to transmit one pilot symbol from each transmit antenna each in another time slot, i.e., pilot symbol $y_m^{(i)}$, $m = 1, \dots, M$, is transmitted in time slot m by the m -th transmit antenna of node S_i . In Figure 5.1, the proposed time slot allocation for the pilot symbols at the transmit node S_i is depicted for $M = 3$. In the figure, the time axis is plotted vs. the transmit antenna index where index $m = 1, \dots, M$ corresponds to the m -th transmit antenna of the transmit node S_i . The notation in each square indicates which node is transmitting from the respective transmit antenna in the respective time slot. The two squares of different shades of gray with the notation S_i in Figure 5.1 correspond to pilot symbols $y_1^{(i)}$ and $y_2^{(i)}$, respectively, and the white square with the notation S_i corresponds to pilot symbol $y_3^{(i)}$. For the white squares with a dot in the center, no pilot symbol is transmitted from the respective antenna in

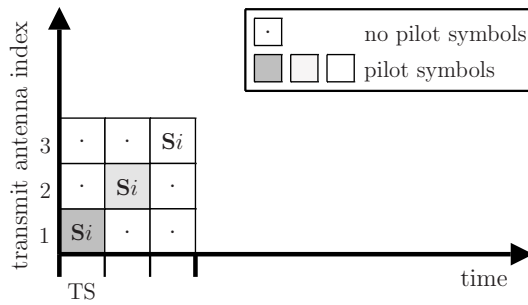


Figure 5.1. Pilot transmission scheme for obtaining local CSI at the receiving node assuming $M = 3$ transmit antennas at the transmitting node S_i .

the respective time slot. The overall transmission of M pilot symbols may be described by pilot matrix

$$\mathbf{Y}^{(i)} = \text{diag} \left[y_1^{(i)}, y_2^{(i)}, \dots, y_M^{(i)} \right]. \quad (5.1)$$

Neglecting the noise at the RS, matrix

$$\tilde{\mathbf{Y}}^{(i)} = \mathbf{H}^{(i)} \mathbf{Y}^{(i)}, \quad (5.2)$$

contains the required ML orthogonally received pilot symbols in order to determine the estimated channel matrix $\hat{\mathbf{H}}^{(i)}$. From Eq. (5.2), $\hat{\mathbf{H}}^{(i)}$ can be obtained by simply multiplying matrix $\tilde{\mathbf{Y}}^{(i)}$ with the inverse of the known pilot matrix $\mathbf{Y}^{(i)}$. The inverse $\mathbf{Y}^{(i)-1}$ is determined by a simple element-wise inversion of the diagonal elements of $\mathbf{Y}^{(i)}$. Thus, the estimated channel matrix $\hat{\mathbf{H}}^{(i)}$ results in

$$\hat{\mathbf{H}}^{(i)} = \tilde{\mathbf{Y}}^{(i)} \mathbf{Y}^{(i)-1}. \quad (5.3)$$

5.2.3 Global CSI at S1 and S2

In the following, a pilot transmission scheme as well as the respective ZF channel estimation algorithm in order to obtain global CSI about channels $\mathbf{H}^{(k)\text{T}}$ and $\mathbf{H}^{(i)}$ at S_k are proposed. The CSI about channel $\mathbf{H}^{(k)\text{T}}$ at node S_k can be obtained by the pilot transmission scheme and the ZF channel estimation algorithm of Section 5.2.2, where the RS transmits L pilot symbols to S_k in L orthogonal time slots. In order to obtain CSI about channel $\mathbf{H}^{(i)}$ at node S_k , pilot symbols are transmitted over the overall channel $\mathbf{H}^{(k)\text{T}} \mathbf{H}^{(i)}$ and channel $\mathbf{H}^{(i)}$ is determined by using the already known channel $\mathbf{H}^{(k)\text{T}}$ and the received pilot symbols over the overall channel $\mathbf{H}^{(k)\text{T}} \mathbf{H}^{(i)}$. This novel pilot transmission scheme and the respective ZF channel estimation algorithm in order to obtain an estimate $\hat{\mathbf{H}}^{(i)}$ of channel $\mathbf{H}^{(i)}$ at node S_k depend on the relation between M and L .

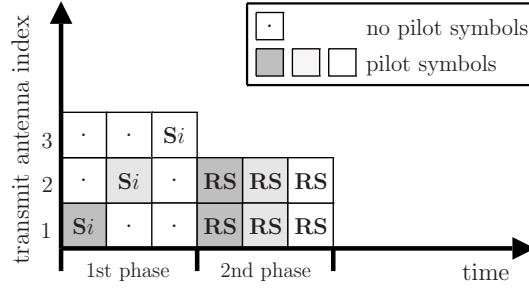
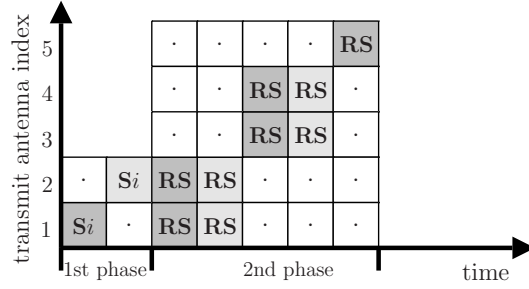
(a) $M = 3, L = 2$ (b) $M = 2, L = 5$

Figure 5.2. Pilot transmission scheme for obtaining global CSI for the cases $M > L$ and $M < L$.

If $M \geq L$, the pilot symbol $y_m^{(i)}$, $m = 1, \dots, M$, is transmitted in time slot m by the m -th antenna of node S_i . The overall transmission of M pilot symbols is described by pilot matrix $\mathbf{Y}^{(i)}$ of Eq. (5.1). The transmission of the pilot symbols from S_i to the RS is indicated by the first phase in Figure 5.2(a). At the RS, the received pilot symbol of each antenna is amplified by weighting factor g satisfying the transmit power constraint at the RS and retransmitted from each antenna. The retransmission is described by matrix

$$\mathbf{Y}_{M \geq L}^{(0,i)} = g\mathbf{H}^{(i)}\mathbf{Y}^{(i)}, \quad (5.4)$$

containing the pilot symbols of pilot matrix $\mathbf{Y}^{(i)}$ which are modified by the channel coefficients of channel matrix $\mathbf{H}^{(i)}$ and the amplification factor g . Matrix $\mathbf{Y}_{M \geq L}^{(0,i)}$ is indicated by the gray squares with the notation RS in the second phase of Figure 5.2(a). The received pilot symbols at node S_k may be described by matrix

$$\tilde{\mathbf{Y}}_{M \geq L}^{(i)} = \mathbf{H}^{(k)\text{T}}\mathbf{Y}_{M \geq L}^{(0,i)} = g\mathbf{H}^{(k)\text{T}}\mathbf{H}^{(i)}\mathbf{Y}^{(i)}, \quad (5.5)$$

which contains the required ML orthogonally received pilot symbols at node S_k . Since the estimated channel matrix $\hat{\mathbf{H}}^{(k)\text{T}}$ is already known at S_k , the estimated channel matrix $\hat{\mathbf{H}}^{(i)}$ can be calculated by

$$\hat{\mathbf{H}}^{(i)} = \frac{1}{g} \left(\hat{\mathbf{H}}^{(k)*} \hat{\mathbf{H}}^{(k)\text{T}} \right)^{-1} \hat{\mathbf{H}}^{(k)*} \tilde{\mathbf{Y}}_{M \geq L}^{(i)} \mathbf{Y}^{(i)-1}, \quad (5.6)$$

where the term $\left(\hat{\mathbf{H}}^{(k)*} \hat{\mathbf{H}}^{(k)\text{T}}\right)^{-1} \hat{\mathbf{H}}^{(k)*}$ is the pseudo-inverse of the estimated channel matrix $\hat{\mathbf{H}}^{(k)\text{T}}$ for $M > L$ which can be replaced by the inverse $\hat{\mathbf{H}}^{(k)\text{T},-1}$ for $M = L$.

In order to give a pilot transmission scheme and a ZF channel estimation algorithm for $M < L$, the colon notation defined in [GL96] is introduced. Let $[\mathbf{X}]_{n_1:n_2,:}$ denote a matrix containing the n_1 -th to n_2 -th row of matrix \mathbf{X} , let $[\mathbf{X}]_{:,n_1:n_2}$ denote a matrix containing the n_1 -th to n_2 -th column of \mathbf{X} , and let $[\mathbf{X}]_{n_1:n_2}$ denote a matrix containing the n_1 -th to n_2 -th row and the n_1 -th to n_2 -th column of \mathbf{X} . Furthermore, the antenna ratio γ is defined as

$$\gamma = \left\lfloor \frac{L}{M} \right\rfloor, \quad (5.7)$$

where $\lfloor \cdot \rfloor$ rounds the argument to the nearest integer towards minus infinity. As for the case $M \geq L$, pilot symbol $y_m^{(i)}$, $m = 1, \dots, M$, is transmitted by the m -th antenna of node S_i in time slot m which is indicated by the first phase in Figure 5.2(b). The overall transmission of M pilot symbols is described by pilot matrix $\mathbf{Y}^{(i)}$ of Eq. (5.1). At the RS, a coordination of the retransmission is required which ensures that LM orthogonal pilot symbols are received at node S_k . For that reason, the retransmission from the RS is processed in groups of M antennas leading to the following block diagonal matrix $\mathbf{Y}_{M < L}^{(0,i)}$ which describes the retransmission from the RS:

$$\mathbf{Y}_{M < L}^{(0,i)} = g \text{diag}_b \left[[\mathbf{H}^{(i)}]_{1:M,:} \mathbf{Y}^{(i)}, [\mathbf{H}^{(i)}]_{2M+1:2M,:} \mathbf{Y}^{(i)}, \dots, [\mathbf{H}^{(i)}]_{\gamma M+1:L,:} [\mathbf{Y}^{(i)}]_{1:L-\gamma M} \right]. \quad (5.8)$$

Each block of matrix $\mathbf{Y}_{M < L}^{(0,i)}$ contains the pilot symbols of pilot matrix $\mathbf{Y}^{(i)}$ which are modified by the amplification factor g and a sub-matrix of channel matrix $\mathbf{H}^{(i)}$. The retransmission of matrix $\mathbf{Y}_{M < L}^{(0,i)}$ is indicated by the gray squares with the notation RS in the second phase of Figure 5.2(b). The received pilot symbols at node S_k may be described by matrix

$$\tilde{\mathbf{Y}}_{M < L}^{(i)} = \mathbf{H}^{(k)\text{T}} \mathbf{Y}_{M < L}^{(0,i)}, \quad (5.9)$$

which contains ML orthogonally received pilot symbols. Note that for a simple retransmission of $g\mathbf{H}^{(i)}\mathbf{Y}^{(i)}$ as in the case of $M \geq L$, node S_k would have received only MM orthogonal pilot symbols and not the required ML pilot symbols. With the proposed pilot transmission scheme for $M < L$, the first γM rows of the estimated channel matrix $\hat{\mathbf{H}}^{(i)}$ can be calculated block-wise by applying

$$\left[\hat{\mathbf{H}}^{(i)} \right]_{(n-1)M+1:nM,:} = \frac{1}{g} \left(\left[\hat{\mathbf{H}}^{(k)} \right]_{(n-1)M+1:nM,:}^{\text{T}} \right)^{-1} \left[\tilde{\mathbf{Y}}_{M < L}^{(i)} \right]_{:, (n-1)M+1:nM} \mathbf{Y}^{(i)-1}, \quad (5.10)$$

for $n = 1, \dots, \gamma$. In case of $L - \gamma M \neq 0$, the last $L - \gamma M$ rows of $\mathbf{H}^{(i)}$ are calculated

by

$$\begin{aligned} \left[\hat{\mathbf{H}}^{(i)} \right]_{\gamma M+1:L,:} = \\ \frac{1}{g} \left(\left[\hat{\mathbf{H}}^{(k)} \right]_{\gamma M+1:L,:}^* \left[\hat{\mathbf{H}}^{(k)} \right]_{\gamma M+1:L,:}^T \right)^{-1} \left[\hat{\mathbf{H}}^{(k)} \right]_{\gamma M+1:L,:}^* \left[\tilde{\mathbf{Y}}_{M < L}^{(i)} \right]_{:, \gamma M+1:(\gamma+1)M} \left[\mathbf{Y}^{(i)} \right]_{1:L-\gamma M}^{-1}. \end{aligned} \quad (5.11)$$

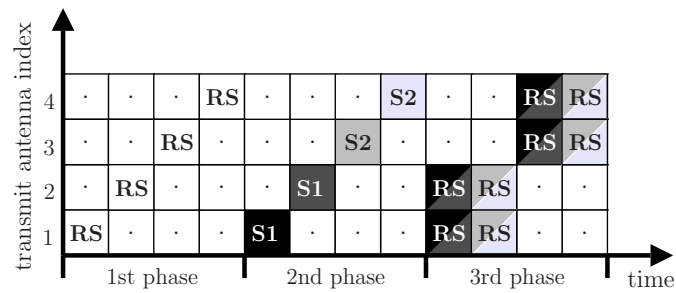
5.2.4 Pilot transmission schemes for different cases of system capabilities

In this section, pilot transmission schemes are proposed for the four cases of system capabilities of Figure 1.4 based on the introduced pilot transmission schemes for obtaining local and global CSI in Sections 5.2.2 and 5.2.3. Furthermore, the number of required time slots for the pilot transmission scheme depending on the number M of antennas at S1 and S2 and on the number L of antennas at the RS is defined by δ , and δ is determined for all cases of system capabilities. The proposed pilot transmission schemes are depicted in Figure 5.3 for $L = 4$ antennas at the RS, and $M = 2$ antennas at S1 and S2, respectively. The figure gives the time slot allocation of the pilot symbols depending on the transmit antenna index, where indices 1 and 2 denote the first and second transmit antenna of the RS, and the first and second transmit antenna of S1, respectively. Indices 3 and 4 denote the third and fourth transmit antenna of the RS, and the first and second transmit antenna of S2, respectively. The respective transmitters can be distinguished by the notation in the squares.

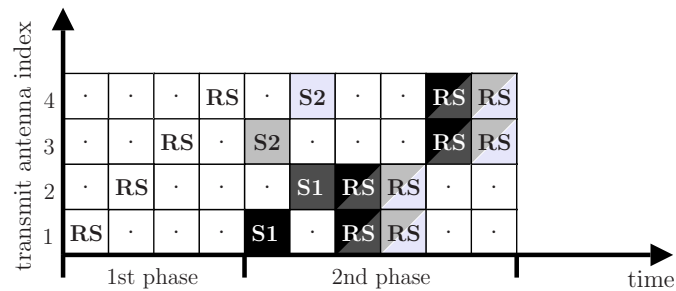
In the following, a pilot transmission scheme for the system with full capabilities (CASE1) is proposed, which is depicted in Figure 5.3(a). The pilot transmission scheme can be divided into three phases:

- first phase: obtaining local CSI at S1 and S2,
- second phase: obtaining global CSI at the RS,
- third phase: obtaining global CSI at S1 and S2.

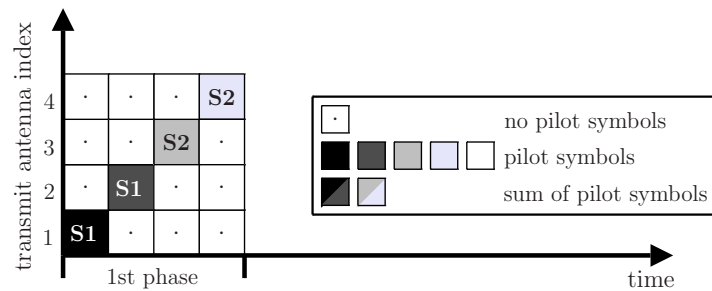
In the first phase, the RS transmits one pilot symbol per transmit antenna according to the pilot transmission scheme introduced in Section 5.2.2. This phase requires L orthogonal time slots.



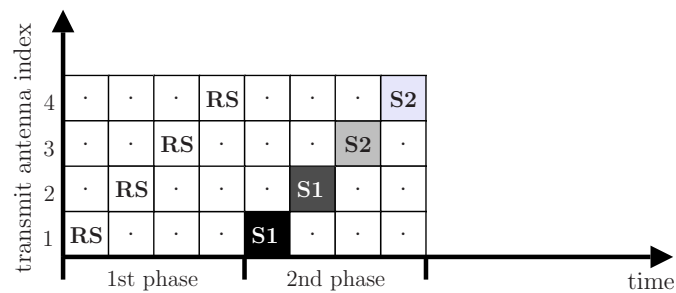
(a) CASE1: system with full capabilities.



(b) CASE2: system with limited capabilities at the RS.



(c) CASE3: system with limited capabilities at S1 and S2.



(d) CASE4: system with local CSI at S1 and S2.

Figure 5.3. Pilot transmission schemes for the different cases of system capabilities, $M = 2, L = 4$.

In the second phase, firstly S1 transmits one pilot symbol per transmit antenna which requires M orthogonal time slots. Secondly, S2 transmits one pilot symbol per

transmit antenna which also requires M orthogonal time slots leading to overall $2M$ time slots in the second phase.

In the third phase, the pilot symbols of the second phase which have been received by the RS are retransmitted by the RS in order to obtain global CSI at S1 and S2 as introduced in Section 5.2.3. Since S1 and S2 already have local CSI from the first phase and since they also know their own transmitted pilot symbols, duplex interference from the own transmitted pilot symbols can be cancelled by CDI at the destination nodes. For that reason, the sum of the pilot symbols received from S1 and S2 in the second phase is retransmitted by the RS, i.e., matrix $\mathbf{Y}^{(0)}$ of Eq. (5.4) and Eq. (5.8), respectively, describing the retransmission from the RS is modified to

$$\mathbf{Y}^{(0,i)} = \begin{cases} g \sum_{i=1}^2 \mathbf{Y}_{M \geq L}^{(0,i)} & \text{for } M \geq L, \\ g \sum_{i=1}^2 \mathbf{Y}_{M < L}^{(0,i)} & \text{for } M < L. \end{cases} \quad (5.12)$$

The sum of two pilot symbols, one from S1 and another from S2, is indicated by the two different shades of gray per square for the pilot symbols of the third phase in Figure 5.3(a). Depending on the ratio between L and M , the number of required time slots during the third phase is either M for $M \geq L$ or $(2L - \gamma M)$ for $M < L$. The overall number of required time slots for the proposed pilot transmission scheme in CASE1 is given by

$$\delta_{\text{CASE1}} = \begin{cases} 3M + L & \text{for } M \geq L, \\ (2 - \gamma)M + 3L & \text{for } M < L. \end{cases} \quad (5.13)$$

In the following, a pilot transmission scheme for the system with limited capabilities at the RS (CASE2) is proposed. The scheme is depicted in Figure 5.3(b) and can be divided into two phases:

- first phase: obtaining local CSI at S1 and S2,
- second phase: obtaining global CSI at S1 and S2.

As for the previous CASE1, L orthogonal time slots are required in the first phase for the pilot transmission scheme of Section 5.2.2.

In the second phase, S1 transmits one pilot symbol per transmit antenna in M orthogonal time slots. Since the RS does not require global CSI and since CDI can

be performed at the destination nodes, S2 transmits one pilot symbol per transmit antenna simultaneously so that a linear combination of two pilot symbols is received at each antenna of the RS. The simultaneous transmission from S1 and S2 corresponds to the first two time slots in the second phase of Figure 5.3(b). The following four time slots correspond to the retransmission of the pilot symbols from the RS in order to obtain global CSI at S1 and S2. As for CASE1, the duplex interference from the own pilot symbols can be cancelled by CDI at the destination nodes. For that reason, the received linear combinations of the pilot symbols from S1 and S2 are just retransmitted by the RS indicated by the two different shades of gray for the last four time slots of the second phase in Figure 5.3(b). Depending on the ratio between L and M , the overall number of required time slots during the two phases of the pilot transmission scheme for CASE2 is given by

$$\delta_{\text{CASE2}} = \begin{cases} 2M + L & \text{for } M \geq L, \\ (1 - \gamma)M + 3L & \text{for } M < L. \end{cases} \quad (5.14)$$

In the following, a pilot transmission scheme for the system with limited capabilities at S1 and S2 (CASE3) is given, which is depicted in Figure 5.3(c) and only consists of one phase:

- first phase: obtaining global CSI at the RS.

Firstly, S1 transmits one pilot symbol per transmit antenna which requires M orthogonal time slots according to the pilot transmission scheme of Section 5.2.2. Secondly, using the same pilot transmission scheme, S2 transmits one pilot symbol per transmit antenna which also requires M orthogonal time slots. Thus, the overall number of required time slots for CASE3 results in

$$\delta_{\text{CASE3}} = 2M. \quad (5.15)$$

In the following, a pilot transmission scheme for the system with local CSI at S1 and S2 (CASE4) is introduced. The scheme is depicted in Figure 5.3(d) and can be divided into two phases:

- first phase: obtaining local CSI at S1 and S2,
- second phase: obtaining global CSI at the RS.

In the first phase, the RS transmits one pilot symbol per transmit antenna according to the pilot transmission scheme introduced in Section 5.2.2. This phase requires L orthogonal time slots.

In the second phase using the same pilot transmission scheme, firstly S1 transmits one pilot symbol per transmit antenna which requires M orthogonal time slots. Secondly, S2 transmits one pilot symbol per transmit antenna which also requires M orthogonal time slots leading to overall $2M$ time slots in the second phase. Thus, the overall number of required time slots for CASE4 results in

$$\delta_{\text{CASE4}} = 2M + L. \quad (5.16)$$

5.2.5 Sum rate degradation

In this section, the degradation of the sum rate due to PACE is considered. The transmission of pilot symbols requires resources in time and frequency. Since these resources are not available for the data transmission, the sum rates for two-way relaying presented in Chapter 4 are too optimistic. Based on the pilot transmission schemes introduced in Section 5.2.4, it shall be determined how many pilot symbols have to be transmitted within the channel coherence bandwidth B_C and during the channel coherence time T_C for a typical OFDM system. The channel coherence bandwidth is given by

$$B_C = \frac{1}{\tau_{\max}}, \quad (5.17)$$

where τ_{\max} is the maximum channel delay [Pro01]. The channel coherence time is given by

$$T_C = \frac{c_0}{2f_0\bar{v}}, \quad (5.18)$$

where f_0 is the carrier frequency, c_0 is the speed of light, and \bar{v} is the relative velocity between transmitter and receiver [Pro01]. In the following, two-dimensional PACE [HKR97] is assumed which means that the pilot symbols are used in order to estimate the channel in time and frequency direction. In this two-dimensional approach, the estimated channel matrices of the previous sections are only valid for one specific time slot and one specific sub-carrier of the OFDM system, i.e., for one specific time-frequency unit. The oversampling factor $u_B \geq 1$ in frequency domain specifies how often the channel is estimated within the channel coherence bandwidth [SFK06]. Likewise, the oversampling factor $u_T \geq 1$ in time domain specifies how often the channel is estimated during the channel coherence time [SFK06]. Finally, the number δ introduced in Section 5.2.4 specifies how many time slots are required due to the application of multiple antennas in two-way relaying depending on the system capabilities.

In the following, the sum rate degradation due to PACE is considered by modifying the sum rate normalization factor of Eq. (2.12). The ratio between the number b_{pilot} of time-frequency units allocated to pilot symbols and the number of overall available time-frequency units b within the coherence bandwidth and the coherence time is given by

$$\frac{b_{\text{pilot}}}{b} = \frac{u_{\text{T}}u_{\text{B}}\delta}{T_{\text{C}}B_{\text{C}}}. \quad (5.19)$$

For a bi-directional transmission in two-way relaying, the number b_{data} of time-frequency units used for data transmission results in

$$b_{\text{data}} = \frac{b + b_{\text{pilot}}}{2}, \quad (5.20)$$

where the factor of 2 is coming from the fact that each data stream is transmitted once by its source node and once by the RS. With Eq. (5.19) and Eq. (5.20), the sum rate normalization factor r_{data} which gives the ratio between the time-frequency units used for data transmission and the number of overall available time-frequency units results in

$$r_{\text{data}} = \frac{b_{\text{data}}}{b} = \frac{1}{2} \left(1 - \frac{u_{\text{T}}u_{\text{B}}\delta}{T_{\text{C}}B_{\text{C}}} \right). \quad (5.21)$$

With the sum rate normalization factor r_{data} of Eq. (5.21), the sum rates defined in Section 2.4 can be re-calculated by considering the different values of δ for each case of system capabilities enabling an improved fairness for the comparison of the different cases.

5.2.6 Performance analysis

In this section, the impact of the pilot transmission schemes on the average sum rate for the different cases of system capabilities is investigated. For that purpose, all simulation parameters are chosen exactly as defined in Section 4.5.1 for the performance analysis of two-way relaying. Additionally, the following parameters of a real relaying system are assumed. The parameters are also summarized in Table 5.1. For the maximum channel delay a value of $\tau_{\text{max}} = 2\mu\text{s}$ is assumed which corresponds to a coherence bandwidth of $B_{\text{C}} = 500\text{kHz}$ in Eq. (5.17). This value is typical for wide area scenarios. The carrier frequency is set to $f_0 = 5\text{GHz}$, and walking speed of $\bar{v} = 5\text{km/h}$ is assumed for the average relative velocity of the nodes since relaying is typically applied in scenarios with low mobility [STIST07a]. This yields a coherence time of $T_{\text{C}} = 5.4\text{ms}$ in Eq. (5.18). If an OFDM system is assumed with an overall bandwidth of $B = 5\text{MHz}$ and with 512 sub-carriers, the sub-carrier spacing results in about 10kHz and the OFDM symbol duration is given by about 0.1ms. Assuming a typical oversampling in

System parameter	value
Maximum channel delay τ_{\max}	$2\mu\text{s}$
Carrier frequency f_0	5GHz
Average velocity \bar{v}	5km/h
Oversampling factor in time domain u_T	5
Oversampling factor in frequency domain u_B	5

Table 5.1. Parameter settings valid for the results presented in Figure 5.4

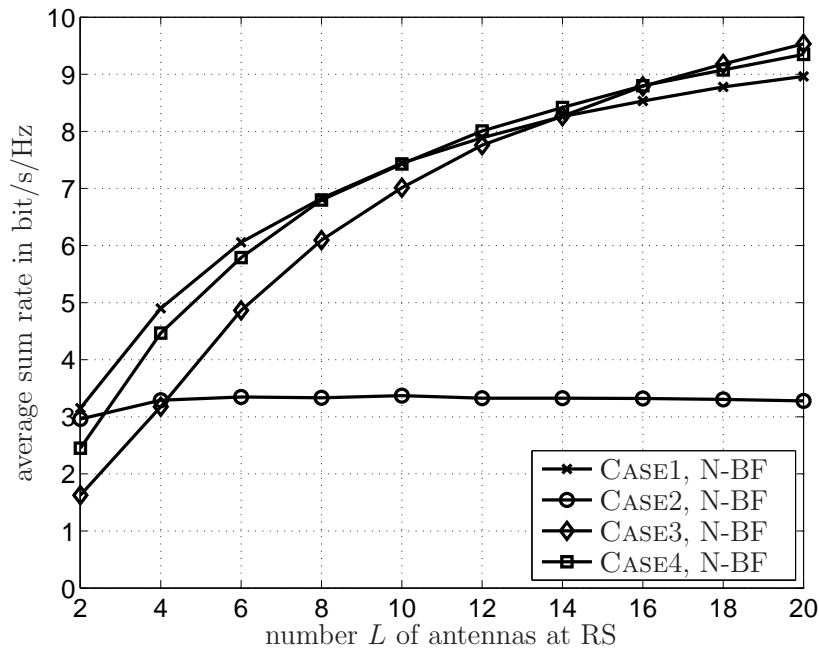


Figure 5.4. Average sum rate vs. number L of antennas at the RS for CASE1, CASE2, CASE3, and CASE4, considering the rate degradation due to the proposed pilot transmission schemes, $\text{SNR}^{(1)} = \text{SNR}^{(2)} = 10\text{dB}$, $M = 2$.

time and frequency domain of $u_T = 5$ and $u_B = 5$ [SFK06], approximately every tenth sub-carrier and every tenth OFDM symbol are used for pilot transmission.

With these system parameters, the results presented in Figure 4.2 are reviewed for the modified sum rate normalization factor of Eq. (5.21). Figure 5.4 gives the average sum rate vs. the number L of antennas at the RS for all cases of system capabilities assuming $\text{SNR}^{(1)} = \text{SNR}^{(2)} = 10\text{dB}$ and $M = 2$. For $M \geq L$, the pilot transmission schemes of all considered cases require almost the same number of resources. For that reason, the relation between the sum rate performances of the different cases does not change compared to Figure 4.2. However, for increasing L the impact of the pilot transmission scheme in order to obtain global CSI at S1 and S2 increases significantly. The sum rates of CASE1 and CASE2 are significantly degraded since these cases require

global CSI at S1 and S2. In contrast to CASE1 and CASE2, the sum rate of CASE3 does not depend on L and the sum rate of CASE4 increases slower depending on L . Thus, CASE4 already achieves the performance of CASE1 for $L = 8$ and outperforms CASE1 for $L > 8$. For $L > 16$, CASE3 with the most limited system capabilities even outperforms all other cases.

Note that these results are only valid for the specific parameter setting of Table 5.1. Nevertheless, the results show that the impact of PACE may not be neglected and the favorable BF algorithm depends on the application and the underlying parameter settings.

5.3 Imperfect CSI

5.3.1 Introduction

In this section, the impact of imperfect CSI on the sum rate performances of the proposed BF algorithms of Chapter 4 is addressed. Previous investigations have been based on perfect CSI in the systems, which means that the exact CSI is known at the nodes. However, in real systems perfect CSI cannot be obtained [KBB⁺05]. There are two main reasons why the CSI obtained by PACE is different compared to the exact CSI:

- There exists some latency between transmitting the pilot symbols for performing PACE and using the obtained CSI for adaptive BF. During this time, the wireless channel may change due to various effects, e.g., due to the movement of a mobile node, reflections, or diffractions. In this case, the CSI obtained by PACE is outdated at the time it is used. Typically, outdated CSI is a bigger problem in systems using only transmit BF since the time duration between receiving the pilot symbols and transmitting the respective data symbols is longer than the time duration between receiving the pilot symbols and receiving the respective data symbols in systems using only receive BF. However, as long as the update time is shorter than the channel coherence time, the impact of the estimation error can be kept small for both cases of adaptive BF.
- There exists some estimation error which is inherent to the applied channel estimation algorithm [HH03] and comes from the receiver noise.

In reality, systems and BF algorithms are required which are not such sensitive to imperfect CSI. In this section, it is shown that the impact of imperfect CSI depends on the case of system capabilities and the considered BF algorithm.

Section 5.3.2 explains how imperfect CSI can be modeled. In Section 5.3.3, the sum rates obtained with imperfect CSI are compared to the sum rates obtained with perfect CSI in two-way relaying.

5.3.2 Modeling imperfect CSI

In this section, the influence of imperfect CSI on the performance of the proposed BF algorithms in two-way relaying is considered. The following modeling of imperfect CSI is taken from [HH03] where it is assumed that the respective nodes perform a linear minimum MSE algorithm for PACE.

The exact channel matrix $\mathbf{H}^{(i)}$ of Eq. (2.4) is separated into two parts resulting in

$$\mathbf{H}^{(i)} = \hat{\mathbf{H}}^{(i)} + \tilde{\mathbf{H}}^{(i)}, \quad (5.22)$$

where $\hat{\mathbf{H}}^{(i)}$ is the estimated channel matrix consisting of zero-mean, independent, circularly symmetric, complex Gaussian random variables of variance $(\sigma^{(i)2} - \tilde{\sigma}^{(i)2})$, and $\tilde{\mathbf{H}}^{(i)}$ is the estimation error matrix with coefficients of variance

$$\tilde{\sigma}^{(i)2} = \frac{1}{1 + \text{SNR}^{(i)}}. \quad (5.23)$$

It is assumed that the estimation errors are zero-mean, independent, circularly symmetric, complex Gaussian random variables. Furthermore, the variance $\tilde{\sigma}^{(i)2}$ depends on $\text{SNR}^{(i)}$ of Eq. (3.61) where it is assumed that each node receives as many pilot symbols as unknown channel coefficients during the channel coherence time [HH03]. This assumption provides a worst case scenario since increasing the number of transmitted pilot symbols during the channel coherence time would improve the channel estimates and decrease the variance of the estimation error. With the previous assumptions, a fair comparison in terms of received signal power between the cases of perfect CSI and the cases of imperfect CSI is ensured since the overall variance of the exact channel coefficients is fixed to $\sigma^{(i)2}$ in any case. For $\tilde{\sigma}^{(i)2} = 0$, i.e., for infinite $\text{SNR}^{(i)}$, the estimated channel matrix corresponds to the exact channel matrix, and for $\tilde{\sigma}^{(i)2}$ to infinity, i.e., for $\text{SNR}^{(i)} = 0$, the estimated channel is completely uncorrelated to the exact channel.

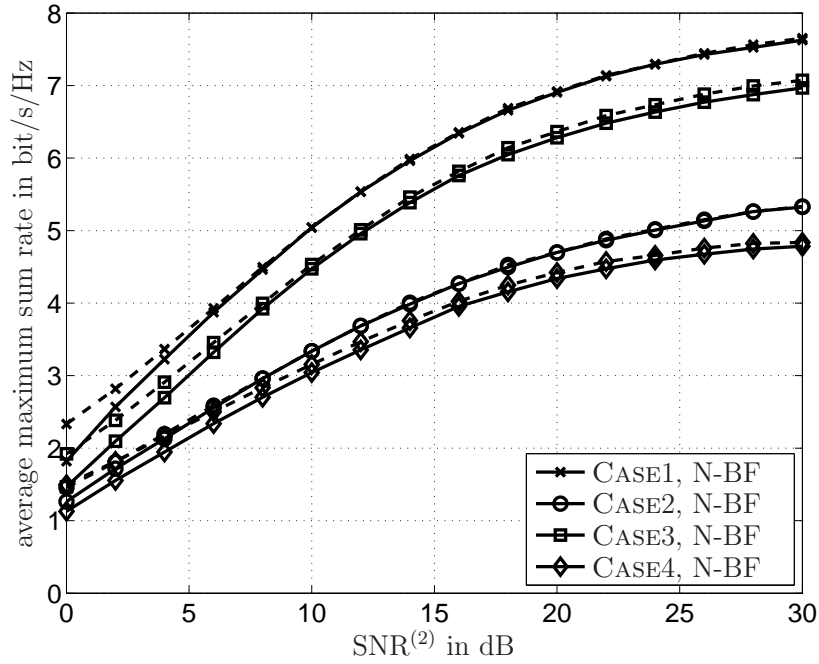


Figure 5.5. Average maximum sum rate vs. $\text{SNR}^{(2)}$ for CASE1, CASE2, CASE3, CASE4, solid lines: imperfect CSI, dashed lines: perfect CSI $\text{SNR}^{(1)} = 10\text{dB}$, $M = 2$ and $L = 4$.

In order to determine the transmission rate in case of imperfect CSI, the transmission rate expressions introduced in Section 2.4 are used in a modified way. Instead of using the exact channel matrices $\mathbf{H}^{(i)}$, $i = 1, 2$, for the calculation of the BF matrices of the system model in Figure 2.1, the estimated channel matrices $\hat{\mathbf{H}}^{(i)}$, $i = 1, 2$ are used [KK08]. This means that the transmission rates of Eq. (2.14) and Eq. (2.21) are evaluated by using the exact channel matrices $\mathbf{H}^{(i)}$, $i = 1, 2$, and the mismatched BF matrices which leads to a degradation of the transmission rate.

5.3.3 Performance analysis

In the following, the average maximum sum rates of CASE1, CASE2, CASE3, and CASE4 are analyzed for imperfect CSI. For that purpose, the same simulation parameters as presented in Section 4.5.1 are assumed. Figure 5.5 gives the average maximum sum rate vs. $\text{SNR}^{(2)}$ for all cases of system capabilities obtained by numerical optimizations. For all following figures, $\text{SNR}^{(1)}$ is fixed to 10dB and S1 and S2 are equipped with $M = 2$ antennas and the RS is equipped with $L = 4$ antennas. The solid lines correspond to the sum rates in case of imperfect CSI and the dashed lines correspond to the previously considered results where the CSI is perfectly known.

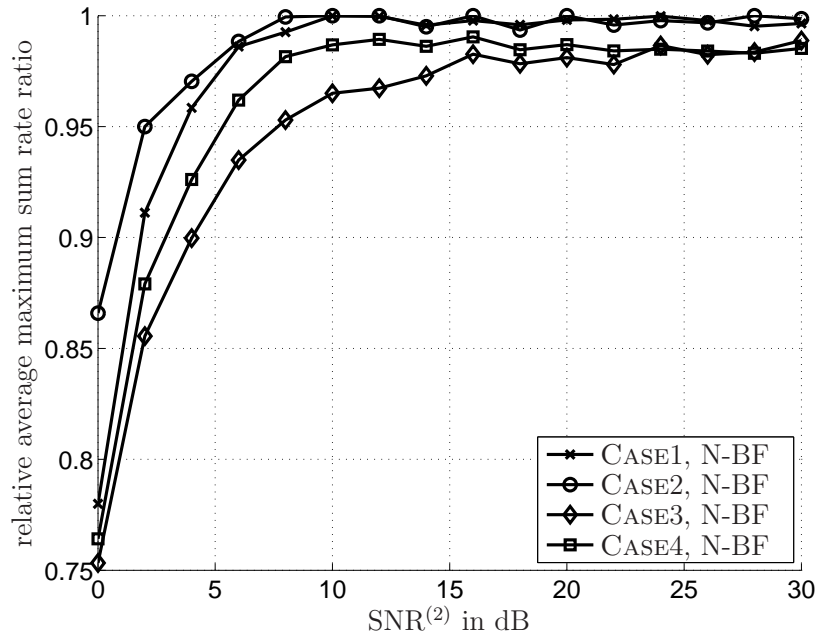


Figure 5.6. Relative average maximum sum rate ratio vs. $\text{SNR}^{(2)}$ for CASE1, CASE2, CASE3, and CASE4, $M = 2$, $L = 4$, $\text{SNR}^{(1)} = 10\text{dB}$.

Obviously, in every case the sum rate is degraded due to the imperfect CSI. However, the degradation is significantly higher for low values of $\text{SNR}^{(2)}$ and the sum rate with imperfect CSI converges to the sum rate with perfect CSI for increasing $\text{SNR}^{(2)}$ in all cases. This observation can be explained by the definition of the variance of the estimation error in Eq. (5.23) which decreases for increasing $\text{SNR}^{(2)}$. Thus, for high $\text{SNR}^{(2)}$ the CSI obtained by PACE differs only slightly from the exact CSI.

In Figure 5.5, it can be seen that the performance of CASE1 is also the best performance in case of imperfect CSI and CASE3 still provides the worst performance while CASE4 still performs better than CASE2. However, for small values of $\text{SNR}^{(2)}$ the performance of CASE4 is degraded more than the performance of CASE2 for example which leads to the assumption that the different cases have different sensitivities to imperfect CSI.

In order to verify the relative effect of imperfect CSI in each of the cases, the average maximum sum rate for imperfect CSI is divided by the average maximum sum rate for perfect CSI and the resulting relative average maximum sum rate ratio vs. $\text{SNR}^{(2)}$ is depicted in Figure 5.6. For CASE3 and CASE4 in which BF is only applied at the RS, the loss in sum rate due to imperfect CSI is up to 10% higher than for CASE1 and CASE2 for values of $\text{SNR}^{(2)}$ between 0dB and 6dB. For high values of $\text{SNR}^{(2)}$, the sum rate ratio of all cases is close to one. The worse sum rate ratio of CASE3 and CASE4

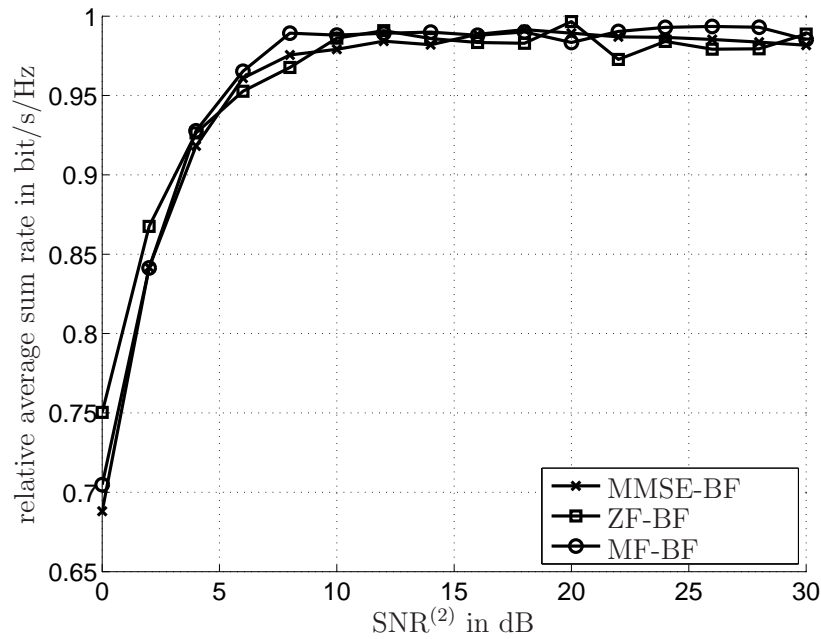


Figure 5.7. Relative average sum rate ratio vs. $\text{SNR}^{(2)}$ for CASE4 with different BF algorithms, $M = 2$, $L = 4$, $\text{SNR}^{(1)} = 10\text{dB}$.

for low values of $\text{SNR}^{(2)}$ comes from the fact that no adaptive BF can be applied at the source and destination nodes, respectively. Hence, a good spatial separation among different data streams has to be provided by the RS. But imperfect CSI significantly affects the performance of the BF algorithms at the RS since the antenna beams are steered in wrong directions. Of course, the BF algorithms at the RS provide incorrect antenna beams in CASE1 and CASE2, too. However, due to the joint encoding and decoding these incorrect antenna beams have a lower impact. Nevertheless, especially CASE4 is still promising since the achieved absolute value of the sum rate always outperforms the sum rate in CASE2 which has been seen in Figure 5.5.

In Figure 5.7, the sum rate ratio vs. $\text{SNR}^{(2)}$ is given for the MMSE-BF, the ZF-BF, and the MF-BF algorithms in CASE4. For low values of $\text{SNR}^{(2)}$, the ZF-BF algorithm provides a slightly smaller relative loss in sum rate than the MMSE-BF and the MF-BF algorithms. For high values of $\text{SNR}^{(2)}$, the loss in sum rate due to imperfect CSI is a constant of about 1% which is the same for all BF algorithms.

5.4 Multiple source-destination pairs

5.4.1 Introduction

In Sections 5.4.2 and 5.4.3, two-way relaying for multiple source-destination pairs is considered. For that purpose, the assumptions of the previous chapters which are summarized in Section 2.2 are partially relaxed and the scenario of Figure 1.2 is extended. In general, the transmissions of multiple source-destination pairs can be separated in time by time division multiple access (TDMA) or in frequency by frequency division multiple access (FDMA) [ZK01]. In this case, each single source-destination pair corresponds to the setup of Figure 1.2 and all BF algorithms introduced in Chapters 3 and 4 are still valid. However, two scenarios are considered exemplarily in the following where additional measures besides TDMA and FDMA promise an improved performance in terms of resource efficiency. Firstly, the spatial domain is additionally used in order to multiplex multiple source-destination pairs which is also referred to as space division multiple access (SDMA). Section 5.4.2 considers a scenario where SDMA can be applied. Secondly, asymmetric rate requirements in bi-directional transmissions are considered, which means that one source node of a bi-directional source-destination pair transmits with a higher rate than the other source node. Section 5.4.3 gives a scenario where two source-destination pairs with asymmetric rate requirements are considered.

5.4.2 Multiple single-antenna source-destination pairs

In this section, spatial multiplexing of multiple single-antenna source-destination pairs is regarded. The considered scenario is depicted in Figure 5.8. The scenario corresponds to an ad-hoc scenario for example [PWS⁺04]. There are M single-antenna source-destination pairs where each pair corresponds to one of the gray arrows in the figure, i.e., node S_i , $i = 1, 2, \dots, M$, and node S_{i+M} form a source-destination pair. Compared to the original scenario of Figure 1.2, the M antennas per node in Figure 1.2 are no longer co-located in the scenario of Figure 5.8, but there are $2M$ independent nodes. This means that the M antennas on the left-hand side as well as the M antennas on the right-hand side cannot cooperate. Furthermore, it is assumed that each node can only obtain local CSI about its own channel to the RS. In this case, different source-destination pairs cannot cooperate. Thus, spatial multiplexing of the M source-destination pairs transmitting $2M$ data streams simultaneously can only be performed by exclusive BF at the RS in the described scenario. For that purpose, the RS has to

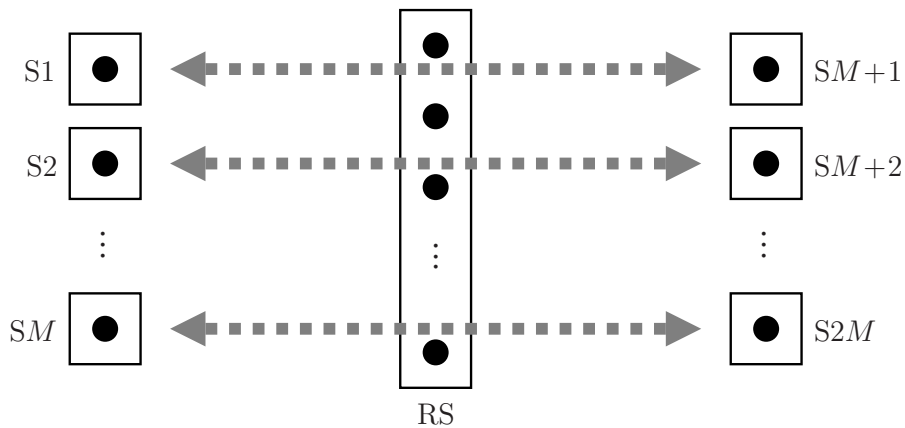


Figure 5.8. Bi-directional two-hop relaying scenario with M single-antenna source-destination pairs and one multiple-antenna RS.

be equipped with at least $2M$ antennas and requires global CSI about all links between the RS and the nodes S_i , $i = 1, 2, \dots, 2M$.

Each source node in Figure 5.8 transmits one data stream which is weighted by a single scalar weighting factor satisfying the transmit power constraint of the node and which is dedicated to one specific destination node. Each destination node desires only one data stream while there exist $2M - 2$ interfering data streams from the other source nodes. Furthermore, in two-way relaying the own transmitted data stream causes duplex interference at each destination node. Thus, there are $2M - 1$ interfering data streams in total at each destination node. Assuming that the nodes S_i , $i = 1, 2, \dots, 2M$ do not cancel the duplex interference of their own data stream by CDI, the BF algorithms developed in Section 4.3 for a system with limited capabilities at S1 and S2 can be directly applied to the described scenario. This means that the $2M$ data streams are separated by adaptive BF at the RS assuming $2M - 1$ interferers. Actually, if the duplex interference from the own transmitted data stream can be cancelled by CDI at nodes S_i , $i = 1, 2, \dots, 2M$, BF algorithms are required at the RS which only suppress $2M - 2$ interferers. Nevertheless, the linear BF algorithms of Section 4.3 provide reasonable performance, especially for high values of M where the difference in interference power of either $2M - 1$ or $2M - 2$ interferers can be neglected. Note that the BF algorithms of Section 4.3 only perform well if there are at least $2M$ antennas at the RS. If there are less than $2M$ antennas at the RS, additional resources in time or frequency are required in order to separate the transmissions of the different source-destination pairs by TDMA or FDMA in the scenario of Figure 5.8.

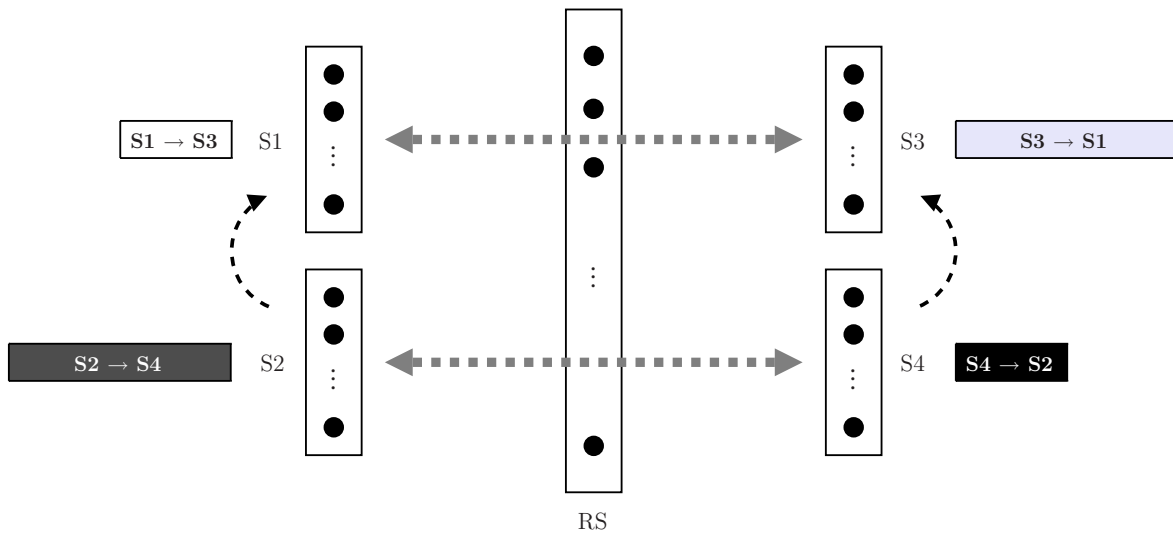


Figure 5.9. Bi-directional two-hop relaying scenario with 2 multiple-antenna source-destination pairs and one multiple-antenna RS for asymmetric rate requirements.

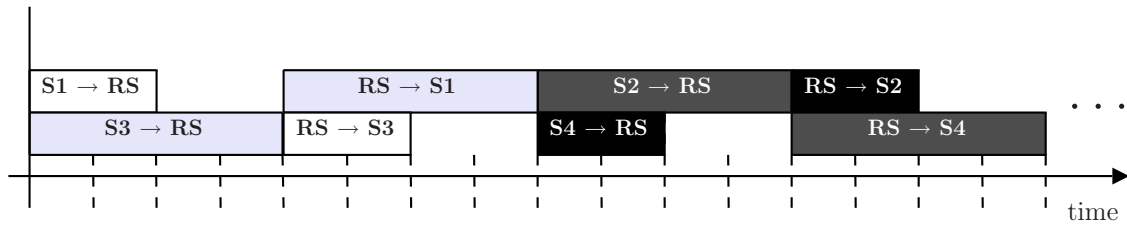
5.4.3 Asymmetric rate requirements of multiple source-destination pairs

In this section, asymmetric rate requirements in bi-directional transmissions with multiple source-destination pairs are considered. So far, only performance bounds like the maximum sum rate have been addressed, which means that the individual transmission rates have been chosen such that the sum rate is maximized. Thus, no requirements of individual transmission rates have been formulated. In this case, the individual transmission rates of both directions of transmission are in the same order of magnitude which can be seen in Figure 4.5. There are only small differences between the individual transmission rates which depend on the ratio between the SNR values of the channel between S1 and the RS and the channel between S2 and the RS. In real systems, there exist rate requirements for each direction of transmission depending on the considered service, e.g., for a file download, a high transmission rate is required for the transmission from the source to the destination of the file, but only a low transmission rate for feedback is required for the transmission from the destination to the source.

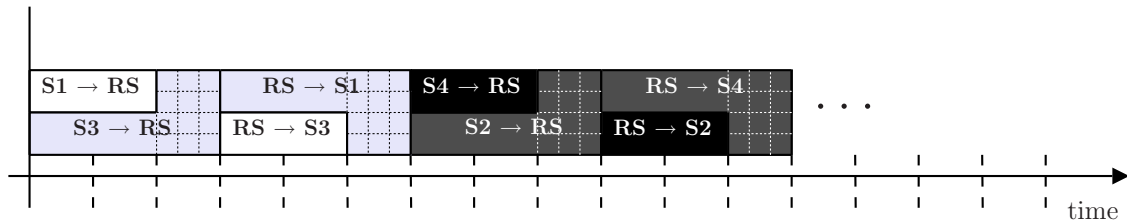
Figure 5.9 gives a simple example how a scenario with asymmetric rate requirements could look like. There exist two source-destination pairs, namely S1 and S3, as well as S2 and S4. The two source-destination pairs are denoted by the two gray arrows in the figure. The lengths of the bars next to the source nodes indicate the rate requirements of the transmitting nodes. For example, the rate required for the transmission from source node S3 to destination node S1 is twice as much as the rate required for the

transmission from S1 to S3. Similarly, the rate requirement for the transmission from S2 to S4 is the same as from S3 to S1, but twice as much as the rate requirement for the transmission from S4 to S2. Corresponding to a system with full capabilities as introduced for a single source-destination pair in the second row and first column of Figure 1.4, it is assumed that all nodes of Figure 5.9 have full SP capabilities and global CSI as defined in Section 1.1.3. In the following, three different schemes are proposed in order to meet the rate requirements of this scenario.

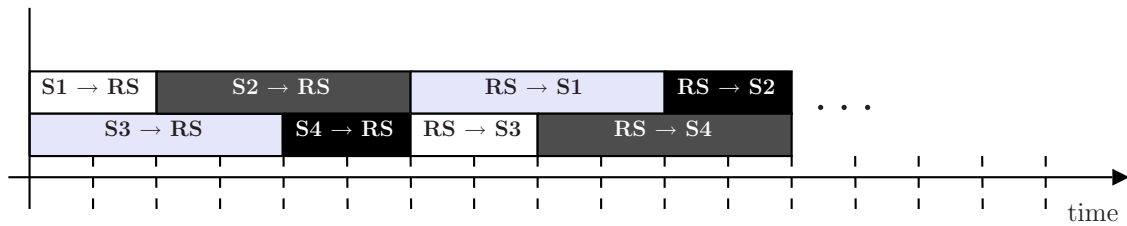
In the first scheme, the two bi-directional transmissions are processed independently in orthogonal time slots, i.e., TDMA is applied. The corresponding time slot allocation is depicted in Figure 5.10(a) where each direction of transmission is indicated by another shade of gray according to the shades of gray presented in Figure 5.9. In order



(a) Orthogonal transmission of the two two-way transmissions.



(b) Adaptation to one-way or two-way relaying.



(c) Pairing source nodes with same amount of data.

Figure 5.10. Time slot allocation for two source-destination pairs with asymmetric rate requirements.

to obtain a transmission rate from S1 to S3 which is half as much as the transmission rate from S3 to S1, source node S1 transmits zeros while S3 transmits its remaining data [EW08]. After the bi-directional transmission between S1 and S3 is finished, the

bi-directional transmission between S2 and S4 is processed where S4 transmits zeros while S2 transmits its remaining data. Instead of transmitting zeros, the node with the lower rate requirement could also perform repetition coding for example.

In the second scheme, the two bi-directional transmissions are also processed independently in orthogonal time slots and the corresponding time slot allocation is depicted in Figure 5.10(b). In contrast to the scheme proposed in Figure 5.10(a), not only two-way relaying is used, but it is possible to change from two-way relaying to one-way relaying and vice versa. In the following, only the bi-directional transmission between S1 and S3 is regarded, since the bi-directional transmission between S2 and S4 is processed in the same way. There exist four phases for each direction of the transmission. During the first phase, BF algorithms from two-way relaying are used which means that S1 and S3 transmit simultaneously. After transmitting the data of S1, the second phase starts. During the second phase, BF algorithms from one-way relaying are used which is indicated by the small squares in the figure. In one-way relaying, the multiple antennas of all nodes may be exclusively used for the transmission from S3 to S1 allowing a higher transmission rate. The higher transmission rate is obtained by multiplexing a higher number of data streams at S3 and/or using a higher order modulation scheme and/or using a higher coding rate than in the two-way relaying case. In the example of Figure 5.10(b), it is assumed that the transmission scheme of the second phase provides a transmission rate from S3 to S1 which is twice as high as the transmission rate of the first phase which allows finishing the transmission of the remaining data during half of the time. During the third phase, two-way relaying is used for the retransmission from the RS to S1 and S3, and during the fourth phase one-way relaying is used for the retransmission from the RS to S1. Obviously, the second transmission scheme requires less time slots than the first one.

In the third scheme, the transmissions of the two bi-directional source-destination pairs are processed simultaneously as depicted for the time slot allocation of Figure 5.10(c). In contrast to the second scheme, only two-way relaying is used. For the scheme, ideas from network coding are applied which are explained briefly in the following. The basic idea is that nodes can receive the signals of adjacent other nodes and can exploit this information in order to cancel interference later on. The scheme consists of six phases. During the first phase, S1 and S3 transmit simultaneously until the data of S1 is transmitted. During the second phase, S3 still transmits and S2 which is the source node requiring the higher transmission rate for the second source-destination pair also starts to transmit. It is assumed that the link quality between S1 and S2 is sufficient in order to receive the signals of S2 at S1 during the second phase which is indicated by the black dashed arrow from S2 to S1 in Figure 5.10(c). Furthermore, it is assumed that S1 knows the channel between S2 and S1 so that it

is possible for S1 to cancel the interference from S2 later on. Similarly, it is possible for S4 to cancel the interference from S3 later on. During the third phase, S2 and S4 transmit simultaneously to the RS. During the fourth phase, the RS retransmits the received data streams from the first phase to S1 and S3, which can both cancel the duplex interference by CDI. During the fifth phase, the RS retransmits the received data streams from the second phase to S1 and S4. At S1 it is possible to extract the data from S3 after canceling the interference from S2 since S1 received the data of S2 during the second phase. In the same way, it is possible to extract the data from S2 at S4 after canceling the interference from S3. During the sixth phase, the RS retransmits the received data streams from the third phase to S2 and S4, which can both cancel the duplex interference of their own transmitted data streams by performing CDI.

In the third scheme, coordination among multiple source-destination pairs is required in order to find source-destination pairs which fit into the time slot allocation proposed in Figure 5.10(c). Furthermore, CSI of channels between nodes which do not transmit to each other is required in order to cancel the interference. This leads to a trade-off between the efficient time slot allocation and the additional effort for obtaining CSI in the third scheme.

Chapter 6

Conclusions

This thesis deals with non-regenerative two-hop relaying for bi-directional transmission between a single source-destination pair of nodes S1 and S2. Multiple antennas at the source node, at the destination node, and at the RS are used in order to perform spatial multiplexing. Two relaying schemes, namely one-way and two-way relaying, are considered for the bi-directional transmission. The performance of the relaying schemes significantly depends on the system capabilities which are defined by the CSI availability at the nodes and the SP capabilities of the nodes. Chapter 1 provides a framework classifying the systems of different capabilities in one-way and two-way relaying. In the framework, four different cases of system capabilities are defined, namely a system with full capabilities, a system with limited capabilities at the RS, a system with limited capabilities at S1 and S2, and a system with local CSI at S1 and S2. While the first three cases are reasonable for both relaying schemes, the fourth case is only reasonable in two-way relaying. For all reasonable cases, several optimization problems are considered in this thesis.

In order to formulate and describe the optimization problems, a general system model for the bi-directional transmission between a single source-destination pair is introduced in Chapter 2. The system model can be applied to one-way relaying as well as to two-way relaying.

In Chapter 3, the sum rate maximization problem is considered for the first three cases of system capabilities in one-way relaying. For a system with full capabilities, a review of the BF algorithm which maximizes the sum rate is given. For the system with limited capabilities at the RS, a sub-optimum analytical BF algorithm is proposed in order to maximize the sum rate. For the maximization of the sum rate in the system with limited capabilities at S1 and S2, only a numerical solution could be found. It is shown that the full spatial multiplexing gain in one-way relaying is only obtained if the number of antennas at the RS is at least as high as the number of antennas at S1 and S2.

For the system with limited capabilities at S1 and S2 in one-way relaying, three additional linear optimization problems known to provide analytical BF algorithms with reasonable performance in point-to-point transmission are considered, namely the minimization of the MSE, the minimization of the MSE under the ZF constraint,

and the maximization of the SNR. These optimization problems are newly formulated for the one-way relaying scheme and the corresponding analytical BF algorithms are derived. In case of a system with limited capabilities at S1 and S2, the BF algorithm which minimizes the MSE provides the best performance in terms of sum rate and BER.

In Chapter 4, the sum rate maximization problem is considered for all four cases of system capabilities in two-way relaying. For all cases, the BF algorithm which maximizes the sum rate could only be found numerically. Nevertheless, methods are proposed in order to simplify the numerical optimizations and for the particular case of one antenna at S1 and S2 a sub-optimum analytical BF algorithm is proposed. It is shown that a significant amount of the loss in achievable sum rate due to the half-duplex constraint in two-hop transmissions can be compensated by two-way relaying. Furthermore, the full spatial multiplexing gain in two-way relaying is only obtained if the number of antennas at the RS is at least twice as high as the number of antennas at S1 and S2.

The three additional linear optimization problems introduced in one-way relaying are also considered for the system with limited capabilities at S1 and S2 and the system with local CSI at S1 and S2 in two-way relaying. For the system with limited capabilities at S1 and S2, it is shown that the corresponding BF algorithms can be derived by introducing an equivalent system model and using the respective BF algorithms developed for one-way relaying. For the system with local CSI at S1 and S2, BF algorithms which minimize the MSE, minimize the MSE under the ZF constraint, and maximize the SNR are newly derived. The BF algorithm which minimizes the MSE provides the best performance in terms of sum rate and BER. The comparison between the system with limited capabilities at S1 and S2 and the system with local CSI at S1 and S2 shows that at least local CSI should be provided to S1 and S2, since significant gains in terms of sum rate and BER can be obtained due to the cancellation of the duplex interference at the destination nodes.

In Chapter 5, pilot transmission schemes for obtaining CSI are proposed for the different cases of system capabilities and the respective channel estimation algorithms are developed. The systems which only require global CSI at the RS and no global CSI at S1 and S2 require less transmissions of pilot symbols. Thus, it is shown that there exists a trade-off between achievable sum rate and required effort in order to obtain CSI. Furthermore, it is shown that systems with global CSI at S1 and S2 are less sensitive to imperfect CSI than systems which do not have global CSI at S1 and S2. Finally, multiple source-destination pairs are addressed in Chapter 5, and approaches to satisfy asymmetric rate requirements in bi-directional transmissions are proposed.

Appendix

A.1 Derivation of (3.38) and (3.39) for the MMSE-BF algorithm in one-way relaying

In the following, the derivation of the BF matrix $\mathbf{G}_{\text{MMSE}}^{(k,i)}$ of Eq. (3.38) and the weighting factor $p_{\text{MMSE}}^{(k)}$ of Eq. (3.39) is sketched for the MMSE-BF algorithm in one-way relaying. From the first KKT condition (3.36a), the conjugate weighting factor $p^{(k)*}$ can be determined as

$$p^{(k)*} = \frac{q^{(i)} \text{tr} \left\{ \mathbf{H}^{(k)\text{T}} \mathbf{G}^{(k,i)} \mathbf{H}^{(i)} \mathbf{R}_{\mathbf{x}^{(i)}} \right\}}{\text{tr} \left\{ \mathbf{H}^{(k)\text{T}} \mathbf{G}^{(k,i)} \boldsymbol{\Upsilon}^{(i)} \mathbf{G}^{(k,i)\text{H}} \mathbf{H}^{(k)*} \right\} + \text{tr} \left\{ \mathbf{R}_{\mathbf{n}_R^{(k)}} \right\}}, \quad (\text{A.1.1})$$

with $\boldsymbol{\Upsilon}^{(i)}$ from (3.34). The conjugate weighting factor from (A.1.1) is inserted into the second KKT condition (3.36b), yielding

$$\begin{aligned} \eta^{(k)} \mathbf{G}^{(k,i)} \boldsymbol{\Upsilon}^{(i)} &= \frac{q^{(i)} \text{tr} \left\{ \mathbf{H}^{(k)\text{T}} \mathbf{G}^{(k,i)} \mathbf{H}^{(i)} \mathbf{R}_{\mathbf{x}^{(i)}} \right\} q^{(i)} \mathbf{H}^{(k)*} \mathbf{R}_{\mathbf{x}^{(i)}} \mathbf{H}^{(i)\text{H}}}{\text{tr} \left\{ \mathbf{H}^{(k)\text{T}} \mathbf{G}^{(k,i)} \boldsymbol{\Upsilon}^{(i)\text{T}} \mathbf{G}^{(k,i)\text{H}} \mathbf{H}^{(k)*} \right\} + \text{tr} \left\{ \mathbf{R}_{\mathbf{n}_R^{(k)}} \right\}} \\ &- \frac{q^{(i)^2 \left| \text{tr} \left\{ \mathbf{H}^{(k)\text{T}} \mathbf{G}^{(k,i)} \mathbf{H}^{(i)} \mathbf{R}_{\mathbf{x}^{(i)}} \right\} \right|^2 \mathbf{H}^{(k)*} \mathbf{H}^{(k)\text{T}} \mathbf{G}^{(k,i)} \boldsymbol{\Upsilon}^{(i)}}{\text{tr}^2 \left\{ \mathbf{H}^{(k)\text{T}} \mathbf{G}^{(k,i)} \boldsymbol{\Upsilon}^{(i)\text{T}} \mathbf{G}^{(k,i)\text{H}} \mathbf{H}^{(k)*} + \mathbf{R}_{\mathbf{n}_R^{(k)}} \right\}}. \end{aligned} \quad (\text{A.1.2})$$

After multiplying both sides of Eq. (A.1.2) with $\mathbf{G}^{(k,i)\text{H}}$, applying the trace operator, and some algebraic manipulations, one gets

$$\eta^{(k)} \text{tr} \left\{ \mathbf{G}^{(k,i)} \boldsymbol{\Upsilon}^{(i)} \mathbf{G}^{(k,i)\text{H}} \right\} = p^{(k)^2} \text{tr} \left\{ \mathbf{R}_{\mathbf{n}_R^{(k)}} \right\}. \quad (\text{A.1.3})$$

With Eq. (A.1.3) and the RS transmit power constraint (3.32b), the Lagrangian multiplier $\eta^{(k)}$ results in

$$\eta^{(k)} = \frac{p^{(k)^2} \text{tr} \left\{ \mathbf{R}_{\mathbf{n}_R^{(k)}} \right\}}{E^{(0)}}. \quad (\text{A.1.4})$$

By rearranging the second KKT condition (3.36b) and inserting the Lagrangian multiplier of Eq. (A.1.4), the BF matrix $\mathbf{G}^{(k,i)}$ results in

$$\mathbf{G}^{(k,i)} = \frac{q^{(i)}}{p^{(k)}} \left(p^{(k)^2} \mathbf{H}^{(k)*} \mathbf{H}^{(k)\text{T}} + \eta^{(k)} \mathbf{I}_L \right)^{-1} \mathbf{H}^{(k)*} \mathbf{R}_{\mathbf{x}^{(i)}} \mathbf{H}^{(i)\text{H}} \boldsymbol{\Upsilon}^{(i)-1}. \quad (\text{A.1.5})$$

Inserting Eq. (A.1.5) into the RS transmit power constraint (3.32b) shows that only the absolute value of the weighting factor $p^{(k)}$ is defined which means that there is no

unique solution to $p^{(k)}$. However, restricting $p^{(k)}$ to be positive real-valued ends up with the unique solution

$$p_{\text{MMSE}}^{(k)} = \sqrt{\frac{q^{(i)2} \text{tr} \{ \mathbf{H}^{(i)} \mathbf{R}_{\mathbf{x}^{(i)}} \mathbf{H}^{(k)\text{T}} \boldsymbol{\Upsilon}^{(k)-2} \mathbf{H}^{(k)*} \mathbf{R}_{\mathbf{x}^{(i)}} \mathbf{H}^{(i)\text{H}} \boldsymbol{\Upsilon}^{(i)-1} \}}{E^{(0)}}} \in \mathbb{R}^+, \quad (\text{A.1.6})$$

with $\boldsymbol{\Upsilon}^{(k)}$ of Eq. (3.37). With Eqs. (A.1.6) and (3.37), the linear BF matrix of Eq. (A.1.5) is rewritten as

$$\mathbf{G}_{\text{MMSE}}^{(k,i)} = \frac{q^{(i)}}{p_{\text{MMSE}}^{(k)}} \boldsymbol{\Upsilon}^{(k)-1} \mathbf{H}^{(k)*} \mathbf{R}_{\mathbf{x}^{(i)}} \mathbf{H}^{(i)\text{H}} \boldsymbol{\Upsilon}^{(i)-1}. \quad (\text{A.1.7})$$

A.2 Derivation of (3.48) and (3.49) for the ZF-BF algorithm in one-way relaying

In the following, the derivation of the BF matrix $\mathbf{G}_{\text{ZF}}^{(k,i)}$ of Eq. (3.48) and the weighting factor $p_{\text{ZF}}^{(k)}$ of Eq. (3.49) is sketched for the ZF-BF algorithm in one-way relaying. The second KKT condition (3.47a) can be rewritten as follows:

$$\mathbf{G}^{(k,i)} = \frac{1}{\eta^{(k)}} \left(-p^{(k)2} \mathbf{H}^{(k)*} \mathbf{H}^{(k)\text{T}} \mathbf{G}^{(k,i)} \mathbf{R}_{\mathbf{n}^{(0)}} + p^{(k)*} q^{(i)} \mathbf{H}^{(k)*} \boldsymbol{\Gamma}^{(k)\text{H}} \mathbf{H}^{(i)\text{H}} \right) \boldsymbol{\Upsilon}^{(i)-1}. \quad (\text{A.2.1})$$

An analytical solution to the optimization problem (3.43) can only be provide if $\mathbf{R}_{\mathbf{n}^{(0)}}$ of the first summand in Eq. (A.2.1) is assumed to be zero, i.e., $\mathbf{R}_{\mathbf{n}^{(0)}} = \mathbf{0}_{L \times L}$. Otherwise, it is not possible to extract BF matrix $\mathbf{G}^{(k,i)}$ in Eq. (A.2.1) and to determine the Lagrangian multiplier $\boldsymbol{\Gamma}^{(k)}$. Regarding the Lagrangian function (3.46), setting the first summand in (A.2.1) equal to zero corresponds to an optimization problem which only minimizes the MSE neglecting the noise at the RS which is actually retransmitted to node Sk . Thus, the following solution is expected to be sub-optimum. Note that the noise at the RS is only neglected for the first summand in Eq. (A.2.1), but for the transmit power constraint (3.43c) at the RS, the noise $\mathbf{R}_{\mathbf{n}^{(0)}}$ is still considered, i.e., $\mathbf{R}_{\mathbf{n}^{(0)}} \neq \mathbf{0}_{L \times L}$ in the covariance matrix $\boldsymbol{\Upsilon}^{(i)}$ of the received signal at the RS of Eq. (3.34) which also depends on $\mathbf{R}_{\mathbf{n}^{(0)}}$.

With this assumption, Eq. (A.2.1) is inserted into the ZF constraint (3.44), yielding the Hermitian of the Lagrangian multiplier

$$\boldsymbol{\Gamma}^{(k)\text{H}} = \frac{\eta^{(k)}}{q^{(i)2} p^{(k)2}} \left(\mathbf{H}^{(k)\text{T}} \mathbf{H}^{(k)*} \right)^{-1} \left(\mathbf{H}^{(i)\text{H}} \boldsymbol{\Upsilon}^{(i)-1} \mathbf{H}^{(i)} \right)^{-1}. \quad (\text{A.2.2})$$

By inserting the Hermitian of the Lagrangian multiplier $\mathbf{\Gamma}^{(k)\text{H}}$ of Eq. (A.2.2) into Eq. (A.2.1) for $\mathbf{R}_{\mathbf{n}^{(0)}} = \mathbf{0}_{L \times L}$, the BF matrix $\mathbf{G}_{\text{ZF}}^{(k,i)}$ at the RS results in

$$\mathbf{G}_{\text{ZF}}^{(k,i)} = \frac{1}{p^{(k)}q^{(i)}} \mathbf{H}^{(k)*} \left(\mathbf{H}^{(k)\text{T}} \mathbf{H}^{(k)*} \right)^{-1} \left(\mathbf{H}^{(i)\text{H}} \mathbf{\Upsilon}^{(i)-1} \mathbf{H}^{(i)} \right)^{-1} \mathbf{H}^{(i)\text{H}} \mathbf{\Upsilon}^{(i)-1}. \quad (\text{A.2.3})$$

Applying the Woodbury identity (A.4.4) for the matrix inversion introduced in Appendix A.4, Eq. (A.2.3) can be rewritten as

$$\mathbf{G}_{\text{ZF}}^{(k,i)} = \frac{1}{p^{(k)}q^{(i)}} \mathbf{H}^{(k)*} \left(\mathbf{H}^{(k)\text{T}} \mathbf{H}^{(k)*} \right)^{-1} \left(\mathbf{H}^{(i)\text{H}} \mathbf{R}_{\mathbf{n}^{(0)}}^{-1} \mathbf{H}^{(i)} \right)^{-1} \mathbf{H}^{(i)\text{H}} \mathbf{R}_{\mathbf{n}^{(0)}}^{-1}. \quad (\text{A.2.4})$$

The RS transmit power constraint can be satisfied subsequently by inserting \mathbf{G}_{ZF} of Eq. (A.2.4) into Eq. (3.43c). Restricting $p_{\text{ZF}}^{(k)}$ to be positive real-valued yields

$$p_{\text{ZF}}^{(k)} = \frac{1}{q^{(i)}} \sqrt{\frac{\text{tr} \left\{ \left(\mathbf{H}^{(i)\text{H}} \mathbf{\Upsilon}^{(i)-1} \mathbf{H}^{(i)} \right)^{-1} \left(\mathbf{H}^{(k)\text{T}} \mathbf{H}^{(k)*} \right)^{-1} \right\}}{E^{(0)}}} \in \mathbb{R}^+. \quad (\text{A.2.5})$$

A.3 Derivation of (3.57) and (3.58) for the MF-BF algorithm in one-way relaying

In the following, the derivation of the BF matrix $\mathbf{G}_{\text{MF}}^{(k,i)}$ of Eq. (3.57) and the weighting factor $p_{\text{MF}}^{(k)}$ of Eq. (3.58) is sketched for the MF-BF algorithm in one-way relaying. The first KKT condition (3.56a) can be rewritten as follows:

$$\mathbf{G}^{(k,i)} = \frac{q^{(i)2}}{\eta^{(k)}} \left(|\alpha^{(k)}|^2 \text{tr} \{ \mathbf{R}_{\mathbf{x}^{(i)}} \} \mathbf{H}^{(k)*} \mathbf{H}^{(k)\text{T}} \mathbf{G}^{(k,i)} \mathbf{R}_{\mathbf{n}^{(0)}} + \alpha^{(k)} \mathbf{H}^{(k)*} \mathbf{R}_{\mathbf{x}^{(i)}} \mathbf{H}^{(i)\text{H}} \right) \mathbf{\Upsilon}^{(i)-1}. \quad (\text{A.3.1})$$

As proposed for the ZF-BF algorithm in Appendix A.2, $\mathbf{R}_{\mathbf{n}^{(0)}}$ of the first summand in Eq. (A.3.1) is assumed to be zero in order to provide an analytical solution to the optimization problem (3.52), i.e., $\mathbf{R}_{\mathbf{n}^{(0)}} = \mathbf{0}_{L \times L}$. Regarding the Lagrangian function (3.54), setting the first summand in (A.3.1) equal to zero corresponds to an optimization problem which only maximizes the SNR between the power of the useful received signal and the noise at destination node S_k neglecting the noise at the RS which is retransmitted. Thus, the following solution is expected to be sub-optimum. Note that the noise at the RS is only neglected for the first summand in Eq. (A.3.1), but for the transmit power constraint (3.52b) at the RS, the noise $\mathbf{R}_{\mathbf{n}^{(0)}}$ is still considered, i.e., $\mathbf{R}_{\mathbf{n}^{(0)}} \neq \mathbf{0}_{L \times L}$ in the covariance matrix $\mathbf{\Upsilon}^{(i)}$ of the received signal at the RS of Eq. (3.34) which also depends on $\mathbf{R}_{\mathbf{n}^{(0)}}$.

Since $p^{(k)}$ can be chosen arbitrarily which can be seen from the Lagrangian function (3.54), the following choice is made:

$$\frac{1}{p^{(k)}} = \frac{q^{(i)^2} \alpha^{(k)}}{\eta^{(k)}}. \quad (\text{A.3.2})$$

With this choice, Eq. (A.3.1) already gives the solution for the BF matrix $\mathbf{G}_{\text{MF}}^{(k,i)}$ under the assumption $\mathbf{R}_{\mathbf{n}^{(0)}} = \mathbf{0}_{L \times L}$. The BF matrix $\mathbf{G}_{\text{MF}}^{(k,i)}$ results in

$$\mathbf{G}_{\text{MF}}^{(k,i)} = \frac{1}{p^{(k)}} \mathbf{H}^{(k)*} \mathbf{R}_{\mathbf{x}^{(i)}} \mathbf{H}^{(i)\text{H}} \boldsymbol{\Upsilon}^{(i)-1} \quad (\text{A.3.3})$$

Assuming that $p_{\text{ZF}}^{(k)}$ is positive real-valued, the BF matrix $\mathbf{G}^{(k,i)}$ of Eq. (A.3.3) can be inserted into the RS transmit power constraint yielding

$$p_{\text{MF}}^{(k)} = \sqrt{\frac{\text{tr} \{ \mathbf{H}^{(k)*} \mathbf{R}_{\mathbf{x}^{(i)}} \mathbf{H}^{(i)\text{H}} \boldsymbol{\Upsilon}^{(i)-1} \mathbf{H}^{(i)} \mathbf{R}_{\mathbf{x}^{(i)}} \mathbf{H}^{(k)\text{T}} \}}{E^{(0)}}} \in \mathbb{R}^+. \quad (\text{A.3.4})$$

A.4 The vectorization, the Kronecker product, and the matrix inversion

For some of the proposed BF algorithms, the following mathematical definitions and identities are required:

- The Kronecker product of matrices $\mathbf{Z} \in \mathbb{C}^{K \times N}$ and $\mathbf{X} \in \mathbb{C}^{U \times V}$ is defined as

$$\mathbf{Z} \otimes \mathbf{X} = \begin{bmatrix} z_{1,1} \mathbf{X} & z_{1,2} \mathbf{X} & \dots & z_{1,N} \mathbf{X} \\ z_{2,1} \mathbf{X} & z_{2,2} \mathbf{X} & \dots & z_{2,N} \mathbf{X} \\ \vdots & \vdots & \ddots & \vdots \\ z_{K,1} \mathbf{X} & z_{K,2} \mathbf{X} & \dots & z_{K,N} \mathbf{X} \end{bmatrix} \in \mathbb{C}^{KU \times NV}, \quad (\text{A.4.1})$$

where $z_{k,n}$, $k = 1, 2, \dots, K$ and $n = 1, 2, \dots, N$, is the element in the k -th row and n -th column of matrix \mathbf{Z} .

- The vectorization operator $\text{vec}[\mathbf{Z}]$ stacks the columns of matrix \mathbf{Z} into a vector, i.e.,

$$\text{vec}[\mathbf{Z}] = [z_{1,1}, z_{2,1}, \dots, z_{K,1}, z_{1,2}, z_{2,2}, \dots, z_{K,2}, \dots, z_{1,N}, z_{2,N}, \dots, z_{K,N}]^{\text{T}}. \quad (\text{A.4.2})$$

- The operator $\text{vec}_{K,N}^{-1}[\cdot]$ is the revision of the operator $\text{vec}[\cdot]$, i.e., a vector of length KN is sequentially divided into N smaller vectors of length K which are combined to a matrix with K rows and N columns.
- The vectorization of a matrix product \mathbf{XYZ} is given by

$$\text{vec}[\mathbf{XYZ}] = (\mathbf{Z}^T \otimes \mathbf{X}) \text{vec}[\mathbf{Y}]. \quad (\text{A.4.3})$$

- The Woodbury identity [PP08] for the matrix inversion with positive definite matrices \mathbf{R} and \mathbf{X} is given by

$$(\mathbf{X}^{-1} + \mathbf{Z}^H \mathbf{R}^{-1} \mathbf{Z})^{-1} \mathbf{Z}^H \mathbf{R}^{-1} = \mathbf{XZ}^H (\mathbf{ZXZ}^H + \mathbf{R})^{-1}. \quad (\text{A.4.4})$$

A.5 Derivation of (4.65) and (4.67) for the MMSE-BF algorithm in two-way relaying

In the following, the derivation of the BF matrix \mathbf{G}_{MMSE} of Eq. (4.65) and the weighting factor p_{MMSE} of Eq. (4.67) is sketched for the MMSE-BF algorithm for a system with local CSI at S1 and S2 in two-way relaying. From the first KKT condition (4.63a), the conjugate weighting factor p^* can be determined as

$$p^* = \frac{\sum_{i=1}^2 q^{(i)} \text{tr} \left\{ \mathbf{H}^{(k)T} \mathbf{G} \mathbf{H}^{(i)} \mathbf{R}_{\mathbf{x}^{(i)}} \right\}}{\sum_{i=1}^2 \text{tr} \left\{ \mathbf{H}^{(k)T} \mathbf{G} \mathbf{\Upsilon}^{(i)} \mathbf{G}^H \mathbf{H}^{(k)*} + \mathbf{R}_{\mathbf{n}_R^{(k)}} \right\}}, \quad (\text{A.5.1})$$

with $\mathbf{\Upsilon}^{(i)}$ of Eq. (3.34). The weighting factor of Eq. (A.5.1) is inserted into the second KKT condition (4.63b), yielding

$$\begin{aligned} \eta \mathbf{G} \mathbf{\Upsilon} &= \frac{\sum_{i=1}^2 q^{(i)} \text{tr} \left\{ \mathbf{H}^{(k)T} \mathbf{G} \mathbf{H}^{(i)} \mathbf{R}_{\mathbf{x}^{(i)}} \right\} \sum_{i=1}^2 q^{(i)} \mathbf{H}^{(k)*} \mathbf{R}_{\mathbf{x}^{(i)}} \mathbf{H}^{(i)H}}{\sum_{i=1}^2 \text{tr} \left\{ \mathbf{H}^{(k)T} \mathbf{G} \mathbf{\Upsilon}^{(i)T} \mathbf{G}^H \mathbf{H}^{(k)*} + \mathbf{R}_{\mathbf{n}_R^{(k)}} \right\}} \\ &\quad - \frac{\sum_{i=1}^2 \left| \text{tr} \left\{ q^{(i)} \mathbf{H}^{(k)T} \mathbf{G} \mathbf{H}^{(i)} \mathbf{R}_{\mathbf{x}^{(i)}} \right\} \right|^2 \mathbf{H}^{(k)*} \mathbf{H}^{(k)T} \mathbf{G} \mathbf{\Upsilon}^{(i)}}{\text{tr}^2 \left\{ \sum_{i=1}^2 \mathbf{H}^{(k)T} \mathbf{G} \mathbf{\Upsilon}^{(i)T} \mathbf{G}^H \mathbf{H}^{(k)*} + \mathbf{R}_{\mathbf{n}_R^{(k)}} \right\}}. \end{aligned} \quad (\text{A.5.2})$$

After multiplying both sides of Eq. (A.5.2) with \mathbf{G}^H , applying the trace operator, and some algebraic manipulations, one gets

$$\eta \operatorname{tr} \{ \mathbf{G} \boldsymbol{\Upsilon} \mathbf{G}^H \} = p^2 \operatorname{tr} \left\{ \sum_{k=1}^2 \mathbf{R}_{\mathbf{n}_R^{(k)}} \right\}. \quad (\text{A.5.3})$$

With Eq. (A.5.3) and the RS transmit power constraint (4.59c), the Lagrangian multiplier results in

$$\eta = \frac{p^2 \operatorname{tr} \left\{ \sum_{k=1}^2 \mathbf{R}_{\mathbf{n}_R^{(k)}} \right\}}{E^{(0)}}. \quad (\text{A.5.4})$$

Let \mathbf{K} be given by

$$\mathbf{K} = \sum_{i=1}^2 \left(\boldsymbol{\Upsilon}^{(i)\top} \otimes \left(\mathbf{H}^{(k)*} \mathbf{H}^{(k)\top} \right) \right) + \left(\boldsymbol{\Upsilon} \otimes \frac{1}{E^{(0)}} \operatorname{tr} \left\{ \sum_{k=1}^2 \mathbf{R}_{\mathbf{n}_R^{(k)}} \right\} \mathbf{I}_L \right). \quad (\text{A.5.5})$$

In order to separate the BF matrix \mathbf{G} , the second KKT condition (4.63b) is vectorized firstly, and secondly, identity (A.4.3) is applied. These operations result in the following vector equation:

$$\operatorname{vec} [\mathbf{G}] = \frac{1}{p} \mathbf{K}^{-1} \operatorname{vec} \left[\sum_{i=1}^2 q^{(i)} \mathbf{H}^{(k)*} \mathbf{R}_{\mathbf{x}^{(i)}} \mathbf{H}^{(i)H} \right]. \quad (\text{A.5.6})$$

From Eq. (A.5.6), the BF matrix \mathbf{G} can be determined by reversing the vectorization. Let auxiliary matrix $\tilde{\mathbf{G}}$ be defined as

$$\tilde{\mathbf{G}} = p \mathbf{G} = \operatorname{vec}_{L,L}^{-1} \left[\mathbf{K}^{-1} \operatorname{vec} \left[\sum_{i=1}^2 q^{(i)} \mathbf{H}^{(k)*} \mathbf{R}_{\mathbf{x}^{(i)}} \mathbf{H}^{(i)H} \right] \right]. \quad (\text{A.5.7})$$

Inserting Eq. (A.5.7) into the RS transmit power constraint (4.59c) shows that only the absolute value of the weighting factor p is defined which means that there is no unique solution to p . However, restricting p to be positive real-valued yields the unique solution

$$p_{\text{MMSE}} = \sqrt{\frac{\operatorname{tr} \{ \tilde{\mathbf{G}} \boldsymbol{\Upsilon} \tilde{\mathbf{G}}^H \}}{E^{(0)}}} \in \mathbb{R}^+, \quad (\text{A.5.8})$$

and

$$\mathbf{G}_{\text{MMSE}} = \frac{1}{p_{\text{MMSE}}} \operatorname{vec}_{L,L}^{-1} \left[\mathbf{K}^{-1} \operatorname{vec} \left[\sum_{i=1}^2 q^{(i)} \mathbf{H}^{(k)*} \mathbf{R}_{\mathbf{x}^{(i)}} \mathbf{H}^{(i)H} \right] \right]. \quad (\text{A.5.9})$$

A.6 Derivation of (4.75) and (4.77) for the ZF-BF algorithm in two-way relaying

In the following, the derivation of the BF matrix \mathbf{G}_{ZF} of Eq. (4.75) and the weighting factor p_{ZF} of Eq. (4.77) is sketched for the ZF-BF algorithm for a system with local CSI at S1 and S2 in two-way relaying. Due to the two ZF constraints in (4.69), the optimization is more complicated than in the one-way relaying case of Appendix A.2. An analytical solution to problem (4.68) can only be provided under the assumption that $\mathbf{R}_{\mathbf{n}^{(0)}} = \mathbf{0}_{L \times L}$ in the first summand of the second KKT condition (4.72b). Thus, for the MSE of Eq. (4.70) the noise of the RS which is actually retransmitted to node S_k is neglected providing a sub-optimum solution to the original optimization problem (4.68). Note that the noise at the RS is only neglected for the first summand in Eq. (4.72b), but for the transmit power constraint (4.68d) at the RS, the noise $\mathbf{R}_{\mathbf{n}^{(0)}}$ is still considered, i.e., $\mathbf{R}_{\mathbf{n}^{(0)}} \neq \mathbf{0}_{L \times L}$ in the covariance matrix $\mathbf{\Upsilon}$ of the received signal at the RS of Eq. (4.61) which also depends on $\mathbf{R}_{\mathbf{n}^{(0)}}$. With these assumptions, the BF matrix \mathbf{G} at the RS can be determined by the second KKT condition (4.72b) yielding

$$\mathbf{G} = \frac{p^*}{\eta} \sum_{i=1}^2 q^{(i)} \mathbf{H}^{(k)*} \mathbf{\Gamma}^{(k)\text{H}} \mathbf{H}^{(i)\text{H}} \mathbf{\Upsilon}^{-1}. \quad (\text{A.6.1})$$

By inserting (A.6.1) into both ZF constraints of Eq. (4.69), it can be shown that the Lagrangian multipliers $\mathbf{\Gamma}^{(k)\text{H}}$, $k = 1, 2$, are proportional to $\eta/|p|^2$ which means that $\mathbf{\Gamma}^{(k)\text{H}}$ can be described by

$$\mathbf{\Gamma}^{(k)\text{H}} = \frac{\eta}{|p|^2} \tilde{\mathbf{\Gamma}}^{(k)\text{H}}, \quad (\text{A.6.2})$$

with the modified Lagrangian multipliers $\tilde{\mathbf{\Gamma}}^{(k)}$, $k = 1, 2$. Thus, by inserting (A.6.2) into Eq. (A.6.1) the BF matrix \mathbf{G} becomes independent of the Lagrangian multiplier η resulting in

$$\mathbf{G} = \frac{1}{p} \sum_{i=1}^2 q^{(i)} \mathbf{H}^{(k)*} \tilde{\mathbf{\Gamma}}^{(k)\text{H}} \mathbf{H}^{(i)\text{H}} \mathbf{\Upsilon}^{-1}. \quad (\text{A.6.3})$$

In the following, the modified Lagrangian multipliers $\tilde{\mathbf{\Gamma}}^{(1)\text{H}}$ and $\tilde{\mathbf{\Gamma}}^{(2)\text{H}}$ are determined by inserting \mathbf{G} of Eq. (A.6.3) into both ZF constraints from (4.69). Let matrices $\mathbf{X}_0^{(k)}$, $\mathbf{X}_1^{(k)}$, $\mathbf{X}_2^{(k)}$, $\mathbf{X}_3^{(k)}$ and $\mathbf{X}_4^{(k)}$ be given by

$$\mathbf{X}_0^{(k)} = \mathbf{H}^{(k)\text{T}} \mathbf{H}^{(i)*} \left(\mathbf{H}^{(i)\text{T}} \mathbf{H}^{(i)*} \right)^{-1} \left(\mathbf{H}^{(k)\text{H}} \mathbf{\Upsilon}^{-1} \mathbf{H}^{(k)} \right)^{-1} \mathbf{H}^{(k)\text{H}} \mathbf{\Upsilon}^{-1} \mathbf{H}^{(i)}, \quad (\text{A.6.4a})$$

$$\mathbf{X}_1^{(k)} = q^{(i)} \mathbf{H}^{(k)\text{T}} \mathbf{H}^{(k)*}, \quad (\text{A.6.4b})$$

$$\mathbf{X}_2^{(k)} = \mathbf{H}^{(i)\text{H}} \mathbf{\Upsilon}^{-1} \mathbf{H}^{(i)}, \quad (\text{A.6.4c})$$

$$\mathbf{X}_3^{(k)} = q^{(k)} \mathbf{H}^{(k)\text{T}} \mathbf{H}^{(i)*} \left(\mathbf{H}^{(i)\text{T}} \mathbf{H}^{(i)*} \right)^{-1} \mathbf{H}^{(i)\text{T}} \mathbf{H}^{(k)*}, \quad (\text{A.6.4d})$$

$$\mathbf{X}_4^{(k)} = \mathbf{H}^{(i)\text{H}} \mathbf{\Upsilon}^{-1} \mathbf{H}^{(k)} \left(\mathbf{H}^{(k)\text{H}} \mathbf{\Upsilon}^{-1} \mathbf{H}^{(k)} \right)^{-1} \mathbf{H}^{(k)\text{H}} \mathbf{\Upsilon}^{-1} \mathbf{H}^{(i)}. \quad (\text{A.6.4e})$$

Solving the first ZF constraint in (4.69) for $\tilde{\mathbf{\Gamma}}^{(1)\text{H}}$, and inserting $\tilde{\mathbf{\Gamma}}^{(1)\text{H}}$ into the second ZF constraint, gives the following two equations depending on $\tilde{\mathbf{\Gamma}}^{(k)\text{H}}$, for $k = 1, 2$:

$$\frac{1}{q^{(k)}} \mathbf{I}_M - \mathbf{X}_0^{(k)} = \mathbf{X}_1^{(k)} \tilde{\mathbf{\Gamma}}^{(k)\text{H}} \mathbf{X}_2^{(k)} - \mathbf{X}_3^{(k)} \tilde{\mathbf{\Gamma}}^{(k)\text{H}} \mathbf{X}_4^{(k)}. \quad (\text{A.6.5})$$

By vectorizing Eq. (A.6.5) and applying identity (A.4.3), $\text{vec} \left[\tilde{\mathbf{\Gamma}}^{(k)\text{H}} \right]$ results in

$$\text{vec} \left[\tilde{\mathbf{\Gamma}}^{(k)\text{H}} \right] = \left(\left(\mathbf{X}_2^{(k)\text{T}} \otimes \mathbf{Y}_1^{(k)} \right) - \left(\mathbf{X}_4^{(k)\text{T}} \otimes \mathbf{X}_3^{(k)} \right) \right)^{-1} \text{vec} \left[\frac{1}{q^{(k)}} \mathbf{I}_M - \mathbf{X}_0^{(k)} \right]. \quad (\text{A.6.6})$$

The reversion of the vectorization provides the modified Lagrangian multipliers

$$\tilde{\mathbf{\Gamma}}^{(k)\text{H}} = \text{vec}_{M,M}^{-1} \left[\left(\left(\mathbf{X}_2^{(k)\text{T}} \otimes \mathbf{X}_1^{(k)} \right) - \left(\mathbf{X}_4^{(k)\text{T}} \otimes \mathbf{X}_3^{(k)} \right) \right)^{-1} \text{vec} \left[\frac{1}{q^{(k)}} \mathbf{I}_M - \mathbf{X}_0^{(k)} \right] \right]. \quad (\text{A.6.7})$$

Let auxiliary matrix $\tilde{\mathbf{G}}$ be defined as

$$\tilde{\mathbf{G}} = p \mathbf{G} = \sum_{i=1}^2 q^{(i)} \mathbf{H}^{(k)*} \tilde{\mathbf{\Gamma}}^{(k)\text{H}} \mathbf{H}^{(i)\text{H}} \mathbf{\Upsilon}^{-1}, \quad (\text{A.6.8})$$

with the modified Lagrangian multiplier of Eq. (A.6.7). Inserting Eq. (A.6.3) into the RS transmit power constraint (4.68d), shows that only the absolute value of the weighting factor p is defined which means that there exists no unique solution to p . However, restricting p to be positive real-valued, yields the unique solution

$$p_{\text{ZF}} = \sqrt{\frac{\text{tr} \left\{ \tilde{\mathbf{G}} \mathbf{\Upsilon} \tilde{\mathbf{G}}^{\text{H}} \right\}}{E^{(0)}}} \in \mathbb{R}^+, \quad (\text{A.6.9})$$

and

$$\mathbf{G}_{\text{ZF}} = \frac{1}{p_{\text{ZF}}} \sum_{i=1}^2 q^{(i)} \mathbf{H}^{(k)*} \tilde{\mathbf{\Gamma}}^{(k)\text{H}} \mathbf{H}^{(i)\text{H}} \mathbf{\Upsilon}^{-1}, \quad (\text{A.6.10})$$

with $\tilde{\mathbf{\Gamma}}^{(k)\text{H}}$ from (A.6.7).

A.7 Derivation of (4.83) and (4.85) for the MF-BF algorithm in two-way relaying

In the following, the derivation of the BF matrix \mathbf{G}_{MF} of Eq. (4.83) and the weighting factor p_{MF} of Eq. (4.85) is sketched for the MF-BF algorithm for a system with local CSI at S1 and S2 in two-way relaying. An analytical solution to problem (4.78) can only be provided under the assumption that $\mathbf{R}_{\mathbf{n}}^{(0)} = \mathbf{0}_{L \times L}$ in the second summand of

the first KKT condition (4.82a). Thus, for the SNR definition of the objective function (4.78a), the noise of the RS which is actually retransmitted to node Sk is neglected providing a sub-optimum solution to the original optimization problem (4.78). Note that the noise at the RS is only neglected for the second summand in Eq. (4.82a), but for the transmit power constraint (4.78c) at the RS, the noise $\mathbf{R}_{\mathbf{n}^{(0)}}$ is still considered, i.e., $\mathbf{R}_{\mathbf{n}^{(0)}} \neq \mathbf{0}_{L \times L}$ in the covariance matrix $\mathbf{\Upsilon}$ of the received signal at the RS of Eq. (4.61) which also depends on $\mathbf{R}_{\mathbf{n}^{(0)}}$. With these assumptions, the BF matrix \mathbf{G} at the RS can be determined by the first KKT condition (4.82a) yielding

$$\mathbf{G} = \frac{1}{\eta} \sum_{i=1}^2 q^{(i)^2} \alpha^{(i)} \mathbf{H}^{(k)*} \mathbf{R}_{\mathbf{x}^{(i)}} \mathbf{H}^{(i)\text{H}} \mathbf{\Upsilon}^{-1}. \quad (\text{A.7.1})$$

By inserting BF matrix \mathbf{G} of Eq. (A.7.1) into (4.81), it can be shown that $|q^{(1)}|^2 \alpha^{(1)} = |q^{(2)}|^2 \alpha^{(2)}$ for

$$\eta = |q^{(2)}|^2 \text{tr} \left\{ \mathbf{H}^{(1)\text{T}} \mathbf{H}^{(2)*} \mathbf{H}^{(1)\text{H}} \mathbf{H}^{(2)} \mathbf{\Upsilon}^{-1} \right\} + |q^{(1)}|^2 \text{tr} \left\{ \mathbf{H}^{(2)\text{T}} \mathbf{H}^{(1)*} \mathbf{H}^{(2)\text{H}} \mathbf{H}^{(1)} \mathbf{\Upsilon}^{-1} \right\}. \quad (\text{A.7.2})$$

For $|q^{(1)}|^2 \alpha^{(1)} = |q^{(2)}|^2 \alpha^{(2)}$, the following choice is made for the scalar weighting factor p which can be chosen arbitrarily except for $p = 0$ due to the Lagrangian function (4.80):

$$\frac{1}{p} = \frac{\alpha^{(1)} |q^{(1)}|^2}{\eta}. \quad (\text{A.7.3})$$

Let auxiliary matrix $\tilde{\mathbf{G}}$ be defined as

$$\tilde{\mathbf{G}} = p\mathbf{G} = \sum_{i=1}^2 \mathbf{H}^{(k)*} \mathbf{R}_{\mathbf{x}^{(i)}} \mathbf{H}^{(i)\text{H}} \mathbf{\Upsilon}^{-1}. \quad (\text{A.7.4})$$

Inserting (A.7.1) into the RS transmit power constraint (4.78c), and restricting p to be positive real-valued, yields

$$p_{\text{MF}} = \sqrt{\frac{\text{tr} \left\{ \tilde{\mathbf{G}} \mathbf{\Upsilon} \tilde{\mathbf{G}}^{\text{H}} \right\}}{E^{(0)}}} \in \mathbb{R}^+, \quad (\text{A.7.5})$$

and

$$\mathbf{G}_{\text{MF}} = \frac{1}{p_{\text{MF}}} \sum_{i=1}^2 \mathbf{H}^{(k)*} \mathbf{R}_{\mathbf{x}^{(i)}} \mathbf{H}^{(i)\text{H}} \mathbf{\Upsilon}^{-1}. \quad (\text{A.7.6})$$

List of Acronyms

3G	Third Generation of wireless communications
4G	Fourth Generation of wireless communications
AF	Amplify-and-Forward
AWGN	Additive White Gaussian Noise
BF	Beamforming
BER	Bit Error Rate
CDI	Cancellation of Duplex Interference
CSI	Channel State Information
DF	Decode-and-Forward
EMC	Electro-Magnetic Compatibility
FDMA	Frequency Division Multiple Access
KKT	Karush-Kuhn-Tucker
MF	Matched Filter
MIMO	Multiple Input Multiple Output
MMSE	Minimum Mean Square Error
MRR	Maximal-Ratio Reception
MRT	Maximal-Ratio Transmission
MSE	Mean Square Error
OFDM	Orthogonal Frequency Division Multiplexing
PA	Power Allocation
PACE	Pilot Assisted Channel Estimation
PSK	Phase Shift Keying
QPSK	Quadrature Phase Shift Keying
RS	Relay Station

SDMA	Spatial Division Multiple Access
SINR	Signal-to-Interference plus Noise Ratio
SNR	Signal-to-Noise Ratio
SQP	Sequential Quadratic Programming
SP	Signal Processing
SVD	Singular Value Decomposition
TDMA	Time Division Multiple Access
TS	Time Slot
WLAN	Wireless Local Area Network
XOR	Exclusive OR
ZF	Zero Forcing

Notation

$\mathbf{0}_{L \times M}$	All zero matrix with L rows and M columns
$\arg \max_{\{x\}} y$	Returns the value of x which maximizes y
$\arg \min_{\{x\}} y$	Returns the value of x which minimizes y
$\mathbf{A}^{(k)}$	Matrix linked with the useful receive signal at node S_k
$A_m^{(k)}$	Useful signal power at the m -th receive antenna of node S_k
$\mathbf{B}^{(k)}$	Matrix describing the overall filtering of the noise at node S_k
$B_m^{(k)}$	Overall noise power at the m -th receive antenna of node S_k
$\beta^{(i)}$	lets pass a signal for $\beta^{(i)} = 1$ and blocks a signal for $\beta^{(i)} = 0$
$C_{EW}^{(k)}$	Transmission rate for the transmission from S_i to S_k
$C^{(\text{sum})}$	Sum rate
\mathbb{C}	Set of complex numbers
$\det[\cdot]$	Determinant
$\text{diag}[\cdot]$	Diagonal matrix consisting of the main diagonal matrix elements if the argument is a matrix, and consisting of the vector elements if the argument is a vector
$\text{diag}_b[\cdot]$	Composes a block diagonal matrix of the matrix arguments
$\mathbf{D}^{(k)}$	Matrix linked with the duplex interference at node S_k
$D_m^{(k)}$	Duplex interference power at the m -th receive antenna of node S_k
$E^{(0)}$	Maximum transmit power of the RS
$E^{(i)}$	Maximum transmit power of node S_i
$E\{\cdot\}$	Expectation operator
$\mathbf{F}^{(k)}$	Matrix linked with the intersymbol interference at node S_k
$F_m^{(k)}$	Intersymbol interference power at the m -th receive antenna of node S_k
$\bar{\mathbf{G}}$	General BF matrix at the RS valid in one-way and two-way relaying
\mathbf{G}	BF matrix at the RS in two-way relaying
\mathbf{G}_T	Transmit BF matrix in the decomposition of \mathbf{G}
\mathbf{G}_R	Receive BF matrix in the decomposition of \mathbf{G}
$\mathbf{G}^{(k,i)}$	BF matrix at the RS for the transmission from S_i to S_k in one-way relaying
$\mathbf{G}_T^{(k)}$	Transmit BF matrix in the decomposition of $\mathbf{G}^{(k,i)}$
$\mathbf{G}_R^{(i)}$	Receive BF matrix in the decomposition of $\mathbf{G}^{(k,i)}$
g	real-valued weighting factor at the RS in two-way relaying

$g^{(k,i)}$	real-valued weighting factor at the RS for the transmission from S_i to S_k in one-way relaying
$h_{n,m}^{(i)}$	Channel fading coefficient between transmit antenna n of node S_i and receive antenna m of the RS
$\mathbf{h}_m^{(i)}$	m -th channel vector between node S_i and the RS
$\mathbf{H}^{(i)}$	Channel matrix between node S_i and the RS
$\mathbf{H}^{(k,i)}$	Overall channel matrix for the transmission from S_i to S_k
\mathbf{H}_R	Joint first hop channel matrix
\mathbf{H}_T	Joint second hop channel matrix
\mathbf{I}_M	Identity matrix of size M
j	$\sqrt{-1}$
L	Number of antennas at the RS
$\mathbf{\Lambda}^{(k)}$	Diagonal matrix containing the eigenvalues of $\mathbf{H}^{(k)}$
$\lambda_m^{(k)}$	m -th eigenvalue of $\mathbf{H}^{(k)}$
$\mathbf{\Lambda}^{(k,i)}$	Diagonal matrix containing the eigenvalues of $\mathbf{H}^{(k,i)}$
$\lambda_m^{(k,i)}$	m -th eigenvalue of $\mathbf{H}^{(k,i)}$
$\log_2(\cdot)$	Logarithm to the base 2
M	Number of antennas at S_1 and S_2
$\mathbf{n}^{(0)}$	Noise vector at the RS
$\mathbf{n}^{(k)}$	Overall noise vector at node S_k
$\mathbf{n}_R^{(k)}$	Noise vector at node S_k
$p^{(k)}$	Scalar receive weighting factor at node S_k
$\mathbf{P}^{(k)}$	Receive BF matrix at node S_k
\mathbf{P}	Joint receive BF matrix of nodes S_1 and S_2
$q^{(i)}$	Scalar transmit weighting factor at node S_i
$\mathbf{Q}^{(i)}$	Transmit BF matrix at node S_i
\mathbf{Q}	Joint transmit BF matrix of nodes S_1 and S_2
r	Sum rate normalization factor
R	Number of non-zero eigenvalues
$\mathbf{R}_{\mathbf{n}}^{(0)}$	Noise covariance matrix at the RS
$\mathbf{R}_{\mathbf{n}}^{(k)}$	Overall noise covariance matrix at node S_k
$\mathbf{R}_{\mathbf{n}_R}^{(k)}$	Noise covariance matrix at node S_k
$\mathbf{R}_{\mathbf{x}}^{(i)}$	Covariance matrix of the data vector transmitted by node S_i
\mathbb{R}	Set of real numbers
\mathbb{R}^+	Set of positive real numbers
$\sigma^{(i)^2}$	Variance of the channel coefficients in $\mathbf{H}^{(i)}$

$\sigma_{\mathbf{n}(0)}^2$	Noise variance at the RS
$\sigma_{\mathbf{n}_R}^2$	Noise variance at node Sk
S	number of orthogonal time slots required for one bi-directional transmission
$\text{SINR}_m^{(k)}$	SINR at the m -th receive antenna of node Sk
$\text{SNR}^{(i)}$	Average SNR for the transmission from Si to the RS and vice versa
$T_m^{(k)}$	Power depending on CDI matrix $\mathbf{T}^{(k)}$ at the m -th receive antenna of node Sk
$\mathbf{T}^{(k)}$	CDI matrix at node Sk
\mathbf{T}	Joint CDI matrix at nodes S1 and S2
$\mathbf{U}^{(i)}$	Left eigenvectors of $\mathbf{H}^{(i)}$
$\mathbf{V}^{(i)}$	Right eigenvectors of $\mathbf{H}^{(i)}$
$\mathbf{U}^{(k,i)}$	Left eigenvectors of $\mathbf{H}^{(k,i)}$
$\mathbf{V}^{(k,i)}$	Right eigenvectors of $\mathbf{H}^{(k,i)}$
$\text{vec}[\cdot]$	vectorization operator, cf. Appendix A.4
w_l	l -th diagonal element of matrix $\tilde{\mathbf{G}}$
$w_l^{(k,i)}$	l -th diagonal element of the RS power allocation matrix $\mathbf{W}^{(k,i)}$
$\mathbf{W}^{(k,i)}$	RS power allocation matrix in the decomposition of $\mathbf{G}^{(k,i)}$
$\text{tr}\{\cdot\}$	Sum of the main diagonal elements of a matrix
$x_m^{(i)}$	m -th data symbol of node Si
\mathbf{x}	Joint data vector transmitted by S1 and S2
$\mathbf{x}^{(i)}$	Data vector transmitted by node Si
$\hat{\mathbf{x}}$	Joint estimated data vector
$\hat{\mathbf{x}}^{(i)}$	Estimated data vector of $\mathbf{x}^{(i)}$
$[\cdot]^H$	Hermitian of a vector or a matrix
$[\cdot]^T$	Transpose of a vector or a matrix
$[\cdot]^*$	Conjugate of a scalar or a vector or a matrix
$(y)^+$	Returns y if $y \geq 0$ and returns 0 if $y < 0$
$\lfloor \cdot \rfloor$	Rounds the argument to the nearest integer towards minus infinity
$ \cdot $	Absolute value
$\ \cdot\ _2^2$	Euclidean norm of a vector
\otimes	Kronecker product operator, cf. Appendix A.4

Bibliography

- [3GP06] 3GPP, “Physical layer aspects for evolved Universal Terrestrial Radio Access (UTRA),” Technical Specification Group Radio Access Network, Tech. Rep. TR 25.814 v7.1.0, Sep. 2006.
- [ACLW00] R. Ahlswede, N. Cai, S. R. Li, and Y. R. W., “Network information flow,” *IEEE Transactions on Information Theory*, vol. 46, no. 4, pp. 1204–1216, Jul. 2000.
- [BFY04] J. Boyer, D. D. Falconer, and H. Yanikomeroglu, “Multihop diversity in wireless relaying channels,” *IEEE Transactions on Communications*, vol. 52, no. 10, pp. 1820–1830, Oct. 2004.
- [BHIM05] C. F. Ball, E. Humburg, K. Ivanov, and R. Müllner, “Rapid estimation method for data capacity and spectrum efficiency in cellular networks,” in *Proc. IST Mobile and Wireless Communications Summit*, Dresden, Germany, Jun. 2005.
- [BUK⁺09] S. Berger, T. Unger, M. Kuhn, A. Klein, and A. Wittneben, “Recent advances in amplify-and-forward two-hop relaying,” *accepted for publication in: IEEE Communications Magazine*, 2009.
- [BV04] S. Boyd and L. Vandenberghe, *Convex Optimization*, 1st ed. Cambridge, UK: Cambridge University Press, 2004.
- [BW05] S. Berger and A. Wittneben, “Cooperative distributed multiuser MMSE relaying in wireless ad-hoc networks,” in *Asilomar Conference on Signals, Systems, and Computers 2005*, Pacific Grove, CA, Nov. 2005.
- [BW08] ———, “A coherent amplify-and-forward relaying demonstrator without global phase reference,” in *Proc. IEEE Symposium on Personal, Indoor and Mobile Radio Communications*, Cannes, France, Sep. 2008.
- [Cav00] J. K. Cavers, “Single-user and multiuser adaptive maximal ratio transmission for rayleigh channels,” *IEEE Transactions on Vehicular Technology*, vol. 49, pp. 2043–2050, Nov. 2000.
- [CEG79] T. M. Cover and A. El Gamal, “Capacity theorems for the relay channel,” *IEEE Transactions on Information Theory*, vol. 25, no. 5, pp. 572–584, Sep. 1979.
- [CGN07] T. Cui, F. Gao, and A. Nallanathan, “Optimal training design for channel estimation in amplify and forward relay networks,” in *Proc. IEEE Global Communications Conference*, Washington DC, USA, Nov. 2007.
- [CLW⁺06] P. W. C. Chan, E. S. Lo, R. R. Wang, E. K. S. Au, V. K. N. Lau, R. S. Cheng, W. H. Mow, R. D. Murch, and K. B. Letaief, “The evolution path of 4G networks: FDD or TDD?” *IEEE Communications Magazine*, vol. 44, no. 12, pp. 42–50, Dec. 2006.

- [CT06] T. Cover and J. Thomas, *Elements of Information Theory*, 2nd ed. New York, USA: Wiley & Sons, 2006.
- [DDA02] M. Dohler, J. Dominguez, and H. Aghvami, "Link capacity analysis for virtual antenna arrays," in *Proc. IEEE Vehicular Technology Conference*, vol. 1, Sep. 2002, pp. 440–443.
- [DEH⁺05] S. Deb, M. Effros, D. R. Ho, T. Karger, R. Koetter, D. S. Lun, M. Médard, and N. Ratnakar, "Network coding for wireless applications: a brief tutorial," in *Proc. International Workshop on Wireless Ad-hoc Networks (invited paper)*, London, UK, May 2005.
- [DGA03] M. Dohler, A. Gkelias, and H. Aghvami, "2-hop distributed MIMO communication system," *IEEE Electronics Letters*, vol. 39, no. 18, pp. 1350–1351, Sep. 2003.
- [DLV⁺06] M. Dohler, Y. Li, B. Vucetic, A. H. Aghvami, M. Arndt, and D. Barthel, "Performance analysis of distributed space-time block-encoded sensor networks," *IEEE Transactions on Vehicular Technology*, vol. 55, no. 6, pp. 1776–1789, Nov. 2006.
- [EBP00] T. H. Eggen, A. B. Baggeroer, and J. C. Preisig, "Communication over doppler spread channels - part I: channel and receiver presentation," *IEEE Journal of Oceanic Engineering*, vol. 25, no. 1, pp. 62–71, Jan. 2000.
- [EBW07] C. Esli, S. Berger, and A. Wittneben, "Optimizing zero-forcing based gain allocation for wireless multiuser networks," in *IEEE International Conference on Communications*, Glasgow, Scotland, Jun. 2007, pp. 5825–5830.
- [EW08] C. Esli and A. Wittneben, "Multiuser MIMO two-way relaying for cellular communications," in *Proc. IEEE Symposium on Personal, Indoor and Mobile Radio Communications*, Cannes, France, Sep. 2008.
- [FATY07] Y. Fan, A. Abdulkareem, J. S. Thompson, and H. Yanikomeroglu, "Antenna combining for multi-antenna multi-relay channels," *European Transactions on Telecommunications*, vol. 18, pp. 617–626, Aug. 2007.
- [FWTP07] Y. Fan, C. Wang, J. S. Thompson, and H. V. Poor, "Recovering multiplexing loss through successive relaying using repetition coding," *IEEE Transactions on Wireless Communications*, vol. 6, no. 12, pp. 4484–4493, Dec. 2007.
- [GL96] G. H. Golub and C. F. Loan, *Matrix Computations*, 3rd ed. Baltimore, USA: Johns Hopkin Unisversity Press, 1996.
- [Ham06] I. Hammerström, "Cooperative relaying and adaptive scheduling for low mobility wireless access networks," Ph.D. dissertation, Institut für Kommunikationstechnik, Eidgenössische Technische Hochschule Zürich, Aug. 2006.

- [Her05] M. Herdin, "MIMO amplify-and-forward relaying in correlated MIMO channels," in *Proc. International Conference on Information, Communications and Signal Processing*, Bangkok, Thailand, Dec. 2005.
- [HH03] B. Hassibi and B. M. Hochwald, "How much training is needed in multiple-antenna wireless links," *IEEE Transactions on Information Theory*, vol. 49, no. 4, pp. 951–963, Apr. 2003.
- [HH06] C. Hausl and J. Hagenauer, "Iterative network and channel decoding for the two-way relay channel," in *Proc. IEEE International Conference on Communications*, Istanbul, Turkey, June 2006.
- [HKE⁺07] I. Hammerström, M. Kuhn, C. Esli, J. Zhao, A. Wittneben, and G. Bauch, "MIMO two-way relaying with transmit CSI at the relay," in *Proc. IEEE Signal Processing Advances in Wireless Communications*, Helsinki, Finland, Jun. 2007.
- [HKR97] P. Hoeher, S. Kaiser, and P. Robertson, "Two-dimensional pilot-symbol-aided channel estimation by Wiener filtering," in *Proc. IEEE International Conference on Acoustics, Speech, and Signal Processing*, Munich, Germany, Apr. 1997.
- [HM72] H. Harashima and H. Miyakawa, "Matched-transmission technique for channels with intersymbol interference," *IEEE Transactions on Communications*, vol. 20, pp. 774–780, Aug. 1972.
- [HU06] M. Herdin and T. Unger, "Performance of single and multi-antenna amplify-and-forward relays in a Manhattan street grid scenario," in *Proc. IST Mobile and Wireless Communications Summit*, Mykonos, Greece, Jun. 2006.
- [HW06] I. Hammerström and A. Wittneben, "On the optimal power allocation for non-regenerative OFDM relay links," in *Proc. IEEE International Conference on Communications*, Istanbul, Turkey, Jun. 2006.
- [HYFP04] H. Hu, H. Yanikomeroglu, D. Falconer, and S. Periyalwar, "Range extension without capacity penalty in cellular networks with digital fixed relays," in *Proc. IEEE Global Telecommunications Conference*, Texas, Dallas, USA, Nov. 2004.
- [HZF04a] P. Herhold, E. Zimmermann, and G. Fettweis, "On the performance of cooperative amplify-and-forward relay networks," in *Proc. ITG Conference on Source and Channel Coding (SCS)*, Erlangen, Germany, 2004.
- [HZF04b] ———, "A simple cooperative extension to wireless relaying," in *Proc. International Zurich Seminar on Communications*, Zurich, Switzerland, 2004.
- [IST05] IST-2003-507581 WINNER, "Final report on link level and system level channel models," Tech. Rep. D5.4 v1.4, Nov. 2005. [Online]. Available: www.ist-winner.org

- [IST07a] IST-4-027756 WINNER II, “Final assessment of relaying concepts for all CGs scenarios under consideration of related WINNER II L1 and L2 protocol functions,” Tech. Rep. D3.5.3 v1.0, Sep. 2007. [Online]. Available: www.ist-winner.org
- [IST07b] —, “WINNER II system concept description,” Tech. Rep. D6.13.14 v1.1, Sep. 2007. [Online]. Available: www.ist-winner.org
- [Joh04] M. Joham, “Optimization of linear and nonlinear transmit signal processing,” Ph.D. dissertation, Lehrstuhl für Netzwerktheorie und Signalverarbeitung, Technische Universität München, Apr. 2004.
- [JT94] S. H. Jamali and L.-N. T., *Coded-modulation Techniques for Fading Channels*, 1st ed. Norwell, USA: Kluwer Academic Publishers, 1994.
- [JUN05] M. Joham, W. Utschick, and J. A. Nossek, “Linear transmit processing in MIMO communication systems,” *IEEE Transactions on Signal Processing*, vol. 53, no. 8, pp. 2700–2712, Aug. 2005.
- [KBB⁺05] T. Kaiser, A. Bourdoux, J. R. Boche, H. Fonollosa, J. B. Andersen, and W. Utschick, *Smart Antennas - State of the Art*. New York, USA: Hindawi Publishing Corporation, EURASIP Book Series on Signal Processing and Communications, 2005, vol. 3.
- [KEHW06] M. Kuhn, A. Etefagh, I. Hammerström, and A. Wittneben, “Two-way communication for IEEE 802.11n WLANs using decode and forward relays,” in *Proc. Asilomar Conference on Signals, Systems, and Computers*, Pacific Grove, CA, USA, Oct. 2006.
- [Kes07] F. Keskin, “Precoding for MIMO multi-user mobile radio downlinks,” Ph.D. dissertation, Technische Universität Kaiserslautern, 2007.
- [KK08] A. Kühne and A. Klein, “Adaptive MIMO-OFDM using OSTBC with imperfect CQI feedback,” in *Proc. International ITG Workshop on Smart Antennas*, Darmstadt, Germany, Feb. 2008.
- [KS95] G. Kaplan and S. Shamai, “Error probabilities for the block-fading gaussian channel,” *Archiv für Elektronik und Übertragungstechnik (AEU)*, vol. 49, no. 4, pp. 192–205, Dec. 1995.
- [Lin03] J. C. Lin, “Health aspects of wireless communication: personal wireless communication radiation and the eye lens,” *Proc. ACM SIGMOBILE Mobile Computing and Communications Review*, vol. 7, no. 3, pp. 4–7, Jul. 2003.
- [LJS06] P. Larsson, N. Johansson, and K.-E. Sunell, “Coded bi-directional relaying,” in *Proc. IEEE Vehicular Technology Conference*, vol. 2, Melbourne, Australia, Apr. 2006, pp. 851–855.
- [LLW⁺03] H. Li, M. Lott, M. Weckerle, W. Zirwas, and E. Schulz, “Multihop communications in future mobile radio networks,” in *Proc. IEEE Personal, Indoor and Mobile Radio Communications*, vol. 1, Sep. 2003, pp. 54–58.

- [Loy01] S. Loyka, “EMC/EMI analysis in wireless communication networks,” in *Proc. IEEE International Symposium on Electromagnetic Compatibility*, vol. 1, Aug. 2001, pp. 100–105.
- [LT02] A. Lozano and A. M. Tulino, “Capacity of multiple-transmit multiple-receive antenna architectures,” *IEEE Transactions on Information Theory*, vol. 48, no. 12, pp. 3117–3128, Dec. 2002.
- [LTW04] J. N. Laneman, D. N. C. Tse, and G. W. Wornell, “Cooperative diversity in wireless networks: efficient protocols and outage behavior,” *IEEE Transactions on Information Theory*, vol. 50, no. 12, pp. 3062–3080, Dec. 2004.
- [LVZD07] Y. Li, B. Vucetic, Z. Zhou, and M. Dohler, “Distributed adaptive power allocation for wireless relay networks,” *IEEE Transactions on Wireless Communications*, vol. 6, no. 2, pp. 948–958, Feb. 2007.
- [LW03] J. N. Laneman and G. W. Wornell, “Distributed space-time-coded protocols for exploiting cooperative diversity in wireless networks,” *IEEE Transactions on Information Theory*, vol. 49, no. 10, Oct. 2003.
- [LZ08] Y.-C. Liang and R. Zhang, “Optimal analogue relaying with multi-antennas for physical layer network coding,” in *Proc. IEEE International Conference on Communications*, Beijing, China, May 2008.
- [MBQ04] M. Meurer, P. W. Baier, and W. Qiu, “Receiver orientation versus transmitter orientation in linear MIMO transmission systems,” *EURASIP Journal on Applied Signal Processing*, vol. 9, pp. 1191–1198, Aug. 2004.
- [MH04] J. Mietzner and P. A. Hoeher, “Distributed space-time codes for cooperative wireless networks in the presence of different propagation delays and path losses,” in *Proc. IEEE Sensor Array and Multichannel Signal Processing Workshop*, Jul. 2004, pp. 264–268.
- [MLM02] W. Mohr, R. Lüder, and K. H. Möhrmann, “Data rate estimates, range calculations and spectrum demand for new elements of systems beyond IMT-2000,” in *Proc. IEEE International Symposium on Wireless Personal Multimedia Communications*, vol. 1, Oct. 2002, pp. 37–46.
- [Mue01] R. Mueller, “Successive vs. joint decoding under complexity and performance constraints,” *International Journal of Electronics and Communications*, vol. 55, no. 2, pp. 141–143, 2001.
- [MVA04] O. Munoz, J. Vidal, and A. Agustin, “A game theoretic approach for cooperative MIMO schemes with cellular reuse of the relay slot,” in *Proc. IEEE International Conference on Acoustics, Speech and Signal Processing*, vol. 4, Montreal, Canada, May 2004, pp. iv–581 – iv–584.
- [MVA05] —, “Non-regenerative MIMO relaying with channel state information,” in *Proc. IEEE International Conference on Acoustics, Speech and Signal Processing*, Philadelphia, PA, USA, Mar. 2005.

- [MVA07] ———, “Linear transceiver design in nonregenerative relays with channel state information,” *IEEE Transactions on Signal Processing*, vol. 55, no. 6, pp. 2593–2604, Jun. 2007.
- [MVBL03] H. Minn, K. Vijay, V. K. Bhargava, and K. B. Letaief, “A robust timing and frequency synchronization for OFDM systems,” *IEEE Transactions on Wireless Communications*, vol. 2, no. 4, pp. 822–839, Jul. 2003.
- [OB06] T. J. Oechtering and H. Boche, “Stability region of an efficient bidirectional regenerative half-duplex relaying protocol,” in *Proc. IEEE Information Theory Workshop*, Chengdu, China, Oct. 2006, pp. 380–384.
- [OB07] ———, “Bidirectional relaying using interference cancellation,” in *Proc. ITG/IEEE International Workshop on Smart Antennas*, Vienna, Austria, Feb. 2007.
- [OB08] ———, “Optimal time-division for bidirectional relaying using superposition encoding,” *IEEE Communications Letters*, vol. 12, no. 4, Apr. 2008.
- [OP06] O. Oyman and A. J. Paulraj, “Design and analysis of linear distributed MIMO relaying algorithms,” *IEE Proceedings-Communication*, vol. 153, no. 4, pp. 565–572, Aug. 2006.
- [PF05] D. P. Palomar and J. R. Fonollosa, “Practical algorithms for a family of waterfilling solutions,” *IEEE Transactions on Signal Processing*, vol. 53, no. 2, pp. 686–695, Feb. 2005.
- [PNG03] A. Paulraj, R. Nabar, and D. Gore, *Introduction to Space-Time Wireless Communications*, 1st ed. Cambridge, UK: Cambridge University Press, 2003.
- [PP08] K. B. Petersen and M. S. Pedersen, *The Matrix Cookbook*, 2008. [Online]. Available: <http://matrixcookbook.com>
- [Pro01] J. Proakis, *Digital Communications*, 4th ed. New York, USA: McGraw-Hill, New York, 2001.
- [PS07] C. S. Patel and G. L. Stüber, “Channel estimation for amplify and forward relay based cooperation diversity systems,” *IEEE Transactions on Wireless Communications*, vol. 6, no. 6, pp. 2348–2355, Jun. 2007.
- [PSP06] C. S. Patel, G. L. Stüber, and T. G. Pratt, “Statistical properties of amplify and forward relay fading channels,” *IEEE Transactions on Vehicular Technology*, vol. 55, no. 1, pp. 1–9, Jan. 2006.
- [PWS⁺04] R. Pabst, B. Walke, D. Schultz, P. Herhold, S. Mukherjee, H. Viswanathan, M. Lott, W. Zirwas, M. Dohler, H. Aghvami, D. Falconer, and G. Fettweis, “Relay-based deployment concepts for wireless and mobile broadband radio,” *IEEE Communications Magazine*, pp. 80–89, Sep. 2004.

- [PY07] P. Popovski and H. Yomo, "Wireless network coding by amplify-and-forward for bi-directional traffic flows," *IEEE Communications Letters*, vol. 11, no. 1, pp. 16–18, Jan. 2007.
- [RW05] B. Rankov and A. Wittneben, "Spectral efficient signaling for half-duplex relay channels," in *Proc. Asilomar Conference on Signals, Systems and Computers*, Pacific Grove, CA, USA, Nov. 2005.
- [RW06] —, "Achievable rate regions for the two-way relay channel," in *Proc. IEEE International Symposium on Information Theory*, Seattle, USA, Jul. 2006.
- [RW07] —, "Spectral efficient protocols for half-duplex fading relay channels," *IEEE Journal on Selected Areas in Communications*, vol. 25, no. 2, pp. 379–389, Feb. 2007.
- [SAY06] H. Shi, T. Asai, and H. Yoshino, "A relay node division duplex relaying approach for MIMO relay networks," in *Proc. IEEE Symposium on Personal, Indoor and Mobile Radio Communications*, Helsinki, Finland, Sep. 2006.
- [SEA03a] A. Sendonaris, E. Erkip, and B. Aazhang, "User cooperation diversity, part i: system description," *IEEE Transactions on Communications*, vol. 15, pp. 1927–1938, Nov. 2003.
- [SEA03b] —, "User cooperation diversity, part ii: implementation aspects and performance analysis," *IEEE Transactions on Communications*, vol. 15, pp. 1939–1948, Nov. 2003.
- [SFK06] A. Sohl, T. Frank, and A. Klein, "Channel estimation for DFT precoded OFDMA with blockwise and interleaved subcarrier allocation," in *Proc. International OFDM Workshop*, Hamburg, Germany, Aug. 2006.
- [SPI03] D. C. Schultz, R. Pabst, and T. Irnich, "Multi-hop based radio network deployment for efficient broadband radio coverage," in *Proc. International Symposium on Wireless Personal Multimedia Communications*, vol. 2, Yokosuka, Japan, Oct. 2003, pp. 377–381.
- [Tel99] I. Telatar, "Capacity of multi-antenna Gaussian channels," *European Transactions on Telecommunications*, vol. 10, no. 6, pp. 585–595, Nov./Dec. 1999.
- [TH07] X. Tang and Y. Hua, "Optimal design of non-regenerative MIMO wireless relays," *IEEE Transactions on Wireless Communications*, vol. 6, no. 4, pp. 1398–1407, Apr. 2007.
- [Tim05] B. Timus, "Break-even costs in a cellular multihop system with fixed relays," in *Proc. International Wireless Summit*, Aalborg, Denmark, Sep. 2005.
- [Tom71] M. Tomlinson, "New automatic equaliser employing modulo arithmetic," *Electronic Letters*, vol. 7, pp. 138–139, Mar. 1971.

- [TSD04] L. Tong, B. M. Sadler, and M. Dong, "Pilot-assisted wireless transmissions," *IEEE Signal Processing Magazine*, vol. 21, no. 6, pp. 12–25, Nov. 2004.
- [UK06] T. Unger and A. Klein, "Cooperative MIMO relaying with distributed space-time block codes," in *Proc. IEEE Symposium on Personal, Indoor and Mobile Radio Communications*, Helsinki, Finland, Sep. 2006.
- [UK07a] —, "Applying relay stations with multiple antennas in the one- and two-way relay channel," in *Proc. IEEE Symposium on Personal, Indoor and Mobile Radio Communications (invited paper)*, Athens, Greece, Sep. 2007.
- [UK07b] —, "Linear transceiver filters for relay stations with multiple antennas in the two-way relay channel," in *Proc. IST Mobile and Wireless Communications Summit*, Budapest, Hungary, Jul. 2007.
- [UK07c] —, "On the performance of distributed space-time block codes in cooperative relay networks," *IEEE Communications Letters*, vol. 11, no. 5, pp. 411–413, May 2007.
- [UK07d] —, "On the performance of two-way relaying with multiple antenna relay stations," in *Proc. IST Mobile and Wireless Communications Summit*, Budapest, Hungary, Jul. 2007.
- [UK08a] —, "Duplex schemes in multiple antenna two-hop relaying," *EURASIP Journal on Advances in Signal Processing*, vol. 2008, Article ID 128592, May 2008.
- [UK08b] —, "Maximum sum rate of non-regenerative two-way relaying in systems with different complexities," in *Proc. IEEE Symposium on Personal, Indoor and Mobile Radio Communications (invited paper)*, Cannes, France, Sep. 2008.
- [vdM71] E. C. van der Meulen, "Three-terminal communication channels," *Advances in Applied Probability*, vol. 3, pp. 120–154, 1971.
- [VH07] R. Vaze and R. W. Heath, "Capacity scaling for MIMO two-way relaying," in *Proc. IEEE International Symposium on Information Theory 2007*, Nice, France, Jun. 2007.
- [VJ98] B. R. Vojcic and W. M. Jang, "Transmitter precoding in synchronous multiuser communications," *IEEE Transactions on Communications*, vol. 46, pp. 1346–1355, Oct. 1998.
- [vNP00] R. van Nee and R. Prasad, *OFDM for Wireless Multimedia Communications*, 1st ed. Artech House, 2000.
- [Wie40] N. Wiener, "Extrapolation, interpolation, and smoothing of stationary time series," *MIT Press*, 1940.

- [WOB08] R. F. Wyrembelski, T. J. Oechtering, and H. Boche, “Decode-and-forward strategies for bidirectional relaying,” in *Proc. IEEE Symposium on Personal, Indoor and Mobile Radio Communications (invited paper)*, Cannes, France, Sep. 2008.
- [Yan02] H. Yanikomeroglu, “Fixed and mobile relaying technologies for cellular networks,” in *Proc. Workshop on Applications and Services in Wireless Networks*, Paris, France, Jul. 2002.
- [YSL06] S. Yiu, R. Schober, and L. Lampe, “Distributed space-time block coding,” *IEEE Transactions on Communications*, vol. 54, no. 7, pp. 1195–1206, Jul. 2006.
- [ZHF03] E. Zimmermann, P. Herhold, and G. Fettweis, “On the performance of cooperative diversity protocols in practical wireless systems,” in *Proc. IEEE Vehicular Technology Conference*, Orlando, Florida, USA, Oct. 2003.
- [ZHF04] —, “The impact of cooperation on diversity-exploiting protocols,” in *Proc. IEEE Vehicular Technology Conference*, Milan, Italy, 2004.
- [ZK01] J. Zander and S.-L. Kim, *Radio Resource Management for Wireless Networks*. Boston, USA: Artech House, 2001.

